Spring 2013

Computational fluid dynamics (CFD) modeling to support the reduction of fish passage exposure to elevated total dissolved gas and predator habitats at McNary Dam

Joseph T. Dvorak
University of Iowa

COMPUTATIONAL FLUID DYNAMICS (CFD) MODELING TO SUPPORT THE REDUCTION OF FISH PASSAGE EXPOSURE TO ELEVATED TOTAL DISSOLVED GAS AND PREDATOR HABITATS AT MCNARY DAM

by

Joseph T. Dvorak

A thesis submitted in partial fulfillment
of the requirements for the Master of
Science degree in Mechanical Engineering
in the Graduate College of
The University of Iowa

May 2013

Thesis Supervisors: Adjunct Associate Professor Marcela Politano

Associate Professor Pablo Carrica

Graduate College
The University of Iowa
Iowa City, Iowa

CERTIFICATE OF APPROVAL

MASTER'S THESIS

This is to certify that the Master's thesis of

Joseph T. Dvorak

has been approved by the Examining Committee
for the thesis requirement for the Master of Science degree
in Mechanical Engineering at the May 2013 graduation.

Thesis Committee: _____
Marcela S. Politano, Thesis Supervisor

_____
Pablo Carrica, Thesis Supervisor

_____
Larry Weber

_____
Albert Ratner

ACKNOWLEDGMENTS

I would like to thank Ryan Laughery of the Army Core of Engineers, Walla Walla District for the sponsorship and aid in this project. I would also like to thank Ken Hansen of CH2M Hill for the insights and helpful reviews of the project.

I would also like to thank my advisor Marcela Politano for giving me this opportunity to be her research assistant. Her guidance and support over the past two years were invaluable to my success as a graduate student. Also my thanks to Pablo Carrica my academic advisor and committee chair for his help as well as the other members of my thesis committee, Professor Larry Weber and Professor Albert Ratner for their review and input of this thesis.

Furthermore I would like to extend my gratitude to Antonio Arenas and Mike Carbone for their help, especially during the first months in the lab. Without their help, I would not have been able to finish this project.

Finally I would like to thank my parents and my sister for their support, both financially and emotionally. They have always been there to help motivate me and help keep my goals in front of me.

ABSTRACT

The safety of migrating salmon, especially salmonids, in the Pacific Northwest has been a concern for decades. With the advent of fish bypass systems, and safer turbines the focus of salmon safety has turned to total dissolved gases. Produced by entrainment of air into tailrace waters, total dissolved gases (TDG) can cause gas bubble disease, a harmful and potential lethal disease in fish. Avian predators are another danger for migrating salmon. In some areas of the world birds common in the Pacific Northwest can account for as much as 65% of salmon smolt losses.

The goal of this thesis is to determine the effects of changing operational conditions at McNary dam on fish exposure to predator habitats and TDG. Computational fluid dynamic models were implemented to predict the hydrodynamics, TDG distribution and inert particle trajectories in the tailrace of McNary dam for varying operational conditions.

A 3D volume of fluid (VOF) model was used first to capture the free surface shape in the tailrace. A rigid-lid model was then used to simulate the hydrodynamics and TDG distribution within the tailrace using the free surface shape from the VOF model. This 3D two phase model utilized an anisotropic Reynolds Stress turbulence model. All grids were generated using the commercial Gridgen software. A lagrangian particle tracking model that followed Newton's laws of motion for a particle was used to track inert particles throughout the domain.

Validation of the model was performed. A grid refinement study with four different refinement levels was performed. Velocities for each grid type were compared against field data taken in 2004, and TDG was compared amongst the four grids. It was determined the medium level of refinement could accurately predict the velocities, and

the TDG was relatively independent of grid density; TDG averages at the grid outlets were within 1.435% of one another. The TDG distribution was then compared, using the grid of medium refinement against field data measured in 1997and were between 1.5 and 3% of error depending on the transect.

After validation of the model 16 predictive simulations were run with varying levels of total river flow and operational conditions. Tailrace hydrodynamics along with TDG production and distribution were compared for simulations with comparable total river flow rates. Fish trajectories were tracked using the particle tracking model. Inert particles were injected into the domain and properties such as velocity, distance to the shore and depth about each were recorded. Statistics were then generated for the particles based on criteria that defined dangerous predation zones within the tailrace.

After completion of the simulations, it was determined that existing operations consistently produced higher levels of TDG due to increased entrainment of the powerhouse flows into the spillway regions. It was also found that with increasing total river flows, TDG levels increased. On average, summer operations had lower TDG than spring due to the lower total river flows. Predation zones were similar for all simulations, but particle statistics varied depending on operational conditions. In general, particles were safer for higher flowrates as fewer low velocity eddies where particles could be trapped formed in simulations with high flowrates.

TABLE OF CONTENTS

LIST OF TABLES

Table

LIST OF FIGURES

Figure

CHAPTER I

INTRODUCTION

Salmon species have long been an essential part of the ecological and economical landscapes of the Pacific Northwest. They were a major source of food and trade for the Native Americans of the Pacific Northwest, and when the first settlers arrived to the area in the 19th century, they too used salmon for support. At that time in the 19th century, as many as 1.5 million Chinook salmon could be found in the Columbia River Basin. A count in 1994 revealed that only 1,800 Chinook salmon had returned the Snake River to spawn. In the 1970's, one could expect to find approximately 4,400 Sockeye salmon in the basin, again however, in 1994 a count revealed that just one solitary Sockeye salmon had returned to Redfish Lake, a lake in Idaho on the outskirts of the Columbia River Basin (NMFS, 1995). Overall wild salmon run sizes have dropped dramatically since the late 19th century. At that time, run sizes in the basin were between 11 and 15 million total salmon. Today they are between 110,000 and 333,000, less than two percent of the historic size (Lackey, 2003).

There are an array of different reasons as to the cause of the decline in Pacific Northwest salmon populations including overfishing, logging and climate change. This thesis focuses on another cause, specifically construction of hydropower dams. There have been many different steps taken to reduce the impact of hydropower dams on the salmon population of the Pacific Northwest. Turbine mortality rates have dropped due to improvements in design, fish passage facilities have been implemented to transport juvenile salmon around dams and the construction of fish ladders have provided routes for adult salmon to complete their salmon runs upriver to spawn. These steps help

mitigate migration problems and mechanical injuries, there is however another threat to the salmon population created by hydropower facilities.

Another method of aiding migrating salmon is to increase spill from a facility during the height of spawning season, specifically spring and summer months. This increased spill creates an alternative route for juvenile salmon to pass through the dam other than via the turbines or a bypass system. A negative effect of increased spill is an increase in the amount of air entrainment into the stilling basin. Here, the entrained air is carried to depths where hydrostatic pressure causes bubbles to dissolve, increasing the gas concentration in the water. High levels of total dissolve gas (TDG) are a serious issue for fish as exposure to high TDG can lead to gas bubble disease. Gas bubble disease is caused by the formation of bubbles within gills, eyes and/or the bloodstream within salmon when high TDG water is absorbed through the gills. Gas bubble disease reduces a fish's swimming abilities, make them more susceptible to disease and can lead to death in the case of extreme exposure.

There have been efforts to reduce TDG levels in tailraces of hydropower facilities, namely the installation of deflectors in the spill bays. Deflectors are ideally used to create what are known as surface jets, where instead of plunging deep into the stilling basin, spill jets are directed parallel to the surface where bubbles will not be subjected to large pressures and dissolve. While deflectors reduce TDG production, they are not a singular solution to the TDG problem. Determining which spillway and powerhouse operations lead to the lowest TDG production is a relatively inexpensive method for further reducing TDG production.

Another problem for the migrating salmon face is predation. Predators, especially birds are able to catch salmon swimming in shallow or slow moving water. Also birds have learned to wait at outfall sites where fish are transported to the tailrace from the forebay. Fish may become confused in this region, making them susceptible to attacks from birds. Areas along the shorelines also present zones of concern as they are generally shallower and are easily accessed by the predators. Determining operational conditions that provide the safest routes for the fish is an important part of maintaining salmon populations. This thesis is part of a research project with the U.S. Army Corps of Engineers (USACE) Walla Walla District who requested numerical modeling to support the reduction of fish exposure to predator habitats in the McNary tailrace (Politano, Dvorak 2012). TDG exposure was also analyzed in this study.

1.1 McNary Dam Background

McNary Dam, operated by the U.S. Army Corps of Engineers (USACE) Walla Walla District, is one of the largest hydroelectric power facilities in the Pacific Northwest. It is the first dam downstream of the confluence of the Snake and Columbia rivers at river mile 292 (see Figure 1.1). It spans 1.4 miles across the river and utilizes 22 50-foot wide spillway bays, and 14 70-megawatt turbines for an installed capacity of 980 megawatts. This massive dam greatly influences anadromous fish migration in the Snake and Columbia River systems. Juvenile fish facilities consist of a collection system in the forebay that captures fish and transports them back to the river downstream of the dam through a pipeline/corrugated metal flume. The adult fish passage facilities at McNary consist of separate north (Washington) and south (Oregon) shore facilities. The north and south shore facilities include fish ladders with counting station, tag antennas in the

ladder, collection systems, and auxiliary water supply systems. The south shore facilities also include two south shore entrances and a powerhouse collection system.

Figure 1.1 Columbia River Basin

Source: http://www.nwcouncil.org/energy/powersupply/dams/default.htm

Figure 1.2 McNary Dam Configuration

Source: http://www.nww.usace.army.mil/Locations/DistrictLocksandDams.aspx

CFD models have been developed for the tailrace of McNary Dam since 2008 (Politano et al. 2009, Politano and Laughery 2010, Politano 2011). The purpose of these models was to assist in the understanding of the effect of operational configurations or fish passage structures on the tailrace flow pattern and TDG production. Special attention was given to operations that could result in elevated powerhouse flow entrainment into the spillway region and high total TDG concentrations. The models have incorporated either existing and/or proposed fish passage related features. CFD models provided a method to quantify the hydraulic performance of these features in both the forebay and tailrace for multiple configurations of turbine and spillway operations.

State and Federal regulations established water quality standards relative to TDG to protect aquatic life. Both Oregon and Washington States wrote Total Maximum Daily Loads (TMDLs) to address TDG in the Columbia and Snake River (Oregon Department of Environmental Quality and Washington State Department of Ecology, 2002). Water quality standards limit TDG levels to 110% at any point of measurement. TDG levels are allowed to exceed the standard, up to 120%, of saturation under two scenarios: to pass a discharge greater or equal than the 7Q10 or to pass voluntary spill to assist out-migrating juveniles.

The effect of TDG supersaturation on fish depends on TDG levels, exposure time and swimming depth. Fish exposed to elevated TDG during a short period of time will unlikely experience significant effects unless the level of supersaturation is extremely high. Fish moving up and down daily at depths of several meters for at least one third of the time will probably experience minor effects for TDG in the range of 120-140%

(Weitkamp, 2000). TDG abatement studies usually focused on meeting TDG water quality standards without considering exposure time.

In order to further increase the survival of migrating fish, USACE is using a more comprehensive approach. After installing spillway deflectors in all spillway bays to reduce TDG production, they seek to optimize dam operations and fish passage structures considering TDG exposure time and exposure to predators. In this study, predator habitat is defined as: A) flow velocities below 4 fps, B) flow depth less than 10 meters, and C) distance from shore less than 75 meters (USACE, 2011).

The approach presented in this paper is a first step for evaluation of threats faced by fish in a tailrace. The expectation is that, when biological models are accessible, the approach presented in this paper can be used to evaluate probability of fish injury or mortality due to gas supersaturation and/or predators. Current migration models are limited to fish behavior in forebays. To the knowledge of the author, a biological model for fish moving in a tailrace has yet to be developed nor has one been developed that models avian predators in a tailrace. The use of current behavioral models for forebays would increase the uncertainty of the results and therefore they were not incorporated in the analysis.

1.2 Study Area

The model used in this study is based on the CFD model of the McNary tailrace developed at IIHR-Hydroscience & Engineering by Politano et al. (2009). The model includes the main structures of the McNary tailrace: 22 spillway bays with deflectors, 14 powerhouse units, two temporary spillway weirs (TSW), north shore fish entrance, north

powerhouse fish entrance, south fish entrance, fish pumps, station service, and a navigation lock.

In this study, existing and proposed juvenile fish bypass outfalls were included into the model. In addition, the model was extended from the end of the navigation lock to a distance of about 8,500 ft downstream of the dam. Figure 1.3 shows the bathymetric information of the entire model together with existing and new outfalls.

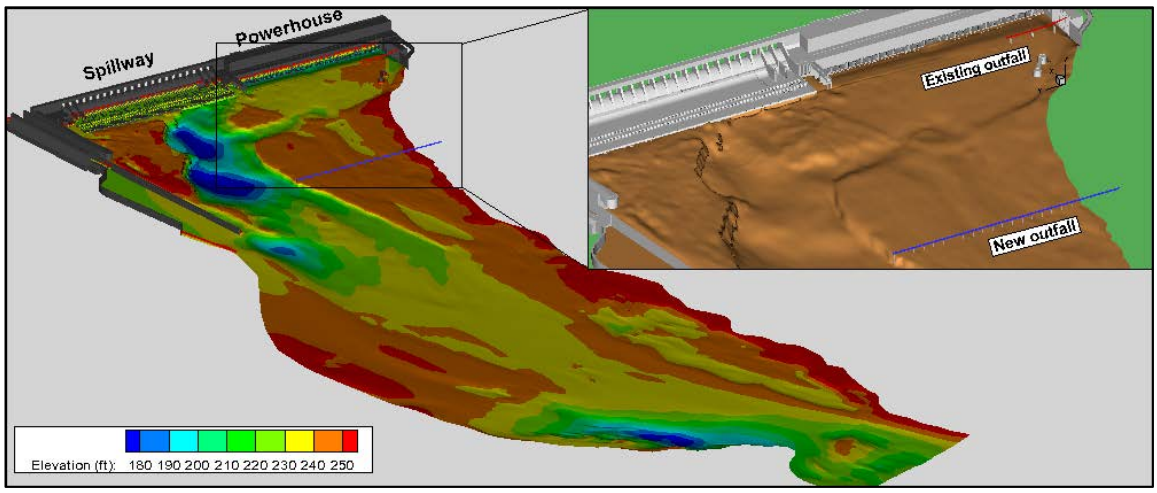

Figure 1.3 McNary CFD Model

1.3 Thesis Objectives

The purpose of this thesis is to provide hydraulic information related to fish predation habitats and TDG within the tailrace of McNary dam for varying operational conditions and/or hydraulic features by developing a CFD model for the tailrace of McNary dam. The steps taken in development were:

1. A grid sensitivity study was performed.

2. The model was validated by comparison of results to TDG and velocity field data.

3. The model was used to perform simulations to predict the hydrodynamics and TDG distribution in the McNary tailrace for a number of varying operational conditions. These simulation conditions were provided by the USACE Walla Walla District.

4. The effects of varying operational conditions on TDG distribution were analyzed.

5. Use of a lagrangian particle tracking model to predict fish locations within the tailrace, and risk levels for the fish were determined based on the criteria also provided by the USACE.

Model overviews are presented in Chapters III and IV, while Chapter V discusses the calibration and validation of the models, and Chapter VI presents results of the simulations. The literature review in chapter two briefly covers related topics such as gas bubble disease, a modeling history of TDG, and current models being used for these simulations.

CHAPTER II

LITERATURE REVIEW

2.1 TDG Modeling History

There are many processes that play roles in the production of TDG in a tailrace. Entrainment of air into the spillway, mass transfer between entrained bubbles and the water, breakup and coalescence of the bubbles, mass transfer at the free surface (degasification) as well as general transport of the bubbles and the TDG. All these processes should be considered when modeling TDG. Further issues arise when one considers the fact that the free surface is not a plane, but a complex three-dimensional shape. Models that are able to predict these complex free surfaces are very expensive and not extensively used today for hydraulic applications. Turan et al. (2008) and Ferrari et al. (2009) had used these types of models.

One also must consider the entrainment of water from the powerhouse region which can either help dilute the TDG concentration, or increase production of TDG as discussed earlier. A complex three-dimensional model is required to accurately predict TDG distribution. Accurately predicting TDG in the tailrace of dams has been an area of study for many years. Initial studies used a one-dimensional empirical model. These studies, while modeling the mass transfer between the water and the bubbles, did not solve hydrodynamics in the tailrace (Hibbs and Gulliver 1997; Geldert et al. 1998; Urban et al. 2008). Orlins and Gilliver (2000) and Weber et al. (2004) created models to include the transportation and mixing of the TDG based on empirical correlations. These models presented several experimental parameters based on measured TDG data, and thus were limited for predicting TDG for varying dam configurations and operational conditions.

Transport and mixing of TDG is a crucial part of accurately predicting the TDG in the tailrace. A two-dimensional (2D) two-phase model was developed by Politano et al. (2007) utilizing transport equations for gas volume fraction, bubble velocity and bubble number density. This model was able to solve the flow field while including the mixing and transport of TDG. However, the model was restricted by an isotropic turbulence model, the lack of free surface computations, the 2D approach, which cannot solve the general three-dimensional (3D) nature of tailrace flow fields, and the one-way coupling of the bubbles and flow field.

The model used in this study is based on the model developed by Politano et al.(2009, 2012) which is not limited as the above 2D approach is. Chapter III presents an overview of the hydrodynamic and TDG models used in this thesis.

2.2 TDG and Gas Bubble Disease

One of the first reports to address the issue of gas supersaturation created by hydroelectric facilities on the Columbia and Snake rivers was written by Beiningen and Ebel (1971). In their report, Beiningen and Ebel noted elevated gas levels, of approximately 120%, including nitrogen levels as high as 140% from 1965 and 1969 in the Columbia river. Meyers et al. (2008) have reported on the effects of total dissolved gas in causing gas bubble disease (GBD). Gas bubble disease is caused by exposure to water containing high saturation levels of oxygen, nitrogen or any combination of the two. Fish swimming at depth will absorb these high levels of gas through their gills, where when returning to shallower depths, the gases form bubbles in the blood stream leading to GBD.

The age and species of a fish, along with water properties such as temperature TDG levels and depth all change the effects of gas bubble disease, which can range from mild to fatal. The literature review provided by Weitkam and Katz (1980) provides an extensive examination of the effects of GBD on fish. Signs of gas bubble disease include blisters/bubbles forming in eyes, around the mouth and in the gills of fish as shown in Figures 2.1 and 2.2. Pop-eye syndrome can also be caused by GBD as shown in Figure 2.3. Below is a list of TDG ranges and their effects on fish (Meyers et al. 2008).

TDG

100-106% Embolic lesions will appear with hemostasis

≥ 103% Certain species of salmonid fry are stressed and may later develop conditions leading to death (i.e., coagulated yolk, fin erosion, tail erosion, etc.)

> 120% Acute levels, fry will die before signs or lesions indicate a problem

Figure 2.1 Gas Bubbles Surrounding Eye of Fish with GBD

Source: Meyers et al. 2008

Figure 2.2 Gas Bubbles Trapped in Gill of a Fish with GBD

Source: Meyers et al. 2008

Figure 2.3 Pop-eye Syndrome in a Fish with GBD

Source: http://www.kissyourfish.com/Pop-Eye.htm

Many studies have reviewed the effects of TDG on fish in the Columbia River Basin. McGrath et al. (2006) studied TDG effects on fish in the Columbia river. They reported that at Bonneville dam (downstream of McNary) just 3% of fry exposed to 115-120% TDG had bubbles form in the body cavity causing erratic swimming behaviors while between 120-125% TDG, 40% of fry had large body cavity bubbles. Below Grand Coulee Dam (upstream of McNary on the Columbia river) fish died after exposure to 125-130% saturation with little signs of the disease, and mortality rates roughly doubled when exposure increased from 125% to 130% (Beeman et al. 2003).

2.3 Predation in Dam Tailraces

There are a number of avian predators in the Columbia River Basin. Some of the most abundant are the California Gull, the Caspian Tern, the Common Merganser, the Double-crested Cormorant and the Ring-billed Gull. The population of birds, and the species of bird changes with regard to salmonid abundance. The peak population of birds occurs in mid-July, averaging over 1000 birds in the reach and about 55% of the birds present were Common Mergansers. Later in the year, after July, seasonally returning Ring-billed gulls return to the area and dominate the population (Wiese et al. 2008).

Common Mergansers are small, typically 3-4 pound, ducks that live year round in the Columbia River Basin. They are forager birds, and eat mostly small fish. Their population has been increasing annually since 1957, however culling programs are used in areas where safety of juvenile fish is important. Figure 2.4 shows a typical Common Merganser pair.

Figure 2.4 Common Merganser Pair

Source: http://www.billhubick.com/photos/birds/common_merganser.php

Weise et al. (2008) studied the relationship between avian predators and salmon in the basin. The area of study was the reach of the Columbia River extending from the Grand Coulee dam at river mile 596.6, to McNary dam at river mile 292. Mergansers consume on average 27,000 salmon annually in the Columbia River basin which makes up approximately 55% of avian consumption in the region. Total salmon consumption in the 300 mile reach ranged from 0.02 to 0.96% of smolts. This result was quite low, considering studies of the Big Qualicum River of Vancouver Island saw 24-65% of smolts were consumed by mergansers alone. Similarly, in Scotland mergansers consumed 3-16% of available salmon smolts (Wood 1987 and Feltham 1995 as cited by Weise et al. 2008).

2.4 Summary of Literature

This chapter discussed the modeling history of TDG, facts about gas bubble disease, its relationship with TDG and the effects it has on fish and avian predation of

salmon in the Columbia River Basin. Models produced by Hibbs and Gulliver in 1997 were able to model the mass transfer between air and water without solving tailrace hydrodynamics. Orlins and Gulliver and Weber et al. then created a model capable of predicting transport and mixing. These works became the basis of the model that is used in this thesis.

TDG created by the entrainment of air into the spillway region of the dam can have many negative effects on fish. It was noted that exposure to elevated TDG levels can result in erratic swimming behavior, erosion of fins and tails and death among other problems.

Avian predators are the most abundant salmon predator in the region, among those the Common Merganser is the most populous. While consuming less than 1% of total available smolts in the basin, in other areas of the world these birds have been responsible for as much as 65% of the loss in smolts.

CHAPTER III

MODEL OVERVIEW

3D two-phase models used in this study are based on the commercial code Fluent, ANSYS which solve discrete Reynolds-averaged Navier-Stokes (RANS) equations using a cell-centered finite volume scheme. Three models were used in this thesis: a) a VOF model, b) a rigid-lid eulerian model and c) a lagrangian model, which will be described in Chapter IV.

The VOF model predicts the flow regime and free-surface shape. Due to the computational requirements of using a small time-step to obtain convergence, the extent of the VOF model is limited to approximately 2,500 ft downstream of the dam. After the statistically steady-state solution is reached, the free-surface shape is extracted and used to generate a grid, fixed throughout the computation, conformed to this geometry.

The rigid-lid mixture model allows for a proper prediction of the tailrace flow pattern and TDG concentration. The model includes about 8500 ft of the tailrace. The model used in this study is based on the model proposed by Politano et al. (2009) which accounts for the effect of the bubbles on the flow field. The mixture model considers the volume occupied by the bubbles as well as the density and viscosity of the mixture gas/water. In addition, the suppression and production of the turbulence by the bubbles is included into the model for proper assessment of water entrainment from the powerhouse into the spillway region and TDG distribution. Bubble velocities are calculated considering buoyancy, pressure, drag and turbulent dispersion forces. The air entrainment (gas volume fraction and bubble size) is a model parameter imposed as a boundary

condition at the spillway bays. It must be noted that the choice of bubble size and volume fraction at the spillway bays has an important effect on the level of entrainment and TDG distribution. In this study a reasonable single-size bubble diameter and volume fraction were used at the spillway gates to match the experimental TDG data measured on Feb. 12, 1997, and the same values are used for all computations.

The lagrangian model simulates fish as neutrally buoyant spherical particles neglecting behavioral responses. The history of particle exposure to predator habitat is calculated as a percentage of time for criteria of velocity magnitude, water depth and distance to the shore.

Specific two phase flow models and boundary conditions were implemented into FLUENT through User Defined Functions (UDFs). Two-phase User Defined Scalar (UDSs) transport equations were used to calculate the distribution of TDG concentration and bubble number density. The development of a two-phase flow model for McNary dam can be found in Politano & Laughery (2010).

In this study, boundary conditions at the spillway inlet were improved and are described in detail. Please refer to Politano & Laughery (2010) for details of the remaining boundary conditions.

3.1 Numerical method

The pressure at the faces was obtained using a body force weighted scheme. The continuity equation was enforced using a Semi-Implicit Method for Pressure-Linked (SIMPLE) algorithm. A first order upwind, realizable k-ε scheme was used for the turbulent quantities in the VOF model while a Reynolds Stress model was used for the rigid-lid model turbulence. Turan et al. (2007) discovered that an anisotropic two-phase

flow model was required to accurately capture the entrainment. Furthermore, attenuation of normal fluctuations at the free surface was also necessary to predict the entrainment. A UDF was then programmed for the free surface boundary condition as FLUENT does not have a default free surface boundary condition. Standard wall functions were used for both models.

Unsteady free surface simulations were performed using variable time-step between 0.001 to 0.003 seconds. Rigid-lid simulations used a constant time step of 1 second. Typically, two to three nonlinear iterations were needed within each time step to converge all variables to a L2 norm of the error $< 10^{-3}$.

Initial conditions for the entire domain for the VOF simulations were: 1) a constant water elevation with zero velocity and turbulent quantities or 2) interpolation from similar VOF simulations with similar operating conditions. For the mixture model, first a single phase model was run and then, after convergence was obtained, bubbles were injected in the domain.

3.2 Grid Generation

All grids were generated using the commercial grid generator Gridgen. Grid points were concentrated near the top to resolve the free surface. The grids, of approximately 1.6 to 2.0 10^6 nodes, were constructed nearly orthogonal in the vicinity of the free surface to improve convergence. The domain was divided into a number of blocks and a structured mesh of hexahedral cells was generated in each block. The grids were refined the free surface and in the spillway where large accelerations were expected. An extra block at the top of the VOF grids was included to accommodate the air volume.

Grids developed in earlier studies were locally modified to incorporate the fish outfalls. Non-conformal grids were used to accommodate blocks near the outfalls in the VOF grids in order to fully capture the shape of the free surface out of the outfalls. Conformal faces were used in all rigid-lid grids.

3.3 Boundary Conditions at Spillway Inflows for the VOF Model

In earlier models, a given mass flowrate was imposed at the spillway gates assuming a uniform velocity profile. The gate opening was obtained with a rating curve. This approach resulted in an under prediction of the contraction after the gate and spillway velocities. In this study, the velocity and water depth downstream of the contraction are used as boundary conditions. Figure 3.1 shows the location of the VOF model inflow.

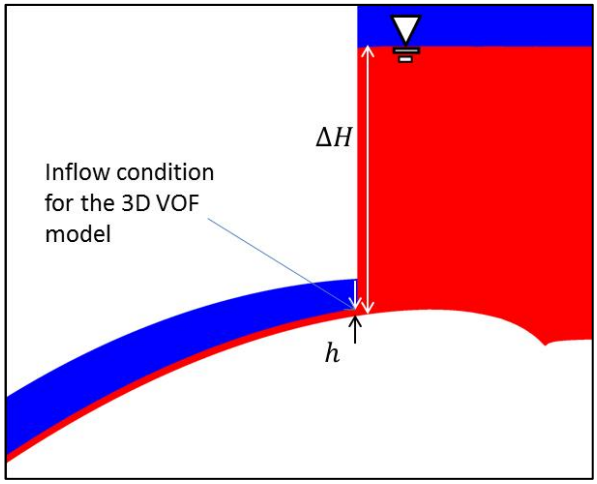

Figure 3.1 Representation of the Model Inflow for the 3D VOF Model

Assuming zero energy loss in the gate, the velocity and water depth at the model inflow can be calculated from:

$$g(\Delta H - h) = \frac{|V|^2}{2} \quad (1)$$

$$q = U\,h\,W \quad (2)$$

$$U = |V|\cos(\phi) \quad (3)$$

where|V|is the velocity magnitude, U the velocity in longitudinal direction, q the gate flowrate, ϕ the local angle of the spillway, and W is the spillway width.

3.4 Boundary Conditions for the Rigid-lid Model at Spillway Inflows

The spillway inflows in the rigid-lid model are defined as velocity inlets at about 25 ft upstream of the deflector end. The value of the velocity was obtained from a 2D VOF model. A 2D model was required for the validation because of the refinement level required for the grids. To ensure maximum accuracy, the grids used contained approximately 15,000 nodes and it would not be feasible to simulate 3D grids with this density. The 2D model includes the forebay and a 15 ft curvature radius deflector. The model was validated using deflector pressures measured in a reduced-scale laboratory model.

3.4.1 Validation of 2D Model

Details of the simulated domain together with the numerical grid and a predicted free surface are shown in Figure 3.2.A 6 ft stop condition with forebay and tailwater elevations of 340 ft and 270 ft were simulated to validate the model.

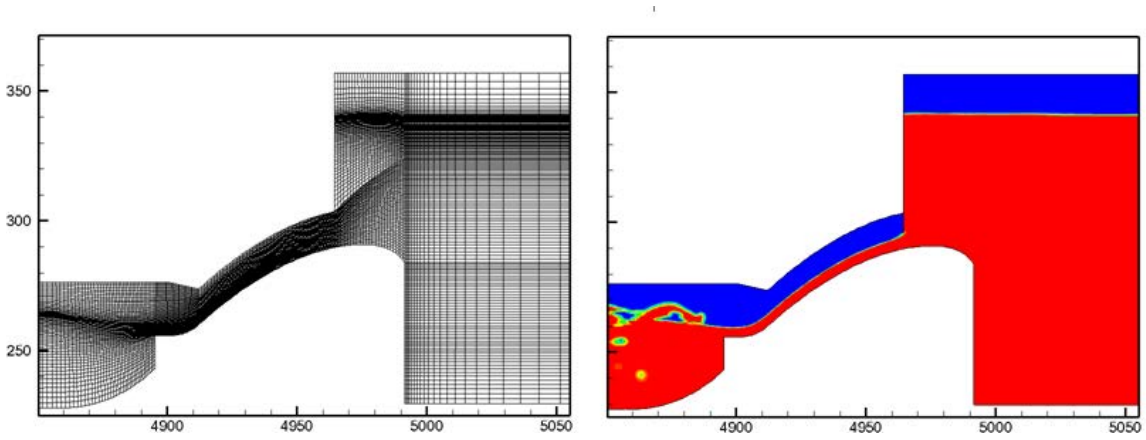

Figure 3.2 Grid and Free Surface Obtained in the Validation Case of the 2D Model

Figure 3.3 shows measured and predicted piezometric elevation contours. Symbols are colored with measured pressure and yellow boxes contain the experimental values. The bold white line represents the free surface, while the thin white lines are labeled pressure contour lines. At the most upstream point, the velocity is extracted to obtain the boundary condition for the 3D model. In this position, the difference between measurements and model prediction is about 4%. In other locations the agreement is good with exception of the downstream points. Note that near the end of the deflector, a very small offset in the experiments creates a significant measurement difference and large discrepancy with model results.

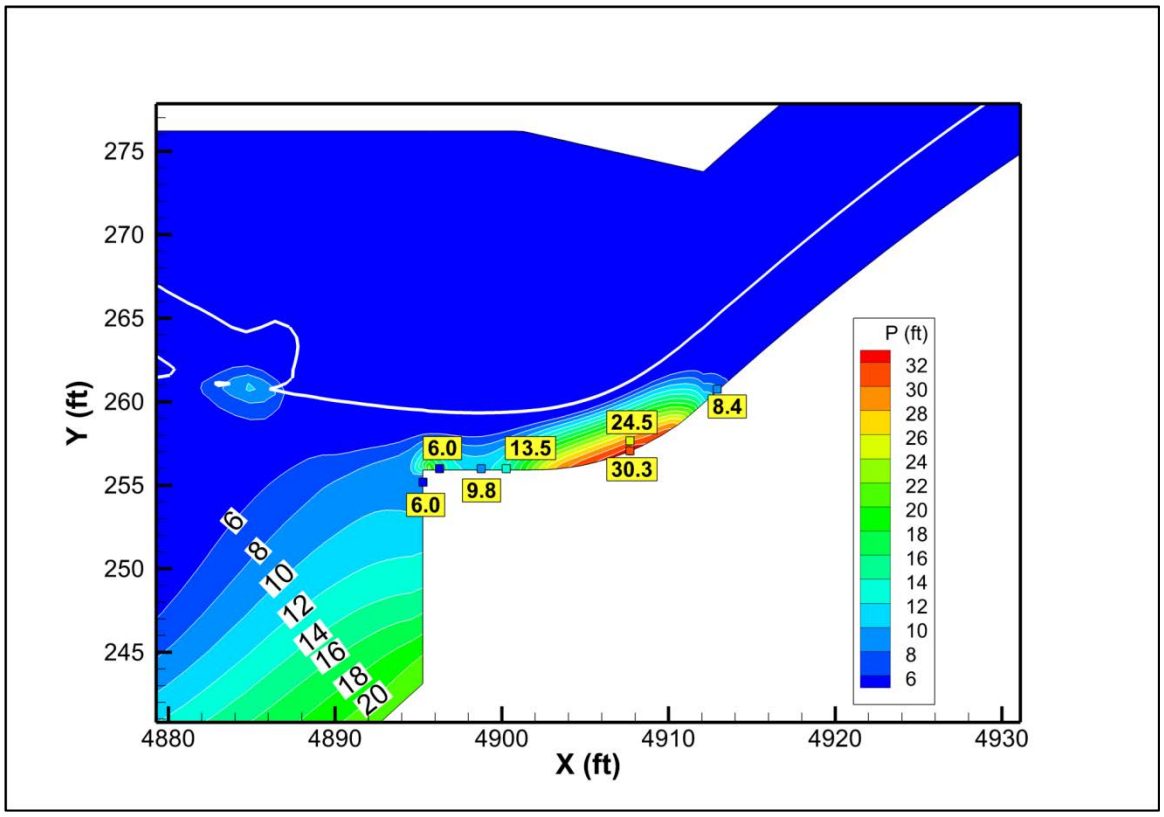

Figure 3.3 Piezometric Elevation Contours for the Validation of the 2D Model

3.4.2 Velocity Magnitude as a Function of Gate Opening

After validation, different gate openings were simulated to obtain boundary conditions for different spill operations. A forebay elevation of 338.5 ft was used for all simulations. A lower tailwater elevation of 256 ft was imposed at the outflow to avoid any influence of the hydraulics on the deflector. Figure 3.4 shows free surface elevation and contours of velocity magnitude for all the simulations. The mass weighted velocity magnitude predicted at 25 ft upstream of the deflector end, used a boundary condition for the rigid lid model, is shown in Figure 3.5 and Table 3.1.

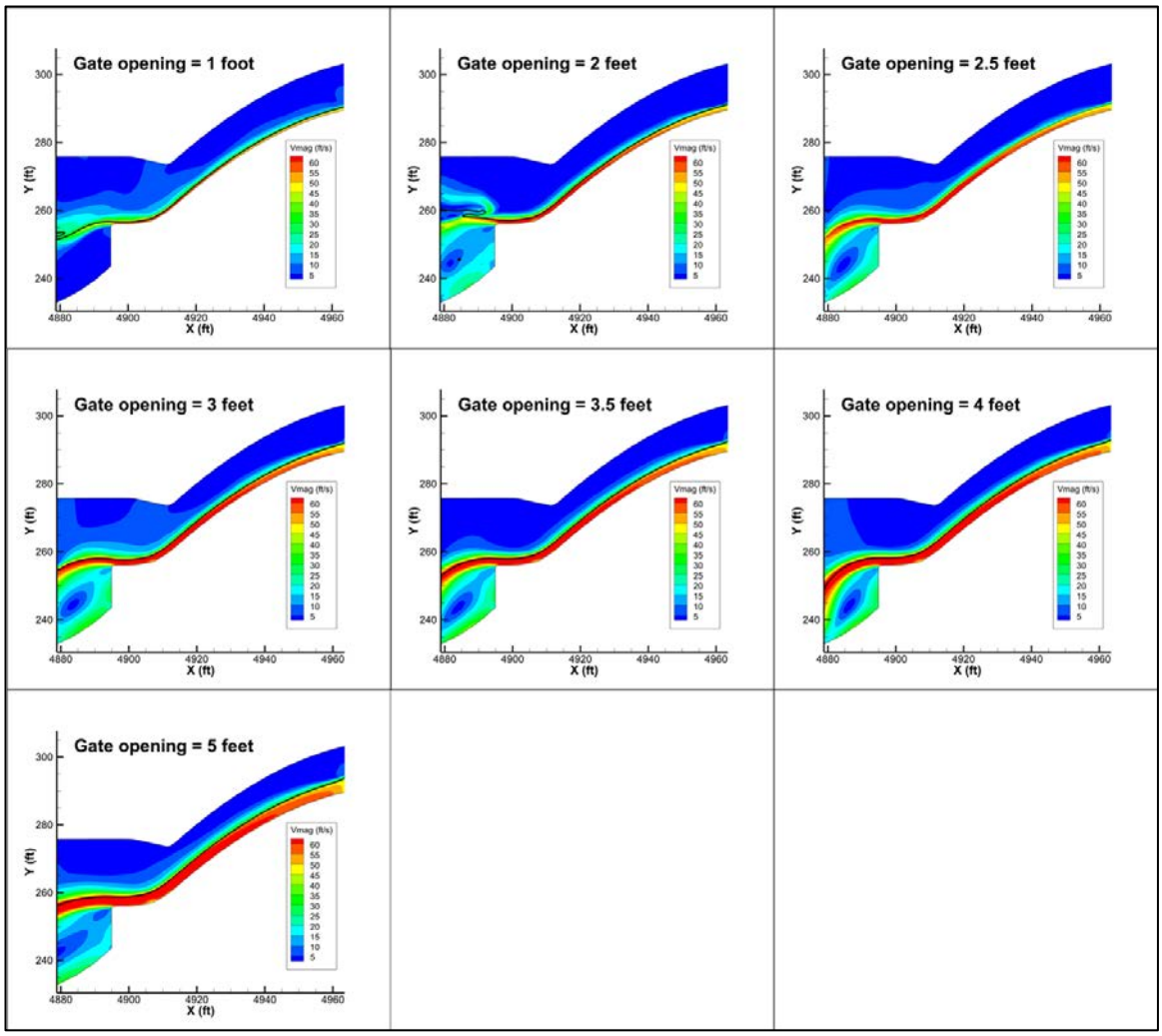

Figure 3.4 Velocity Magnitude Contours for Different Gate Openings

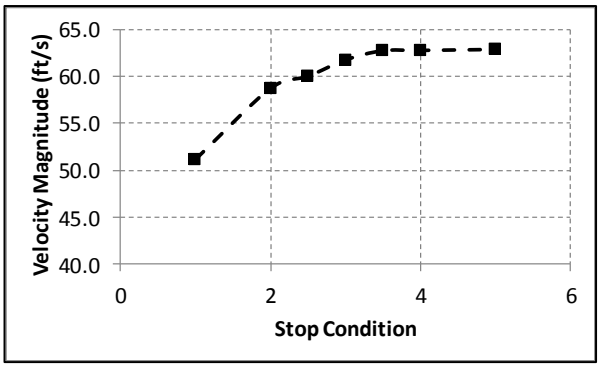

Figure 3.5 Velocity Magnitudes as a Function of Gate Opening

Table 3.1 Predicted Velocity Magnitudes to be Used at the Spillway Inflows of the 3D TDG Model

Stop	1	2	2.5	3	3.5	4	5
Velocity	51.2	58.7	60.0	61.7	62.7	62.7	62.8

3.4.3 Free Surface Shape

The free surface is obtained from the 3D VOF model of the McNary tailrace. Near the spillway inflows the free surface is adjusted to satisfy the velocity condition predicted with the 2D model.

In Figure 3.6, velocities and free surface obtained with the 2D and 3D VOF models are compared. Though the 3D model is significantly coarser than the 2D model, the velocity magnitude predicted with these models is comparable. Therefore, free surface adjustments near the model inflows were minor. Note that spillway regimes predicted with the 2D and 3D models were different. For small spillway flowrates, the 2D model the jet is unstable, oscillating between plunging and surface regimes. On the other hand, the 3D model predicts a stable surface jet due to lateral currents toward the jet region. Furthermore, the tail water elevations for the 2D simulations were below the deflector for easier convergence whereas the tail water elevations in the 3D models are above the deflector.

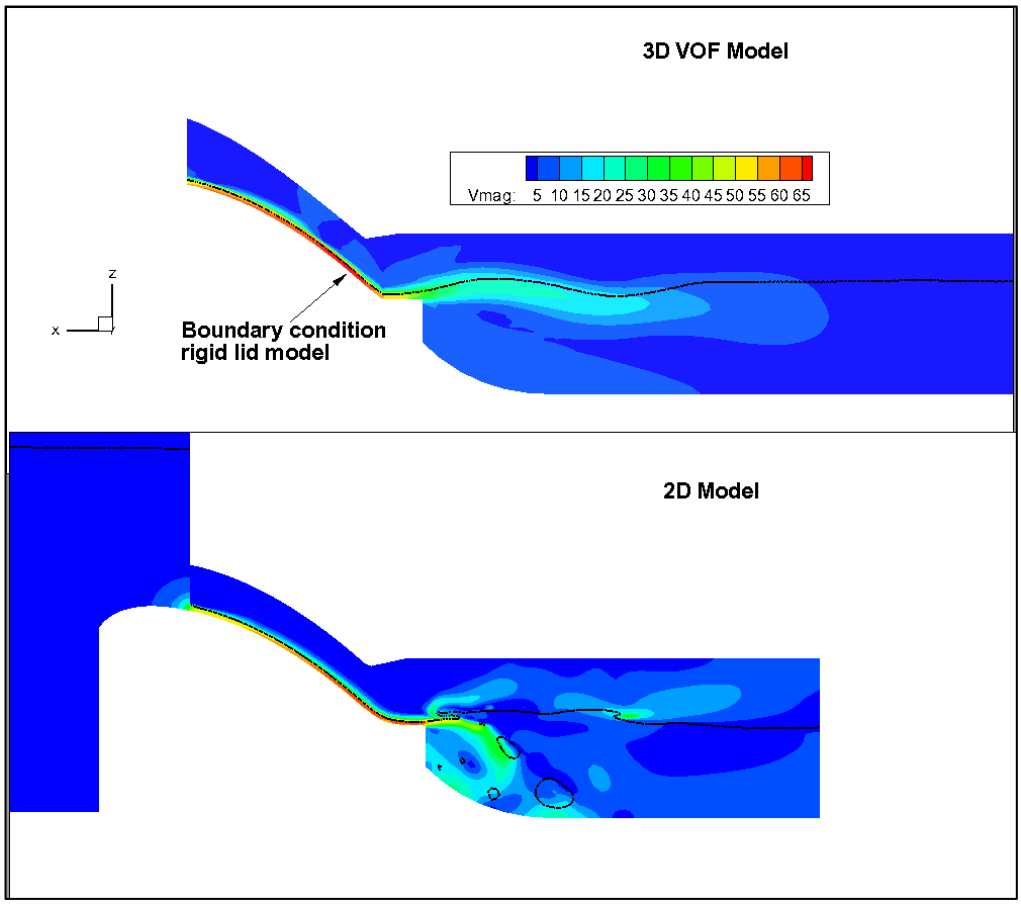

Figure 3.6 Free Surface and Velocity Magnitude Obtained with the 3D Model (top) and 2D Model (bottom)

3.5 Boundary Conditions at Bays with Temporary Spillway Weirs for the Rigid-lid Model

The model developed by Haque and Weber (2008) was used to obtain boundary conditions for spillway bays operating with temporary spillway weirs (TSW). These temporary spillway weirs are top spill weirs that can aid in fish passage. Forebay and tailrace elevations were changed to represent conditions used in this study. Figure 3.7 shows a free surface and velocity obtained with the 3D model downstream of the TSW1.

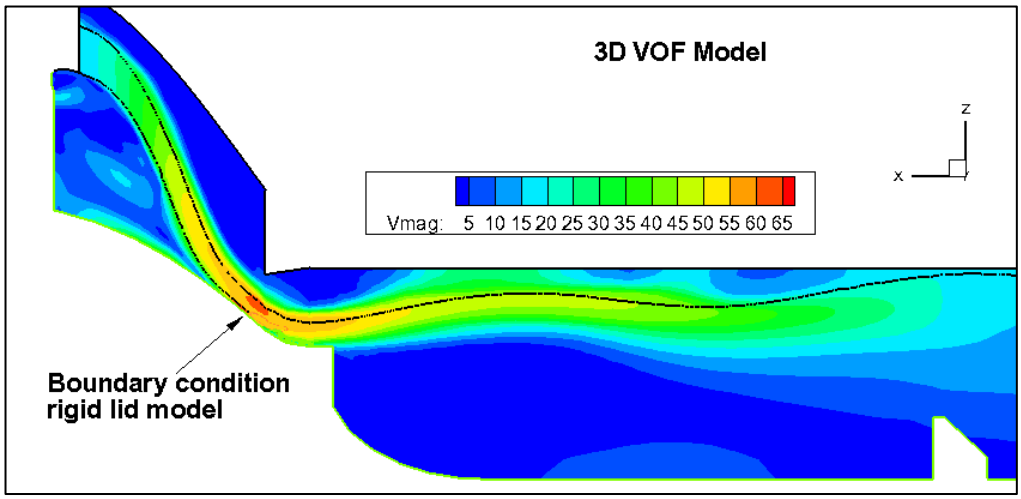

Figure 3.7 Free Surface and Velocity Magnitude Obtained with the 3D Model Downstream of TSW1.

3.6 Model Summary

Two models were used to simulate the hydrodynamics and TDG in the tailrace of McNary dam. The first VOF model utilized the SIMPLE algorithm along with a realizable k-ε turbulence model to predict the free surface shape to be used in the second model. When the VOF model had converged to a given flowrate at the outflow, the free surface was extracted as a database for the rigid-lid model. The rigid-lid model also utilized the SIMPLE algorithm, but used the Reynolds Stress turbulence model.

A new boundary condition for the spillway inflows was proposed. Two-dimensional VOF simulations were performed to validate the proposed inflow boundary conditions for the rigid-lid model. The results of the 3D simulations were comparable to the 2D simulations after applying the proposed boundary conditions.

All grids were generated using the commercial software Gridgen and consisted of structured blocks containing hexahedral cells. Appropriate refinement was used to capture areas of interest, typically with high velocities or at air/water interfaces. Non-

conforming grids were utilized when extreme levels of refinement were required to capture outfall jet shapes.

CHAPTER IV

PARTICLE TRACKING MODEL

A Lagrangian particle tracking model was used to simulate fish in the tailrace. Inert particles representing the fish were injected into the domain through the spillway and powerhouse inflows. Properties of each individual particle were tracked such as position, velocity and time spent in the domain. These properties were then used to perform a statistical analysis based on predation criteria given by USACE. Results of this model are discussed in sections 6.4 and 6.5.

4.1 Mathematical Model

The prediction of the particles trajectories is calculated integrating the Newton's law of motion on a particle:

$$\frac{d\vec{u}_p}{dt} = F_D \tag{1}$$

where F_D is the drag force per unit mass. The sub index p stands for particle and $\vec{u}$ is the velocity. For a spherical particle the equation for the drag force per unit mass reads:

$$F_D = -\frac{3}{8}\frac{\rho_l}{\rho_p} C_D \left(\vec{u}_p - \vec{u}_l\right)\left|\vec{u}_p - \vec{u}_l\right| \tag{2}$$

where ρ stands for density and the sub index l for liquid phase. The drag coefficient C_D depends on the flow regime. For a spherical particle it is given by:

$$C_D = \begin{cases} \dfrac{24}{\mathrm{Re}} & \mathrm{Re} < 0.1 \\ a_1 + \dfrac{a_2}{\mathrm{Re}} + \dfrac{a_3}{\mathrm{Re}^2} & 0.1 < \mathrm{Re} < 10000 \\ 0.4 & \mathrm{Re} > 10000 \end{cases} \tag{3}$$

where $\mathrm{Re} = \frac{\rho_l d_p \left| \vec{u}_p - \vec{u}_l \right|}{\mu_l}$, d_p is the particle diameter, μ the dynamic viscosity, and the constants a_1, a_2, and a_3 depend on the Reynolds number (Morsi and Alexander 1972).

4.2 Boundary Conditions

Particles are injected into the domain with the liquid velocity. In fish pumps and model exit an escape boundary condition is used. Particles are reflected off the free surface and all walls.

4.3 Statistical Analysis

The criteria for determining dangerous zones are again: A) flow velocities below 4 fps, B) flow depth less than 10 meters, and C) distance from shore less than 75 meters. The properties recorded for each particle were as follows: coordinate (x, y, z) velocity magnitude, x, y and z velocity components, Particle ID, TDG at current position, distances from the free surface, bottom, north and south shores and the particle residence time. Using this data, two forms of analysis were performed using Fortran codes developed for this thesis. The first was a 'met criteria' analysis. For this analysis, a particle was counted if at any point in its time in the domain it met any of the three criteria A B or C. Results are shown as averages of all particles released from spillway X or powerhouse Y. The second analysis was a time averaged analysis. Here the time particles spent meeting criteria was calculated. A time average meeting any criteria based on total residence time was then calculated. Again, the results are presented as averages of all particles released from spillway X or powerhouse Y.

4.4 Particle Tracking Model Summary

The particle tracking model was utilized to simulate fish trajectories within the tailrace. Newton's laws of motion were used to simulate the particles. Particles remained in the domain until they reached the outlet, where an escape boundary condition was used. Particles were reflected off of all other surfaces. Properties of each particle were tracked and used for a subsequent statistical analysis.

CHAPTER V

CALIBRATION AND VALIDATION OF THE 3D MODEL

5.1 Grid Sensitivity Study

The first step in the model validation was to perform a grid sensitivity study for the rigid-lid model. Three grids were generated by refining in the x, y and z directions by approximately a factor of 1.4. A non-conforming grid was also created and used the refinement near the spillways from the fine level and the remaining blocks had the same level of refinement as the medium grid. The four refinement grids were defined as coarse, with approximately 847,000 nodes, medium, with approximately 2.1 10^6 nodes, fine, 6.4 10^6 nodes and non-conforming grid with 2.5 10^6 nodes. Examples of the fine and medium grid refinements are shown in Figure 5.1.

For the sensitivity study, a less traditional method was used. Normally, the free surface would be extracted from the VOF model and used as a database to project the rigid lid grid. The actual geometry of the free surface for the rigid-lid grid is highly dependent on the grid density however; more refined grids will more accurately capture the free surface shape. Therefore, grid refinement also implies geometric changes. This posed a problem as slight changes in geometry can have large effects on spillway jet regimes and TDG production. To avoid this, the coarsest grid was projected onto the database extracted from the VOF model, and that coarse grid's surface was then extracted and used as the database for the more refined grids' free surfaces.

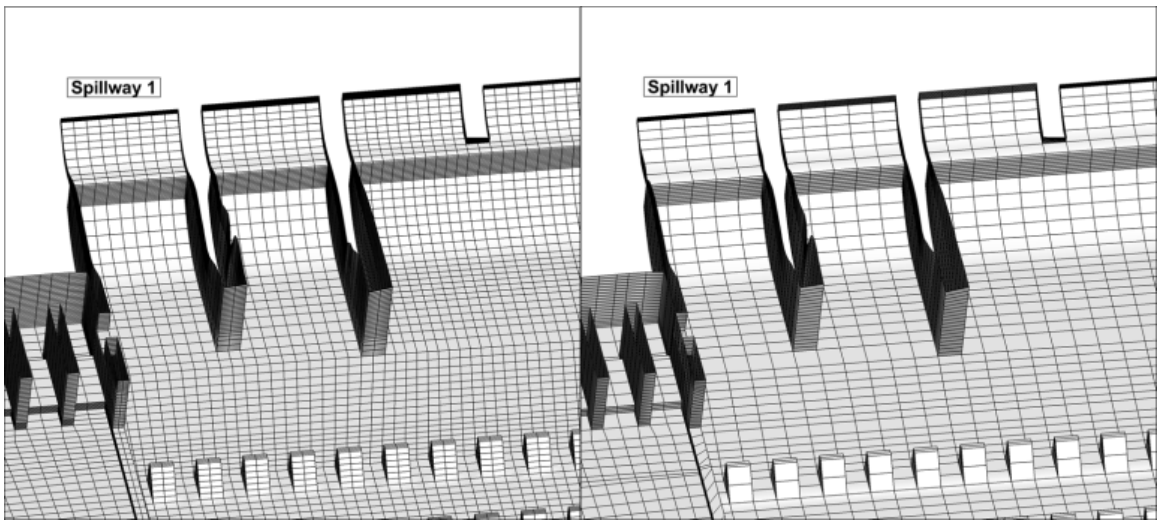

Figure 5.1 Fine (left) and Medium (right) Grids

5.2 Simulation Conditions

The new boundary conditions at the spillway inflows proposed in this thesis changed the flow pattern and TDG distribution in the tailrace. Therefore, a new calibration of the TDG model and validation of the capability of the model to predict the hydrodynamics was needed. During the calibration process, the gas volume fraction at the spillway bays were selected to match TDG field data collected in 1997 (Wilhelms and Schneider, 1997). Three gas volume fractions, $\alpha = 0.03, 0.035$ and 0.04 were evaluated. The bubble diameter, $D_d = 0.8mm$, was the same as used in Politano et al. (2009). The gas volume fraction used in the grid sensitivity study was 0.03. Velocity collected in 2004 (Wilhelms, 2005) was used to validate the hydrodynamics. Table 5.1 are the operational conditions for the spillways and powerhouses for the grid sensitivity study. The operational conditions used for the validation of the model are shown in Table 5.2. Additional operational conditions are as follows. The forebay and tailwater elevations were 338.5 ft and 266.3 ft. The North shore fish entrance was operating at 1 kcfs at 8 ft

deep. Two South gates of the North powerhouse fish entrance were operating at 1 kcfs at 9 ft deep. Both gates of the South powerhouse fish entrance were operating at 1 kcfs at 9 ft deep. Fish pumps were pulling 5 kcfs of water and the South station service outlet was operating with 0.6 kcfs.

All simulations were run on a Dell PowerEdge 7500 with the following specifications: 4 socket 8 core Intel(R) Xeon(R) CPU X7560 @ 2.27GHz – 32 cores total 128GB of RAM 500GB SAS Raid 5 disk space and the Redhat Enterprise Linux 5.5 operating system. VOF operations running with 32 cores took between two and three weeks of computational time to reach convergence while rigid-lid simulations generally were run with 16 processors and took 3 to 4 days to reach convergence.

Table 5.1 Operational conditions used for calibration of the TDG model

Jun. 4, 2004														
Total River Flow: 278.0 kcfs - Tailwater Elevation: 266.9 ft														
Powerhouse Unit Discharge (kcfs)														
Total	**U1**	**U2**	**U3**	**U4**	**U5**	**U6**	**U7**	**U8**	**U9**	**U10**	**U11**	**U12**	**U13**	**U14**
	11.9	12.1	12.0	11.9	12.1	11.9	11.9	12.0	12.1	12.2	12.0	11.9	12.0	12.1
North	**U1**	**U2**	**U3**	**U4**	**U5**	**U6**	**U7**	**U8**	**U9**	**U10**	**U11**	**U12**	**U13**	**U14**
Unit	5.95	6.05	6.0	5.95	6.05	5.95	5.95	6.0	6.05	6.1	6.0	5.95	6.0	6.05
South	**U1**	**U2**	**U3**	**U4**	**U5**	**U6**	**U7**	**U8**	**U9**	**U10**	**U11**	**U12**	**U13**	**U14**
Unit	5.95	6.05	6.0	5.95	6.05	5.95	5.95	6.0	6.05	6.1	6.0	5.95	6.0	6.05
Powerhouse Total: 168.1 (kcfs)														
Spillway Unit Discharge (kcfs)														
	S1	**S2**	**S3**	**S4**	**S5**	**S6**	**S7**	**S8**	**S9**	**S10**	**S11**			
	5.5	8.8	10.8	5.6	5.6	4.9	5.0	3.9	4.0	4.0	5.4			
	S12	**S13**	**S14**	**S15**	**S16**	**S17**	**S18**	**S19**	**S20**	**S21**	**S22**			
	0.0	5.6	5.4	5.6	5.7	5.5	5.5	5.4	3.9	4.0	5.0			
Spillway Total: 109.9 (kcfs)														

Table 5.2 Operational conditions used for validation of the TDG model

Feb. 12, 1997														
Total River Flow: 227.3 kcfs - Tailwater Elevation: 267.6 ft														
Powerhouse Unit Discharge (kcfs)														
Total	U1	U2	U3	U4	U5	U6	U7	U8	U9	U10	U11	U12	U13	U14
	16.1	16.1	16.1	16.1	16.1	16.1	16.1	16.1	16.1	16.1	16.1	16.1	16.1	0
North	U1	U2	U3	U4	U5	U6	U7	U8	U9	U10	U11	U12	U13	U14
Unit	8.05	8.05	8.05	8.05	8.05	8.05	8.05	8.05	8.05	8.05	8.05	8.05	8.05	0
South	U1	U2	U3	U4	U5	U6	U7	U8	U9	U10	U11	U12	U13	U14
Unit	8.05	8.05	8.05	8.05	8.05	8.05	8.05	8.05	8.05	8.05	8.05	8.05	8.05	0
Powerhouse Total: 177.1 (kcfs)														
Spillway Unit Discharge (kcfs)														
	S1	S2	S3	S4	S5	S6	S7	S8	S9	S10	S11			
	3.9	5.0	3.8	3.8	3.8	3.8	5.5	5.5	5.5	5.5	5.5			
	S12	S13	S14	S15	S16	S17	S18	S19	S20	S21	S22			
	5.5	5.5	5.5	7.1	5.5	5.5	3.8	3.8	1.4	5.0	5.0			
Spillway Total: 100.2 (kcfs)														

5.3 Model Results

5.3.1 Grid Sensitivity Study

5.3.1.1 Hydrodynamic Validation

In 2004, the USACE performed a field study in support of the McNary General Model Investigation to obtain velocity data within the tailrace. Acoustic Doppler Current Profiles were used to measure the velocities in two regions of the dam: downstream of the powerhouses and at the downstream end of the navigation lock. These velocities are detailed in the Wilhelms, S.C. (2005) and were used for comparison with the numerical model developed for this thesis. Figure 5.2 was taken from the Memorandum and displays the velocities measured by the USACE.

Similarly, in 1997 a TDG study was performed to determine TDG levels in the McNary dam tailrace. Thirty four remote logging instruments were used in an area extending to 1,000 feet downstream of the spillway to record TDG data at regular intervals. The study was able to determine TDG gradients in the lateral and longitudinal

direction, as well as the vertical direction. A detailed report of the investigation can be found in Wilhelms, S.C., and Schneider M.L. (1997). Figure 5.3 shows the instrument locations and bathymetry data for the study.

Figure 5.2 Measured Velocities in 5 transects of McNary Tailrace

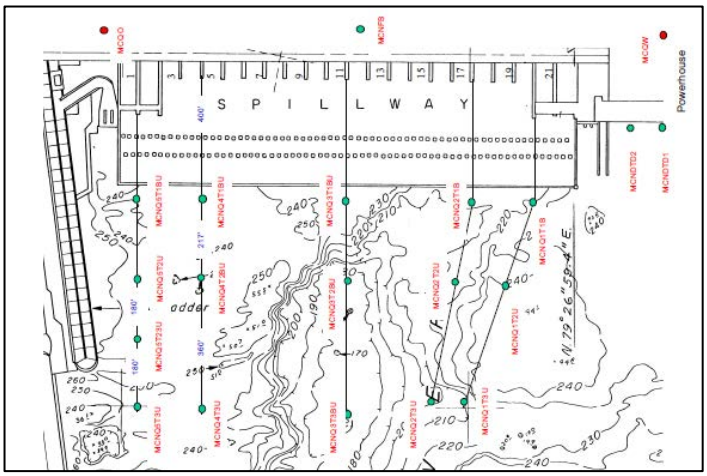

Figure 5.3 Locations of TDG Measuring Instruments and Bathymetry Data

Figure 5.4 displays the regions in the tailrace for the six transects downstream of the powerhouse near the dam. The comparisons of depth-averaged velocity data collected in the field and those predicted by the rigid-lid model for the six transects, A-F, are presented in Figures 5.5-5.10. Reasonable agreement is observed between field data and model predictions of the velocity vectors near the dam. The water entrainment is noted in Transect A near the trash sluiceway. Though at this location field data may be affected by turbulent and unsteady flows, the flow of water from the powerhouse into the spillway region is clearly observed. A very noticeable difference in the velocities near the navigation lock is observed in Figure 5.10. The Army Corps noted that it is difficult to accurately measure bathymetry near structures such as the navigation lock. Due to the imprecise measurements, the bathymetry here does could not be extended as deep as the actual river thus producing a much higher velocity in the region.

Little difference in velocities is seen when comparing the results from the various grids. The effect of grid refinement on the results will be discussed in detail later in this chapter.

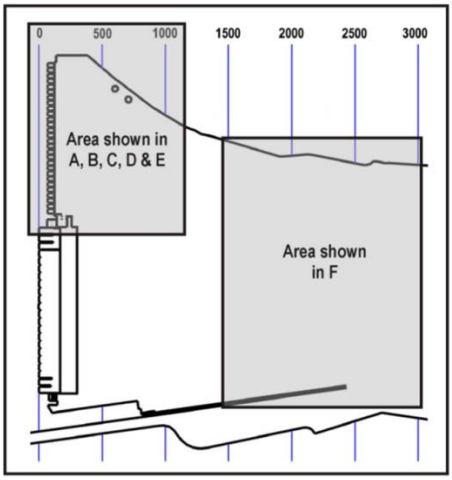

Figure 5.4 Regions of the six transects for June 4, 2004

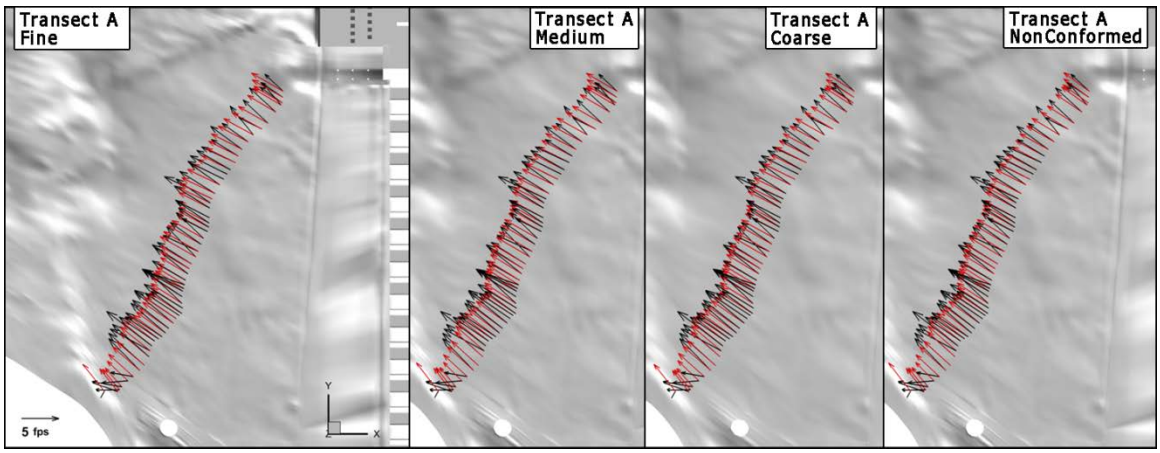

Figure 5.5 Predicted (red) and measured (black) velocity vectors on June 4, 2004 for transect A

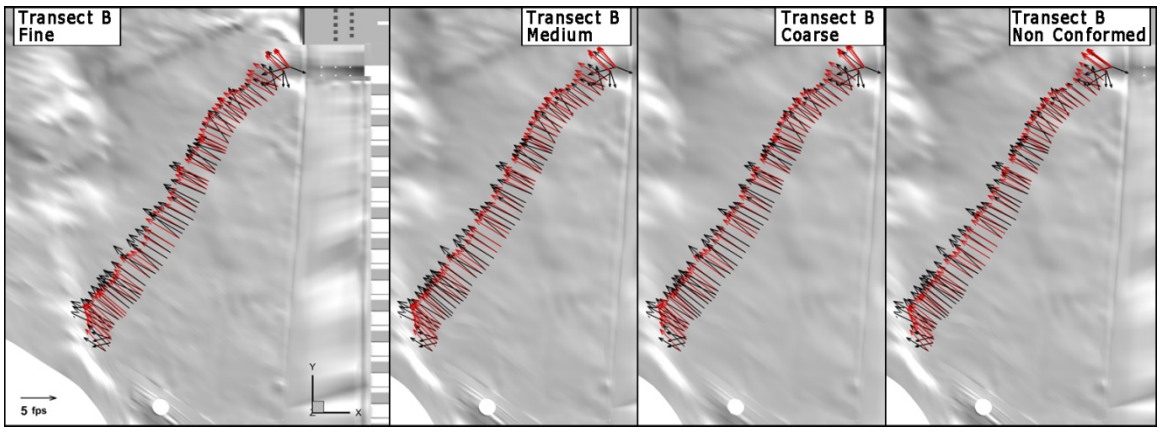

Figure 5.6 Predicted (red) and measured (black) velocity vectors on June 4, 2004 for transect B

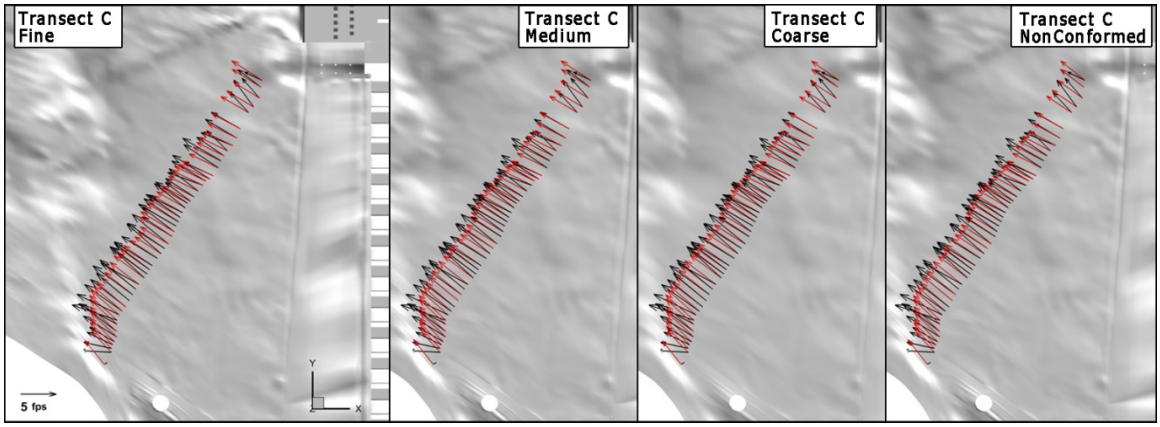

Figure 5.7 Predicted (red) and measured (black) velocity vectors on June 4, 2004 for transect C

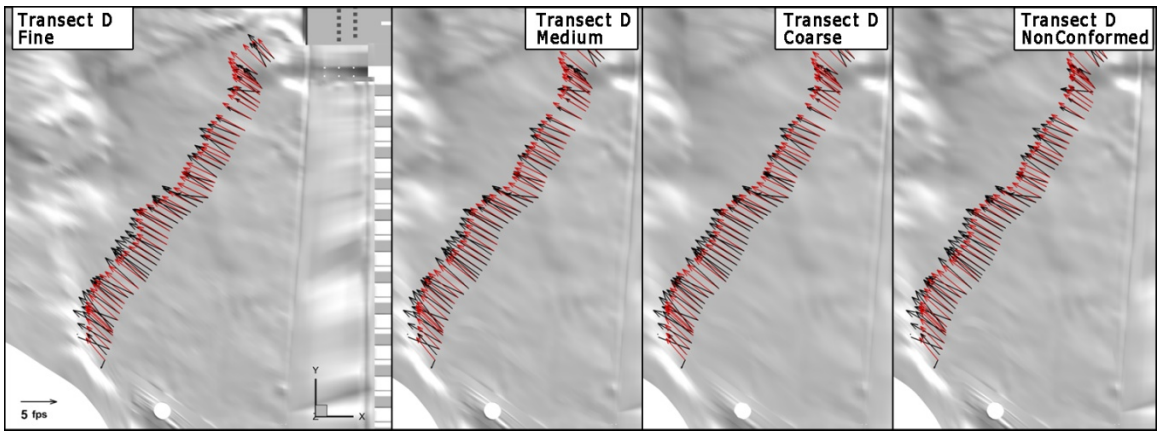

Figure 5.8 Predicted (red) and measured (black) velocity vectors on June 4, 2004 for transect D

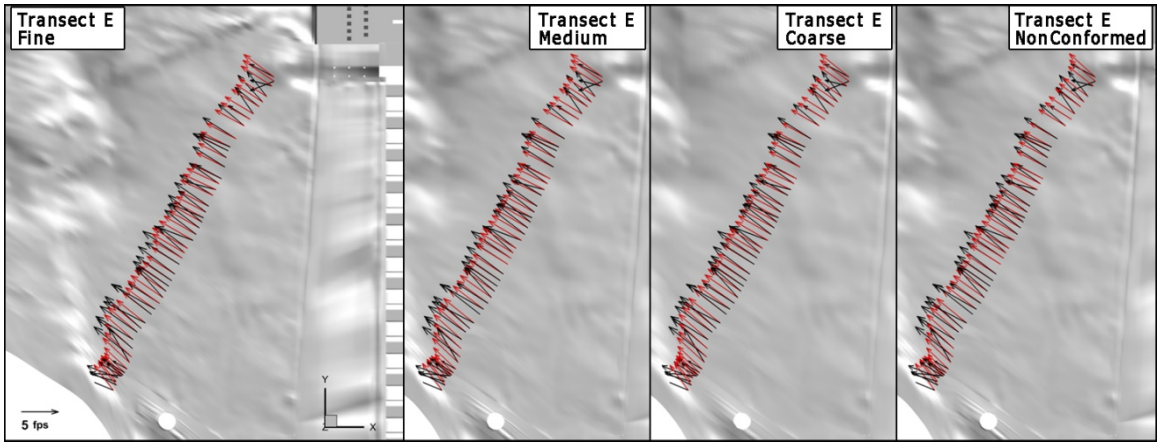

Figure 5.9 Predicted (red) and measured (black) velocity vectors on June 4, 2004 for transect E

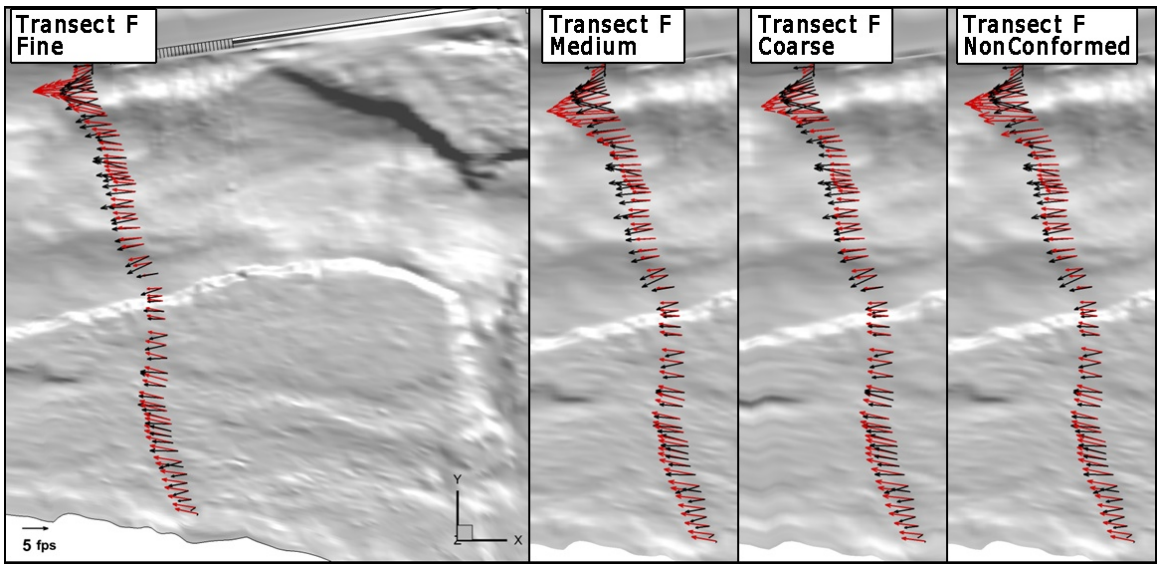

Figure5.10 Predicted (red) and measured (black) velocity vectors on June 4, 2004 for transect F

Figures 5.11 to 5.16 show field data and velocities predicted by the model. Dotted green lines represent the averaged measured velocity magnitude. Solid green lines indicate velocity magnitude within ±10% error, assuming that the field data present zero deviation. The four grids are also represented with colored solid lines. The x-axis variable "Distance" is a measurement from the beginning of the transect to the south shore of the river for figures5.11, 5.13 and 5.15. For figures 5.12 and 5.14 the distance labeled "0" is at a point in the middle of the domain and as the numbers approach 1000, the data is collected closer to the south shore. Therefore, the important regions near the sluiceway where entrainment is expected, are for figures 5.10,12 and 14 near distance = 1000, while for figures 5.12 and 5.14 these regions are where distance = 0. In the case of Figure 5.16, the distance is measured from the north shore. The velocity near the navigation lock

(Distance 0 – 100m) is again noticeably higher as shown in Figure 5.16. Reasonable agreement is observed between measured and predicted velocity vectors near the dam, however as the refinement of the grid increases, velocities do not appear to be converging to the field data.

There are many explanations for this. One reason known to the author is the difference in free surface elevation between the model and the actual river. The model controls the free surface elevation via a hydrostatic pressure condition at the outlet. The river elevation is measured near the southern end of the powerhouse. To ensure the model had the same exact free surface elevation as the river, an iterative process would be required. After convergence, velocities would be compared and adjustments to the hydrostatic pressure condition would be made and a new VOF simulation would be required to generate a new surface. This iterative process would continue until the free simulated free surface at the measurement station is the same as the measured free surface. As a VOF simulations currently require between 2 and 3 weeks of computing time, this scenario is not feasible with current computer resources. Imposing the elevation at the outflow resulted in free surfaces higher than at the river, thus the simulations consistently under predicted the velocities.

Another issue is one discussed previously. Grid geometries are dependent on the grid densities. A refined grid will be able to more accurately capture shapes in the river bed than a coarser grid. The shape of the bathymetry has a profound effect on the local velocity, as seen near the navigation lock where the bathymetry is known to be inaccurate. Two scenarios occur in this situation. The first, which the author does not believe to be the problem, is that a grid of proper refinement has not yet been created or

that the refinement of the grid did not help. If this was the issue, it would be one that cannot be addressed as resources to simulate further refined grids are not available at this time. A second scenario is that the current level of refinement captures more of the noise than the signal. That is, there are errors in the measurement of the bathymetry, and a super-fine grid would "more accurately" capture these errors which would then result in a predictive simulation that suffers from over fitting. These issues, coupled with the geometric changes with varying grid refinement explain why no convergence is seen with increasing refinement levels.

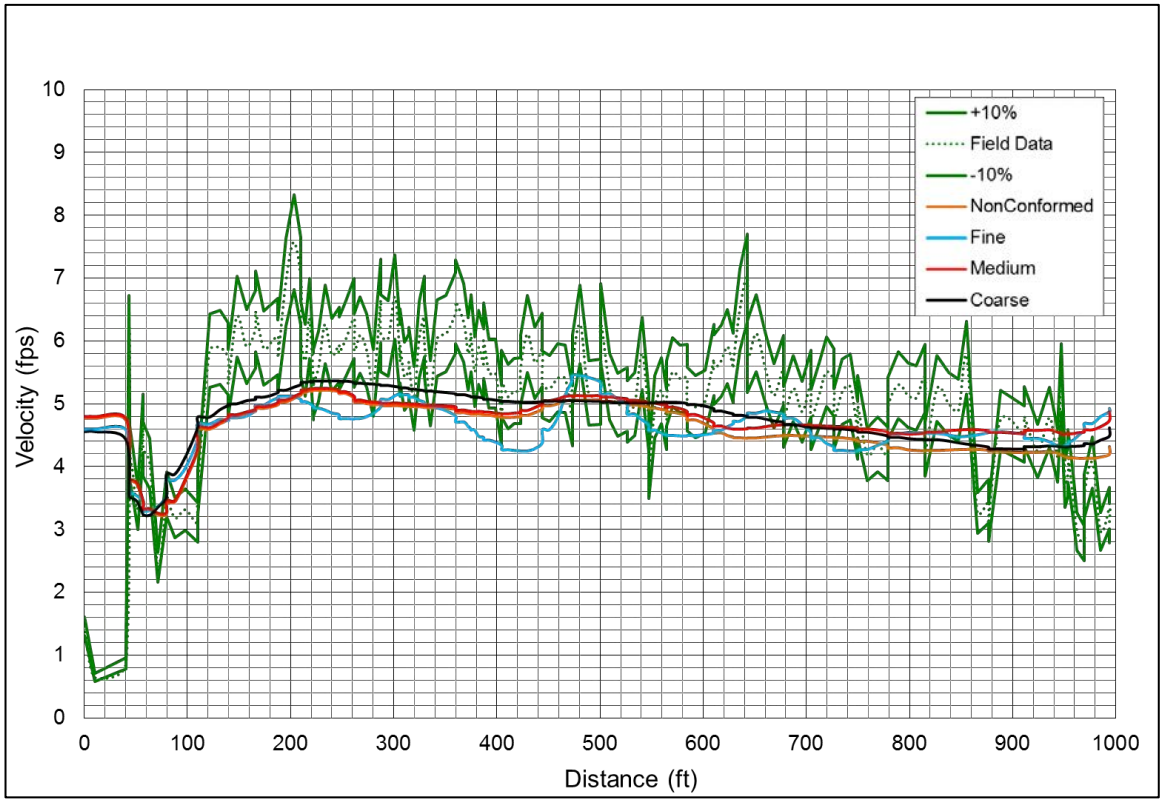

Figure 5.11 Comparison between field data and CFD results at Transect A for June 4, 2004

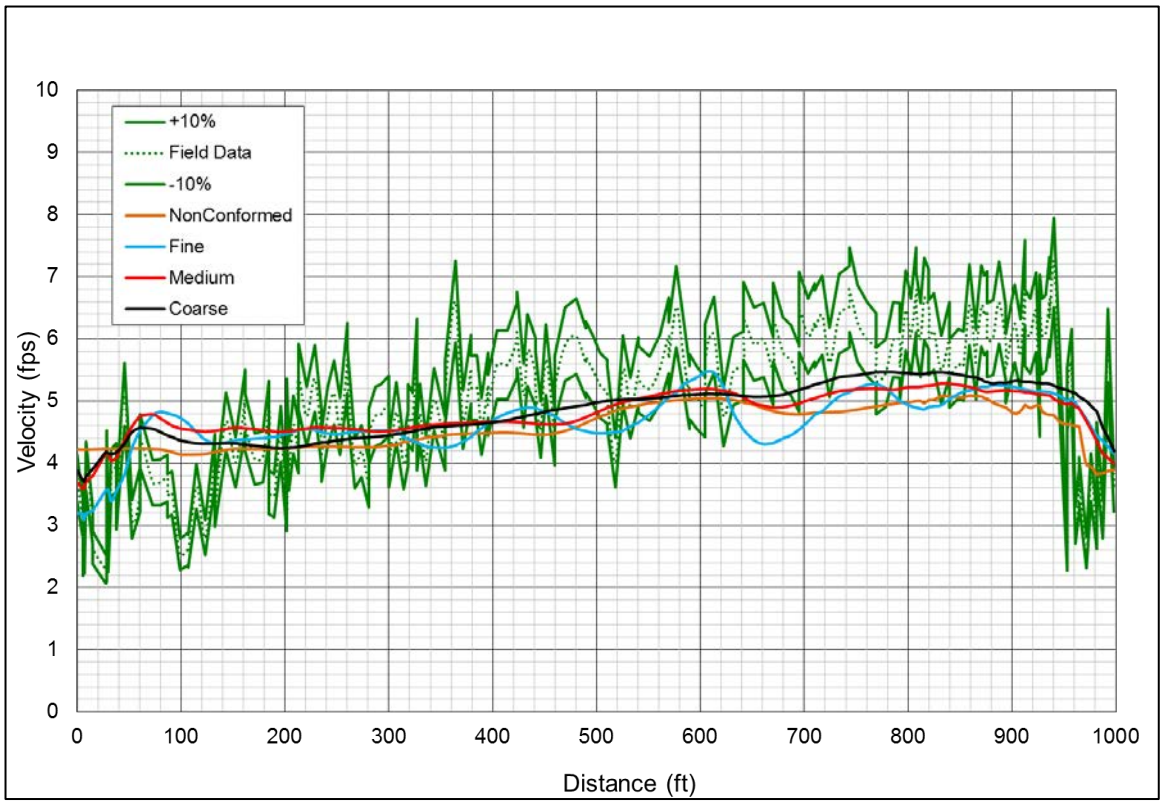

Figure 5.12 Comparison between field data and CFD results at Transect B for June 4, 2004

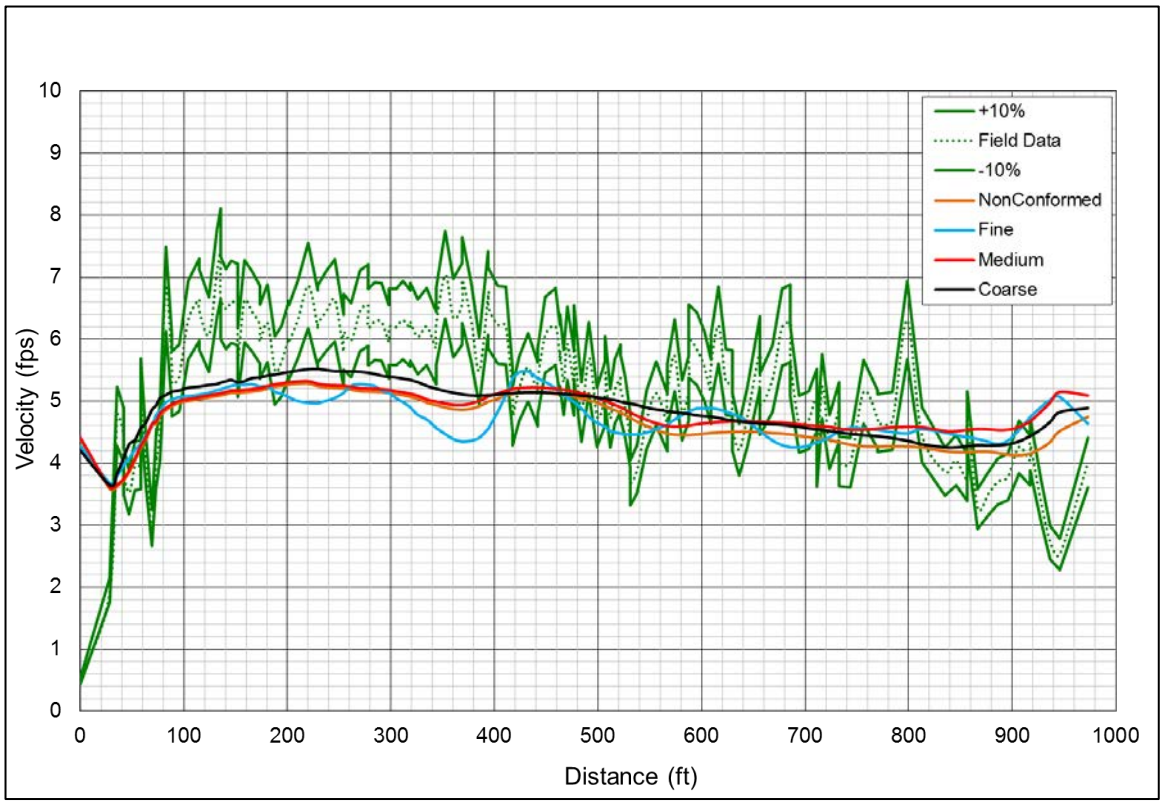

Figure 5.13 Comparison between field data and CFD results at Transect C for June 4, 2004

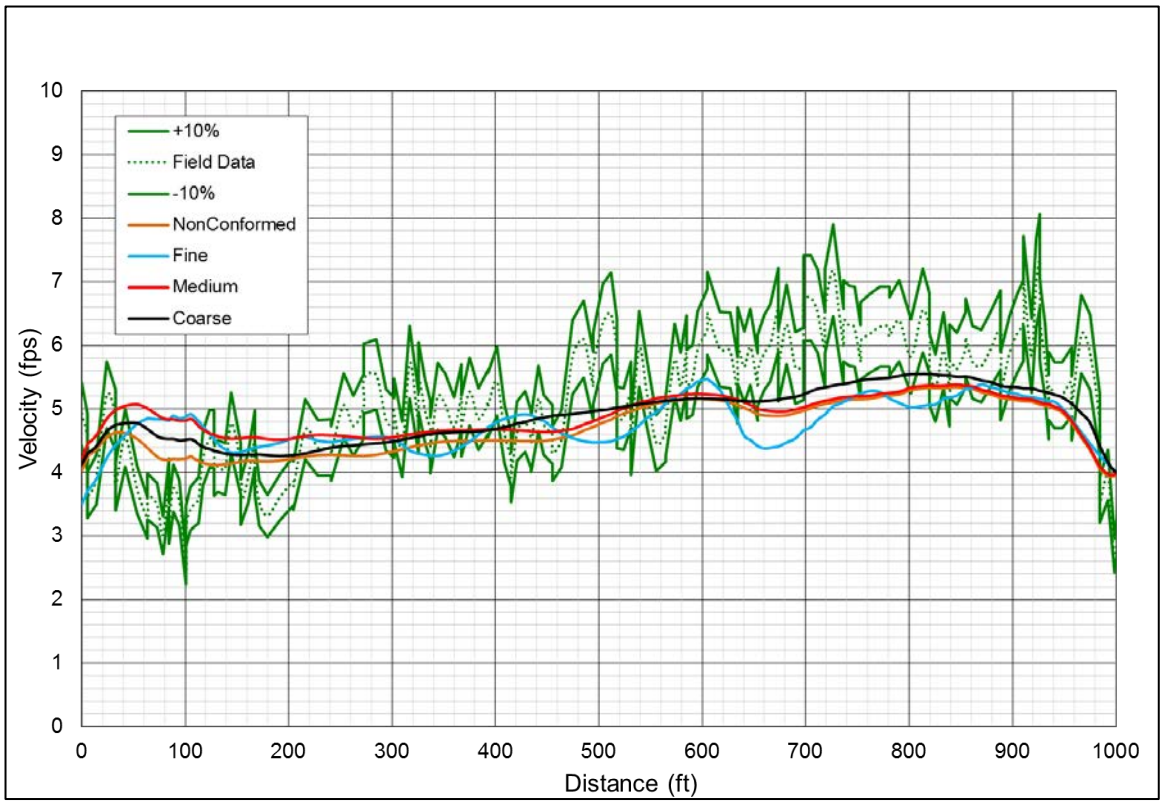

Figure 5.14 Comparison between field data and CFD results at Transect D for June 4, 2004

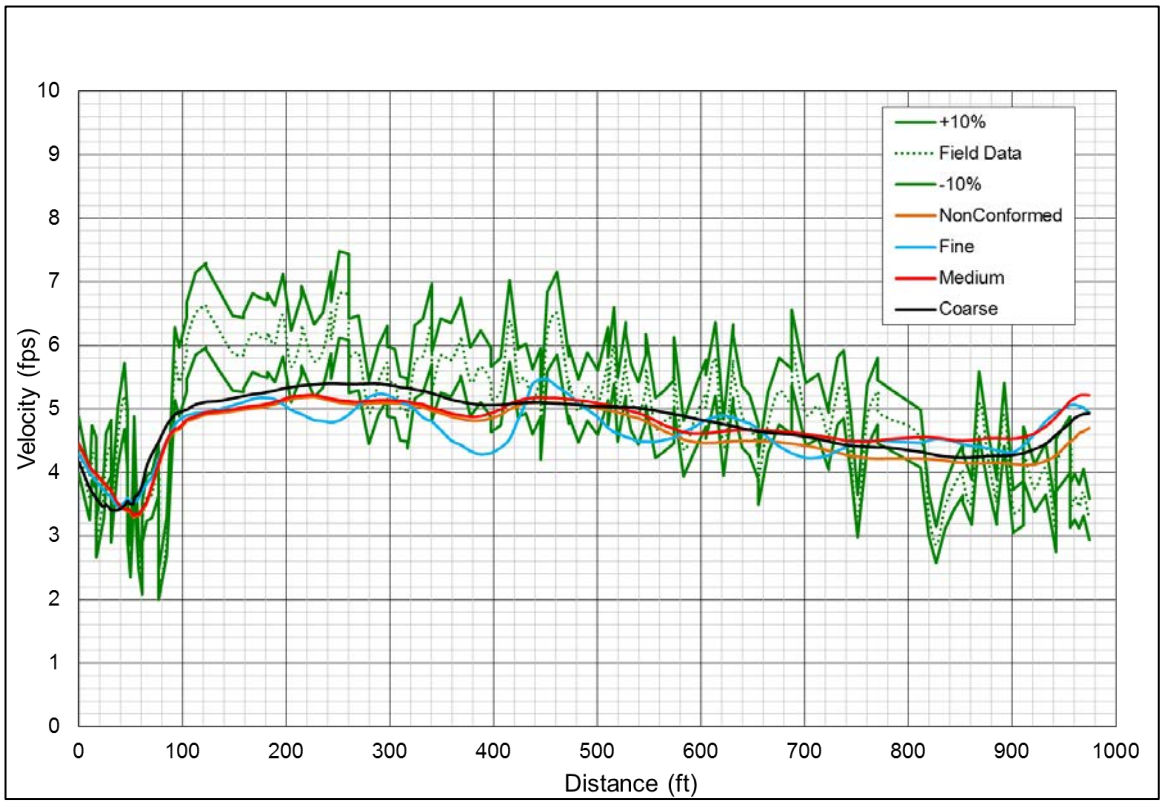

Figure 5.15 Comparison between field data and CFD results at Transect E for June 4, 2004

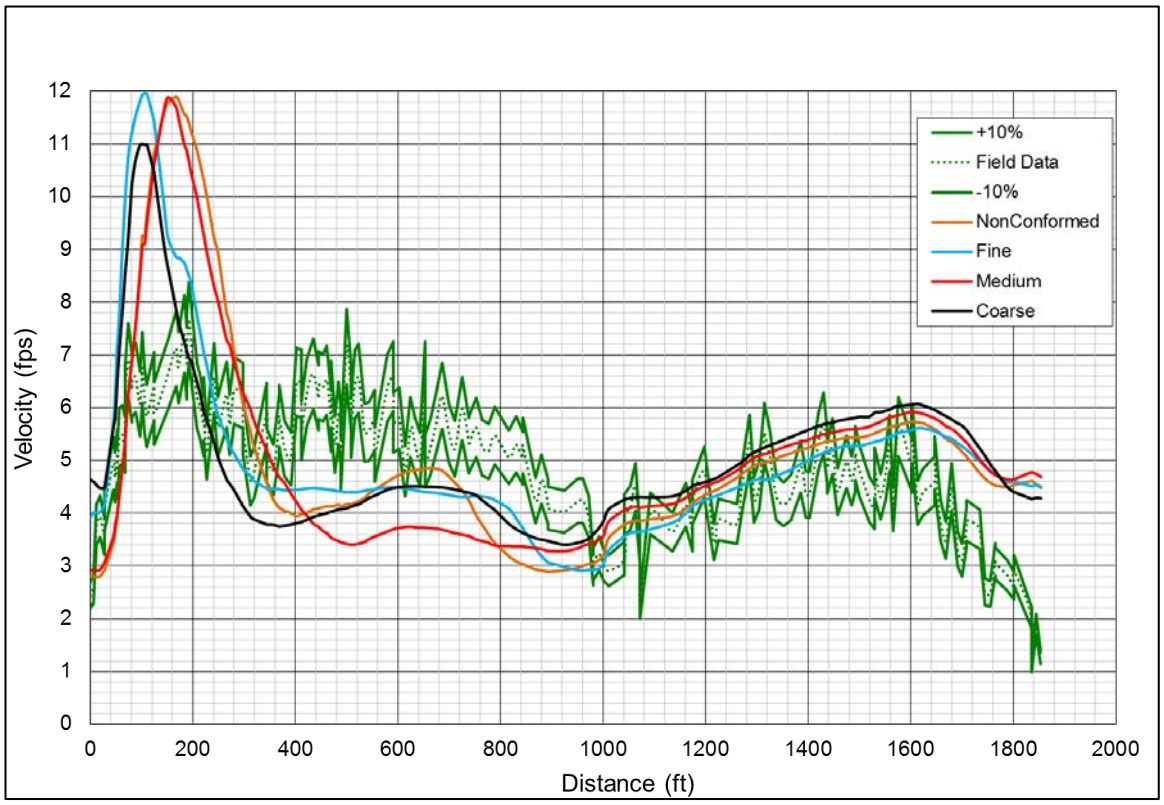

Figure 5.16 Comparison between field data and CFD results at Transect F for June 4, 2004

The effect of grid refinement on TDG production and distribution was also considered. Figure 5.17 shows plots of TDG for the four grids. TDG averages were computed at two transects and the outlet as shown in the figure. Table 5.3 shows the computed averages for all four grids' transects and outlet. TDG differences at the outlet were within 1.435% for the four grids. Slight differences in TDG can be attributed to the minor differences in geometry which have an effect on the type of spillway jet that is formed.

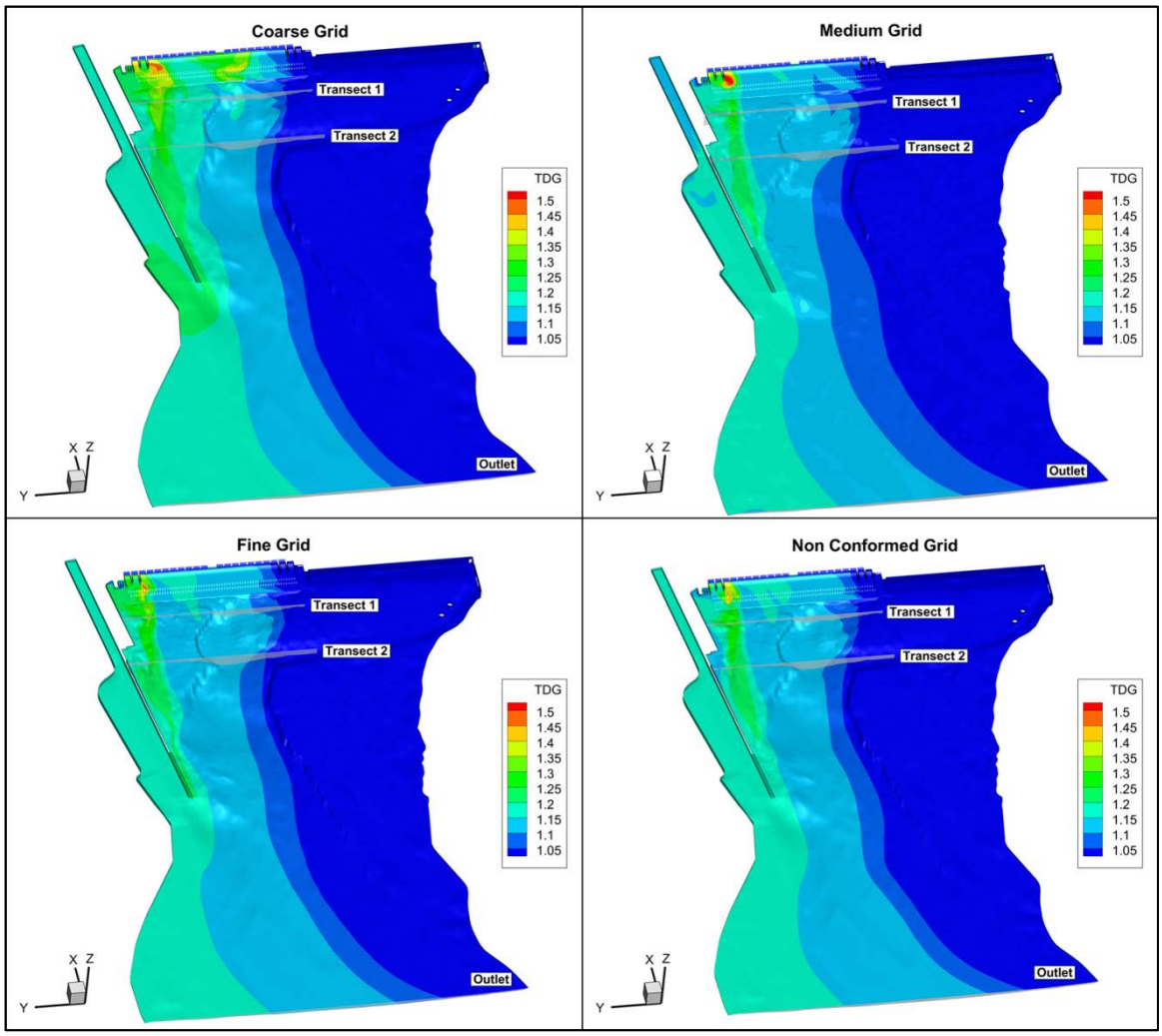

Figure 5.17 TDG Distribution for the Four Grids

Table 5.3 TDG Averages for Four Grids

TDG Average				
Transect	Coarse	Medium	Fine	NonConform
1	1.139	1.111	1.120	1.123
2	1.115	1.094	1.105	1.106
Outlet	1.115	1.099	1.108	1.113

Figure 5.18 shows slices of gas volume fraction (phase 3) with velocity vectors and TDG for the Fine, Medium and Coarse grids in spill bay #11. In the top half of the

figures, the spillway jet can be seen. For the Fine and Medium grids, a surface jet is created, and the bubbles stay near the free surface. The coarse grid predicts more plunging flow which creates a large recirculation just downstream of the deflector. This plunging flow carries bubbles to depth and produces more TDG than the surface jets as seen in the bottom figures. Velocity vectors are interpolated onto uniform planes to enhance visualization.

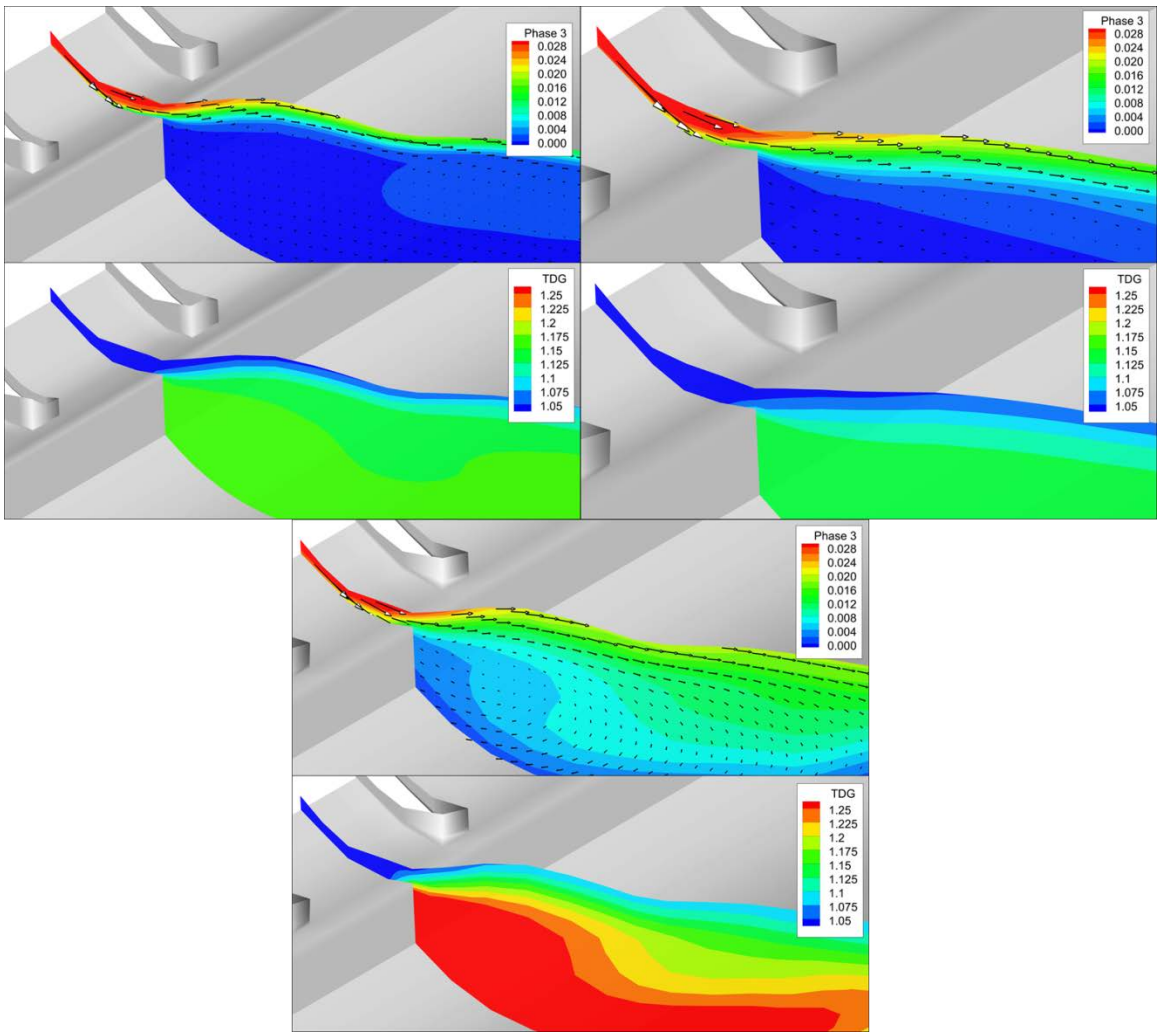

Figure 5.18 Slices Contoured by Gas Volume Fraction (top) and TDG (bottom) for the Fine (left) Medium (right) and Coarse (bottom) grids

5.3.1.2 TDG Validation

After analysis of the grid sensitivity study, the medium grid was selected to perform the TDG comparison. This selection was made because the medium grid, while not having the highest resolution, still accurately replicated the experimental data considering the computational cost of the larger grids. The gas volume fraction that resulted in the smallest difference between predicted and measured averaged TDG was $\alpha = 0.03$. Figure 5.19 shows measured and predicted TDG values at each TDG sensor location. In yellow boxes are the names of sensors and measured TDG data. Contour lines with labels show predicted TDG. The percent saturation of TDG measured in the field at each station and the mean TDG in each of the three transects are shown in Table 5.4. The same table displays predicted values with old and current models. The average errors in transects T1, T2 and T3 with the current model were of -0.3%, 0.5% and 2.3%, respectively.

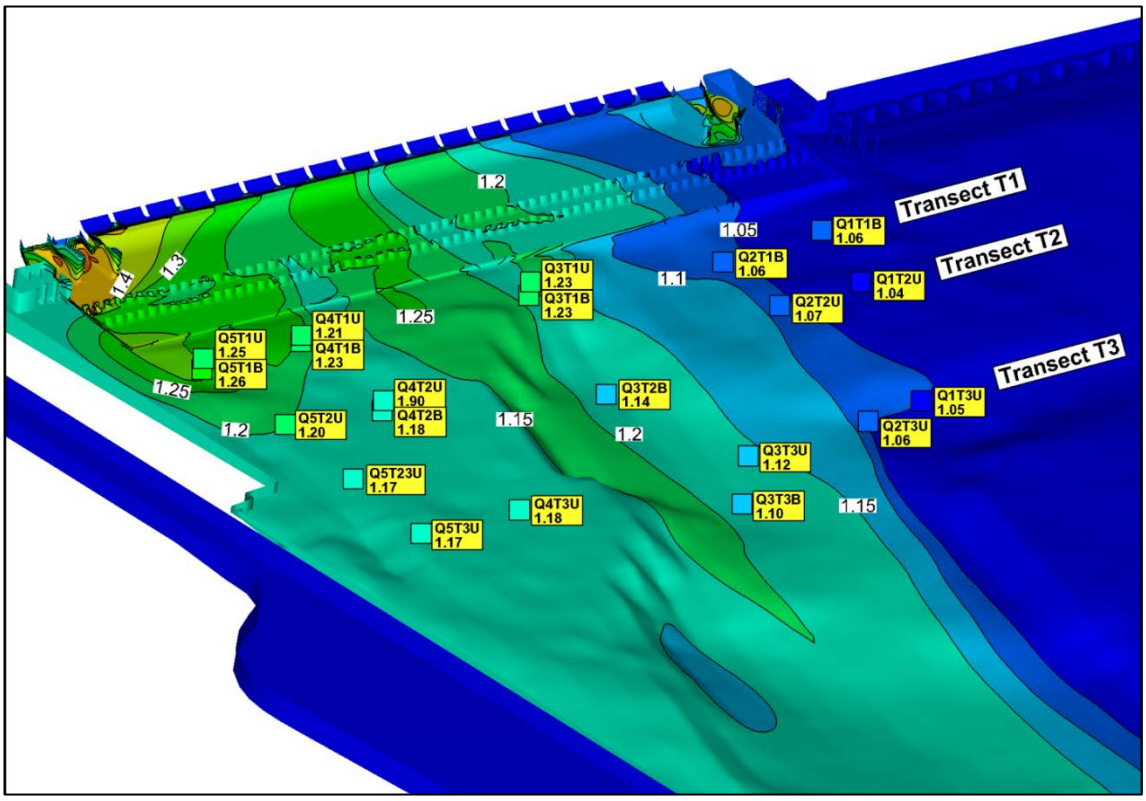

Figure 5.19 Contours of predicted TDG at the river bed and walls. Symbols and yellow labels show field data

The latitudinal TDG gradient is the result of high TDG production in spillway bays 1 and 2, and the entrainment of the low-saturated water from the powerhouse regions. The high production in spillway bays 1 and 2 is caused by a few factors: flowrates for these two bays are high which will increase TDG production, and the walls around the bays encase the jets causing them to plunge and produce more TDG.

Two factors cause the longitudinal TDG gradient. As the bubbles flow downstream, they begin to rise toward the free surface. During this time, mass is transferred from the liquid phase back into the bubbles, reducing TDG levels. Mass is also transferred from the liquid phase at the free surface and out of the domain further reducing TDG levels in the longitudinal direction. In this model, only pressure forces

and bubble dissolution affect the size of the bubbles. The more complex phenomena of breakup and coalescence is not taken into account for this thesis.

Figure 5.20 shows isosurfaces of bubble diameter and gas volume fraction. In the top figure, showing bubble diameter, the effect of large bubbles leaving the domain faster than the small bubbles is evident; further downstream of the spillway only the smallest diameter bubbles remain. The bottom figure of gas volume fraction illustrates the effect of bubbles leaving the domain, lowering TDG levels.

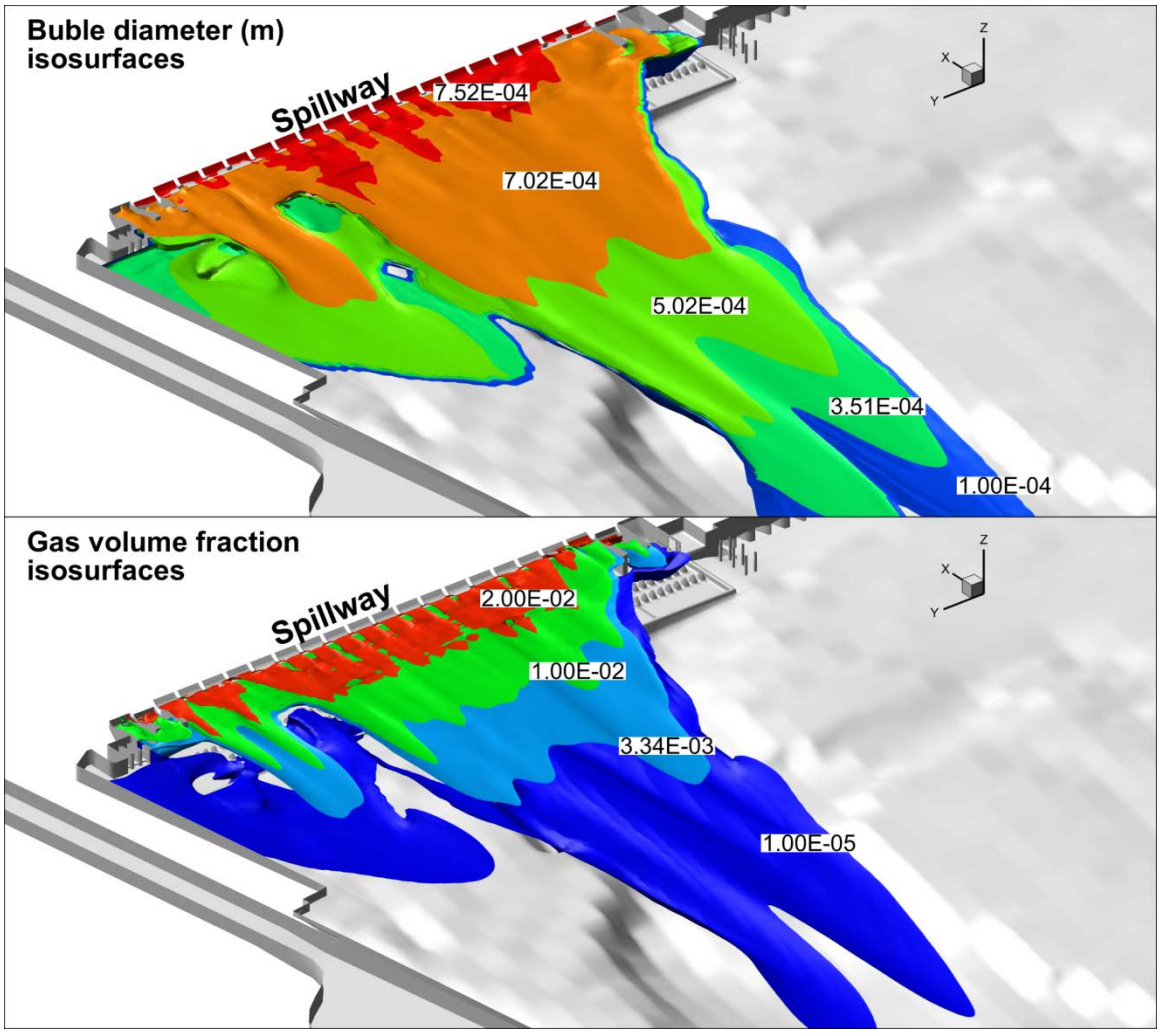

Figure 5.20 Isosurfaces of bubble diameter and gas volume fraction

Table 5.4 Measured and predicted TDG on Feb. 12, 1997

Station	Measured TDG	Predicted TDG Old Model	Predicted TDG Current Model	Error (%) Old Model	Error (%) Current Model	Abs. Error (%) Old Model	Abs. Error (%) Current Model
Q1T1B	1.060	1.059	1.050	-0.07	-0.07	0.07	0.94
Q2T1B	1.057	1.057	1.083	0.04	2.42	0.04	2.42
Q3T1B	1.235	1.235	1.210	-0.01	-2.02	0.01	2.02
Q3T1U	1.227	1.223	1.179	-0.30	-3.91	0.30	3.91
Q4T1B	1.227	1.137	1.231	-7.30	0.33	7.30	0.33
Q4T1U	1.214	1.142	1.183	-5.92	-2.59	5.92	2.59
Q5T1B	1.263	1.180	1.280	-6.56	1.35	6.56	1.35
Q5T1U	1.246	1.176	1.273	-5.64	2.17	5.64	2.17
Average T1	1.191	1.151	1.186	-3.22	-0.29	3.23	1.97
Q1T2U	1.042	1.040	1.040	-0.17	-0.17	0.17	0.17
Q2T2U	1.068	1.088	1.095	1.88	2.54	1.88	2.54
Q3T2B	1.143	1.204	1.193	5.35	4.40	5.35	4.40
Q4T2B	1.184	1.152	1.175	-2.67	-0.79	2.67	0.79
Q4T2U	1.192	1.138	1.174	-4.52	-1.47	4.52	1.47
Q5T2U	1.204	1.170	1.192	-2.86	-0.97	2.86	0.97
Q5T23U	1.166	1.166	1.170	1.17	0.00	0.00	0.34
Average T2	1.139	1.132	1.149	-0.26	0.50	2.49	1.53
Q1T3U	1.050	1.042	1.045	-0.74	-0.45	0.74	0.45
Q2T3U	1.063	1.081	1.107	1.70	4.15	1.70	4.15
Q3T3B	1.104	1.183	1.186	7.17	7.45	7.17	7.45
Q3T3U	1.116	1.174	1.165	5.22	4.42	5.22	4.42
Q4T3U	1.178	1.162	1.165	-1.32	-1.08	1.32	1.08
Q5T2U	1.166	1.165	1.159	-0.10	-0.59	0.10	0.59
Average T3	1.113	1.135	1.138	1.99	2.32	2.71	3.02

5.4 Calibration and Validation Summary

A grid sensitivity study was performed to determine the effects of grid density on velocity and TDG production and distribution predictions. Due to complexities in the free surface elevation prediction, the model consistently under predicted velocities when compared to field data. Furthermore, with increasing refinement, numerical velocities did not converge to the field data. Possible reasons for the lack of convergence were errors in the bathymetry, or that perhaps finer grids are actually over-fit models and capture noise created by the imprecise field measurements. TDG was not seen to be affected greatly by varying grid densities.

Because new boundary conditions at the spillway inlets were used, recalibration of the TDG model was required. Three initial gas volume fractions were analyzed using an initial bubble diameter found in previous studies. After calibration, the model was able to predict TDG field data gathered in February 1997.

CHAPTER VI

PREDICTIVE SIMULATIONS

6.1 Simulation Conditions

After validation, the model was used to simulate 16 scenarios. Tables A1 to A16 in Appendix A describe the operational conditions of these simulations. The focus of the simulations was to contrast different operations of the powerhouse for the same pattern and magnitude of spillway operations and river flow. Eight different river flows were simulated. Tailrace free surface shape depends primarily on spillway flows. Since the spillway operations are the same for current and proposed operations, only 8 VOF simulations were performed.

Total river flows ranged from approximately 100 kcfs to 300 kcfs. Two spill conditions, spring and summer, were simulated. In spring, bays 19 and 20 operate with TSWs that provide surface withdraw from the forebay to facilitate fish migration. In summer, spill is operating the standard gates only. The TSW crest was 325.38 ft. The outfall, or pipeline, that returns fish to the river from the juvenile bypass system, was relocated from the north shore to the center of the spillway approximately 1900 ft from the dam in 2012. The effect of relocating the fish outfall was also numerically studied. The water flow through the outfall was 32 cfs. The water depths in the outfall at the terminus where it discharges into the river for the current and proposed outfall are 1.01 ft and 1.55 ft, respectively.

The forebay elevation was 338.5 ft. Forebay TDG concentration was 115.5%. The flowrate for each gate of the west shore fish entrance was 1 kcfs at 8 ft deep. The north shore fish entrance was operating at 1 kcfs at 8 ft deep. Two south gates of the north

powerhouse fish entrance were operating at 1 kcfs at 9 ft deep. Both gates of the south powerhouse fish entrance were operating at 1 kcfs at 9 ft deep. Fish pumps were pulling 5 kcfs of water and the south station service outlet was operating with 0.6 kcfs.

6.2 VOF Model Results

Plots showing numerical solutions for the free surface simulations are shown in Appendix B. The evolution of Simulation 9 is illustrated in Figure 6.1. The remainder of the simulation evolutions are shown in Figure B1. The red line represents the flow rate at the exit and the black line indicates the target flowrate. The target flowrate for simulation 9 was 152.5 kcfs as shown by the dotted black line. Convergence was reached after approximately 35 minutes of simulation time. Statistically steady solutions were obtained for the other simulations after approximately 8 to 40 minutes of computed flow time, depending on the initial condition used. Some simulations converged more quickly because they shared river flowrates with simulations that had been completed previously. For example, both Simulations 5 and 11, while having different operational conditions, had the same total flowrate. Because of this, solution data from Simulation 5 was interpolated to Simulation 11 initially, reducing the time to convergence.

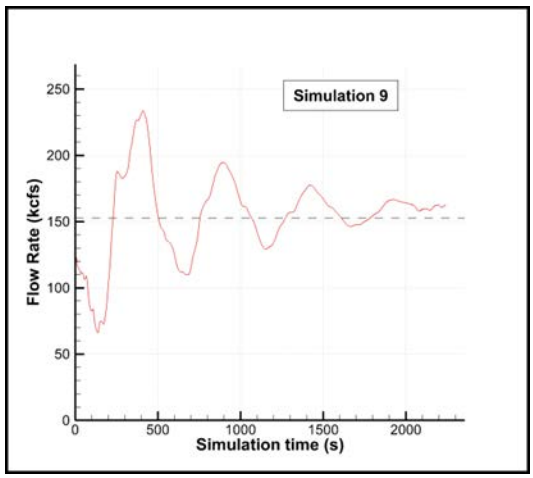

Figure 6.1 Evolution of the Flowrate for Simulation 9

The grid used for Simulation 9 is shown in Figure 6.2. Detail of the spillway region is shown in the top half of the figure, and the entire VOF model can be seen in the bottom half of the figure. Grids used for the remaining simulations are shown in Figures B2 to B8. The grid refinement in the free surface region is can be seen when inspecting the spillway walls. Figures B4 and B7 also show a profile view of the grid generated to capture the plunging jet from the permanent and relocated outfalls, respectively. Fifty six feet of the outfall pipe were simulated in order to have a developed flow condition within the pipe before plunging.

Figure 6.3 shows the isosurface for a gas volume fraction, $\alpha_w = 0.5$ colored by elevation for Simulation 9. This isosurface would then be extracted and later used as a database for the top boundary of the rigid-lid grid. Again, detail near the spillways is shown in the top half while the entire VOF model can be seen in the bottom half of the figure. Figures B9 to B15 show the remainder of the simulation's free surface shapes. For the spring operations, spillbays #19 and #20 have the TSW structure; this too can be

seen in Figure 6.3. In Figures B11 and B14 the resolved jets for the permanent and relocated outfalls, respectively, can be seen. The use of a k-ε turbulence model has some effect on the overall free surface shape.

This turbulence model is unable to capture the effects of the bubbles or the entrainment. This effect is minimal in comparison with the main limitation of the model developed for this thesis: using a fixed free surface for the rigid-lid simulations.

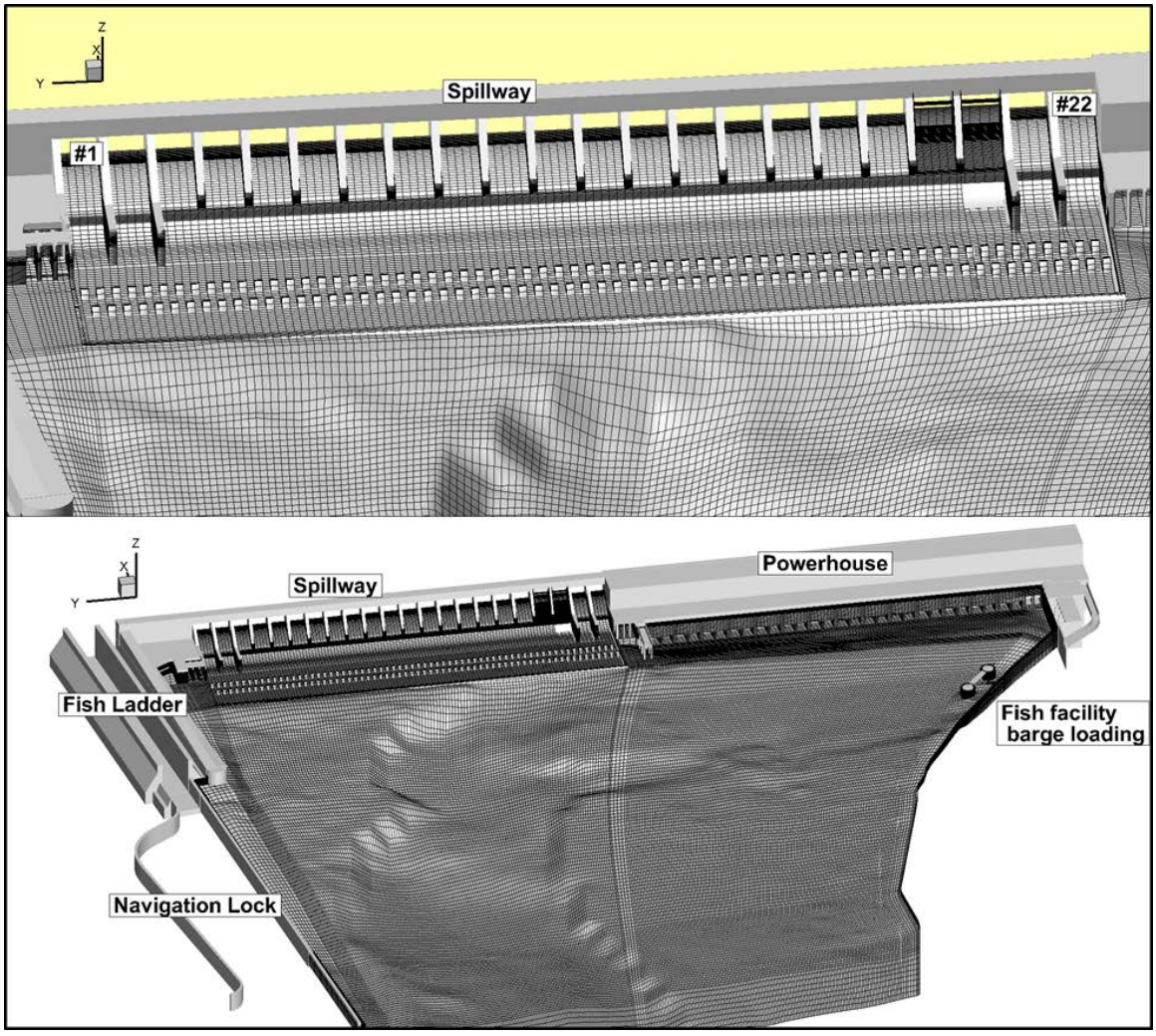

Figure 6.2 Grid Used for VOF Model for Simulation 9. Top: Detail Near the Spillway Bottom: Entire VOF Model

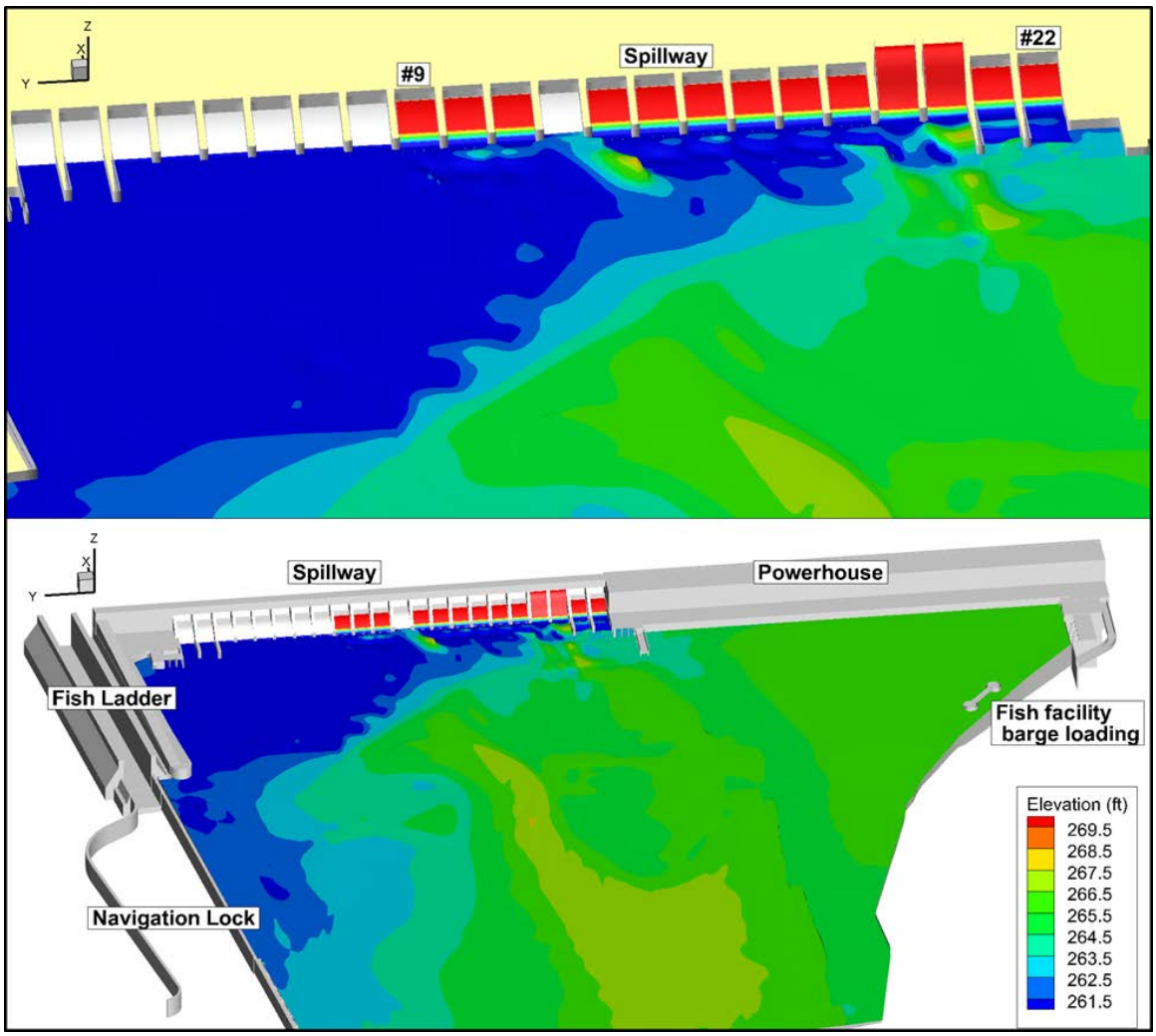

Figure 6.3 Predicted Free Surface Shape for Simulation 9. Top: Detail Near Spillway, Bottom: Entire VOF Model

The large depression in the northern section of the free surface is an effect of the closed spillways 1-8. This effect is seen to a lesser degree in other simulations downstream of closed spillways. The tailwater elevation increases with increased total river flow. With the increase in river flow, spillway flowrates are increased. These increased flowrates create a rougher free surface shape near the spillways due to the increased magnitude of the waves.

6.3 Tailrace Hydrodynamics

Appendix C contains plots showing numerical results related to the hydrodynamics in the tailrace obtained with the rigid-lid model. The rigid-lid meshes used for Simulations 9 and 10 are shown in Figure 6.4. Simulations 9 and 10 had a unique spillway configuration. The northern most bays 1-8 were closed, resulting in the large surface depression in the north spillway region seen in Figure 6.4. Powerhouse flowrates for Simulation 10 were higher, as three more powerhouse units were closed than for Simulation 9. This had a large effect on entrainment and TDG production and will be discussed in detail in later sections. Meshes used for the remaining simulations are shown in Figures C1 to C7. Displayed in these plots are the projections of the bathymetry onto the extracted databases from the VOF model colored by elevation. In the top half of Figure 6.4 refinement in the south east corner (top right in the plot) of the mesh can be seen for Simulation 9. This refinement was used to capture the impact shape of the jet created by the permanent outfall. In the bottom half similar refinement can be seen in the center of the tailrace for Simulation 10. This refinement was then used to capture the shape of the relocated outfall's jet shape in the tailrace. These refinement regions are the same for the remaining rigid-lid plots shown in Appendix C as the outfalls were simulated in all rigid-lid simulations.

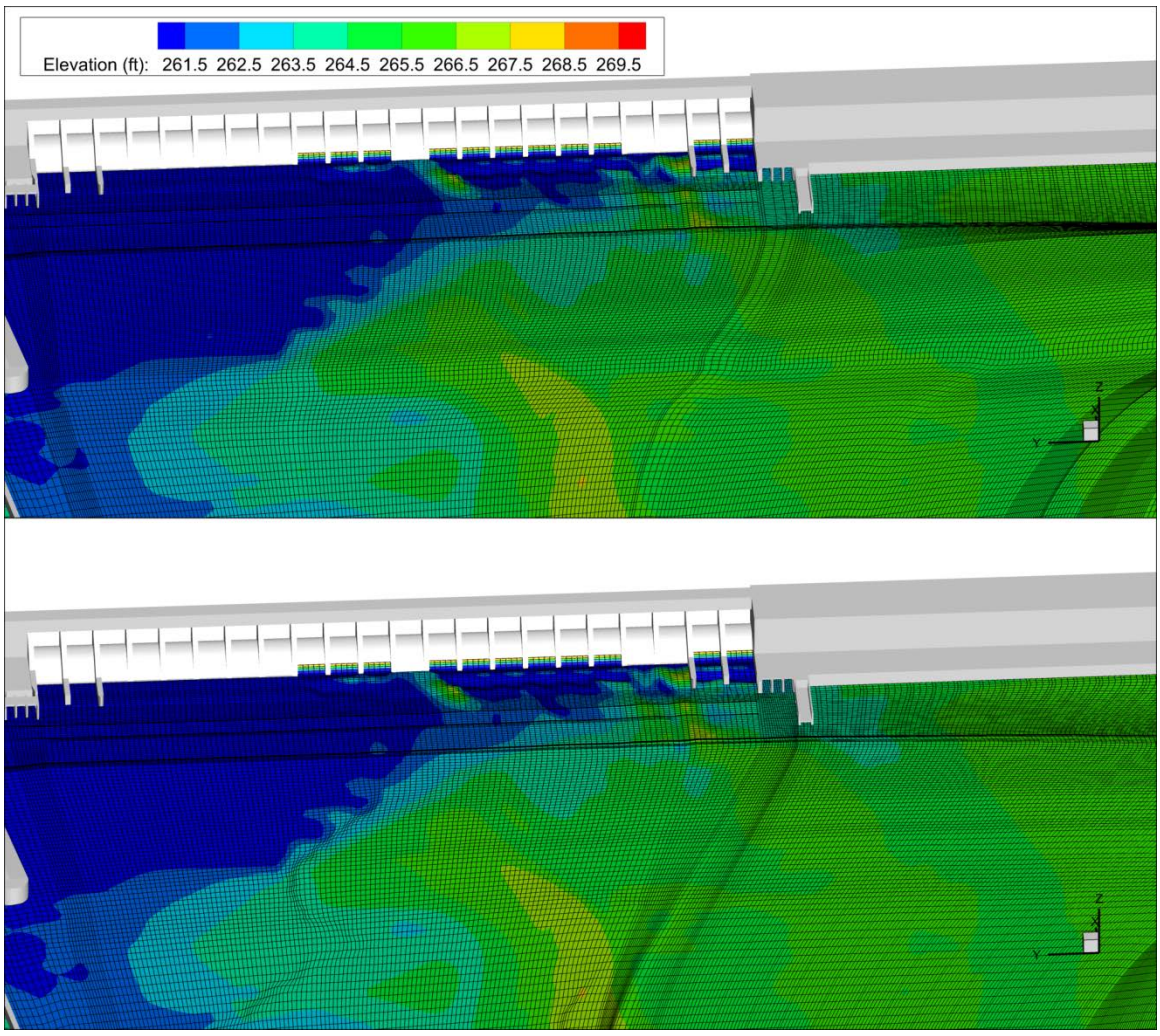

Figure 6.4 Grids Used for Rigid-Lid Simulations 9 (top) and 10 (bottom)

Figure 6.5 shows velocity contours and vectors at 2 meters from the free surface near the dam for Simulations 9 and 10. Velocity vectors are interpolated on to coarse uniform grids for easier visualization. Blue regions are zones with velocity smaller than 4 ft/s which is the criteria specified by USACE as a low-velocity danger area. In the case of these two simulations, as is seen in the simulation condition tables, spill is

concentrated in the southern region of the spillway. This creates a large recirculation in the northern most spillway region as shown by the velocity vectors.

The flow field for these simulations in the powerhouse region is fairly straight forward. Simulation 9 operates with 11 of the 14 turbines so there is little recirculation. Simulation 10 illustrates the case when a large number of turbines are closed. Here turbines 2-7 are closed, and downstream of the turbines a significant recirculation is formed in the region of the fish collection system. Propagation of high velocity from spillway surface jets can be observed at the exit of the domain as far as 8,000 ft. In Simulations 1 and 2, powerhouse flows deflect spillway jets towards the navigation lock. This effect was created by the combination of low spillway flowrates and high entrainment of the powerhouse water.

In summer operations, high velocities are observed in the southern region of the spillway due to strong surface jets created in bays 18 and 20. At higher flowrates, bay 19 is also operating, increasing the velocity further in this zone. During spring operations, higher velocities are predicted downstream of bays with TSWs. As spill increases, surface jets move in a straighter path along the main channel. These trends can be seen when comparing Figures C8 to C14, which show the results for the remaining simulations.

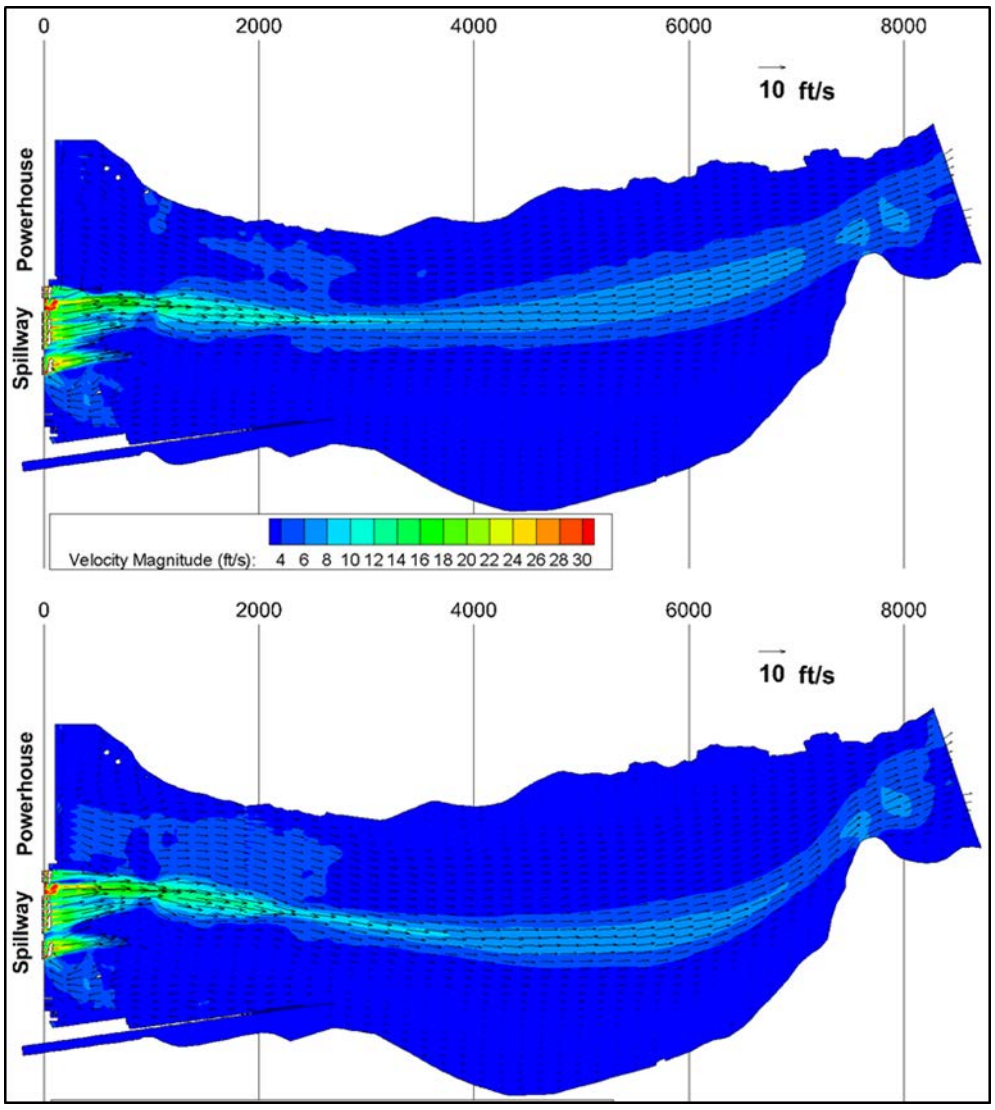

Figure 6.5 Contours of Velocity Magnitude and Velocity Vectors at 2m Beneath the Free Surface for Simulations 9 (top) and 10 (bottom)

Figure 6.6 shows a zoom of the previous figure near the powerhouse. In the latest figures velocity contours had been changed to illustrate better the lower velocities near the powerhouse. This plot more clearly demonstrates the effects of not using turbines, as well as the effect of powerhouse flowrate on entrainment into the spillway region. Comparing the region of entrainment for Simulations 9 and 10 (the area just south of the

final spill bay), it can be seen that the entrainment is stronger for Simulation 9, on the left, than Simulation 10. For Simulation 9, the northern most powerhouse units are operating at approximately 8 kcfs, while the same units operate at 12 kcfs for Simulation 10. This lower flowrate in Simulation 9 results in smaller streamwise velocity which allows for more water to be entrained into the spillway region for the same spillway flowrates.

Results for the simulations show that recirculation in the powerhouse region are eliminated with the use of all units. Results also show a trend in the entrainment of powerhouse water into the spillway region. The existing simulations (odd numbered simulations) have, on average, lower powerhouse flows than proposed simulations thus they have more entrainment than existing simulations. Also, even though powerhouse flows increase with total river flow, entrainment is still observed for all simulations. This is because spill is also increased as powerhouse flow is increased. These trends can be observed when comparing Figures C15 to C21 which show these plots for the remainder of the simulations.

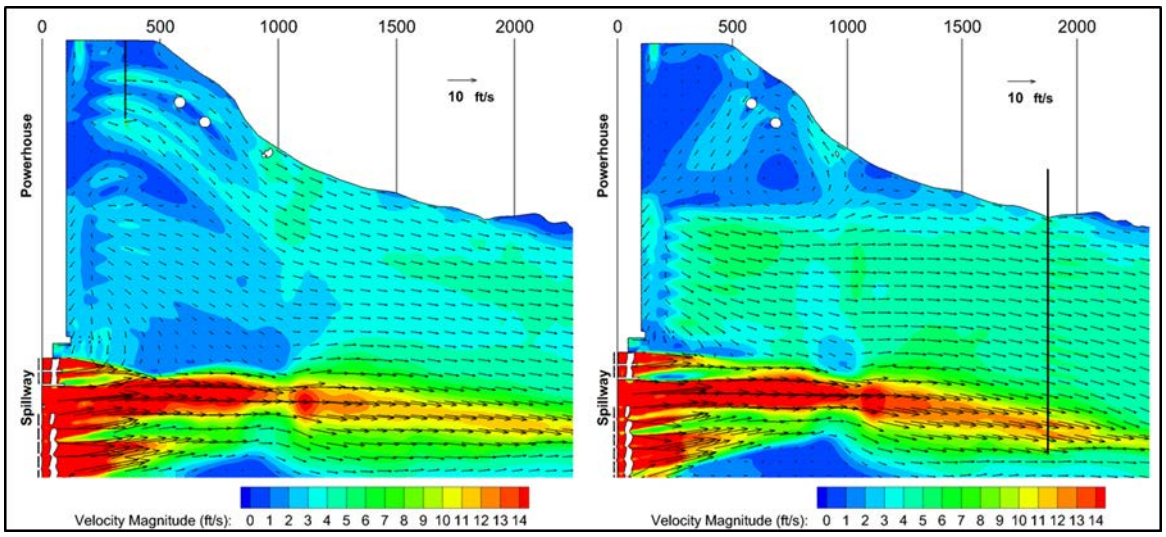

Figure 6.6 Contours of Velocity Magnitude and Velocity Vectors at 2m Beneath the Free Surface Near the Dam for Simulations 9 (left) and 10 (right)

The flow patterns in the powerhouse regions are displayed with streamlines colored by velocity magnitude in Figure 6.7. Figure 6.8 shows the flow patterns in the spillway region of Simulations 9 and 10. A small recirculation in front of the fishway entrances WFE are observed for both simulations. A low-velocity eddy is formed in the deepest central region of the spillway at about 1000 ft from the dam as can be seen in both simulations (Figure 6.8). The velocity of spillway jets is significantly reduced when water reaches this eddy. For both cases, the entrainment of the powerhouse flow is also visible, and in both cases water from the first powerhouse unit enters the fish pumps on the south edge of the structure. The large recirculation area in Simulation 10 where the powerhouse units are closed can also be seen. For Simulation 9, a small area of high velocity in the middle of the powerhouse region can be seen; this is the inflow for the permanent outfall. For all simulations, a large eddy is formed in front of non-operating units. This eddy is more pronounced for simulations where many central units are closed.

As powerhouse flow increases, streamwise velocity increases and powerhouse water from northern units entrains later into the spillway region. In addition, water from the central units travel downstream with minimal mixing with spillway flows. Figures C22 to C28 show the plots of the southern region and Figures C29 to C35 show the plots of the northern region.

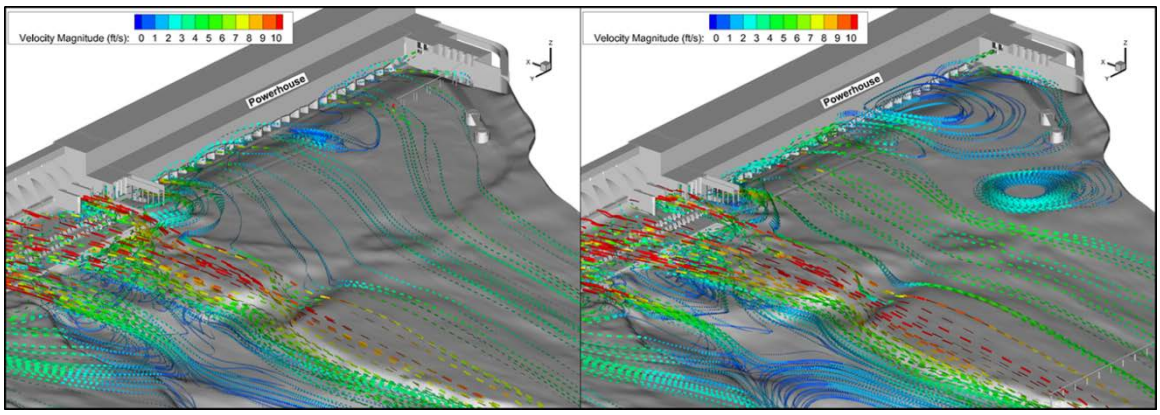

Figure 6.7 Streamlines in the Southern Region of the Tailrace Colored by Velocity Magnitude for Simulations 9 (left) and 10 (right)

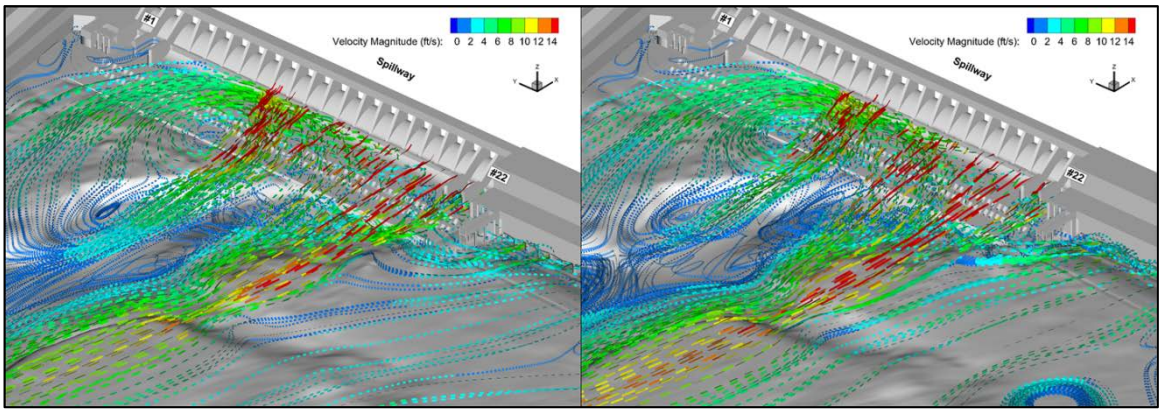

Figure 6.8 Streamlines in the Northern Region of the Tailrace Colored by Velocity Magnitude for Simulations 9 (left) and 10 (right)

Figure 6.9 shows streamlines released from the fish outfalls in Simulations 9 and 10. Water from the existing outfall mixes with powerhouse flows while water from the relocated outfall combines with higher velocity spill flows. Most of the time water from the existing outfall travels near the southern shore. This region, due to its low average velocity and shallow depth is a dangerous predation zone as it meets all of the criteria established by USACE. The exception is simulation 1 (Figure C33), where outfall water is entrained into the spillway region. Streamlines released from fish outfalls for the remainder of the simulations are shown in Figures C36 to C42.

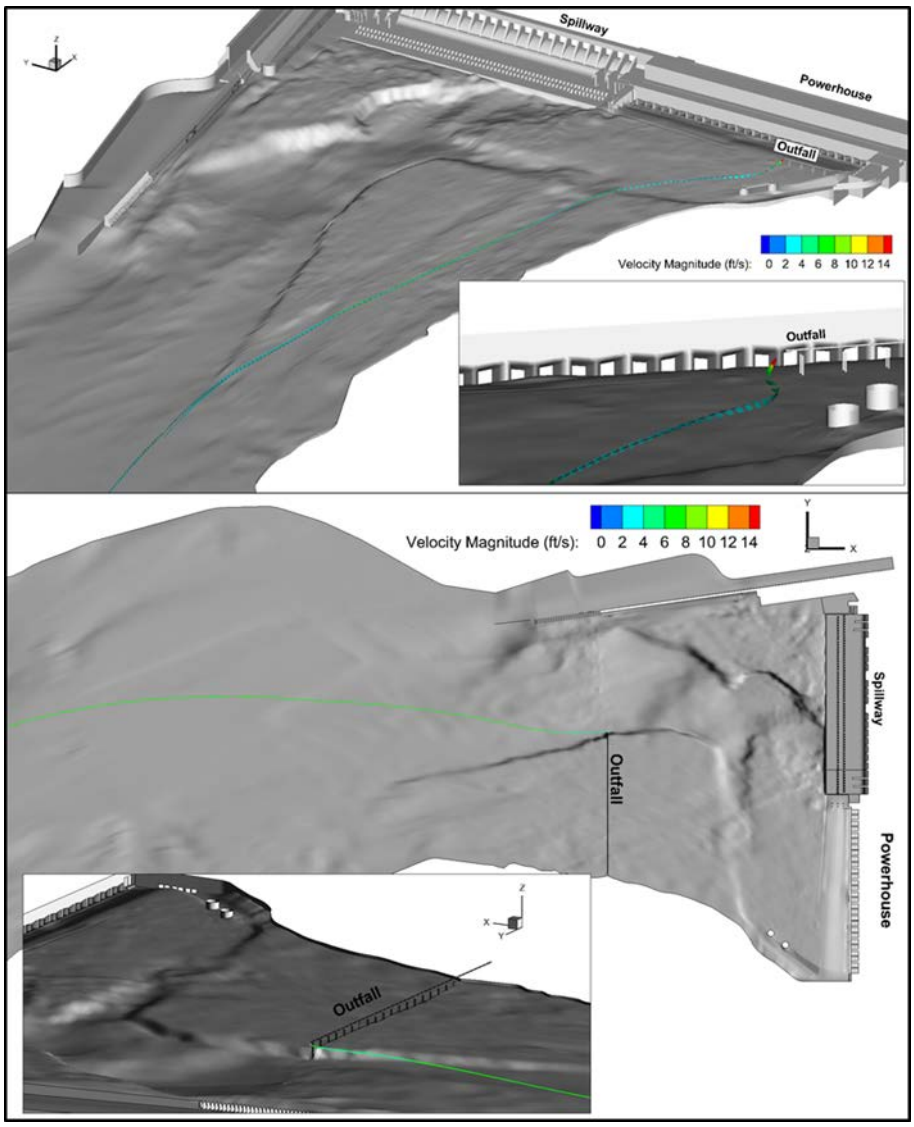

Figure 6.9 Streamlines Released from the Outfall Colored by Velocity Magnitude for the Existing Outfall (Sim. 9, top) and Relocated Outfall (Sim. 10, bottom)

6.4 Particle Tracking

Particle paths and particle statistics are shown in Appendixes D and E. Particle paths after 10 sec., 60 sec. and 10 min. of being injected for Simulation 9 are shown in Figure 6.10. Particles are colored by injections; white particles are released from the outfalls, green particles from the TSW, and particles in the red and blue ranges are

released from the powerhouse and spillway, respectively. Zones with blue and red particles indicate regions of mixing between powerhouse and spillway flows. In the summer operations, some particles from the northern powerhouse units can be entrained into the low velocity eddy in the center of the spillway. This is of some concern, as velocities in this eddy are lower than 4 ft/s, however this is the deepest section of the reach and very far from either shore which reduces the risk associated with this region. In the spring operations, most of these particles are mixed with TSW particles.

It is important to note differences in particles released from the outfalls. Particles released from the existing outfall are released into a zone of low velocity where the river is shallow and they follow a trajectory that stays near to the southern shore. This can be seen in all of the existing (odd numbered simulations) with the main exception being Simulation 1. Here, the effect of closing the majority of the powerhouse units (5-12) results in all of the powerhouse trajectories to be entrained to the spillway region. The level of entrainment depends on the number of central powerhouse units that are closed. Particles released from the proposed outfall follow a trajectory that flows down the center of the river. They are released into a zone of high velocity that is deep. Also, they are far from either shore making it an ideal location to avoid the predation criteria. However, TDG levels are highest in this region of the river. The TDG distribution will be discussed in depth in section 6.6. Slight variations on the trajectory are seen from varying simulations due to the different powerhouse operational conditions' effect on the flow field.

The density of the particles that are entrained from the northern powerhouse units into the spillway region can be seen in the 10 minute portion of Figure6.10. For

Simulation 9, particles are entrained immediately into the spillway region, where as for Simulation 10, more mixing is seen downstream of even the relocated outfall. This is a pattern that can be seen when comparing existing versus proposed simulations for all river flowrates.

The effect of varying the spillway operations, spring versus summer, has an effect on the particles. As seen in Figure 6.10, closing the northern most spillways creates a large eddy in that region. This eddy is slow moving and traps a large portion of the particles released from the spillways. As more spillways are opened, particle trajectories move either toward the north shore or the center where velocities from the southern spillways are high, avoiding the deep area of the reach downstream of the spillways where velocities are low. Eddies form just downstream of closed spillbays trapping particles.

Lower total river flows are conducive to more mixing, as evident when comparing Simulations 1 and 2 with 15 and 16. Therefore, there is more mixing in summer simulations than spring. The particle paths for the remaining simulations are shown in Figures D1 to D15.

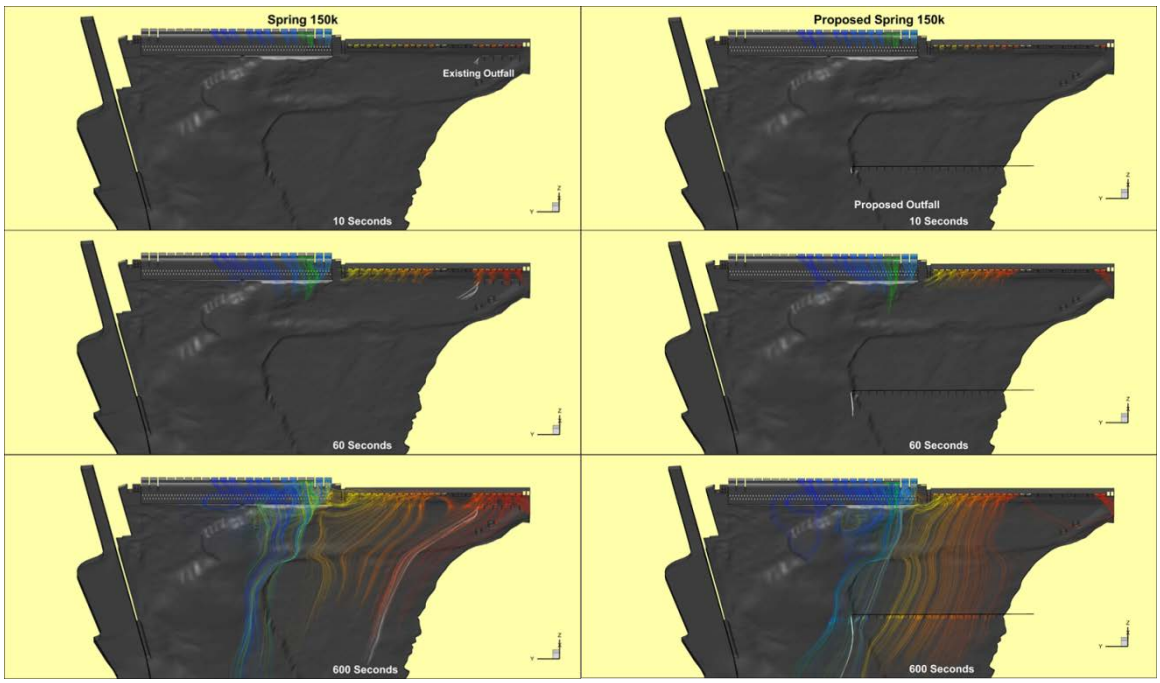

Figure 6.10 Particle Tracks for 10 Seconds, One Minute and 10 Minutes for Simulation 9 (left) and Simulation 10 (right)

Particle statistics were calculated considering predator velocity criteria and all predator criteria together. Two parameters were used:

$$\text{Total particle exposure } (\%): \frac{\text{number of particles that meet a predator criteria}}{\text{total particles injected}} \cdot 100$$

$$\text{Particle exposure time } (\%): \frac{\text{time a particle meet a predator criteria}}{\text{total time}} \cdot 100$$

Tables 6.1 and 6.2 show the percentages of particles exposed, and Table 6.3 and 6.4 show particle exposure time percentages for Simulations 9 and 10. For an example in Table 6.1, particles injected into spillway 15 and the outfall are used. Table 6.1 counts the number of particles that met predator criteria at any point in their path through the

domain. These criteria again are: 1) traveling in flows with velocity less than 4 ft/s, 2) traveling in water depth less than 33 feet, and 3) distance to the shore less than 250 feet.

Particles injected into spillway 15 enter into an area of high velocity, and as such after 10 seconds none of the particles had experienced a flow of less than 4 ft/s and therefore none were in an area where all criteria were met. This 'area where all criteria were met' will be referred to as an 'all-area' for simplicity. Likewise, the outfall initially injects particles into an area of high velocity and 2% of the particles spent any length of time within an area of low velocity after just 10 seconds. Contrasting those results with the data after 1 minute of flow time, 56% of the particles from spillway 15 had at some point entered into an area where flow was less than 4 ft/s, but still none of the particles entered an all-area. All of the outfall particles reached an area of low velocity, and none reached an all-area. The trend continues after 10 minutes, 94% of particles from spillway 15 reached low velocity, and due to the fact that these particles flowed through the center of the tailrace, none ever reached an all-area. The statistics after 10 minutes for the outfall were 100% reached low velocity and 60% reached an all-area.

Effects of varying powerhouse flow conditions are the strongest shortly after release. The proposed simulation has higher flow rates in the powerhouse units, so initially the velocity percentages are lower than the existing operation (simulation 9). After one minute, this difference is still evident but the effect is not as strong. After 10 minutes, flows have slowed to dangerous levels regardless of initial conditions and the percentages are comparable.

Table 6.1 Particle Exposure Percentage for Simulation 9.

Spring 150k- Exposure Percentage After 10 Seconds

Powerhouse Flow Exposure

	U1	U2	U3	U4	U5	U6	U7	U8	U9	U10	U11	U12	U13	U14	Outflow
Velocity	50	51	51	51	n/a	n/a	n/a	50	50	50	50	50	50	50	2
All	0	0	0	0	n/a	n/a	n/a	0	0	0	0	0	0	0	0

Spillway Flow Exposure

	S1	S2	S3	S4	S5	S6	S7	S8	S9	S10	S11	S12	S13	S14	S15	S16	S17	S18	S19	S20	S21	S22
Velocity	n/a	n/a	n/a	n/a	n/a	n/a	n/a	n/a	0	0	0	n/a	0	0	0	0	0	2	2	0	14	4
All	n/a	n/a	n/a	n/a	n/a	n/a	n/a	n/a	0	0	0	n/a	0	0	0	0	0	0	0	0	0	0

Spring 150k- Exposure Percentage After 1 Minute

Powerhouse Flow Exposure

	U1	U2	U3	U4	U5	U6	U7	U8	U9	U10	U11	U12	U13	U14	Outflow
Velocity	100	95	99	96	n/a	n/a	n/a	100	100	100	100	100	100	100	100
All	4	31	5	0	n/a	n/a	n/a	0	0	0	0	0	0	0	0

Spillway Flow Exposure

	S1	S2	S3	S4	S5	S6	S7	S8	S9	S10	S11	S12	S13	S14	S15	S16	S17	S18	S19	S20	S21	S22
Velocity	n/a	n/a	n/a	n/a	n/a	n/a	n/a	n/a	82	97.8	100	n/a	100	70	56	100	78	74	20	38	90	90
All	n/a	n/a	n/a	n/a	n/a	n/a	n/a	n/a	0	0	0	n/a	0	0	0	0	0	0	0	0	0	0

Spring 150k- Exposure Percentage After 10 Minutes

Powerhouse Flow Exposure

	U1	U2	U3	U4	U5	U6	U7	U8	U9	U10	U11	U12	U13	U14	Outflow
Velocity	100	100	100	100	n/a	n/a	n/a	100	100	100	100	100	100	100	100
All	49	80	28	3	n/a	n/a	n/a	0	0	0	0	0	0	0	60

Spillway Flow Exposure

	S1	S2	S3	S4	S5	S6	S7	S8	S9	S10	S11	S12	S13	S14	S15	S16	S17	S18	S19	S20	S21	S22
Velocity	n/a	n/a	n/a	n/a	n/a	n/a	n/a	n/a	100	100	100	n/a	100	100	94	100	100	94	80	100	100	100
All	n/a	n/a	n/a	n/a	n/a	n/a	n/a	n/a	0	0	0	n/a	0	0	0	0	0	0	0	0	0	0

Table 6.2 Particle Exposure Percentage for Simulation 10

Spring 150k Proposed- Exposure Percentage After 10 Seconds

Powerhouse Flow Exposure

	U1	U2	U3	U4	U5	U6	U7	U8	U9	U10	U11	U12	U13	U14	Outflow
Velocity	50	n/a	n/a	n/a	n/a	n/a	n/a	50	27	27	26	27	27	28	20
All	0	n/a	n/a	n/a	n/a	n/a	n/a	0	0	0	0	0	0	0	0

Spillway Flow Exposure

	S1	S2	S3	S4	S5	S6	S7	S8	S9	S10	S11	S12	S13	S14	S15	S16	S17	S18	S19	S20	S21	S22
Velocity	n/a	n/a	n/a	n/a	n/a	n/a	n/a	n/a	0	0	0	n/a	0	0	0	8	0	2	2	6	2	0
All	n/a	n/a	n/a	n/a	n/a	n/a	n/a	n/a	0	0	0	n/a	0	0	0	0	0	0	0	0	0	0

Spring 150k Proposed- Exposure Percentage After 1 Minute

Powerhouse Flow Exposure

	U1	U2	U3	U4	U5	U6	U7	U8	U9	U10	U11	U12	U13	U14	Outflow
Velocity	100	n/a	n/a	n/a	n/a	n/a	n/a	100	70	73	77	77	75	94	20
All	0	n/a	n/a	n/a	n/a	n/a	n/a	0	0	0	0	0	0	0	0

Spillway Flow Exposure

	S1	S2	S3	S4	S5	S6	S7	S8	S9	S10	S11	S12	S13	S14	S15	S16	S17	S18	S19	S20	S21	S22
Velocity	n/a	n/a	n/a	n/a	n/a	n/a	n/a	n/a	88	73.5	86	n/a	100	74	56	64	76	88	22	80	100	100
All	n/a	n/a	n/a	n/a	n/a	n/a	n/a	n/a	0	0	0	n/a	0	0	0	0	0	0	0	0	0	0

Spring 150k Proposed- Exposure Percentage After 10 Minutes

Powerhouse Flow Exposure

	U1	U2	U3	U4	U5	U6	U7	U8	U9	U10	U11	U12	U13	U14	Outflow
Velocity	100	n/a	n/a	n/a	n/a	n/a	n/a	100	87	100	100	100	100	100	20
All	23	n/a	n/a	n/a	n/a	n/a	n/a	33	36	6	0	0	0	0	0

Spillway Flow Exposure

	S1	S2	S3	S4	S5	S6	S7	S8	S9	S10	S11	S12	S13	S14	S15	S16	S17	S18	S19	S20	S21	S22
Velocity	n/a	n/a	n/a	n/a	n/a	n/a	n/a	n/a	100	100	100	n/a	100	100	100	100	100	100	92	92	100	100
All	n/a	n/a	n/a	n/a	n/a	n/a	n/a	n/a	0	0	0	n/a	0	0	0	0	0	0	0	0	0	0

Table 6.3 shows the statistics for the total time particles spent in either an area of low velocity or an all-area. The same units will be used as an example, spillway 15 and the outfall. After 10 seconds, the particles from spillway 15 spent no time in either type of area, and the same can be seen for the outfall. After 1 minute the particles from

spillway 15 spent on average 25.5% of their time in an area of low velocity, again no time spent in an all-area. The outfall particles spent, on average, 52.2% of their time in areas of low velocity after 1 minute. After 10 minutes, particles form spillway 15 spent on average 38.8% of their time in areas of low velocity. Particles from the outfall spent 70.8% of their time in areas of low velocity and 2.82% of their time in all-areas. This is in fairly stark contrast from the 60% of particles exposed to the all-areas from Table 5.1, but the explication is simple. A large portion of the particles released from the outfall passed through an all-area, as represented by Table 6.1, but as Table 6.2 shows, these particles spent very little time in those regions. Unlike Table 6.1, values in Table 6.2 can decrease with time if particles spend time in fast moving flows for example. The effects of varying powerhouse conditions are similar to those described above.

Table 6.3 Exposure Time Percentage for Simulation 9

Spring 150k- Exposure Time Percentage After 10 Seconds

Powerhouse Flow Exposure

	U1	U2	U3	U4	U5	U6	U7	U8	U9	U10	U11	U12	U13	U14	Outflow
Velocity	38.5	38.4	38.3	38.2	n/a	n/a	n/a	37.8	37.8	38.1	37.7	37.6	37.6	37.6	0
All	0	0	0	0	n/a	n/a	n/a	0	0	0	0	0	0	0	0

Spillway Flow Exposure

	S1	S2	S3	S4	S5	S6	S7	S8	S9	S10	S11	S12	S13	S14	S15	S16	S17	S18	S19	S20	S21	S22
Velocity	n/a	n/a	n/a	n/a	n/a	n/a	n/a	n/a	0	0	0	n/a	0	0	0	0	0	0.89	0.34	0	4.56	0.36
All	n/a	n/a	n/a	n/a	n/a	n/a	n/a	n/a	0	0	0	n/a	0	0	0	0	0	0	0	0	0	0

Spring 150k- Exposure Time Percentage After 1 Minute

Powerhouse Flow Exposure

	U1	U2	U3	U4	U5	U6	U7	U8	U9	U10	U11	U12	U13	U14	Outflow
Velocity	74.2	69.9	71.7	66	n/a	n/a	n/a	79.9	72.7	74.8	75.3	76.6	77.3	75.3	52.2
All	0.67	6.89	1.11	0	n/a	n/a	n/a	0	0	0	0	0	0	0	0

Spillway Flow Exposure

	S1	S2	S3	S4	S5	S6	S7	S8	S9	S10	S11	S12	S13	S14	S15	S16	S17	S18	S19	S20	S21	S22
Velocity	n/a	n/a	n/a	n/a	n/a	n/a	n/a	n/a	31.4	32.9	38.6	n/a	46.9	22.4	25.5	46.9	10.9	36.6	6.75	7.35	40.5	24.7
All	n/a	n/a	n/a	n/a	n/a	n/a	n/a	n/a	0	0	0	n/a	0	0	0	0	0	0	0	0	0	0

Spring 150k- Exposure Time Percentage After 10 Minutes

Powerhouse Flow Exposure

	U1	U2	U3	U4	U5	U6	U7	U8	U9	U10	U11	U12	U13	U14	Outflow
Velocity	96.9	92.7	84.3	93.2	n/a	n/a	n/a	94.5	96.3	85.1	78.4	65.7	66.7	55.5	70.8
All	7.72	58.2	4.01	0.32	n/a	n/a	n/a	0	0	0	0	0	0	0	2.82

Spillway Flow Exposure

	S1	S2	S3	S4	S5	S6	S7	S8	S9	S10	S11	S12	S13	S14	S15	S16	S17	S18	S19	S20	S21	S22
Velocity	n/a	n/a	n/a	n/a	n/a	n/a	n/a	n/a	50.5	57.8	66.7	n/a	55.5	55.7	38.8	55.5	85.1	48.2	42.7	61.8	68.6	61.2
All	n/a	n/a	n/a	n/a	n/a	n/a	n/a	n/a	0	0	0	n/a	0	0	0	0	0	0	0	0	0	0

Table 6.3 Exposure Time Percentage for Simulation 10

Spring 150k Proposed- Exposure Time Percentage After 10 Seconds

Powerhouse Flow Exposure

	U1	U2	U3	U4	U5	U6	U7	U8	U9	U10	U11	U12	U13	U14	Outflow
Velocity	38.7	n/a	n/a	n/a	n/a	n/a	n/a	38.1	16.8	17	16.7	17	17	17.1	0.18
All	0	n/a	n/a	n/a	n/a	n/a	n/a	0	0	0	0	0	0	0	0

Spillway Flow Exposure

	S1	S2	S3	S4	S5	S6	S7	S8	S9	S10	S11	S12	S13	S14	S15	S16	S17	S18	S19	S20	S21	S22
Velocity	n/a	n/a	n/a	n/a	n/a	n/a	n/a	n/a	0	0	0	n/a	0	0	0	1.09	0	1	0.67	2.91	0.09	0
All	n/a	n/a	n/a	n/a	n/a	n/a	n/a	n/a	0	0	0	n/a	0	0	0	0	0	0	0	0	0	0

Spring 150k Proposed- Exposure Time Percentage After 1 Minute

Powerhouse Flow Exposure

	U1	U2	U3	U4	U5	U6	U7	U8	U9	U10	U11	U12	U13	U14	Outflow
Velocity	72.9	n/a	n/a	n/a	n/a	n/a	n/a	71.9	33.3	35	42.2	44.7	47.8	46.7	0.03
All	0	n/a	n/a	n/a	n/a	n/a	n/a	0	0	0	0	0	0	0	0

Spillway Flow Exposure

	S1	S2	S3	S4	S5	S6	S7	S8	S9	S10	S11	S12	S13	S14	S15	S16	S17	S18	S19	S20	S21	S22
Velocity	n/a	n/a	n/a	n/a	n/a	n/a	n/a	n/a	24.8	28.8	36.1	n/a	34.6	27.9	23.4	22.7	24.2	41.5	14.4	28.7	57.4	47.6
All	n/a	n/a	n/a	n/a	n/a	n/a	n/a	n/a	0	0	0	n/a	0	0	0	0	0	0	0	0	0	0

Spring 150k Proposed- Exposure Time Percentage After 10 Minutes

Powerhouse Flow Exposure

	U1	U2	U3	U4	U5	U6	U7	U8	U9	U10	U11	U12	U13	U14	Outflow
Velocity	96.9	n/a	n/a	n/a	n/a	n/a	n/a	42.3	23.3	13.1	20.9	26.7	36.7	71.9	0
All	4.47	n/a	n/a	n/a	n/a	n/a	n/a	11.1	9.32	0.26	0	0	0	0	0

Spillway Flow Exposure

	S1	S2	S3	S4	S5	S6	S7	S8	S9	S10	S11	S12	S13	S14	S15	S16	S17	S18	S19	S20	S21	S22
Velocity	n/a	n/a	n/a	n/a	n/a	n/a	n/a	n/a	51.6	70.3	64.4	n/a	53	83.8	79.4	78.9	71.1	60	48.1	56.1	36.7	58.7
All	n/a	n/a	n/a	n/a	n/a	n/a	n/a	n/a	0	0	0	n/a	0	0	0	0	0	0	0	0	0	0

Differences in particle exposure are found for particles released from the same spillway bay or turbine under similar operational conditions. This is particularly noticeable for total particle exposure. In this case, if a particle is in a low velocity region for a very short period of time it is counted as in the predator zone (independently of for

how long it was exposed). Analyzing particle trajectories, it was noted that the particle track algorithm used in this study depends on grid topology. Outfalls were included in a base tailrace grid developed in previous studies refining blocks near the new structures. This approach resulted in two different grid topologies for spring and summer operations and differences in some particle trajectories. However, differences due to distinct operational conditions during spring and summer are larger than numerical uncertainties.

The split of powerhouse flow through the north or south draft tube should be noted. The simulation conditions require that 75% of powerhouse flow be directed through the southern draft tube. This split can lead to slightly unexpected statistical results.

For example, all particles released from the northern draft tube when powerhouse flowrates are 8.33 kcfs meet the low velocity criteria and therefore the particle exposure in the first 10 s is 50%. When powerhouse flow increases to 12.2 kcfs the percentage is reduced to about 25%. These particles' velocities reduce as they move to the larger cross-sectional area in the draft tube. Particles from powerhouse unit #14 entrain faster in the spillway region. However, before particles join the high velocity surface jets they travel in a low velocity region downstream of the trash sluiceway. Depending on the flowrate, some particles meet the velocity criteria in this zone. After 10 minutes, most of the particles at some point meet the velocity criteria. All predator criteria are met when particles are in shallow regions with low velocity near one of the shores. Depending on flowrates, some particles released from southern spillway bays can travel to the north shore and meet all predator criteria. Tables for the remaining simulations can be found in Appendix E.

This approach is limited in that the particles are inert. A more accurate modeling technique would be to include a fish movement model. To the author's knowledge, no such model has been designed for the McNary dam tailrace, and the development of such a model is not within the scope of this thesis. While the plots do not show large differences when comparing operational conditions or total river flow rates, exposure percentages do provide insight into the problem. The main concern of this thesis are juvenile salmon. These salmon are very small and unlikely to be able to resist the large drag forces and high velocities near the dam. The majority of salmon smolts are unable to escape from flow fields moving greater than 2 m/s (6.6 ft/s) (Swanson et al. 1998). Thus, use of inert particles near the dam is a good approximation of how a juvenile salmon would behave.

6.5 Predator Regions

Figure 5.11 shows predation criteria habitat zones for Simulation 9. The zones are colored by velocity magnitude and indicate what are described earlier as an all-area, where all three of the predation criteria are met. The goal is to see how these areas change for varying flow conditions with the goal of minimizing the areas of concern. In the existing condition, powerhouse flows are concentrated in the south units favoring higher velocities near the south shore. At higher flowrates, there is a zone in the south shore near the outfall where the velocity criteria is not met. Differences in the predator zones in the north shore due to different operational conditions are minor. Figures F1-F7 show the all-areas for the remaining simulations.

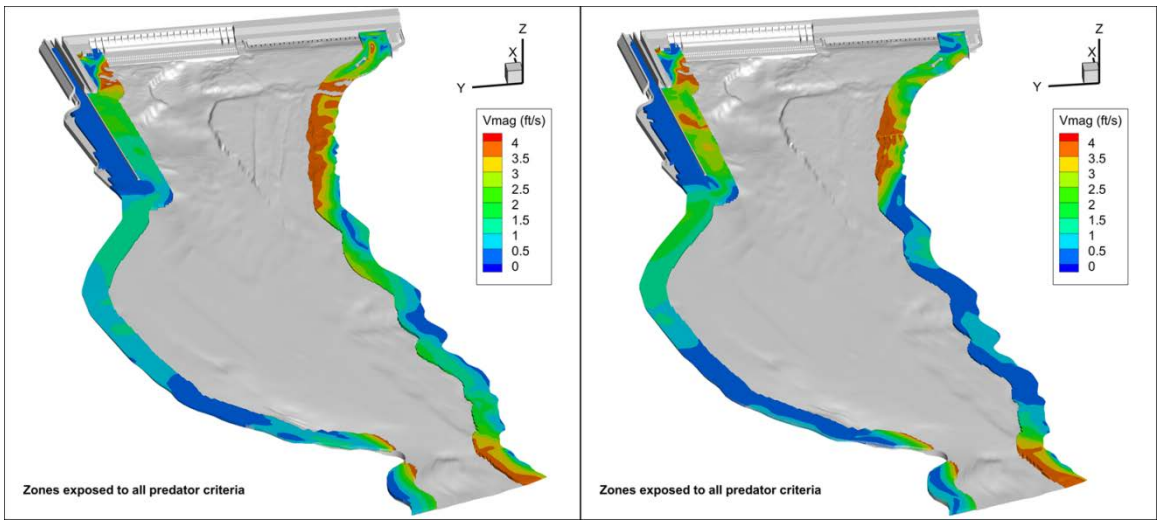

Figure 6.11 Zones Exposed to All Predator Criteria for Simulation 9 (right) and Simulation 10 (left)

Figure 6.12 shows the "safe" zones where velocities are higher than 4 ft/s. These zones may meet the other criteria of depth or proximity to the shore however. The tailrace velocity increases with flowrate thus the regions shown in Figure 6.12 grow with increasing total river flowrate. In the proposed operation (Simulation 10), powerhouse flows concentrate in the north units creating a large zone formed by high velocity spillway and powerhouse flows. The remaining "safe" zone plots can be seen in Figures F8-F14.

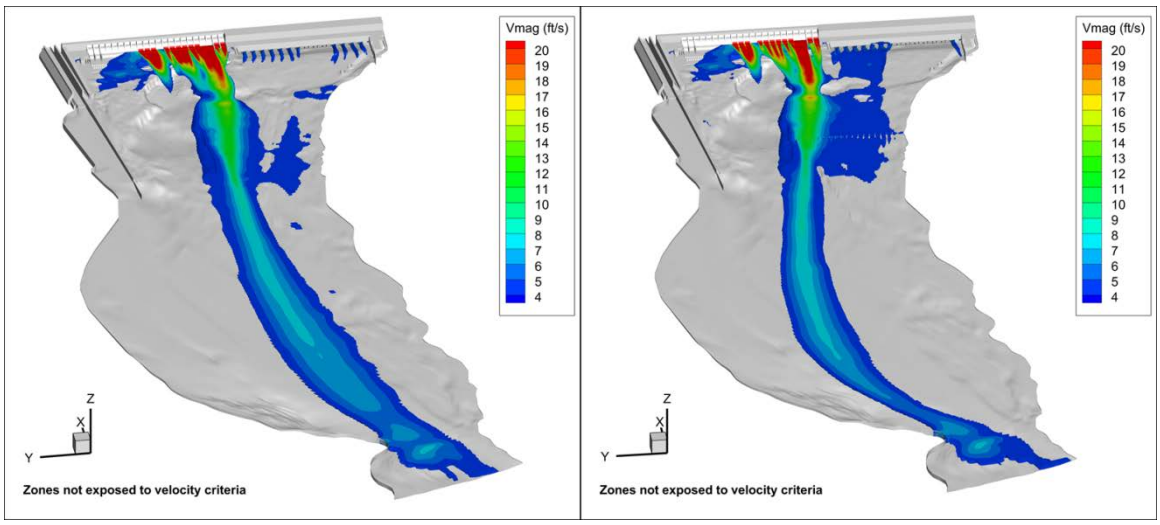

Figure 6.12 "Safe" Zones with Velocity Greater Than 4 ft/s for Simulation 9 (left) and Simulation 10 (right)

6.6 TDG and two-phase Flow Variables

Appendix G contains plots related to TDG and two phase flow variables such as gas volume fraction and bubble size. Figure 6.13 shows TDG and velocity vectors at 2 meters from the free surface for Simulations 9 and 10. Contour levels are the same between the two operations. When comparing the two simulations, it is obvious there is more TDG production for Simulation 9 than 10. This has to do with the entrainment of the powerhouse flows. As stated earlier, more water is entrained into the spillway region from the powerhouse for Simulation 9 due to the lower draft tube exit velocities. This water is entrained into the region where TDG is being produced. Assuming the water has not reached the maximum supersaturation level at the local condition, bubbles will transfer mass into the water. The addition of this under saturated water provides more opportunity for mass transfer to occur and more TDG is produced. Simulation 10 on the

other hand experiences water entrainment further downstream. Instead of adding water for addition TDG production, the powerhouse water dilutes the water downstream of the spillways, reducing the TDG concentration there. The TDG effect on the outfall location is also important to note here. The existing outfall location empties into an area of low TDG concentration, and as seen in the top half of Figure 6.13, increases the TDG in that area between 5 and 10%. The relocated outfall on the other hand, empties into the area downstream of the spillways where the TDG concentration is large enough that there is no noticeable increase in TDG at this location. In addition, the relocated outfall is closer to the free surface which minimizes air entrainment to depth.

TDG production increases with spill flowrate and therefore higher values are observed for summer operations. As powerhouse flow increases, low TDG powerhouse water travels farther along the south shore increasing lateral TDG gradients. Plots for the remaining simulations are shown in Figures G1 to G7.

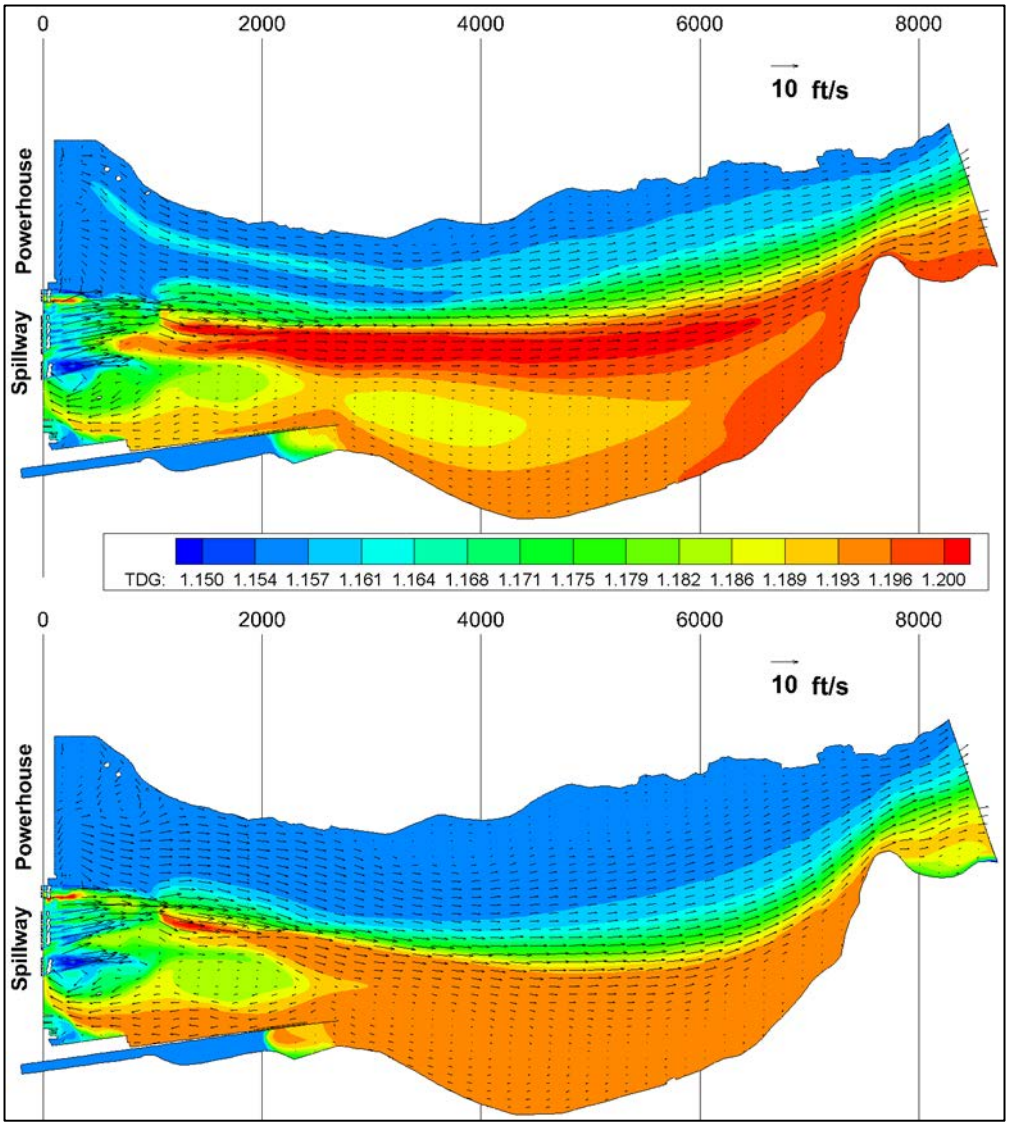

Figure 6.13 Contours of TDG and Velocity Vectors at 2m Beneath the Free Surface for Simulations 9 (top) and 10 (bottom).

Figure 6.14 shows TDG distributions and velocity vectors near the river bed. Streamwise velocities downstream of powerhouse units are considerably higher than those observed near the free surface. Velocities downstream of the spillway near the river bed are significantly smaller than those at the free surface. However, predicted velocities and flow pattern at the free surface and bottom of the tailrace downstream of the

navigation lock are comparable. Higher TDG values are observed near the river bed due to increased bubble dissolution at depth. This effect is more pronounced near the dam, where bubbles are present. Again the effect of the entrained water from the powerhouse region can be seen. The area of TDG production, the dark red region just downstream of the southernmost spill bays, is significantly larger in Simulation 9 than 10. The remaining plots are shown in Figures G8 to G14.

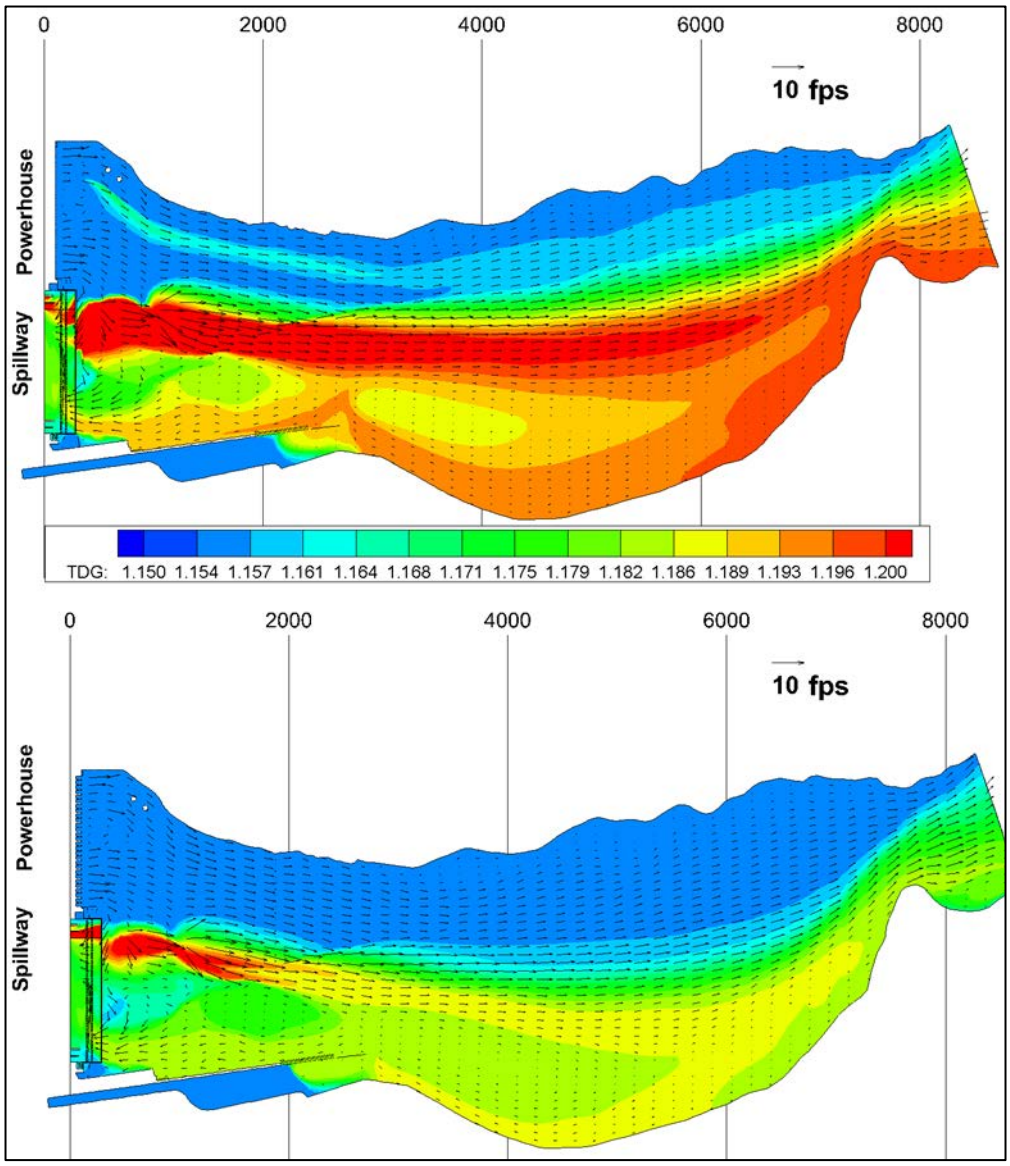

Figure 6.14 Contours of TDG and Velocity Vectors at the River Bed for Simulations 9 (top) and 10 (bottom).

Figure 6.15 shows isosurfaces of TDG for Simulations 9 and 10. Similar levels of TDG are found with the existing and proposed operations with the exception of the outfall. TDG production from the permanent outfall can be seen on the left side of Figure 6.15. Again, in these plots, the green isosurfaces represent higher TDG concentrations. Larger TDG production in Simulation 9 can also be seen downstream of the spill bays.

This entrainment-TDG production effect can be seen throughout all simulations; the existing simulations (odd numbered) always produce higher levels of TDG than the proposed conditions due to the larger entrainment of powerhouse water. When comparing varying river flows, the higher total flows will produce more TDG. This result is expected as larger spill flowrates will create more bubbles and consequently more TDG. Figures G15 to G21 show the remaining TDG isosurface plots.

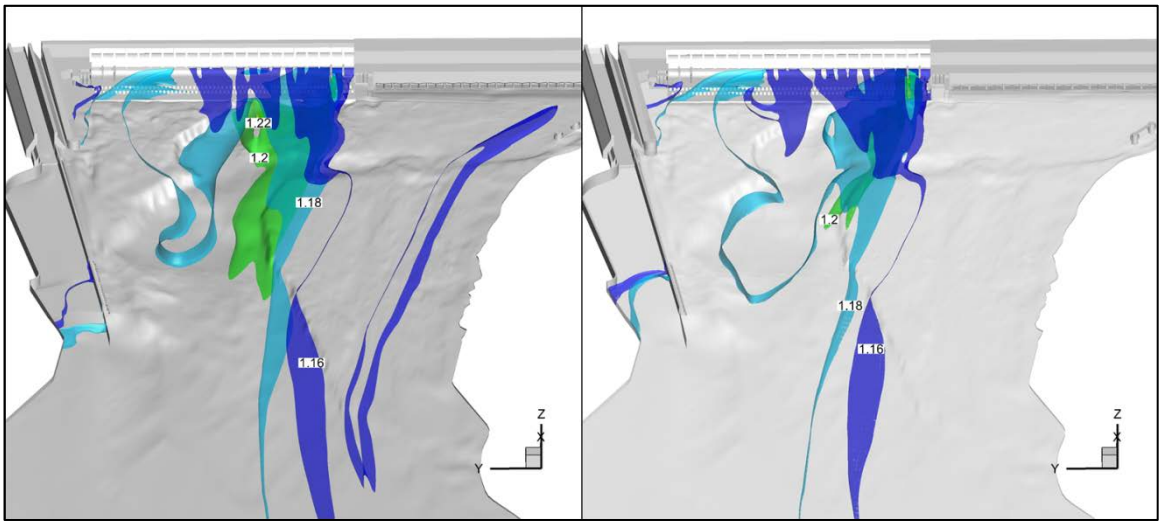

Figure 6.15 Isosurfaces of TDG for Simulations 9 (left) and 10 (right).

Figure 6.16 shows gas volume fraction contours and velocity vectors at 2 meters below the free surface for Simulations 9 and 10. The colored zone indicates the regions where bubbles can be observed in the tailrace. A small bubble plume is created downstream of the existing outfall. The effect of the proposed outfall on the gas volume fraction distribution is negligible. Similar gas volume fraction distributions are observed with the existing (9) and proposed (10) operations. Bubbles entrained in spillway bays

with smaller flowrate leave the domain faster, at about 500 ft from the dam. On the other hand, bubbles are transported farther downstream when entrained in higher velocity spillway jets. As bubbles are only produced by the spillways or outfall, the gas volume fractions only vary between different river flowrates. As expected, greater gas volume fractions are found as spillway flow is increased. Figures G22 to G28 show bubble diameter plots for the remaining simulations.

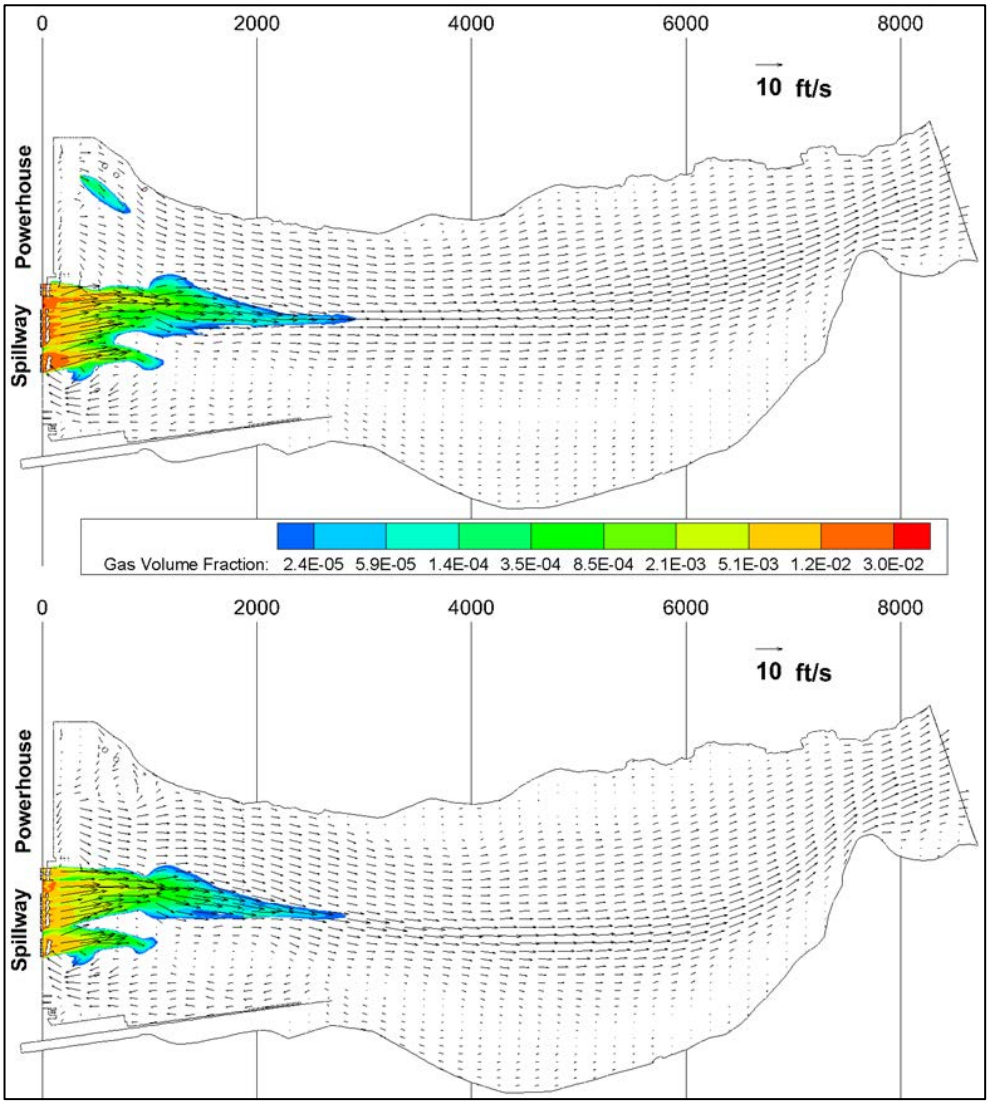

Figure 6.16 Contours of Gas Volume Fraction and Velocity Vectors at 2m Beneath the Free Surface for Simulations 9 (top) and 10 (bottom).

Isosurfaces of bubble diameter are shown in Figure 6.17. Bigger bubbles, of the order of 0.8 mm, leave the domain more quickly near the dam. Some bubbles are entrained deep in the tailrace where they shrink due to pressure and dissolution. These small bubbles can travel farther into the tailrace. When comparing Simulations 9 and 10 in Figure 6.17, it is apparent that powerhouse operations have very little impact on the bubbles. Comparing varying river flowrates shows that more bubbles of all sizes are produced and those bubbles are carried further downstream of the dam for higher total river flows. Figures G29 to G35 show the remaining bubble diameter isosurface plots.

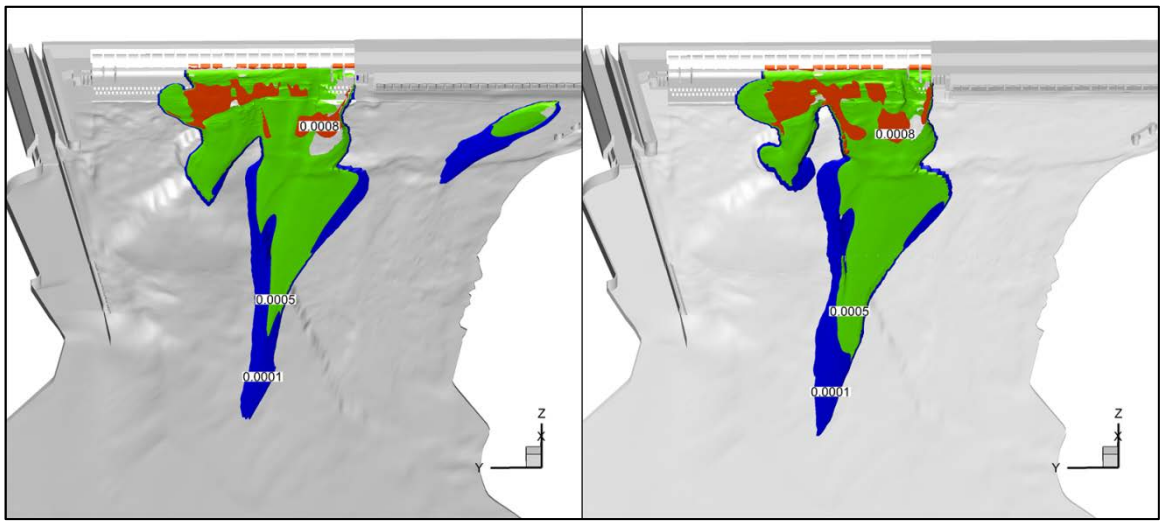

Figure 6.17 Isosurfaces of Bubble Diameter for Simulations 9 (left) and 10 (right).

6.7 Results Summary

The VOF model for the 16 simulations was run, and the free surfaces for the varying total river flows were extracted and used to generate a rigid-lid grid with the free surface approximation. Sixteen rigid-lid simulations were performed to compare the

operational effects on TDG production and fish exposure to predator habitats. A statistical model was used with a lagrangian particle tracking model to calculate risk percentages for simulated fish trajectories.

When comparing plots of TDG production, some fairly clear trends can be seen. The existing operation (odd numbered simulations) operate with more powerhouse units, thus the average flowrate in each powerhouse is lower when comparing to proposed operational conditions (even number simulations). These lower flowrates cause entrainment of the powerhouse flows into the spillway region to happen much closer to the dam. The effect is higher production of TDG due to the increased amount of water in the spill region. On the other hand, the proposed operation operates with higher powerhouse velocities in the northern units. In these situations, the water from the powerhouse region is entrained further downstream of the dam. The effect of this delayed entrainment is the lower TDG concentrated powerhouse water mixes with the high concentrations in the spillway region causing the overall TDG levels to decrease.

Comparing different seasonal operations for the same river flow, for example Simulations 5 and 6 (summer), to Simulations 11 and 12 (spring) also leads to some conclusions. Summer operations have larger spillway flowrates in the region of most TDG production, spillways 18-22, closest to the powerhouse. TDG levels for the summer operations are slightly higher because of these operational conditions. The spring simulations utilize the top spill weirs to aid in fish passage. The effectiveness of these weirs on aiding fish passage is not known to the author and was not considered in this thesis. While individually the TSWs have higher flowrates, the overall flowrate of spillways close to the powerhouse is lower, thus reducing TDG production.

There is little visible evidence when examining the specific zones associated as high risk from normal to proposed operational conditions. However, the trajectories of the simulated fish can change significantly. For instance, the higher flowrates in powerhouses for the proposed cases provide increased velocities, which decrease the time simulated fish spend in dangerous areas of low velocity in that region. When comparing seasonal operations, the effect of closing a spillway gate completely has a greater effect than operating with more, albeit with lower flowrates, spillway gates open. This effect can be seen when comparing again Simulations 5 and 6 with 11 and 12. Exposure percentages are higher for 11 and 12 where the spillways have higher average flowrates, but three gates are closed when compared to Simulations 5 and 6 that have no closed gates.

CHAPTER VII

CONCLUSIONS AND FUTURE WORK

7.1 Conclusions

Two-phase flow models were developed and calibrated in this thesis and used to predict the hydrodynamics, TDG distribution and flow exposure to predator habitat in McNary Dam. A mixture model that takes into account the effect of the bubbles on the flow field and turbulence was used. Two transport equations were used to predict TDG and bubble number density. Variable bubble size was used to compute dissolution and the consequent source of TDG. The model uses an anisotropic RSM turbulence model with attenuation of normal fluctuations at the free surface. A Lagrangian model is incorporated to compute exposure to velocity, water depth and distance to the shore.

New boundary conditions were implemented to capture the water contraction downstream of spillway gates and velocities in the spillway face. A grid refinement study was performed in which four grids were generated to compare predicted velocity data against velocity data collected on April 2, 2000 and June 4, 2004. The grid refinement study was also used to analyze the effect of grid density on TDG production. Good agreement was seen when comparing the numerical and field data, although the model tended to under predict velocities due to complexities in correctly predicting the free surface elevation. Grid density had little effect on production and distribution of TDG as average TDG calculations at the domain's outlet for all four grids were within 1.435% of each other. The effect of grid refinement on the velocity could not be determined however as with increasing refinement numerical data did not converge to the field data. The medium grid was selected for the predictive simulations. The gas volume fraction at

the spillway inlet was adjusted to fit TDG field data measured on February 12, 1997. The model was able to replicate TDG field data within 3% of error.

Eight operational conditions, with two different fish outfalls, were numerically evaluated. High velocities are observed in the center of the dam due to strong surface jets created in the southern spillway bays. In the proposed operation, powerhouse flows from the northern units are entrained by spillway jets contributing to high velocity flows downstream of the dam. A low-velocity eddy is formed in the deepest central region of the spillway at about 1000 ft from the dam. The velocity of spillway jets from central bays is significantly reduced in this region. According to the model, the proposed fish passage releases fish in a region of high velocity and far from the shore minimizing exposure to predator criteria. The approach presented in this thesis is a first step for evaluation of threats suffered by fish in the McNary tailrace. This approach can be further improved incorporating predator-prey models to evaluate probability of fish survival under different operational conditions.

After completion of the predictive simulations, it was determined that existing operations consistently produced higher levels of TDG due to increased entrainment of the powerhouse flows into the spillway regions. It was also found that with increasing total river flows, TDG levels increased. On average, summer operations had higher TDG than spring due to the higher spillway flowrates. The existing outfall relocated fish from upstream of the dam into as region of low velocity near the north shore, two criteria of a predation zone. The relocated outfall transported fish to a region of high velocity in the center of the tailrace, a safer zone from predators but into a region with significantly

higher TDG: TDG produced in the spillway region and transported down the central channel of the tailrace.

Predation zones were similar for all simulations, but particle statistics varied depending on operational conditions. In general, particles were safer for higher flowrates as fewer low velocity eddies where particles could be trapped formed in simulations with high flowrates. The same higher powerhouse flowrates for proposed operations that reduced entrainment and helped lower TDG levels also provide higher velocities for fish passing through the powerhouse regions.

7.2 Future Work

The following recommendations are included as suggestions for future work that would improve on the findings of this thesis.

Fish-predator interactions:

The inclusion of a fish movement model that includes migration rules as well as behavioral reactions to predators to simulate the fish in place of inert particles would provide significantly more insight as to the statistical dangers faced by fish in the McNary dam tailrace. Furthermore, the creation of a predator-pray model to simulate the action of birds and their ability to hunt the simulated fish would provide further insight into the true level of dangers fish are exposed to from avian predators. The combination of these models would also provide a way to validate the criteria that denotes a predator region used in this thesis.

Free surface for TDG model:

The use of an unsteady model that is capable of simultaneously predicting free surface shapes and hydrodynamics along with TDG would provide an increased level of accuracy of the TDG distribution within the McNary dam tailrace.

Field Data:

Increased levels of detail are required in the TDG, velocity and especially bathymetry measurements. It was shown that errors in the bathymetry greatly affect model results, increasing uncertainties when comparing model results with the field data.

REFERENCES

Beeman J.W., Venditti D.A., Moris R.G., Gadomski D.M., Adams B.J., Vanderkooi S.P., Robinson T.C., and Maule A.G. 2003. Gas Bubble Disease in Resident Fish Below Grand Coulee Dam. http://wfrc.usgs.gov/products/reportpdf/usgsfrgbdgrandcouleedam.pdf

Gulliver, J.S., Hibbs, D.E. and McDonald, J.P. (1997)."Measurement of effective saturation concentration for gas transfer." Journal of Hydraulic Engineering, 123(2): 86-97.

Lackey, Robert T. 2003. Pacific Northwest Salmon: Forecasting Their Status in 2100. Reviews in Fisheries Science. 11(1): 35-88.

McGrath K.E., Dawley E.M., Geist D.R., 2006. Total Dissolved Gas effects on Fishes of the Lower Columbia River. PNNL-15525 Final Report, U.S. Army Corps of Engineers.

Meyers T., Burton T., Bentz C., and Starkey N., 2008.Common Diseases of Wild and Cultured Fishes in Alaska. Alaska Department of Fish and Game Fish Pathology Laboratories.http://www.adfg.alaska.gov/static/species/disease/pdfs/fish_disease_book.pdf

Morsi, S. A., and Alexander, A. J., 1972.An Investigation of Particle Trajectories in Two-Phase Flow Systems. Journal of Fluid Mechanics. 55(2),193-208.

National Marine and Fisheries Service. (1995). Proposed Recovery Plan for Snake River Salmon. National Oceanic and Atmospheric Administration

Oregon Department of Environmental Quality and Washington State Department of Ecology, 2002.Total Maximum Daily Load (TMDL) for Lower Columbia River Total Dissolved Gas. http://www.ecy.wa.gov/pubs/0203004.pdf.

Politano M., and Dvorak J., Computational Fluid Dynamics (CFD) Modeling to Support the Reduction of Fish Passage Exposure to Predator Habitat at McNary Dam. IIHR LDR 377.

Politano M., Fu X., Luellen L. and Weber L. 2009. Computational Fluid Dynamics Model to Evaluate Total Dissolved Gas Field within the Tailrace at McNary Dam. IIHR LDR 359.

Politano M. and Laughery R., 2010.Prediction of the Hydrodynamics and Total Dissolved Gas in the Tailrace of McNary Dam. Hydrovision Conference.

Politano M., 2011. Computational Fluid Dynamics (CFD) Modeling to Support Development of Surface Passage Alternatives at McNary Dam. Tailrace Simulations. 2011. IIHR Letter Report.

Swanson C., Young P.S., Cech J. J., 1998. Swimming Performance of Delta Smelt: Maximum Performance, and Kinematic Limitations on Swimming at Submaximal Velocities. The Journal of Experimental Biology 201, 333-345.

Turan C., Politano M., Carrica P. M. and Weber L., (2007) Water Entrainment Due to Spillway Surface Jets. International Journal of Computational Fluid Dynamics, 21:3, 137-153

USACE, Scope of Work for CFD Modeling to Support the Reduction of Fish Passage Exposure to Predator Habitat at McNary Dam 2011. Ecological Applications. 18(3),681-700.

Weber L., Huang H., Lai Y. & McCoy A. (2004). "Modeling Total Dissolved Gas Production and Transport Downstream of Spillways: Three-Dimensional Development and Applications," Int. J. of River Basin Management. 2, 3, 157-16.

Wiese F.K., Parrish J.K., Thompson C.W., and Maranto C., 2008. Ecosystem-Based Management of Predator-Prey Relationships: Piscivorous Birds and Salmonids.

Wilhelms, S.C., and Schneider M.L. (1997).Near-field study of TDG in the McNary spillway. CEWES-CR-F Memorandum for Record dated August 22 1997, U.S. Army Engineer Waterways Experiment Station.

Wilhelms, S.C. (2005). Draft data documentation for field investigation at McNary Dam. CEERD-HC-IE Memorandum for Record dated May 20 2005, Coastal and Hydraulics Laboratory.

APPENDIX A. SIMULATION CONDITIONS

Table A1. Operational Conditions for Simulations 1 and 2

Simulation 1														
Total River Flow: 100.7 kcfs - Tailwater Elevation: 264.7 fmsl														
Powerhouse Unit Discharge (kcfs)														
Total	U1	U2	U3	U4	U5	U6	U7	U8	U9	U10	U11	U12	U13	U14
	8.33	8.33	8.33	8.33	0	0	0	0	0	0	0	0	8.33	8.33
North	U1	U2	U3	U4	U5	U6	U7	U8	U9	U10	U11	U12	U13	U14
Unit	2.0825	2.0825	2.0825	2.0825	0	0	0	0	0	0	0	0	2.0825	2.0825
South	U1	U2	U3	U4	U5	U6	U7	U8	U9	U10	U11	U12	U13	U14
Unit	6.2475	6.2475	6.2475	6.2475	0	0	0	0	0	0	0	0	6.2475	6.2475
Powerhouse Total: 50.0 (kcfs)														
Spillway Unit Discharge (kcfs)														
	S1	S2	S3	S4	S5	S6	S7	S8	S9	S10	S11			
	3.9	3.9	3.9	0	2.01	0	2.01	0	0	0	2.01			
	S12	S13	S14	S15	S16	S17	S18	S19	S20	S21	S22			
	0	0	0	2.01	2.01	3.9	8.8	0	8.8	3.9	2.01			
Spillway Total: 49.1 (kcfs)														

Simulation 2														
Total River Flow: 100.7 kcfs - Tailwater Elevation: 264.7 fmsl														
Powerhouse Unit Discharge (kcfs)														
Total	U1	U2	U3	U4	U5	U6	U7	U8	U9	U10	U11	U12	U13	U14
	8.53	0	0	0	0	0	0	0	0	0	8.53	8.53	12.2	12.2
North	U1	U2	U3	U4	U5	U6	U7	U8	U9	U10	U11	U12	U13	U14
Unit	2.1325	0	0	0	0	0	0	0	0	0	2.1325	2.1325	3.05	3.05
South	U1	U2	U3	U4	U5	U6	U7	U8	U9	U10	U11	U12	U13	U14
Unit	6.3975	0	0	0	0	0	0	0	0	0	6.3975	6.3975	9.15	9.15
Powerhouse Total: 50.0 (kcfs)														
Spillway Unit Discharge (kcfs)														
	S1	S2	S3	S4	S5	S6	S7	S8	S9	S10	S11			
	3.9	3.9	3.9	0	2.01	0	2.01	0	0	0	2.01			
	S12	S13	S14	S15	S16	S17	S18	S19	S20	S21	S22			
	0	0	0	2.01	2.01	3.9	8.8	0	8.8	3.9	2.01			
Spillway Total: 49.1 (kcfs)														

Table A2. Operational Conditions for Simulations 3 and 4

Simulation 3														
Total River Flow: 150.8 kcfs - Tailwater Elevation: 265.4 fmsl														
Powerhouse Unit Discharge (kcfs)														
Total	**U1**	**U2**	**U3**	**U4**	**U5**	**U6**	**U7**	**U8**	**U9**	**U10**	**U11**	**U12**	**U13**	**U14**
	8.33	8.33	8.33	8.33	0	0	0	0	0	8.33	8.33	8.33	8.33	8.33
North	**U1**	**U2**	**U3**	**U4**	**U5**	**U6**	**U7**	**U8**	**U9**	**U10**	**U11**	**U12**	**U13**	**U14**
Unit	2.0825	2.0825	2.0825	2.0825	0	0	0	0	0	2.0825	2.0825	2.0825	2.0825	2.0825
South	**U1**	**U2**	**U3**	**U4**	**U5**	**U6**	**U7**	**U8**	**U9**	**U10**	**U11**	**U12**	**U13**	**U14**
Unit	6.2475	6.2475	6.2475	6.2475	0	0	0	0	0	6.2475	6.2475	6.2475	6.2475	6.2475
Powerhouse Total: 75.0 (kcfs)														
Spillway Unit Discharge (kcfs)														
		S1	**S2**	**S3**	**S4**	**S5**	**S6**	**S7**	**S8**	**S9**	**S10**	**S11**		
		4.75	3.9	5.57	2.01	2.01	2.01	3.9	2.01	2.01	2.01	3.9		
		S12	**S13**	**S14**	**S15**	**S16**	**S17**	**S18**	**S19**	**S20**	**S21**	**S22**		
		2.01	2.01	2.01	2.01	2.01	4.75	8.8	0	8.8	3.9	3.9		
Spillway Total: 74.2 (kfcs)														

Simulation 4														
Total River Flow: 150.8 kcfs - Tailwater Elevation: 265.4 fmsl														
Powerhouse Unit Discharge (kcfs)														
Total	**U1**	**U2**	**U3**	**U4**	**U5**	**U6**	**U7**	**U8**	**U9**	**U10**	**U11**	**U12**	**U13**	**U14**
	8.73	0	0	0	0	0	0	0	8.73	8.73	12.2	12.2	12.2	12.2
North	**U1**	**U2**	**U3**	**U4**	**U5**	**U6**	**U7**	**U8**	**U9**	**U10**	**U11**	**U12**	**U13**	**U14**
Unit	2.1825	0	0	0	0	0	0	0	2.1825	2.1825	3.05	3.05	3.05	3.05
South	**U1**	**U2**	**U3**	**U4**	**U5**	**U6**	**U7**	**U8**	**U9**	**U10**	**U11**	**U12**	**U13**	**U14**
Unit	6.5475	0	0	0	0	0	0	0	6.5475	6.5475	9.15	9.15	9.15	9.15
Powerhouse Total: 75.0 (kcfs)														
Spillway Unit Discharge (kcfs)														
		S1	**S2**	**S3**	**S4**	**S5**	**S6**	**S7**	**S8**	**S9**	**S10**	**S11**		
		4.75	3.9	5.57	2.01	2.01	2.01	3.9	2.01	2.01	2.01	3.9		
		S12	**S13**	**S14**	**S15**	**S16**	**S17**	**S18**	**S19**	**S20**	**S21**	**S22**		
		2.01	2.01	2.01	2.01	2.01	4.75	8.8	0	8.8	3.9	3.9		
Spillway Total: 74.2 (kcfs)														

Table A3. Operational Conditions for Simulations 5 and 6

Simulation 5														
Total River Flow: 201.5 kcfs - Tailwater Elevation: 266.3 fmsl														
Powerhouse Unit Discharge (kcfs)														
Total	**U1**	**U2**	**U3**	**U4**	**U5**	**U6**	**U7**	**U8**	**U9**	**U10**	**U11**	**U12**	**U13**	**U14**
	8.33	8.33	8.33	8.33	0	0	8.33	8.33	8.33	8.33	8.33	8.33	8.33	8.33
North	**U1**	**U2**	**U3**	**U4**	**U5**	**U6**	**U7**	**U8**	**U9**	**U10**	**U11**	**U12**	**U13**	**U14**
Unit	2.0825	2.0825	2.0825	2.0825	0	0	2.0825	2.0825	2.0825	2.0825	2.0825	2.0825	2.0825	2.0825
South	**U1**	**U2**	**U3**	**U4**	**U5**	**U6**	**U7**	**U8**	**U9**	**U10**	**U11**	**U12**	**U13**	**U14**
Unit	6.2475	6.2475	6.2475	6.2475	0	0	6.2475	6.2475	6.2475	6.2475	6.2475	6.2475	6.2475	6.2475
Powerhouse Total: 100.0 (kcfs)														
Spillway Unit Discharge (kcfs)														
		S1	**S2**	**S3**	**S4**	**S5**	**S6**	**S7**	**S8**	**S9**	**S10**	**S11**		
		4.75	3.9	5.57	2.01	3.9	3.9	3.9	2.01	3.9	3.9	3.9		
		S12	**S13**	**S14**	**S15**	**S16**	**S17**	**S18**	**S19**	**S20**	**S21**	**S22**		
		3.9	3.9	2.01	3.9	3.9	4.75	8.8	8.8	8.8	4.75	4.75		
Spillway Total: 99.9 (kcfs)														

Simulation 6														
Total River Flow: 201.5 kcfs - Tailwater Elevation: 266.3 fmsl														
Powerhouse Unit Discharge (kcfs)														
Total	**U1**	**U2**	**U3**	**U4**	**U5**	**U6**	**U7**	**U8**	**U9**	**U10**	**U11**	**U12**	**U13**	**U14**
	8.93	0	0	0	0	0	8.93	8.93	12.2	12.2	12.2	12.2	12.2	12.2
North	**U1**	**U2**	**U3**	**U4**	**U5**	**U6**	**U7**	**U8**	**U9**	**U10**	**U11**	**U12**	**U13**	**U14**
Unit	2.2325	0	0	0	0	0	2.2325	2.2325	3.05	3.05	3.05	3.05	3.05	3.05
South	**U1**	**U2**	**U3**	**U4**	**U5**	**U6**	**U7**	**U8**	**U9**	**U10**	**U11**	**U12**	**U13**	**U14**
Unit	6.6975	0	0	0	0	0	6.6975	6.6975	9.15	9.15	9.15	9.15	9.15	9.15
Powerhouse Total: 100.0 (kcfs)														
Spillway Unit Discharge (kcfs)														
		S1	**S2**	**S3**	**S4**	**S5**	**S6**	**S7**	**S8**	**S9**	**S10**	**S11**		
		4.75	3.9	5.57	2.01	3.9	3.9	3.9	2.01	3.9	3.9	3.9		
		S12	**S13**	**S14**	**S15**	**S16**	**S17**	**S18**	**S19**	**S20**	**S21**	**S22**		
		3.9	3.9	2.01	3.9	3.9	4.75	8.8	8.8	8.8	4.75	4.75		
Spillway Total: 99.9 (kcfs)														

Table A4. Operational Conditions for Simulations 7 and 8

Simulation 7														
Total River Flow: 253.3 kcfs - Tailwater Elevation: 267.4 fmsl														
Powerhouse Unit Discharge (kcfs)														
Total	U1	U2	U3	U4	U5	U6	U7	U8	U9	U10	U11	U12	U13	U14
	9	9	9	9	9	9	9	9	9	9	9	9	9	9
North	U1	U2	U3	U4	U5	U6	U7	U8	U9	U10	U11	U12	U13	U14
Unit	2.25	2.25	2.25	2.25	2.25	2.25	2.25	2.25	2.25	2.25	2.25	2.25	2.25	2.25
South	U1	U2	U3	U4	U5	U6	U7	U8	U9	U10	U11	U12	U13	U14
Unit	6.75	6.75	6.75	6.75	6.75	6.75	6.75	6.75	6.75	6.75	6.75	6.75	6.75	6.75
Powerhouse Total: 126.0 (kcfs)														
Spillway Unit Discharge (kcfs)														
		S1	S2	S3	S4	S5	S6	S7	S8	S9	S10	S11		
		4.75	4.75	7.2	4.75	5.57	4.75	5.57	4.75	5.57	4.75	5.57		
		S12	S13	S14	S15	S16	S17	S18	S19	S20	S21	S22		
		4.75	5.57	4.75	4.75	4.75	6.4	8.8	8.8	8.8	5.57	4.75		
Spillway Total: 125.7 (kcfs)														

Simulation 8														
Total River Flow: 253.3 kcfs - Tailwater Elevation: 267.4 fmsl														
Powerhouse Unit Discharge (kcfs)														
Total	U1	U2	U3	U4	U5	U6	U7	U8	U9	U10	U11	U12	U13	U14
	8.1	0	0	0	8.1	12.2	12.2	12.2	12.2	12.2	12.2	12.2	12.2	12.2
North	U1	U2	U3	U4	U5	U6	U7	U8	U9	U10	U11	U12	U13	U14
Unit	2.025	0	0	0	2.025	3.05	3.05	3.05	3.05	3.05	3.05	3.05	3.05	3.05
South	U1	U2	U3	U4	U5	U6	U7	U8	U9	U10	U11	U12	U13	U14
Unit	6.075	0	0	0	6.075	9.15	9.15	9.15	9.15	9.15	9.15	9.15	9.15	9.15
Powerhouse Total: 126.0 (kcfs)														
Spillway Unit Discharge (kcfs)														
		S1	S2	S3	S4	S5	S6	S7	S8	S9	S10	S11		
		4.75	4.75	7.2	4.75	5.57	4.75	5.57	4.75	5.57	4.75	5.57		
		S12	S13	S14	S15	S16	S17	S18	S19	S20	S21	S22		
		4.75	5.57	4.75	4.75	4.75	6.4	8.8	8.8	8.8	5.57	4.75		
Spillway Total: 125.7 (kcfs)														

Table A5. Operational Conditions for Simulations 9 and 10

Simulation 9														
Total River Flow: 152.5 kcfs - Tailwater Elevation: 265.5 fmsl														
Powerhouse Unit Discharge (kcfs)														
Total	**U1**	**U2**	**U3**	**U4**	**U5**	**U6**	**U7**	**U8**	**U9**	**U10**	**U11**	**U12**	**U13**	**U14**
	8.18	8.18	8.18	8.18	0	0	0	8.18	8.18	8.18	8.18	8.18	8.18	8.18
North	**U1**	**U2**	**U3**	**U4**	**U5**	**U6**	**U7**	**U8**	**U9**	**U10**	**U11**	**U12**	**U13**	**U14**
Unit	2.045	2.045	2.045	2.045	0	0	0	2.045	2.045	2.045	2.045	2.045	2.045	2.045
South	**U1**	**U2**	**U3**	**U4**	**U5**	**U6**	**U7**	**U8**	**U9**	**U10**	**U11**	**U12**	**U13**	**U14**
Unit	6.135	6.135	6.135	6.135	0	0	0	6.135	6.135	6.135	6.135	6.135	6.135	6.135
Powerhouse Total: 89.98 (kcfs)														
Spillway Unit Discharge (kcfs)														
		S1	**S2**	**S3**	**S4**	**S5**	**S6**	**S7**	**S8**	**S9**	**S10**	**S11**		
		0	0	0	0	0	0	0	0	3.9	3.9	3.9		
		S12	**S13**	**S14**	**S15**	**S16**	**S17**	**S18**	**S19**	**S20**	**S21**	**S22**		
		0	3.9	3.9	3.9	3.9	3.9	3.9	9.01	9.01	3.9	3.9		
Spillway Total: 60.92 (kcfs)														

Simulation 10														
Total River Flow: 152.5 kcfs - Tailwater Elevation: 265.5 fmsl														
Powerhouse Unit Discharge (kcfs)														
Total	**U1**	**U2**	**U3**	**U4**	**U5**	**U6**	**U7**	**U8**	**U9**	**U10**	**U11**	**U12**	**U13**	**U14**
	8.4	0	0	0	0	0	0	8.4	12.2	12.2	12.2	12.2	12.2	12.2
North	**U1**	**U2**	**U3**	**U4**	**U5**	**U6**	**U7**	**U8**	**U9**	**U10**	**U11**	**U12**	**U13**	**U14**
Unit	2.1	0	0	0	0	0	0	2.1	3.05	3.05	3.05	3.05	3.05	3.05
South	**U1**	**U2**	**U3**	**U4**	**U5**	**U6**	**U7**	**U8**	**U9**	**U10**	**U11**	**U12**	**U13**	**U14**
Unit	6.3	0	0	0	0	0	0	6.3	9.15	9.15	9.15	9.15	9.15	9.15
Powerhouse Total: 90.0 (kcfs)														
Spillway Unit Discharge (kcfs)														
		S1	**S2**	**S3**	**S4**	**S5**	**S6**	**S7**	**S8**	**S9**	**S10**	**S11**		
		0	0	0	0	0	0	0	0	0	3.9	3.9		
		S12	**S13**	**S14**	**S15**	**S16**	**S17**	**S18**	**S19**	**S20**	**S21**	**S22**		
		0	3.9	3.9	3.9	3.9	3.9	3.9	3.9	9.01	9.01	3.9		
Spillway Total: 60.9 (kcfs)														

Table A6. Operational Conditions for Simulations 11 and 12

Simulation 11														
Total River Flow: 201.7 kcfs - Tailwater Elevation: 266.3 fmsl														
Powerhouse Unit Discharge (kcfs)														
Total	**U1**	**U2**	**U3**	**U4**	**U5**	**U6**	**U7**	**U8**	**U9**	**U10**	**U11**	**U12**	**U13**	**U14**
	8.57	8.57	8.57	8.57	8.57	8.57	8.57	8.57	8.57	8.57	8.57	8.57	8.57	8.57
North	**U1**	**U2**	**U3**	**U4**	**U5**	**U6**	**U7**	**U8**	**U9**	**U10**	**U11**	**U12**	**U13**	**U14**
Unit	2.1425	2.1425	2.1425	2.1425	2.1425	2.1425	2.1425	2.1425	2.1425	2.1425	2.1425	2.1425	2.1425	2.1425
South	**U1**	**U2**	**U3**	**U4**	**U5**	**U6**	**U7**	**U8**	**U9**	**U10**	**U11**	**U12**	**U13**	**U14**
Unit	6.4275	6.4275	6.4275	6.4275	6.4275	6.4275	6.4275	6.4275	6.4275	6.4275	6.4275	6.4275	6.4275	6.4275
Powerhouse Total: 119.98 (kcfs)														
Spillway Unit Discharge (kcfs)														
		S1	**S2**	**S3**	**S4**	**S5**	**S6**	**S7**	**S8**	**S9**	**S10**	**S11**		
		4.75	3.9	6.4	0	3.9	2.01	3.9	0	3.9	2.01	3.9		
		S12	**S13**	**S14**	**S15**	**S16**	**S17**	**S18**	**S19**	**S20**	**S21**	**S22**		
		0	3.9	2.01	3.9	2.01	3.9	3.9	9.01	9.01	3.9	3.9		
Spillway Total: 80.11 (kcfs)														

Simulation 12														
Total River Flow: 201.7 kcfs - Tailwater Elevation: 266.3 fmsl														
Powerhouse Unit Discharge (kcfs)														
Total	**U1**	**U2**	**U3**	**U4**	**U5**	**U6**	**U7**	**U8**	**U9**	**U10**	**U11**	**U12**	**U13**	**U14**
	8.65	0	0	0	8.65	8.65	8.65	12.2	12.2	12.2	12.2	12.2	12.2	12.2
North	**U1**	**U2**	**U3**	**U4**	**U5**	**U6**	**U7**	**U8**	**U9**	**U10**	**U11**	**U12**	**U13**	**U14**
Unit	2.1625	0	0	0	2.1625	2.1625	2.1625	3.05	3.05	3.05	3.05	3.05	3.05	3.05
South	**U1**	**U2**	**U3**	**U4**	**U5**	**U6**	**U7**	**U8**	**U9**	**U10**	**U11**	**U12**	**U13**	**U14**
Unit	6.4875	0	0	0	6.4875	6.4875	6.4875	9.15	9.15	9.15	9.15	9.15	9.15	9.15
Powerhouse Total: 120.0 (kcfs)														
Spillway Unit Discharge (kcfs)														
		S1	**S2**	**S3**	**S4**	**S5**	**S6**	**S7**	**S8**	**S9**	**S10**	**S11**		
		4.75	3.9	6.4	0	3.9	2.01	3.9	0	3.9	2.01	3.9		
		S12	**S13**	**S14**	**S15**	**S16**	**S17**	**S18**	**S19**	**S20**	**S21**	**S22**		
		0	3.9	2.01	3.9	2.01	3.9	2.01	9.01	9.01	3.9	3.9		
Spillway Total: 80.1 (kcfs)														

Table A7. Operational Conditions for Simulations 13 and 14

Simulation 13														
Total River Flow: 250.7 kcfs - Tailwater Elevation: 267.3 fmsl														
Powerhouse Unit Discharge (kcfs)														
Total	**U1**	**U2**	**U3**	**U4**	**U5**	**U6**	**U7**	**U8**	**U9**	**U10**	**U11**	**U12**	**U13**	**U14**
	10.7	10.7	10.7	10.7	10.7	10.7	10.7	10.7	10.7	10.7	10.7	10.7	10.7	10.7
North	**U1**	**U2**	**U3**	**U4**	**U5**	**U6**	**U7**	**U8**	**U9**	**U10**	**U11**	**U12**	**U13**	**U14**
Unit	2.675	2.675	2.675	2.675	2.675	2.675	2.675	2.675	2.675	2.675	2.675	2.675	2.675	2.675
South	**U1**	**U2**	**U3**	**U4**	**U5**	**U6**	**U7**	**U8**	**U9**	**U10**	**U11**	**U12**	**U13**	**U14**
Unit	8.025	8.025	8.025	8.025	8.025	8.025	8.025	8.025	8.025	8.025	8.025	8.025	8.025	8.025
Powerhouse Total: 149.8 (kcfs)														
Spillway Unit Discharge (kcfs)														
		S1	**S2**	**S3**	**S4**	**S5**	**S6**	**S7**	**S8**	**S9**	**S10**	**S11**		
		4.75	3.9	6.4	2.01	3.9	3.9	3.9	3.9	3.9	3.9	3.9		
		S12	**S13**	**S14**	**S15**	**S16**	**S17**	**S18**	**S19**	**S20**	**S21**	**S22**		
		3.9	3.9	3.9	3.9	3.9	3.9	3.9	9.01	9.01	4.75	4.75		
Spillway Total: 99.18 (kcfs)														

Simulation 14														
Total River Flow: 250.7 kcfs - Tailwater Elevation: 267.3 fmsl														
Powerhouse Unit Discharge (kcfs)														
Total	**U1**	**U2**	**U3**	**U4**	**U5**	**U6**	**U7**	**U8**	**U9**	**U10**	**U11**	**U12**	**U13**	**U14**
	9.33	0	9.33	9.33	12.2	12.2	12.2	12.2	12.2	12.2	12.2	12.2	12.2	12.2
North	**U1**	**U2**	**U3**	**U4**	**U5**	**U6**	**U7**	**U8**	**U9**	**U10**	**U11**	**U12**	**U13**	**U14**
Unit	2.3325	0	2.3325	2.3325	3.05	3.05	3.05	3.05	3.05	3.05	3.05	3.05	3.05	3.05
South	**U1**	**U2**	**U3**	**U4**	**U5**	**U6**	**U7**	**U8**	**U9**	**U10**	**U11**	**U12**	**U13**	**U14**
Unit	6.9975	0	6.9975	6.9975	9.15	9.15	9.15	9.15	9.15	9.15	9.15	9.15	9.15	9.15
Powerhouse Total: 150.0 (kcfs)														
Spillway Unit Discharge (kcfs)														
		S1	**S2**	**S3**	**S4**	**S5**	**S6**	**S7**	**S8**	**S9**	**S10**	**S11**		
		4.75	3.9	6.4	2.01	3.9	3.9	3.9	3.9	3.9	3.9	3.9		
		S12	**S13**	**S14**	**S15**	**S16**	**S17**	**S18**	**S19**	**S20**	**S21**	**S22**		
		3.9	3.9	3.9	3.9	3.9	3.9	3.9	9.01	9.01	4.75	4.75		
Spillway Total: 99.1 (kcfs)														

Table A8. Operational Conditions for Simulations 15 and 16

Simulation 15														
Total River Flow: 301.7 kcfs - Tailwater Elevation: 268.5 fmsl														
Powerhouse Unit Discharge (kcfs)														
Total	**U1**	**U2**	**U3**	**U4**	**U5**	**U6**	**U7**	**U8**	**U9**	**U10**	**U11**	**U12**	**U13**	**U14**
	12.2	12.2	12.2	12.2	12.2	12.2	12.2	12.2	12.2	12.2	12.2	12.2	12.2	12.2
North	**U1**	**U2**	**U3**	**U4**	**U5**	**U6**	**U7**	**U8**	**U9**	**U10**	**U11**	**U12**	**U13**	**U14**
Unit	3.05	3.05	3.05	3.05	3.05	3.05	3.05	3.05	3.05	3.05	3.05	3.05	3.05	3.05
South	**U1**	**U2**	**U3**	**U4**	**U5**	**U6**	**U7**	**U8**	**U9**	**U10**	**U11**	**U12**	**U13**	**U14**
Unit	9.15	9.15	9.15	9.15	9.15	9.15	9.15	9.15	9.15	9.15	9.15	9.15	9.15	9.15
Powerhouse Total: 170.8 (kcfs)														
Spillway Unit Discharge (kcfs)														
	S1	**S2**	**S3**	**S4**	**S5**	**S6**	**S7**	**S8**	**S9**	**S10**	**S11**			
	4.75	4.7	8.8	5.57	5.57	5.57	5.57	5.57	5.57	5.57	5.57			
	S12	**S13**	**S14**	**S15**	**S16**	**S17**	**S18**	**S19**	**S20**	**S21**	**S22**			
	5.57	5.57	4.75	5.57	5.57	5.57	5.57	9.01	9.01	5.57	4.75			
Spillway Total: 129.32 (kcfs)														

Simulation 16														
Total River Flow: 301.7 kcfs - Tailwater Elevation: 268.5 fmsl														
Powerhouse Unit Discharge (kcfs)														
U1	**U2**	**U3**	**U4**	**U5**	**U6**	**U7**	**U8**	**U9**	**U10**	**U11**	**U12**	**U13**	**U14**	**U14**
12.2	12.2	12.2	12.2	12.2	12.2	12.2	12.2	12.2	12.2	12.2	12.2	12.2	12.2	344843.7
U1	**U2**	**U3**	**U4**	**U5**	**U6**	**U7**	**U8**	**U9**	**U10**	**U11**	**U12**	**U13**	**U14**	**U14**
3.05	3.05	3.05	3.05	3.05	3.05	3.05	3.05	3.05	3.05	3.05	3.05	3.05	3.05	86210.93
U1	**U2**	**U3**	**U4**	**U5**	**U6**	**U7**	**U8**	**U9**	**U10**	**U11**	**U12**	**U13**	**U14**	**U14**
9.15	9.15	9.15	9.15	9.15	9.15	9.15	9.15	9.15	9.15	9.15	9.15	9.15	9.15	258632.8
Powerhouse Total: 170.8 (kcfs)														
Spillway Unit Discharge (kcfs)														
S1	**S2**	**S3**	**S4**	**S5**	**S6**	**S7**	**S8**	**S9**	**S10**	**S11**				
4.75	4.7	8.8	5.57	5.57	5.57	5.57	5.57	5.57	5.57	5.57				
S12	**S13**	**S14**	**S15**	**S16**	**S17**	**S18**	**S19**	**S20**	**S21**	**S22**				
5.57	5.57	4.75	5.57	5.57	5.57	5.57	9.01	9.01	5.57	4.75				
Spillway Total: 129.3 (kcfs)														

APPENDIX B. VOF MODEL PLOTS

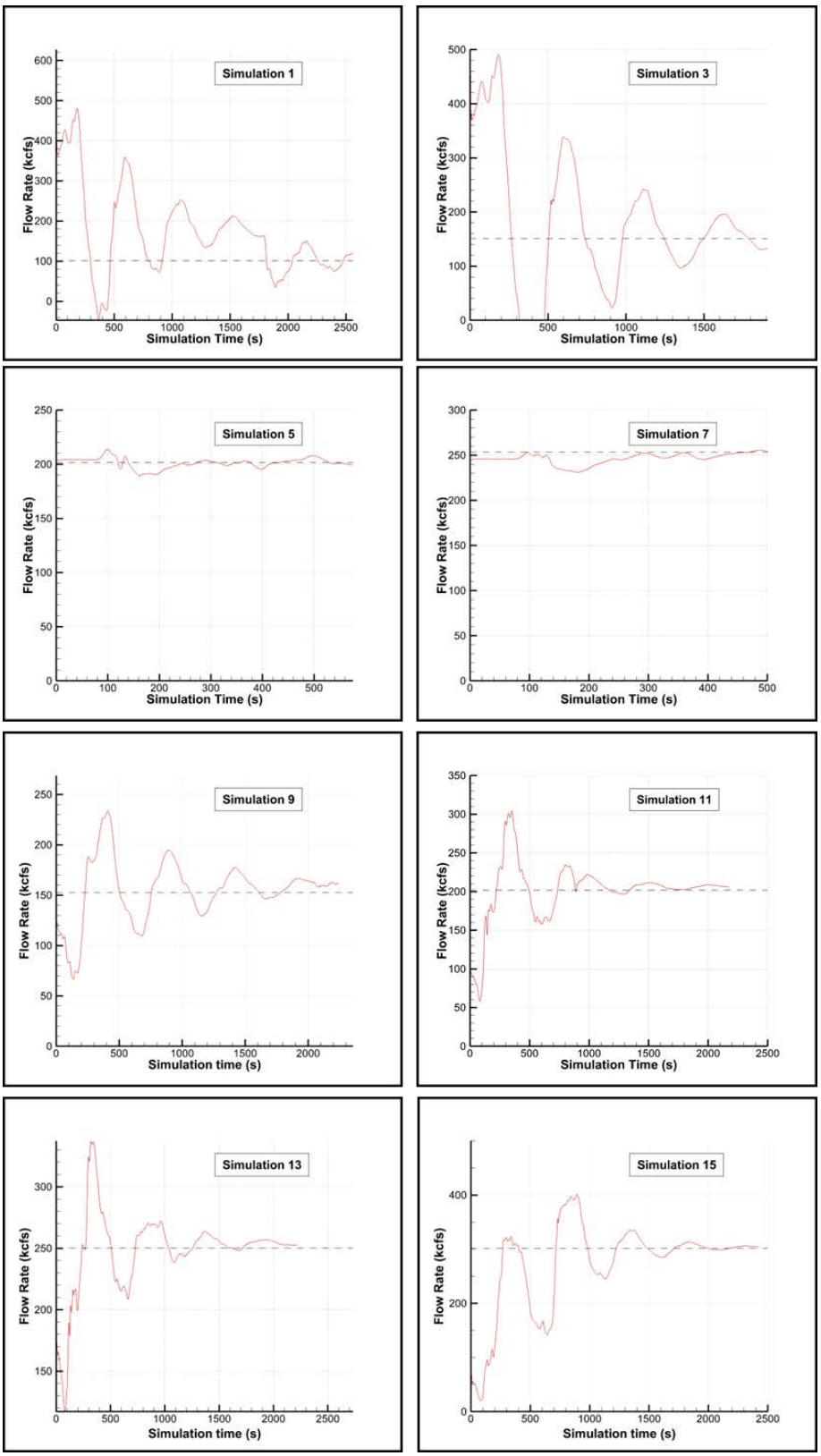

Figure B1. Evolution of Flowrate for the Predictive Simulations

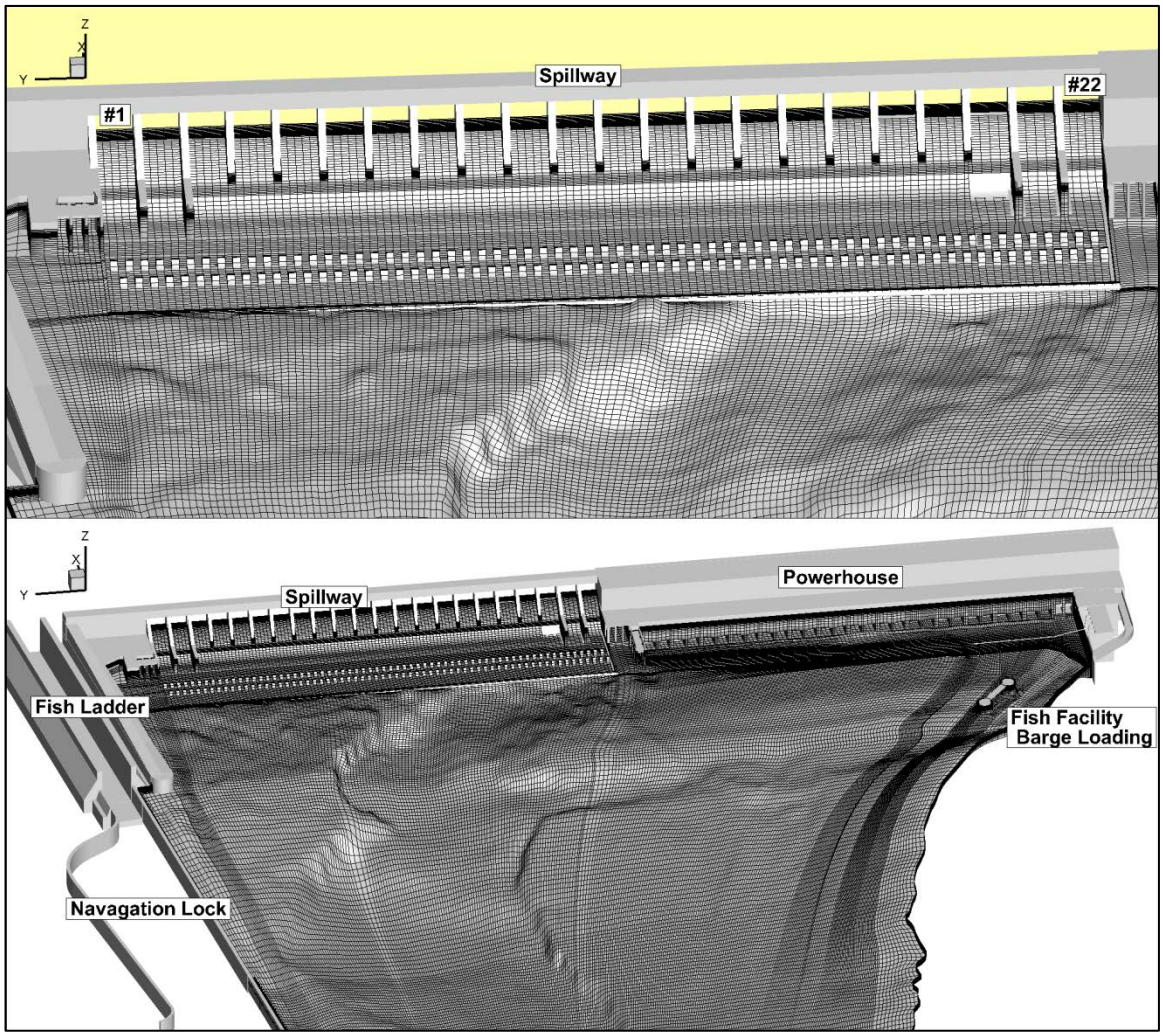

Figure B2. Grid used for the VOF model in simulation 1. Top: detail near the spillway, bottom: entire VOF model

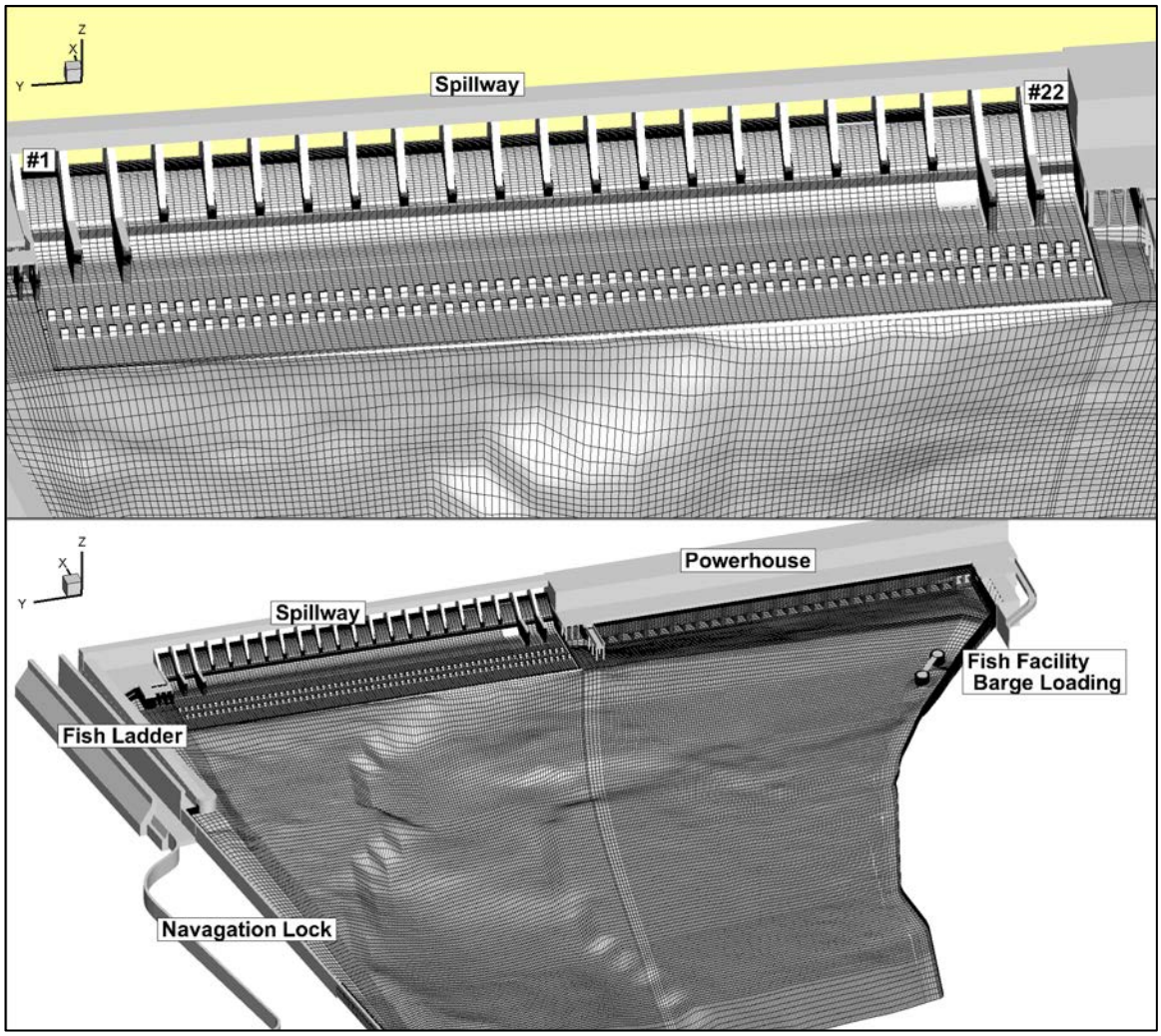

Figure B3. Grid used for the VOF model in simulation 3. Top: detail near the spillway, bottom: entire VOF model

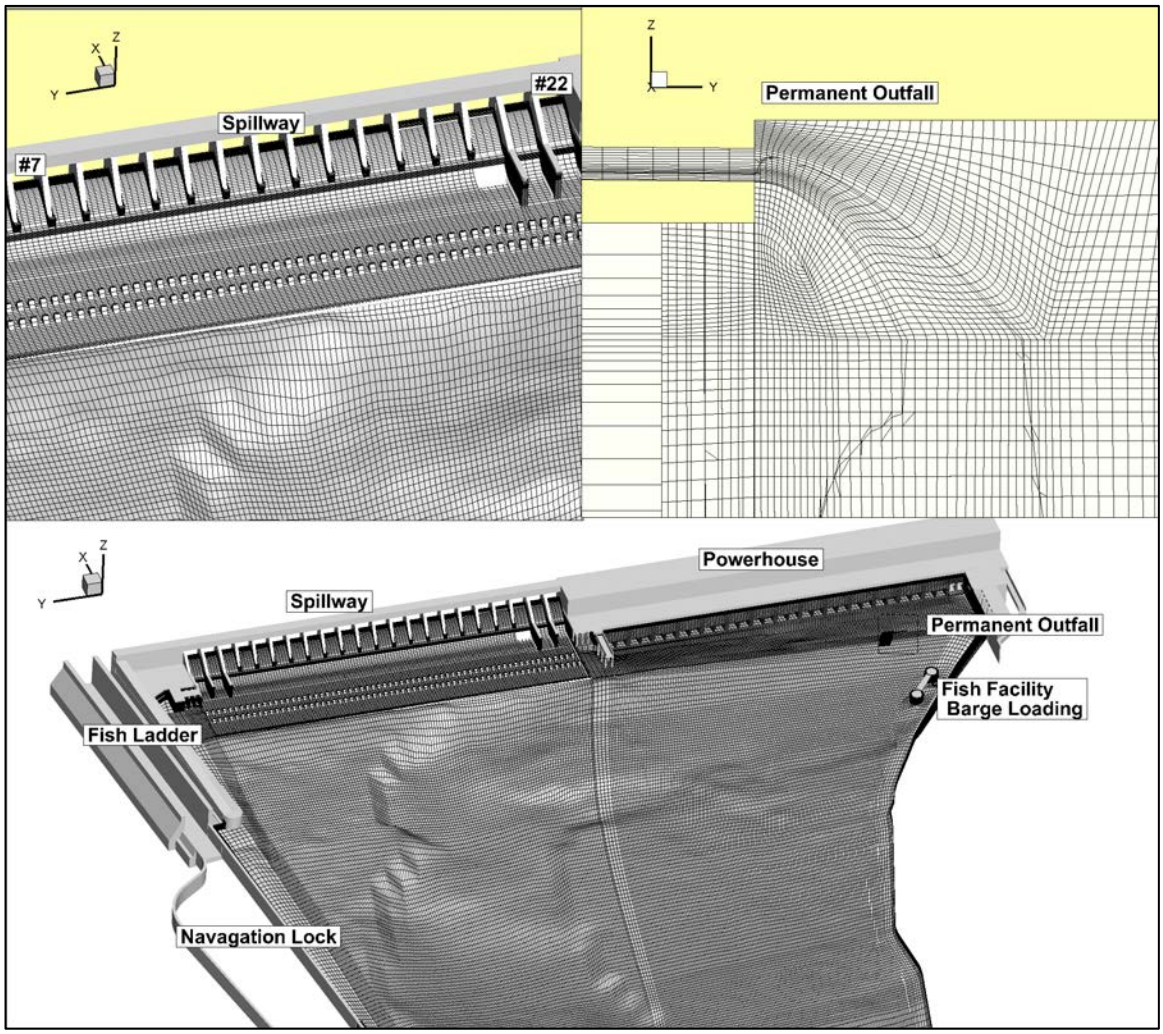

Figure B4. Grid used for the VOF model in simulation 5. Top left: detail near the spillway, top right: current outfall and bottom: entire VOF model

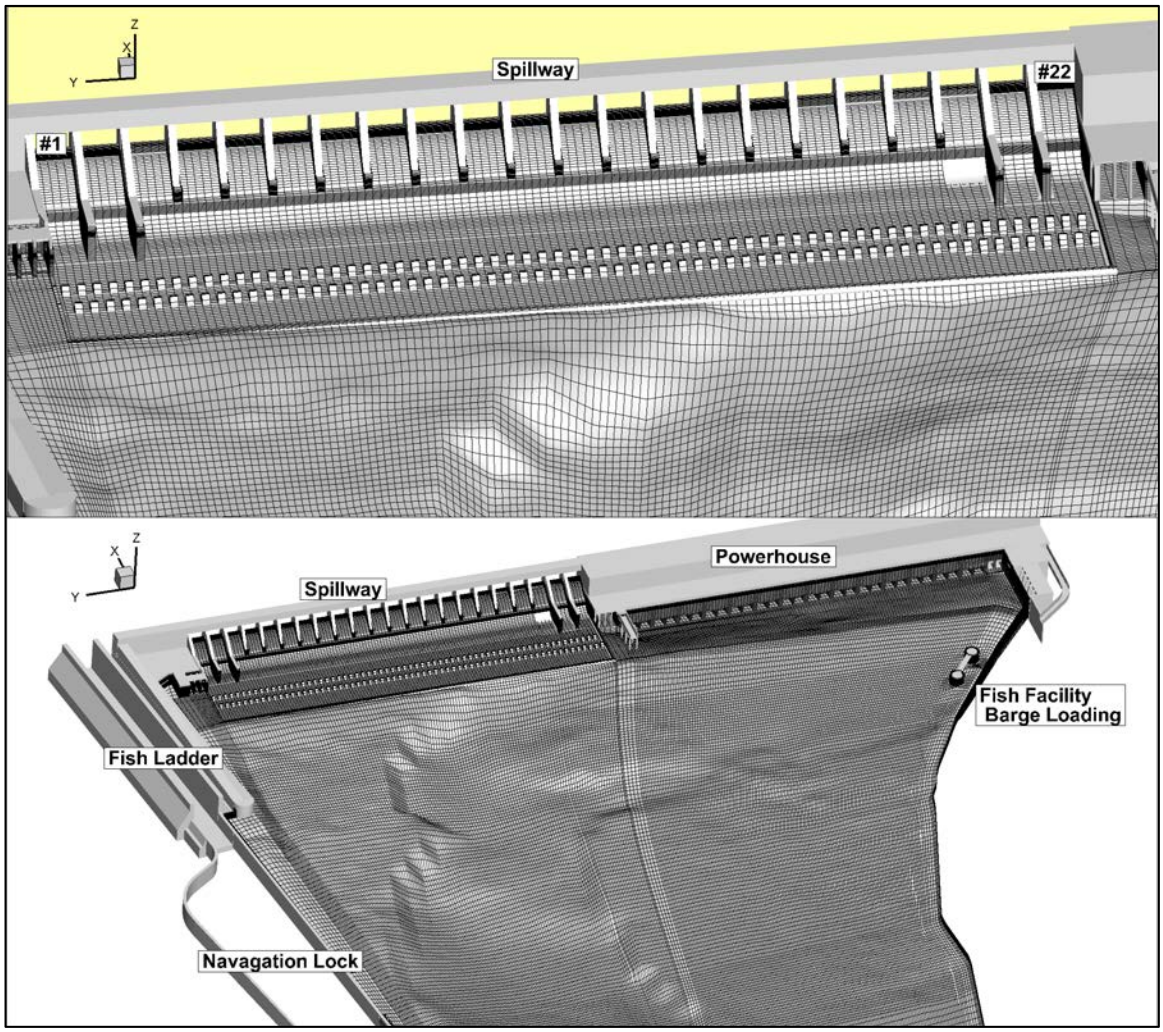

Figure B5. Grid used for the VOF model in simulation 7. Top: detail near the spillway, bottom: entire VOF model

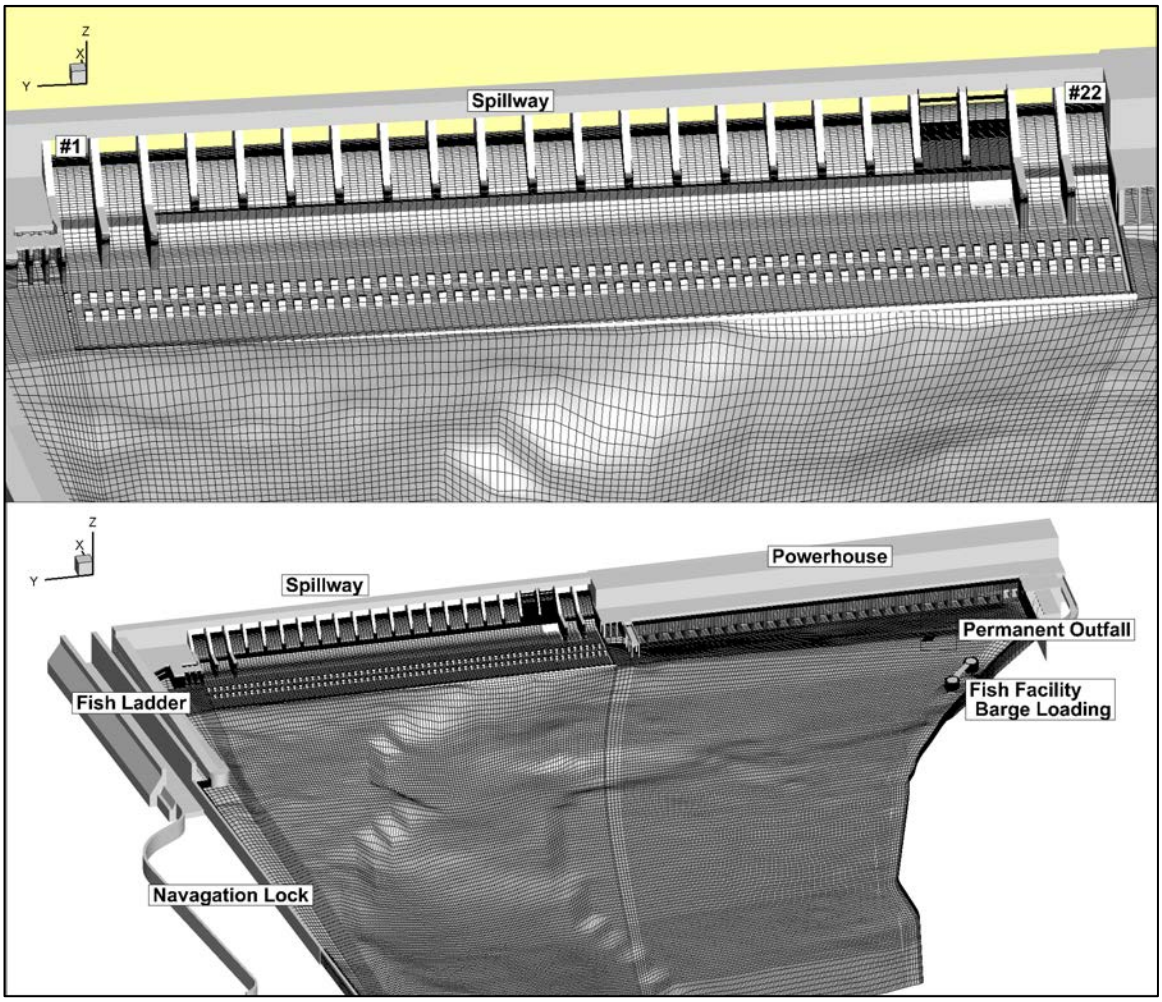

Figure B6. Grid used for the VOF model in simulation 11. Top: detail near the spillway, bottom: entire VOF model

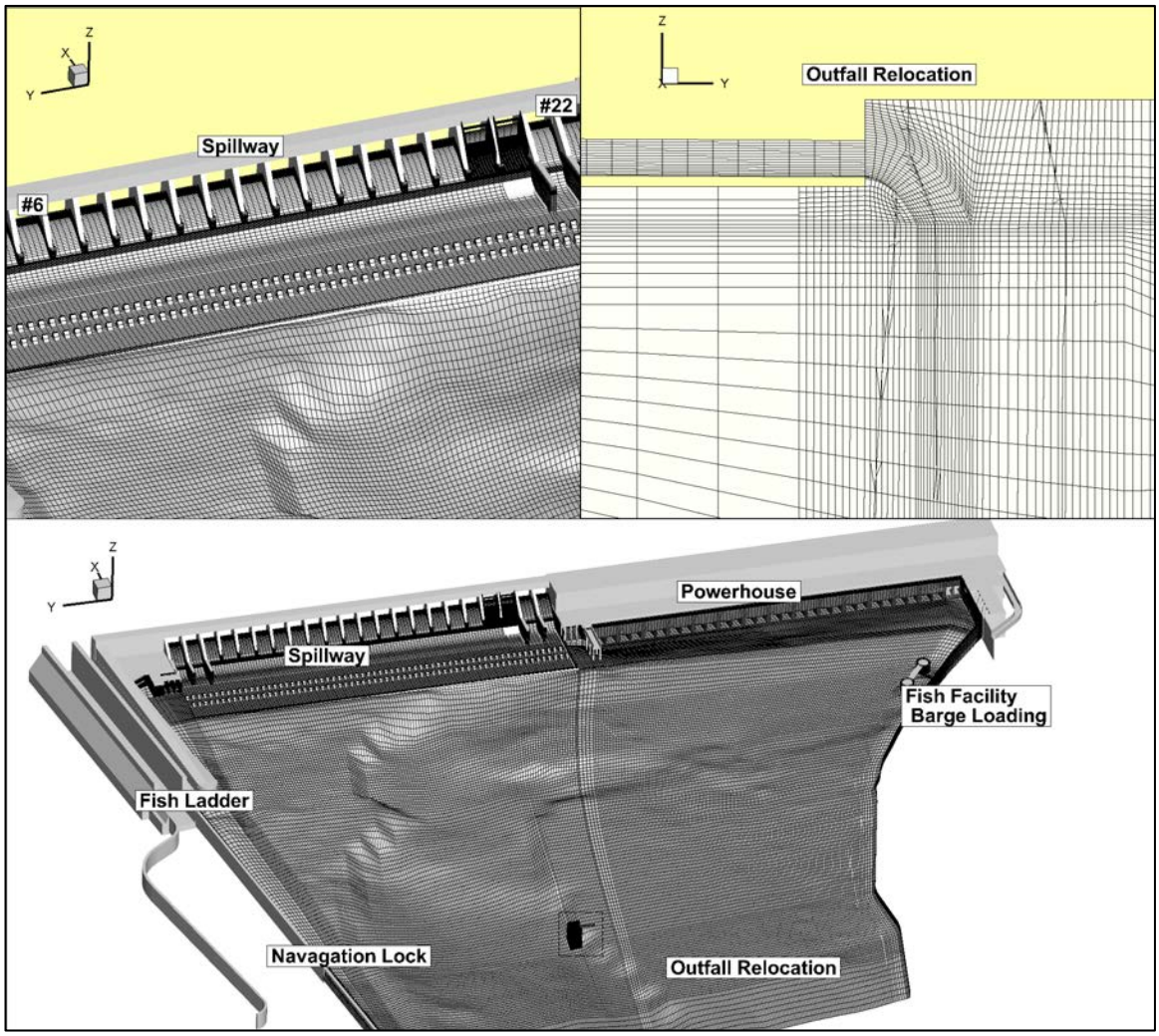

Figure B7. Grid used for the VOF model in simulation 13. Top left: detail near the spillway, top right: new outflow and bottom: entire VOF model

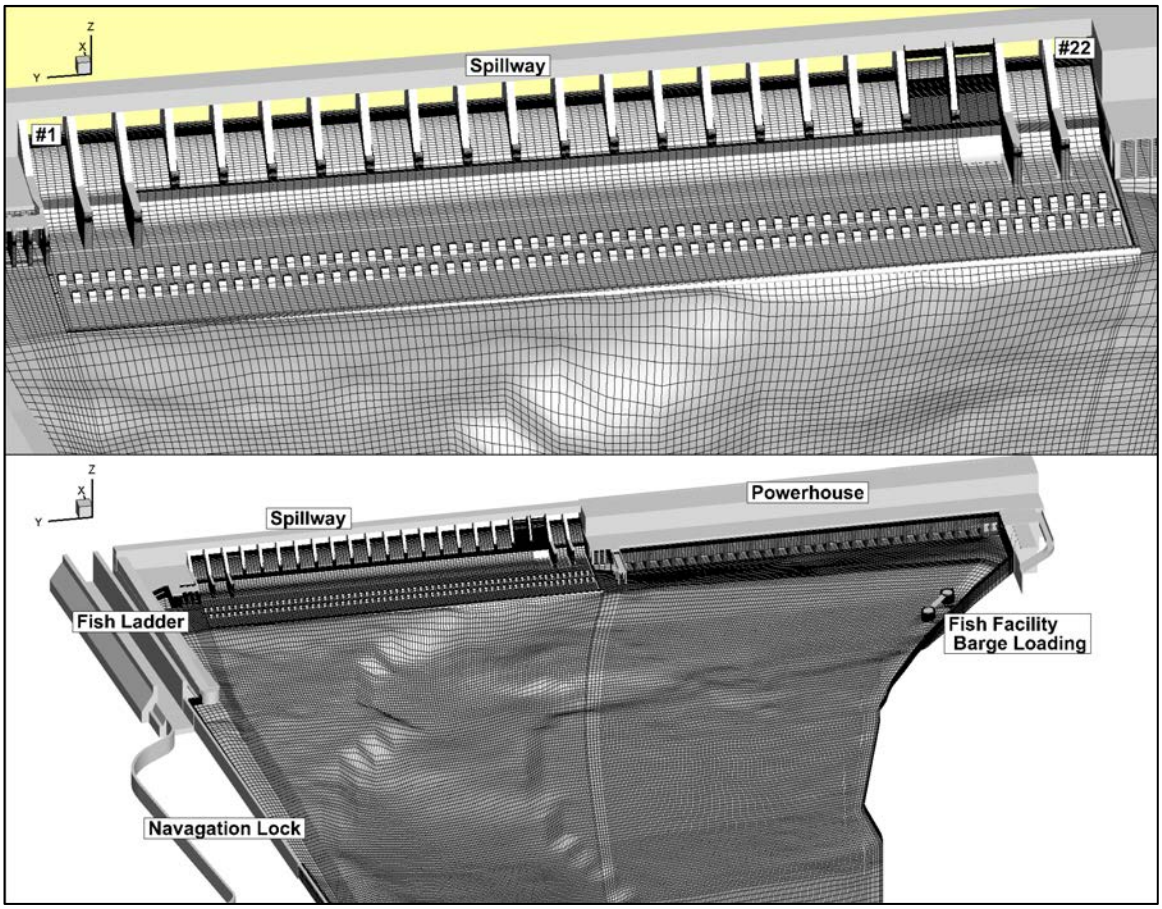

Figure B8. Grid used for the VOF model in simulation 15. Top: detail near the spillway, bottom: entire VOF model

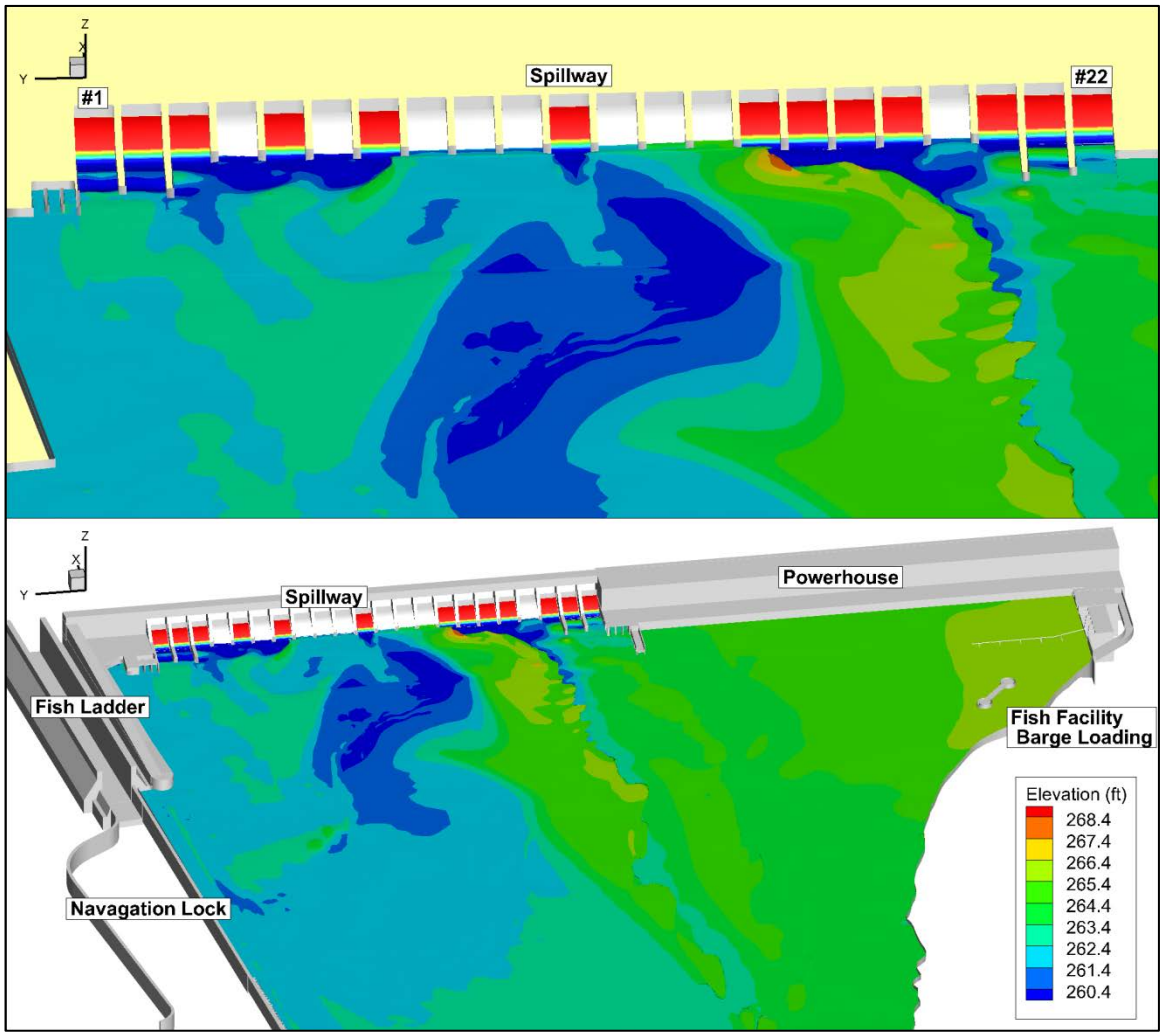

Figure B9 Predicted free surface shape for simulation 1. Top: detail near the spillway, bottom: entire VOF model

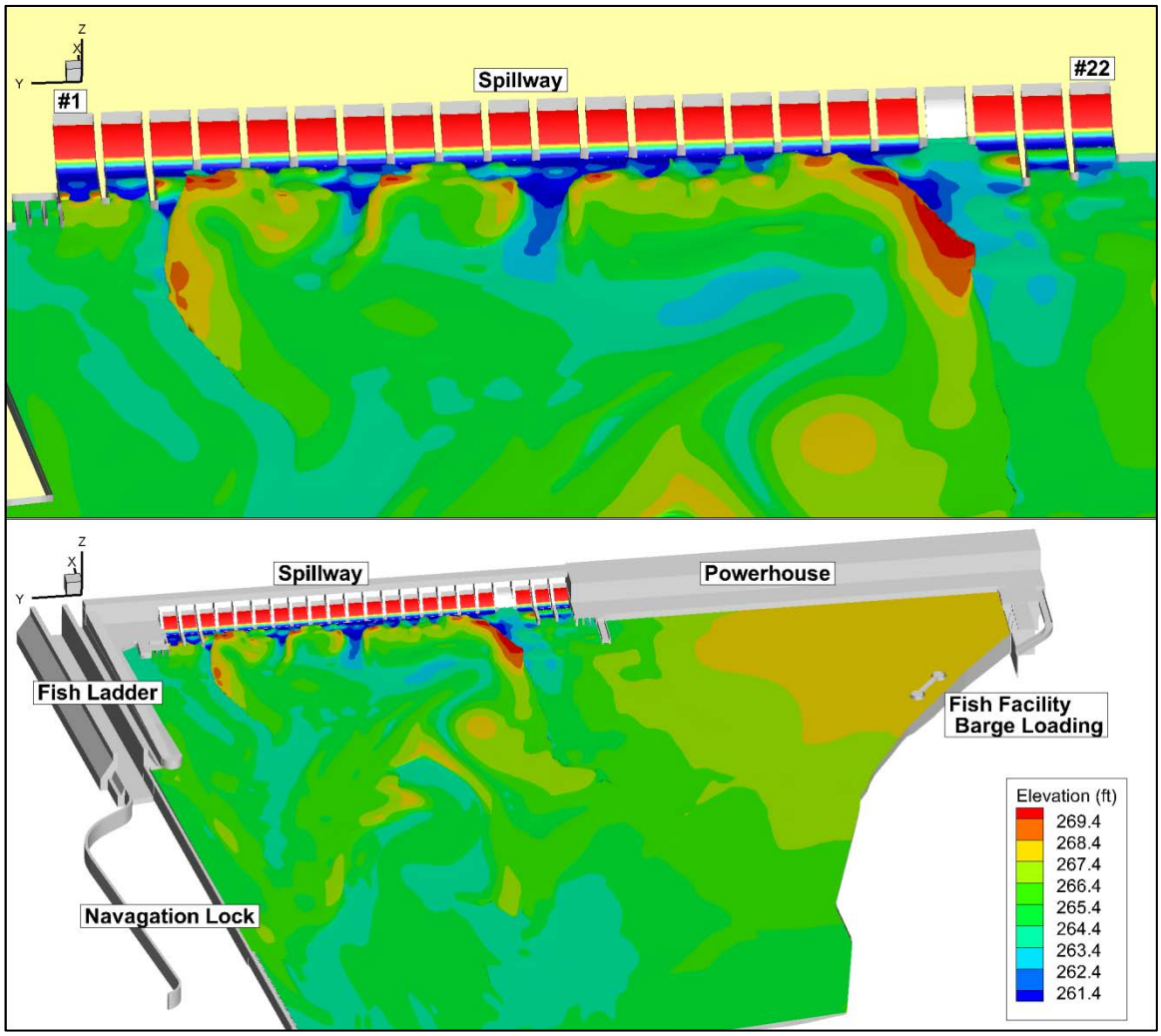

Figure B10 Predicted free surface shape for simulation 3. Top: detail near the spillway, bottom: entire VOF model

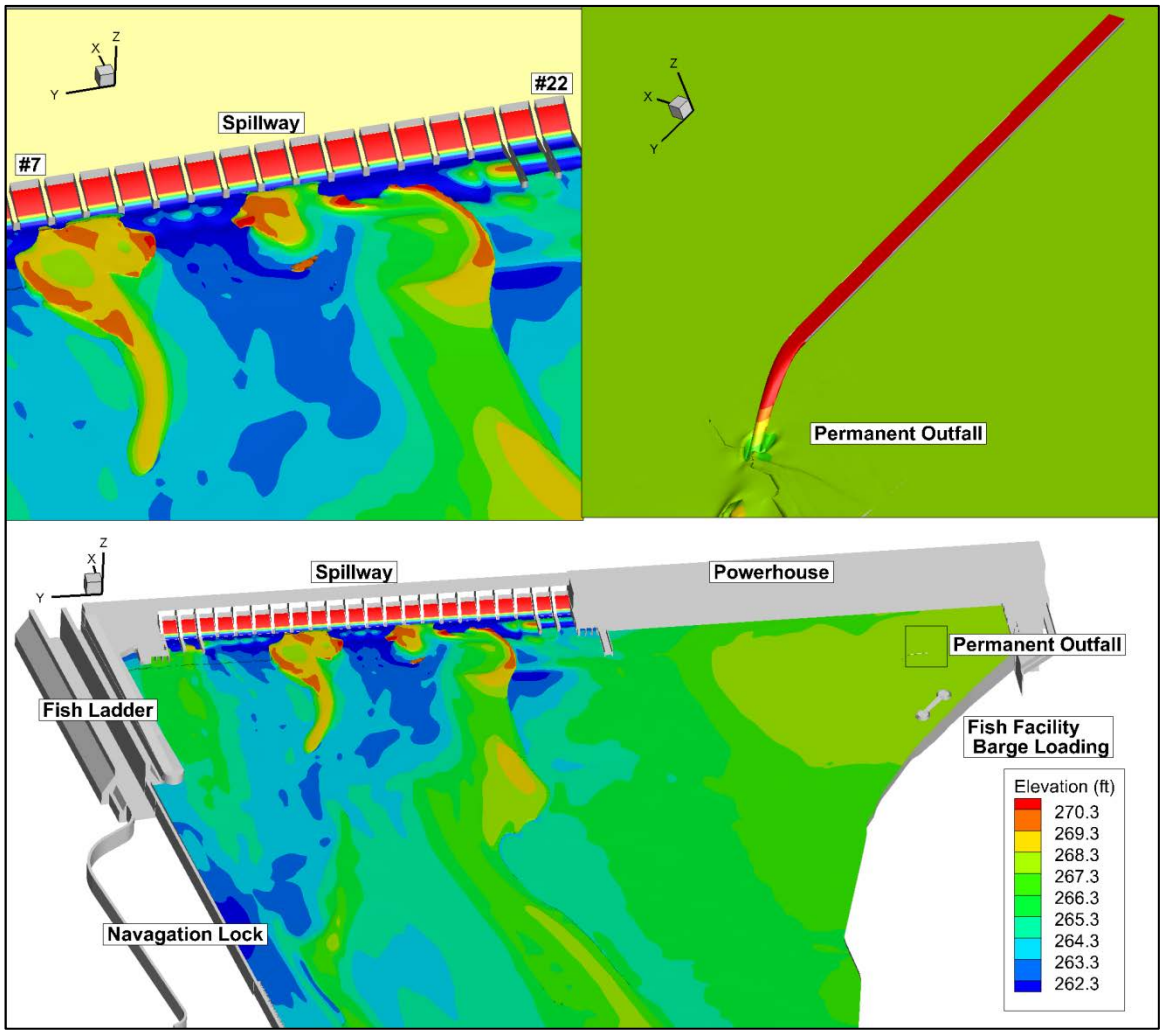

Figure B11 Predicted free surface shape for simulation 5. Top left: detail near the spillway, top right: current outfall and bottom: entire VOF model

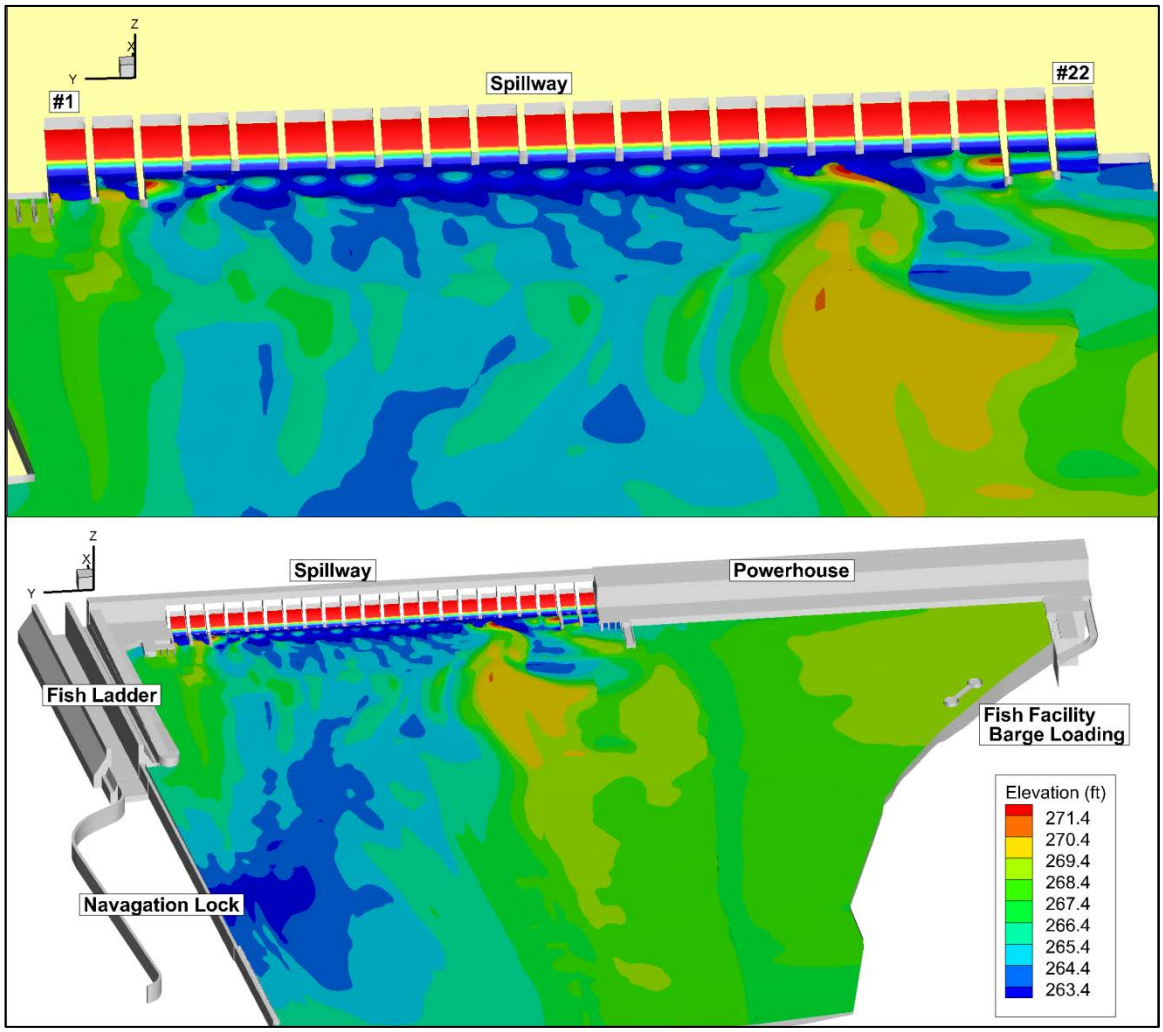

Figure B12 Predicted free surface shape for simulation 7. Top: detail near the spillway, bottom: entire VOF model

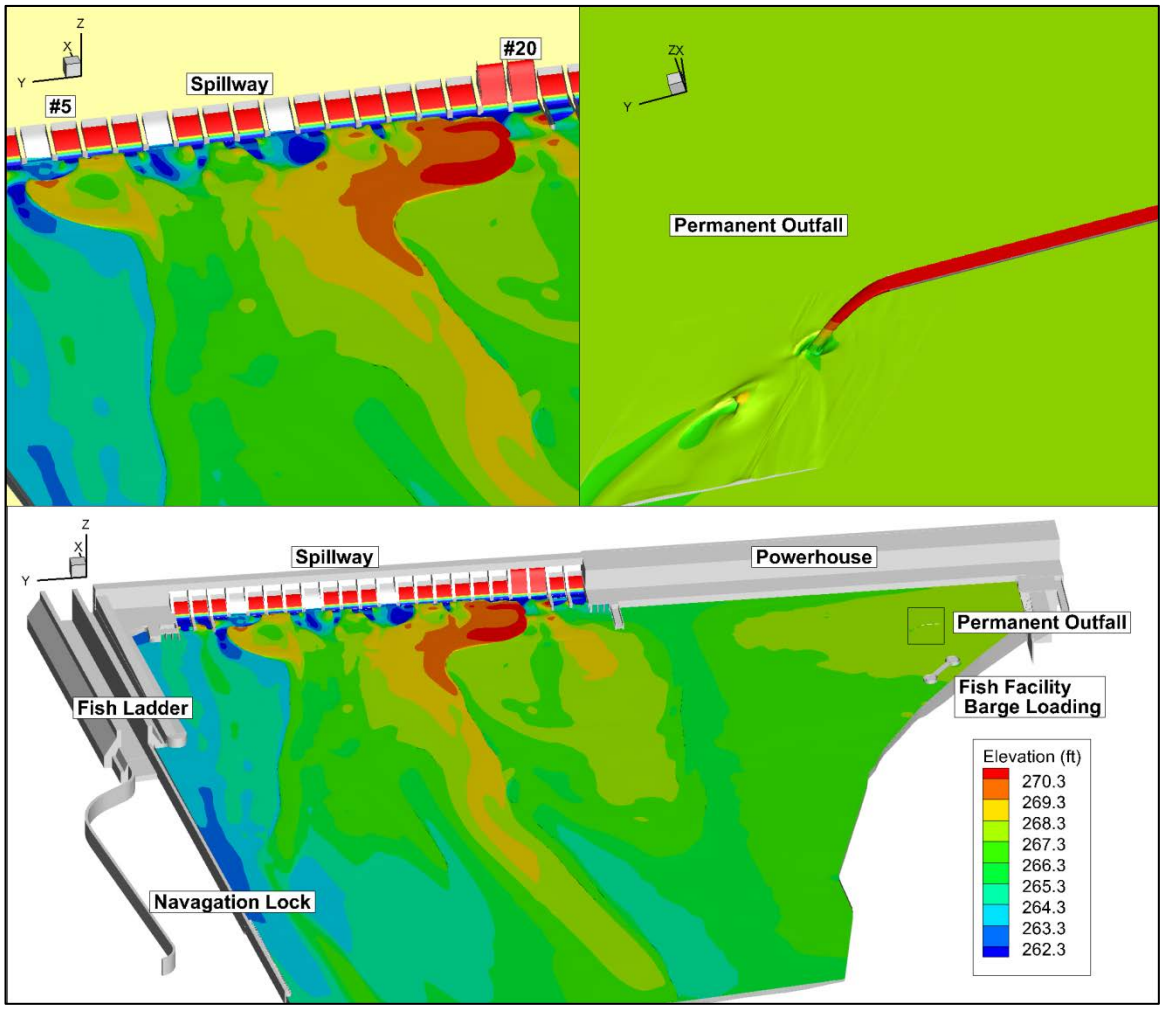

Figure B13 Predicted free surface shape for simulation 11. Top: detail near the spillway, bottom: entire VOF model

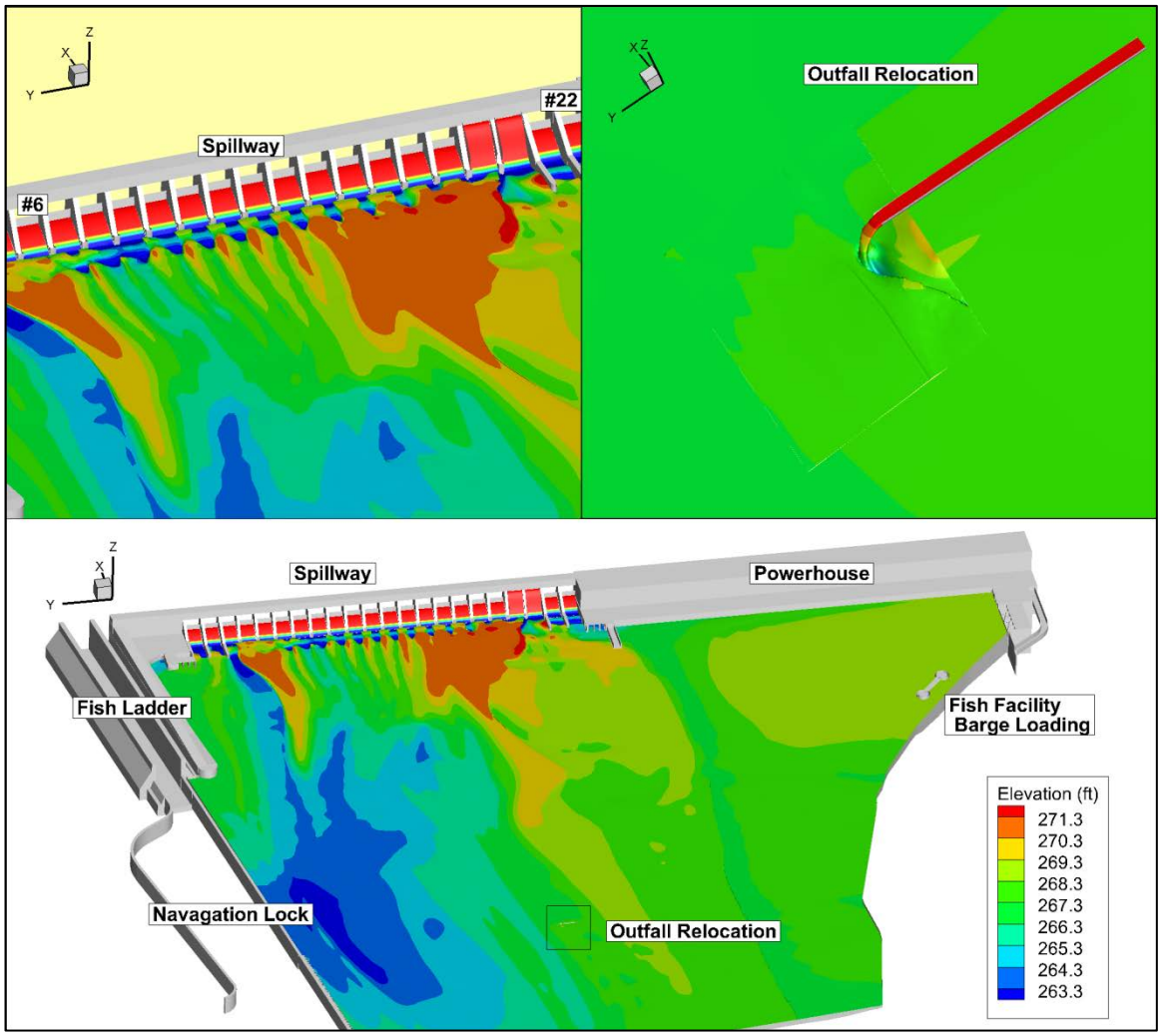

Figure B14 Predicted free surface shape for simulation 13. Top left: detail near the spillway, top right: proposed outfall and bottom: entire VOF model

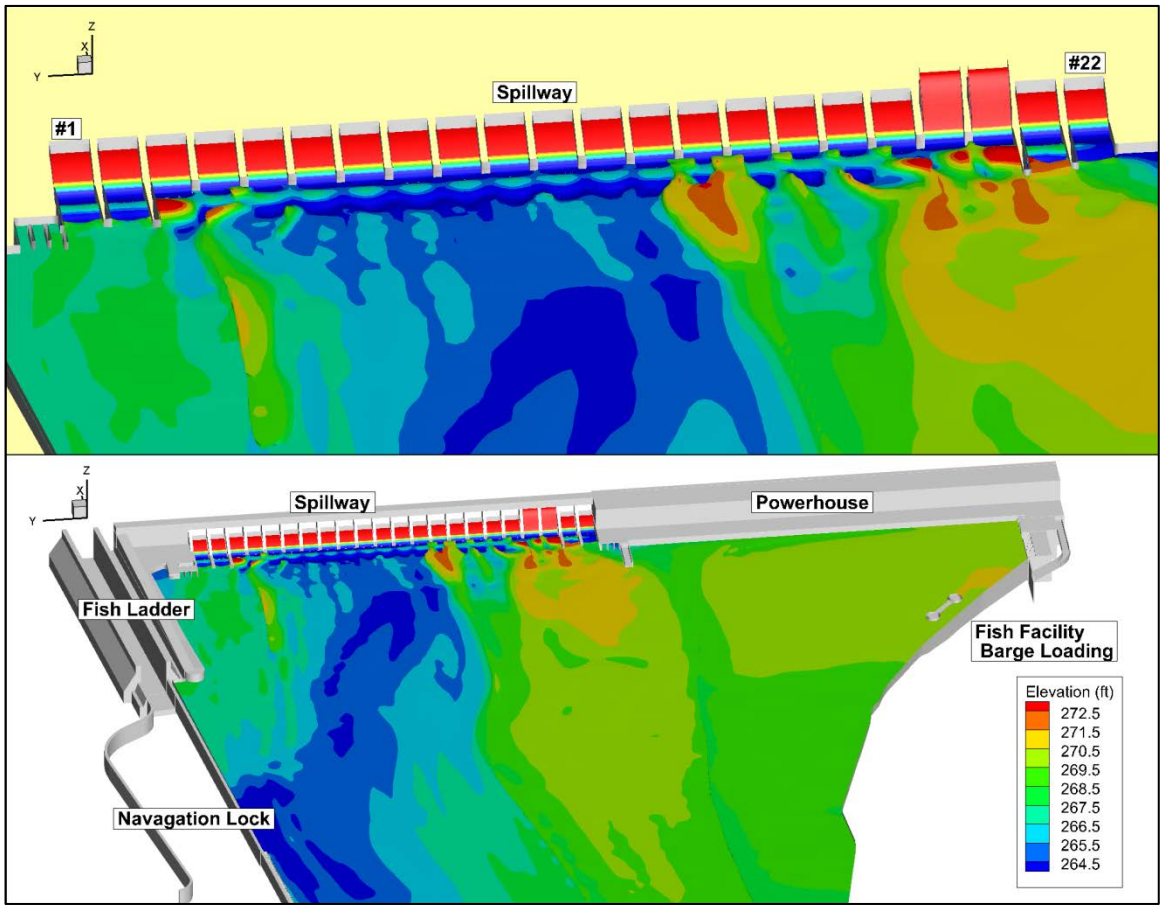

Figure B15 Predicted free surface shape for simulation 15. Top: detail near the spillway, bottom: entire VOF model

APPENDIX C. HYDRODYNAMIC PLOTS

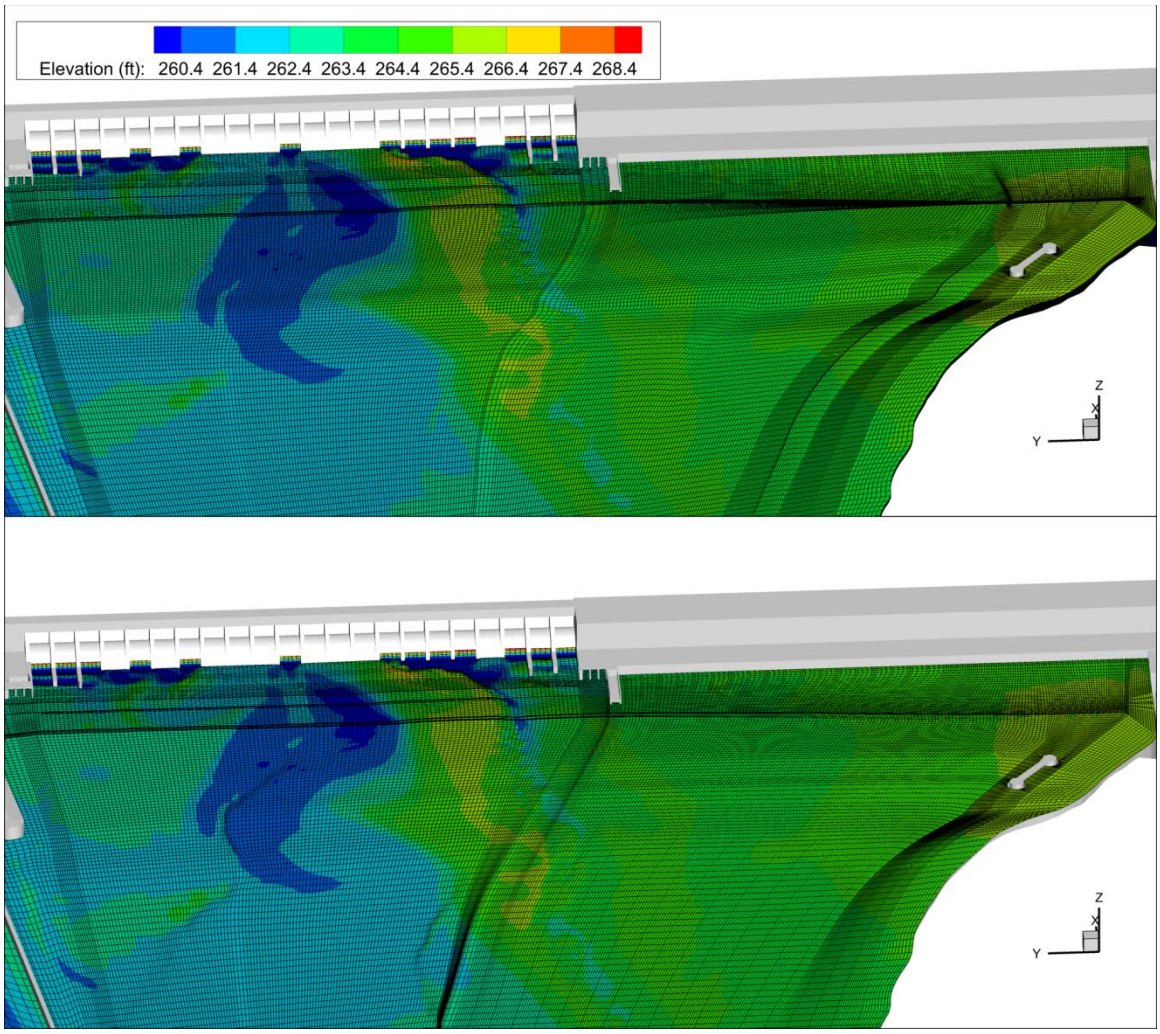

Figure C1. Grid used for rigid-lid model. Top: Simulation 1. Bottom: Simulation 2.

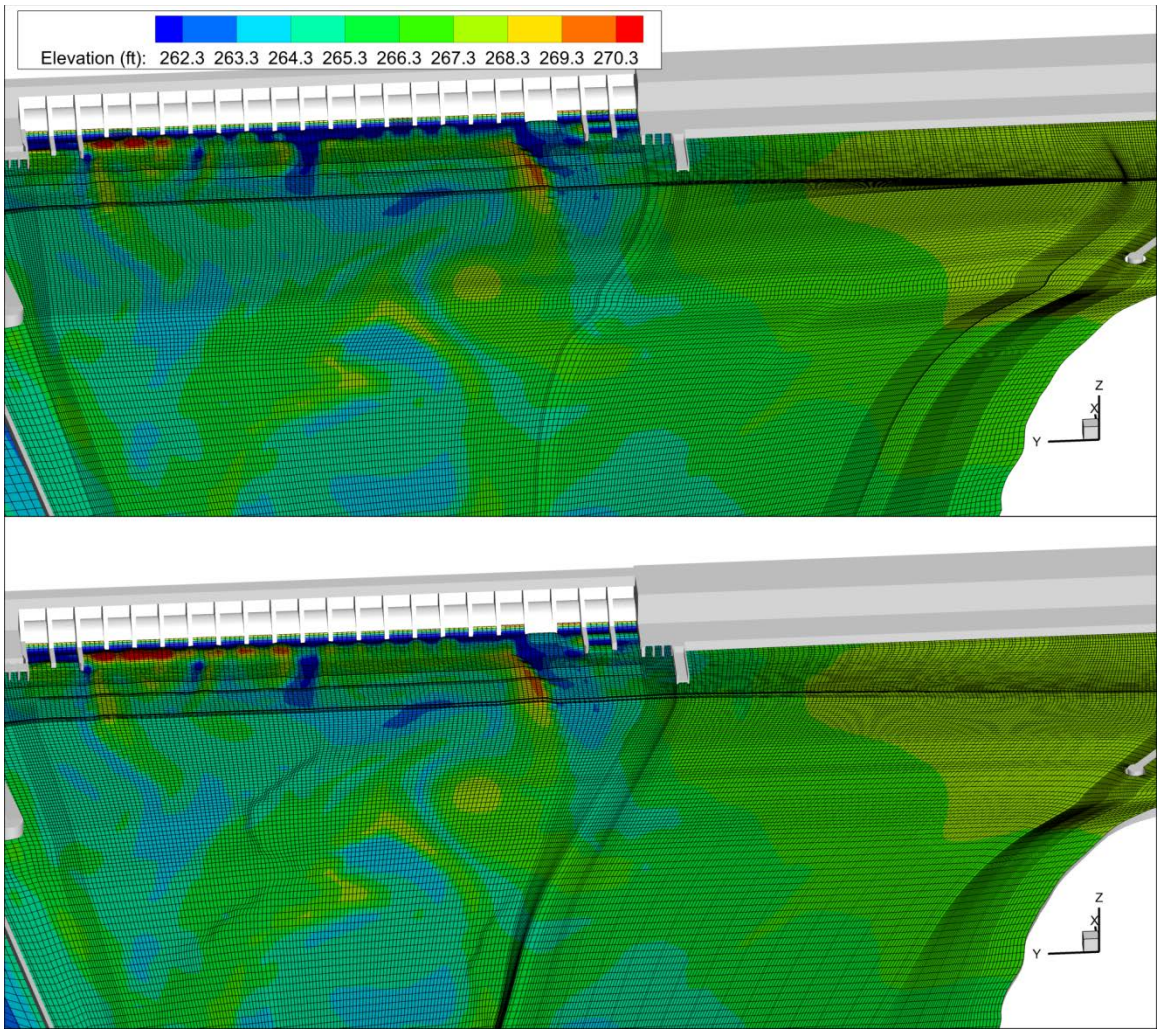

Figure C2. Grid used for rigid-lid model. Top: Simulation 3. Bottom: Simulation 4.

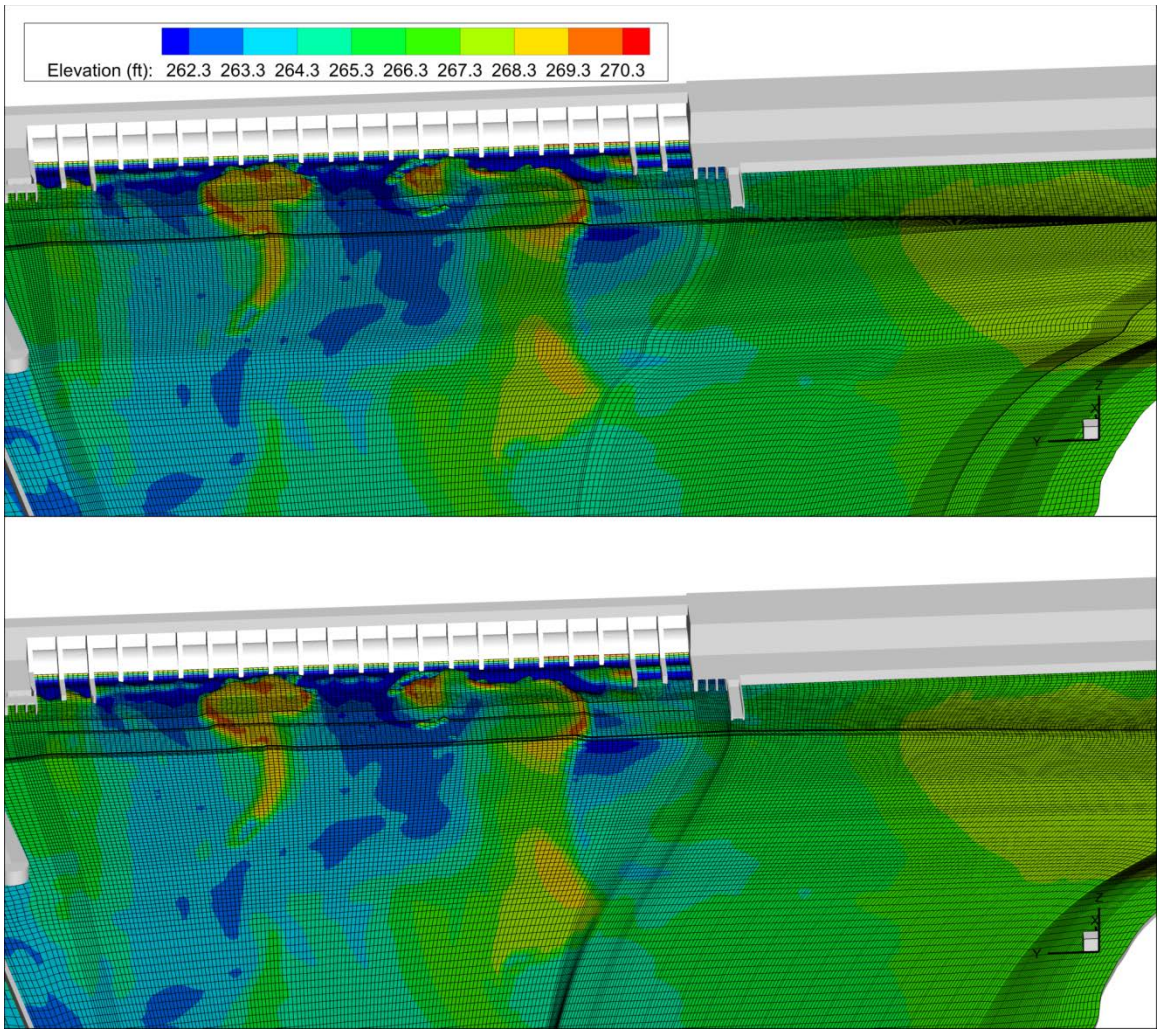

Figure C3. Grid used for rigid-lid model. Top: Simulation 5. Bottom: Simulation 6.

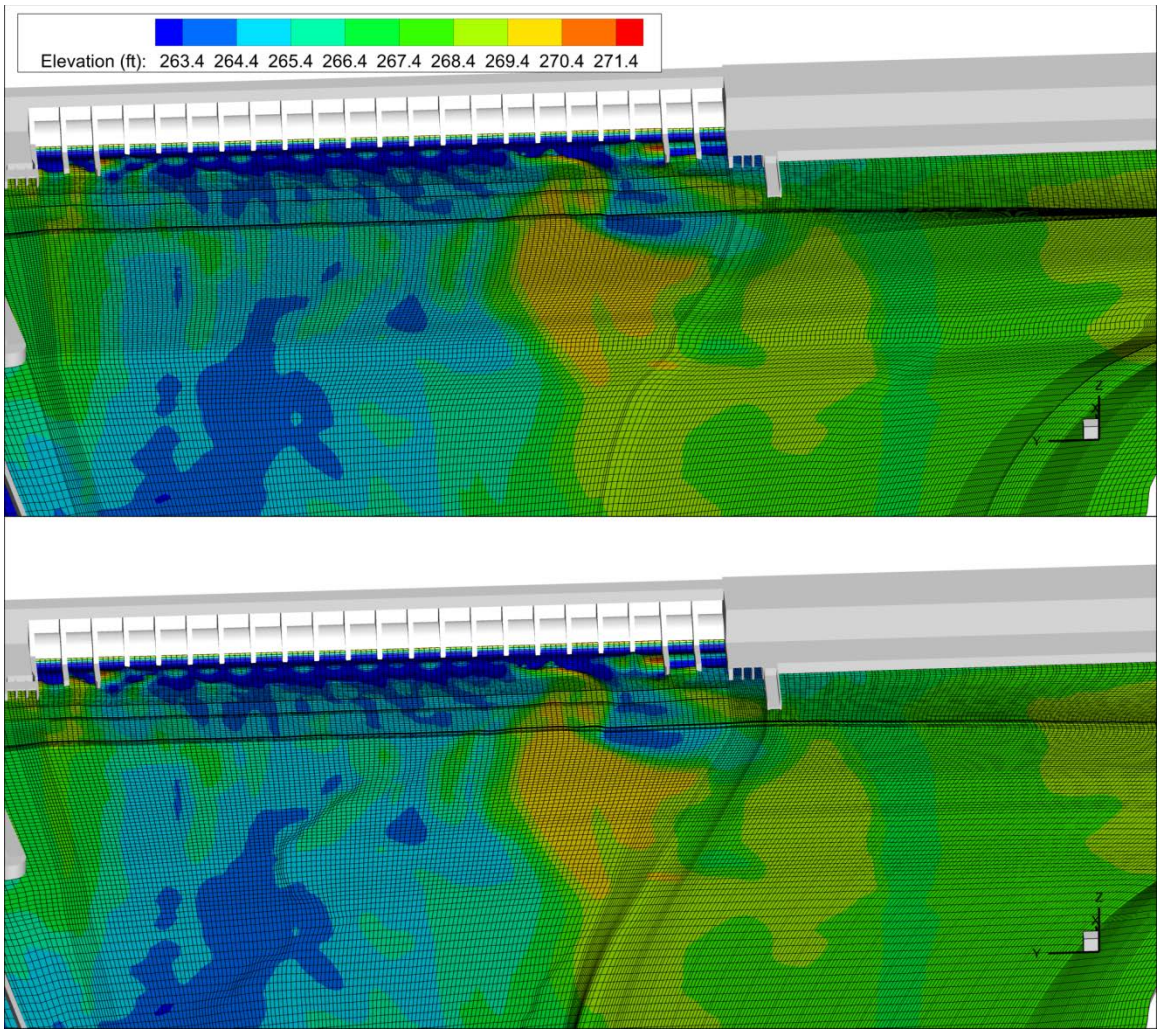

Figure C4. Grid used for rigid-lid model. Top: Simulation 7. Bottom: Simulation 8.

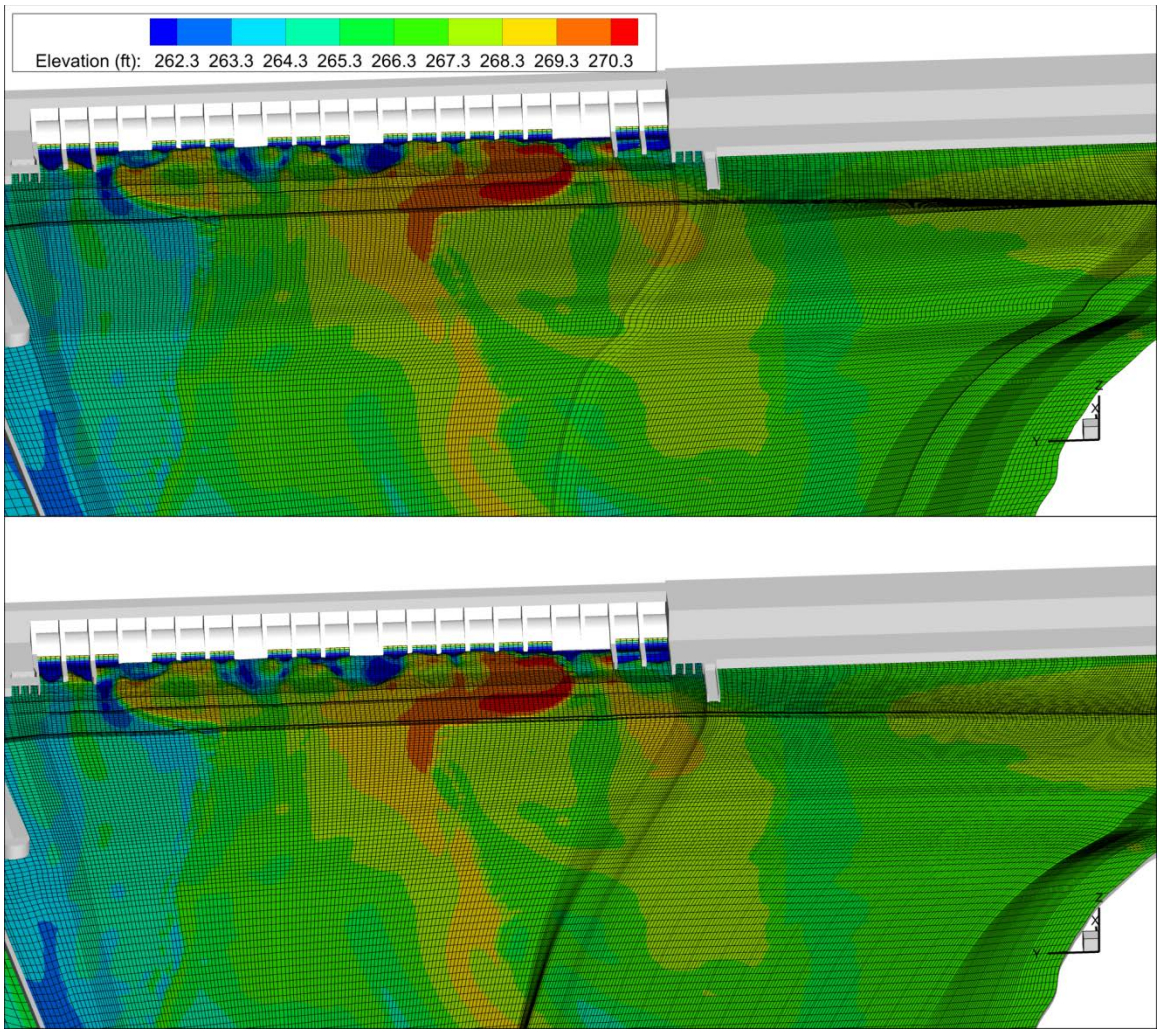

Figure C5. Grid used for rigid-lid model. Top: Simulation 11. Bottom: Simulation 12.

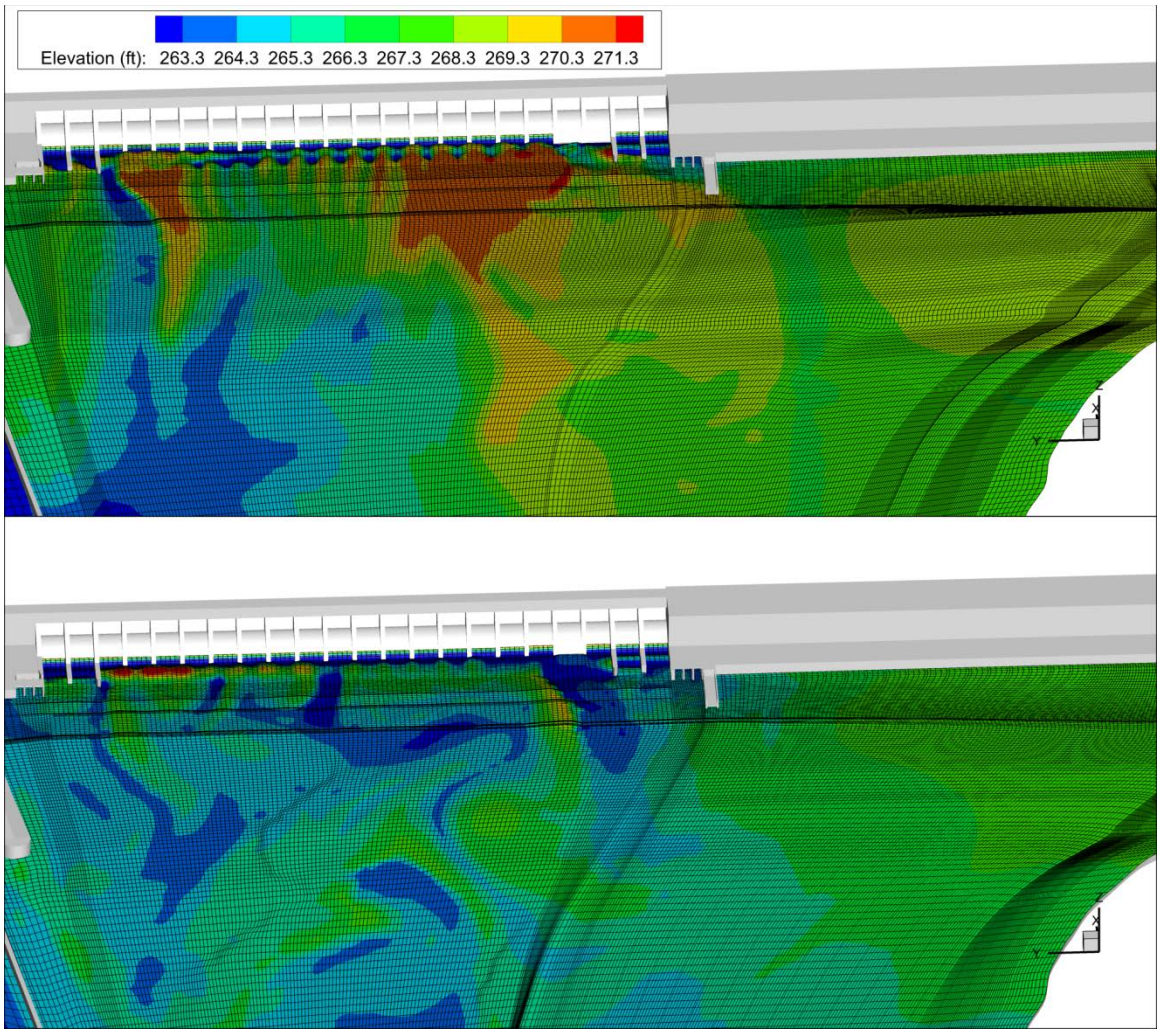

Figure C6. Grid used for rigid-lid model. Top: Simulation 13. Bottom: Simulation 14.

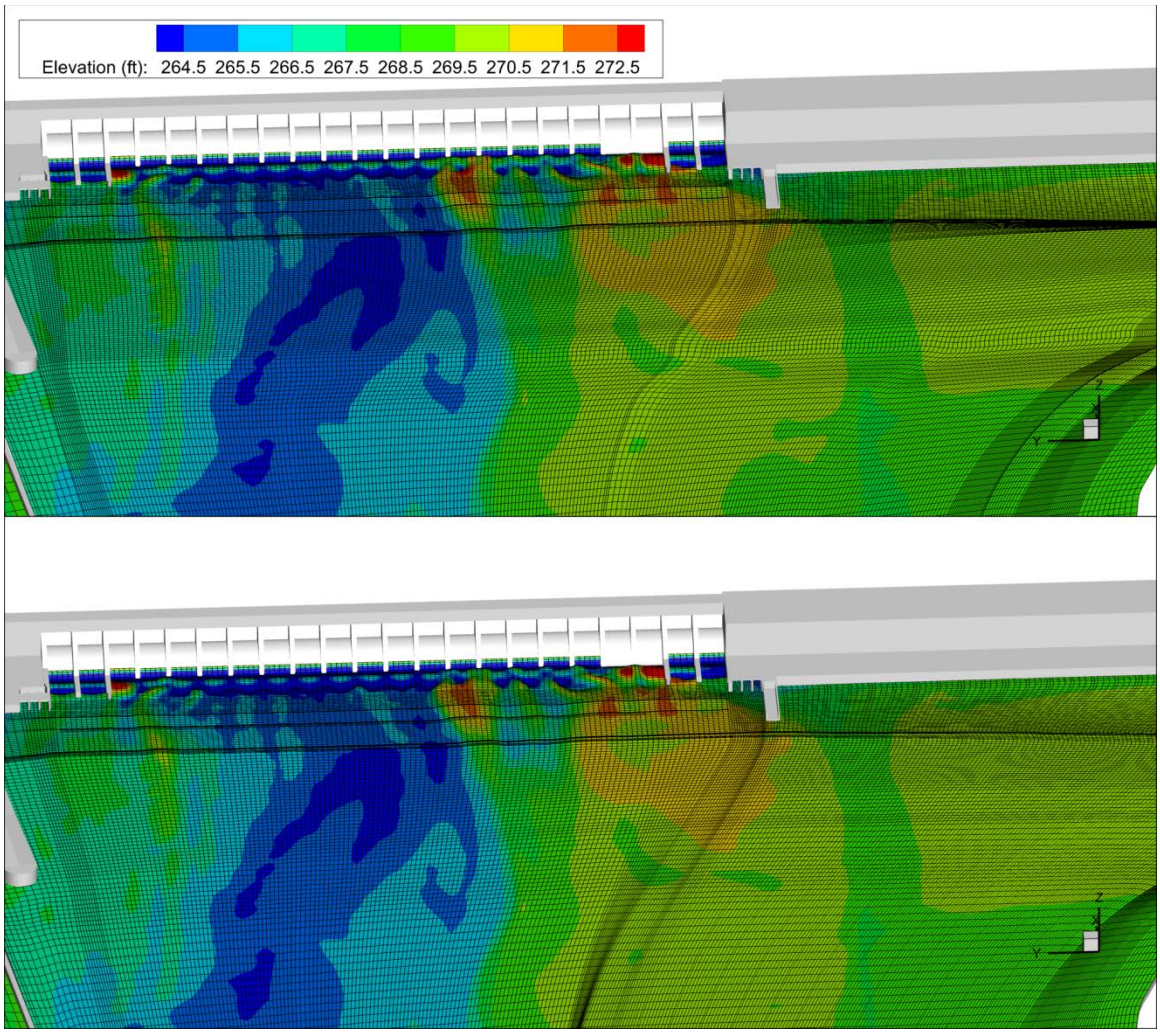

Figure C7. Grid used for rigid-lid model. Top: Simulation 15. Bottom: Simulation 16.

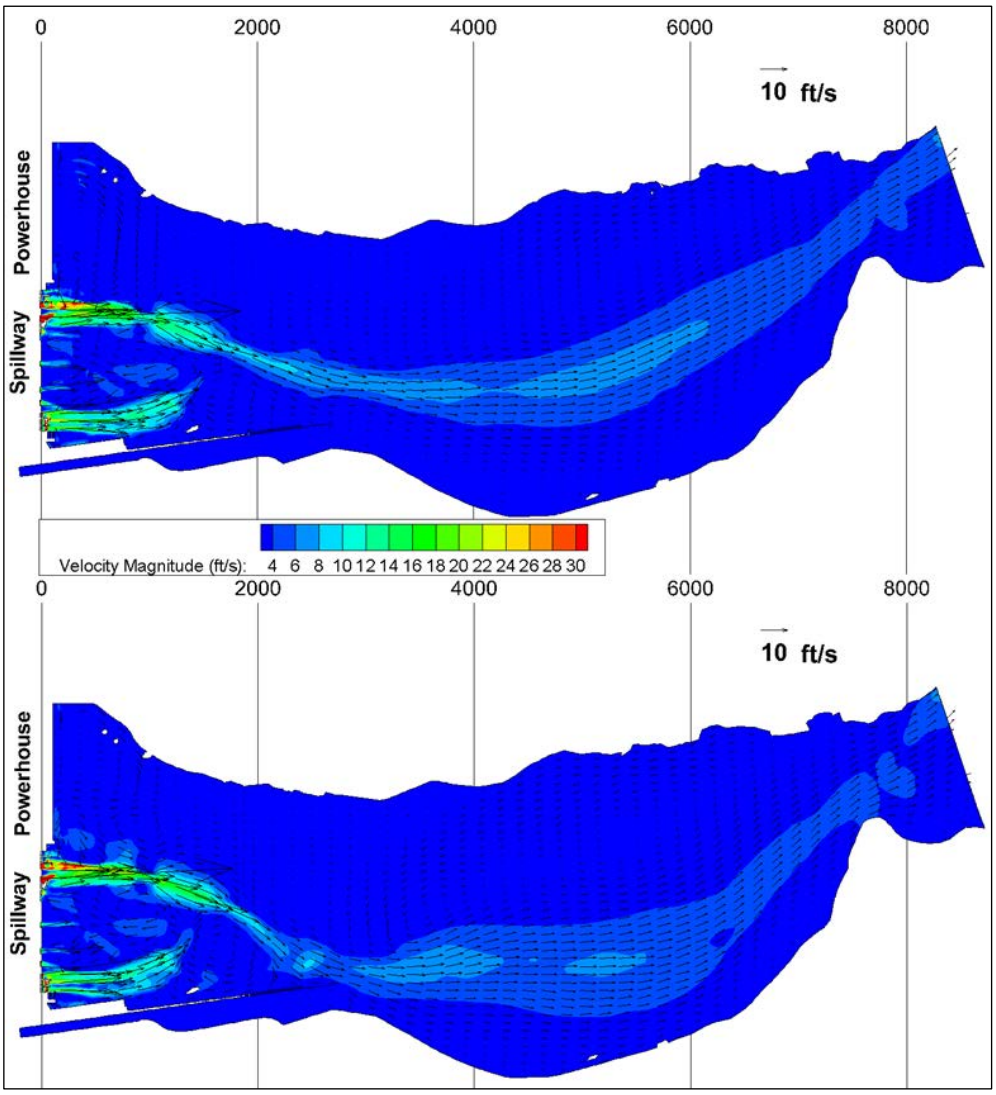

Figure C8 Contours of velocity magnitude and velocity vectors at 2m beneath the free surface. Top: Simulation 1. Bottom: Simulation 2.

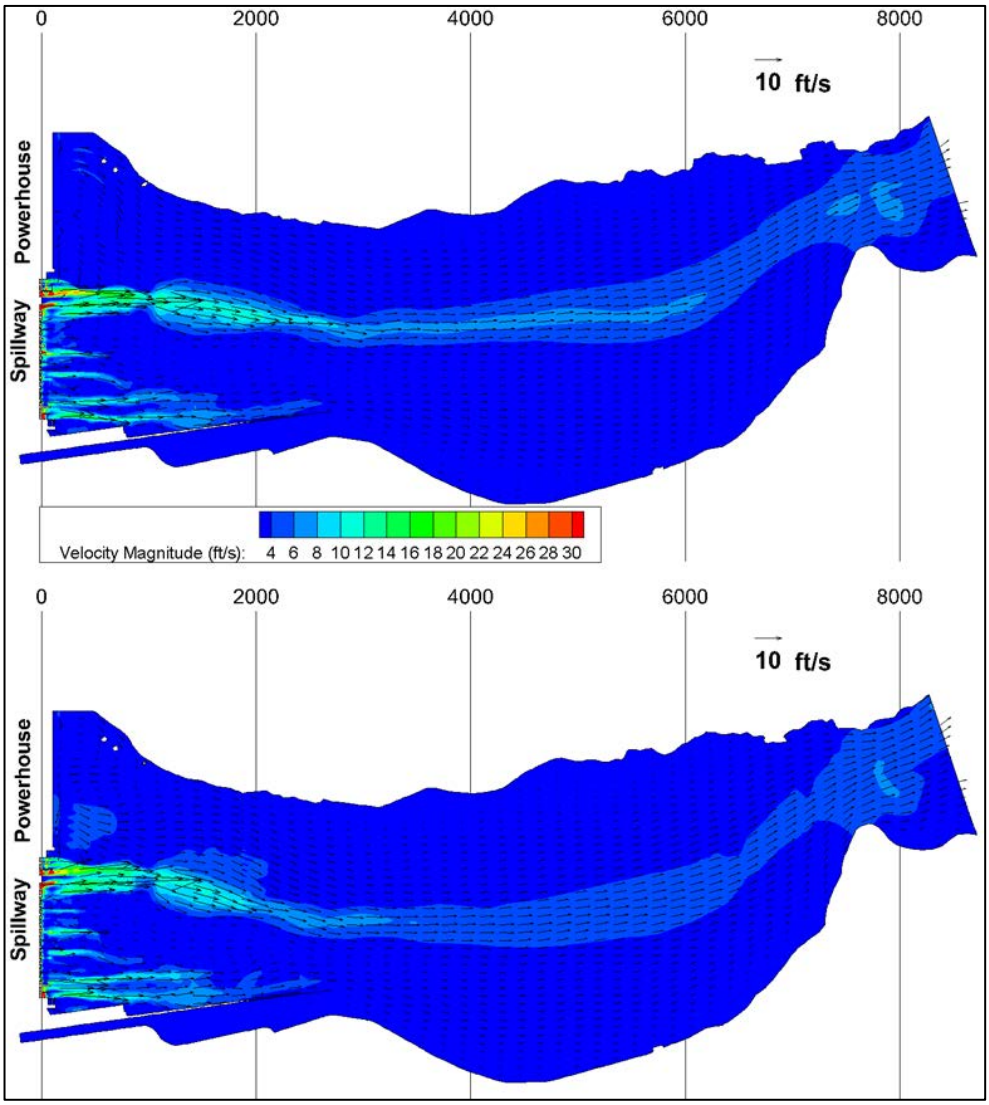

Figure C9 Contours of velocity magnitude and velocity vectors at 2m beneath the free surface. Top: Simulation 3.Bottom:
Simulation 4.

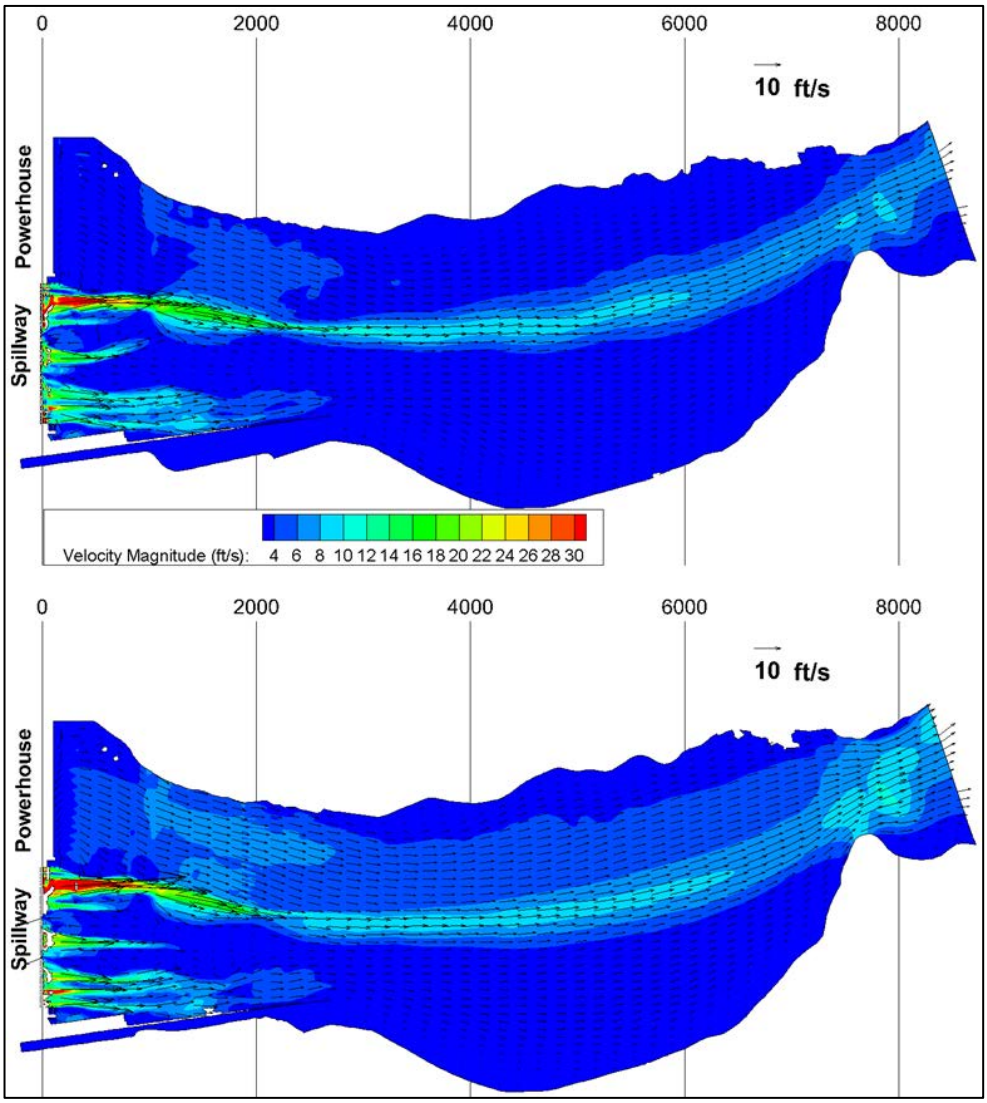

Figure C10 Contours of velocity magnitude and velocity vectors at 2m beneath the free surface. Top: Simulation 5. Bottom: Simulation 6.

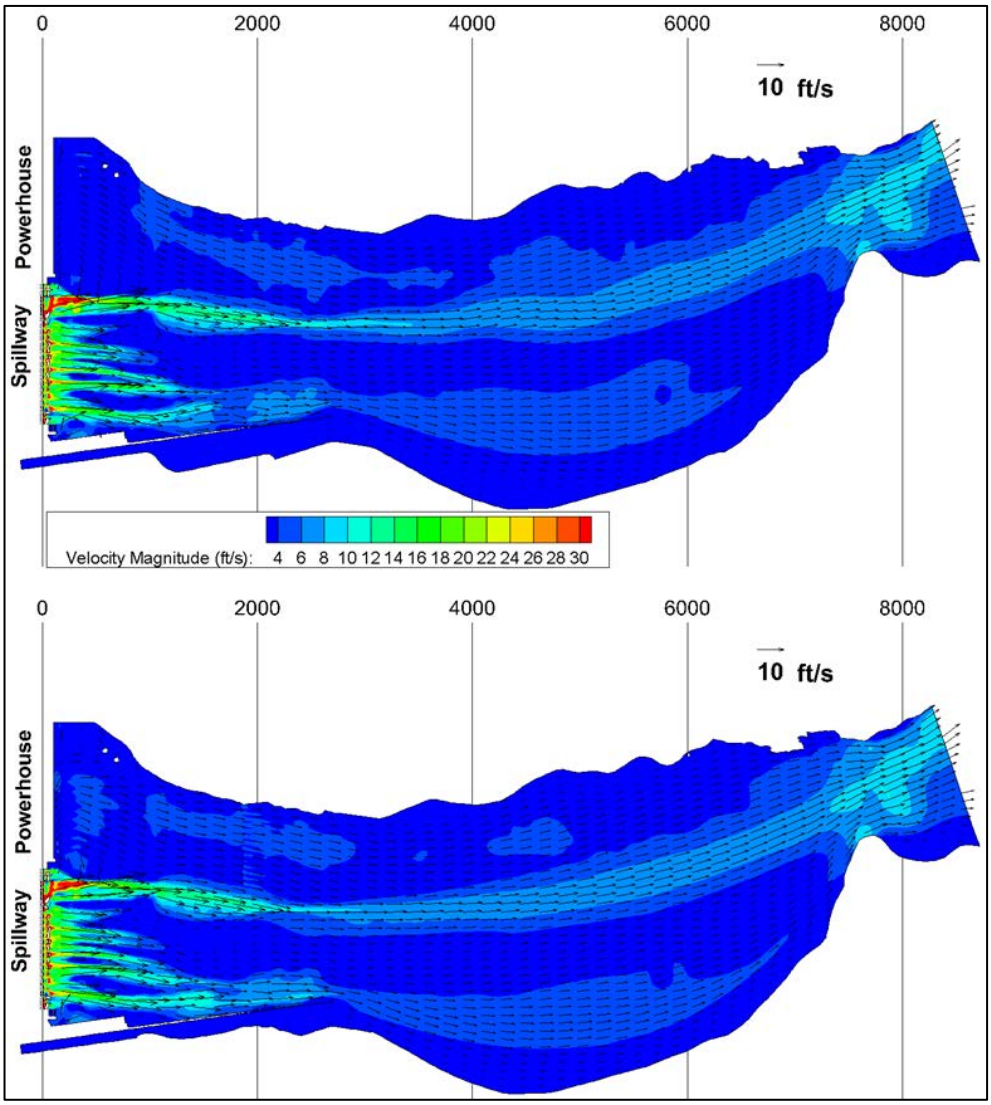

Figure C11 Contours of velocity magnitude and velocity vectors at 2m beneath the free surface. Top: Simulation 7. Bottom: Simulation 8.

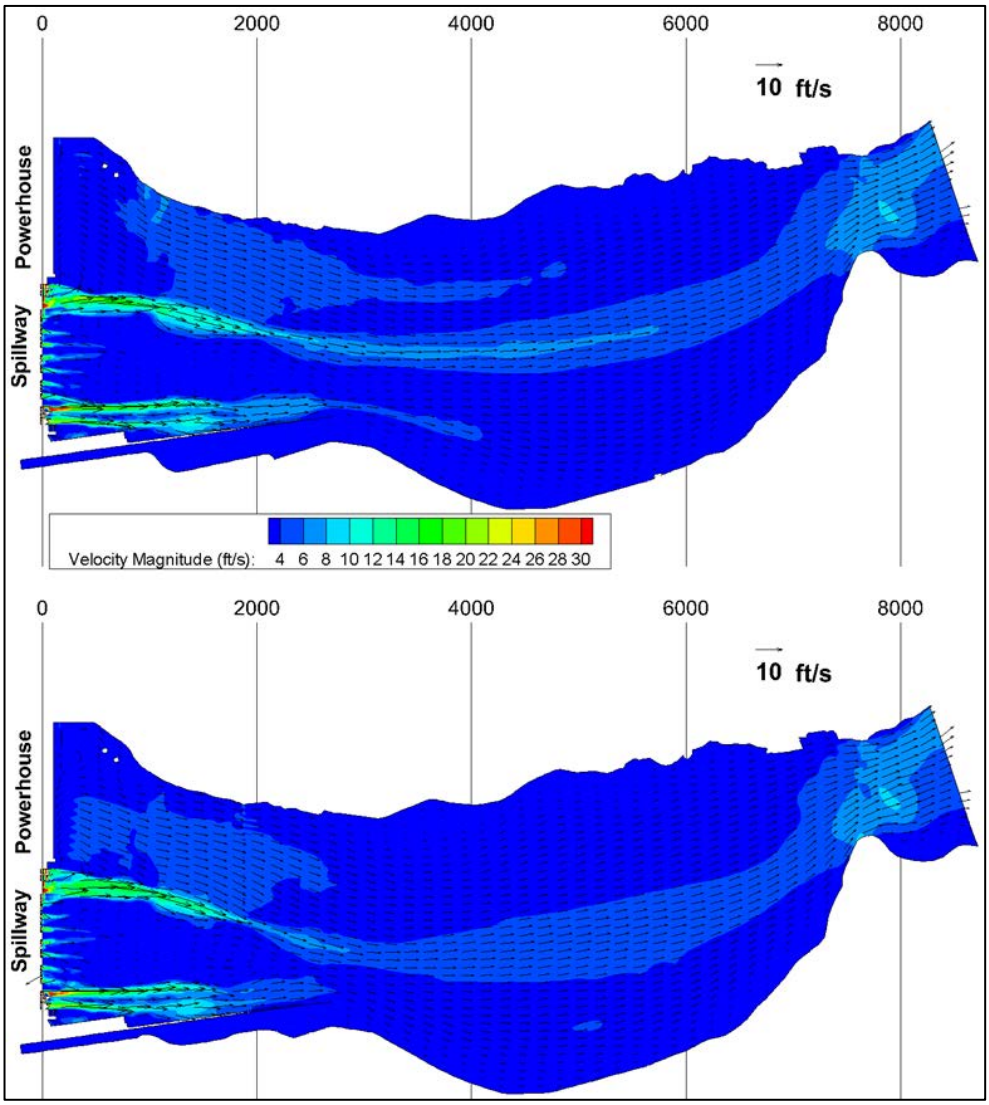

Figure C12 Contours of velocity magnitude and velocity vectors at 2m beneath the free surface. Top: Simulation 11. Bottom: Simulation 12.

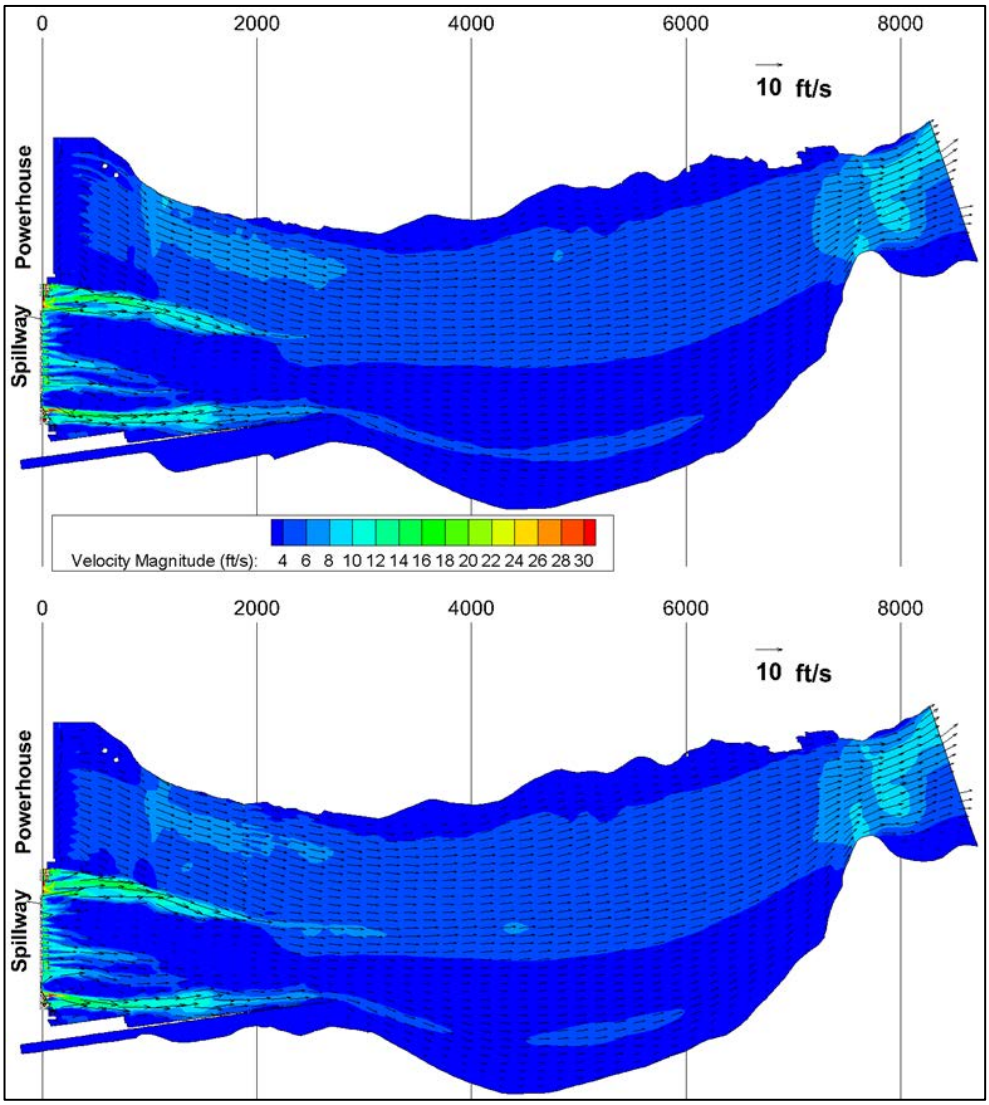

Figure C13 Contours of velocity magnitude and velocity vectors at 2m beneath the free surface. Top: Simulation 13. Bottom: Simulation 14.

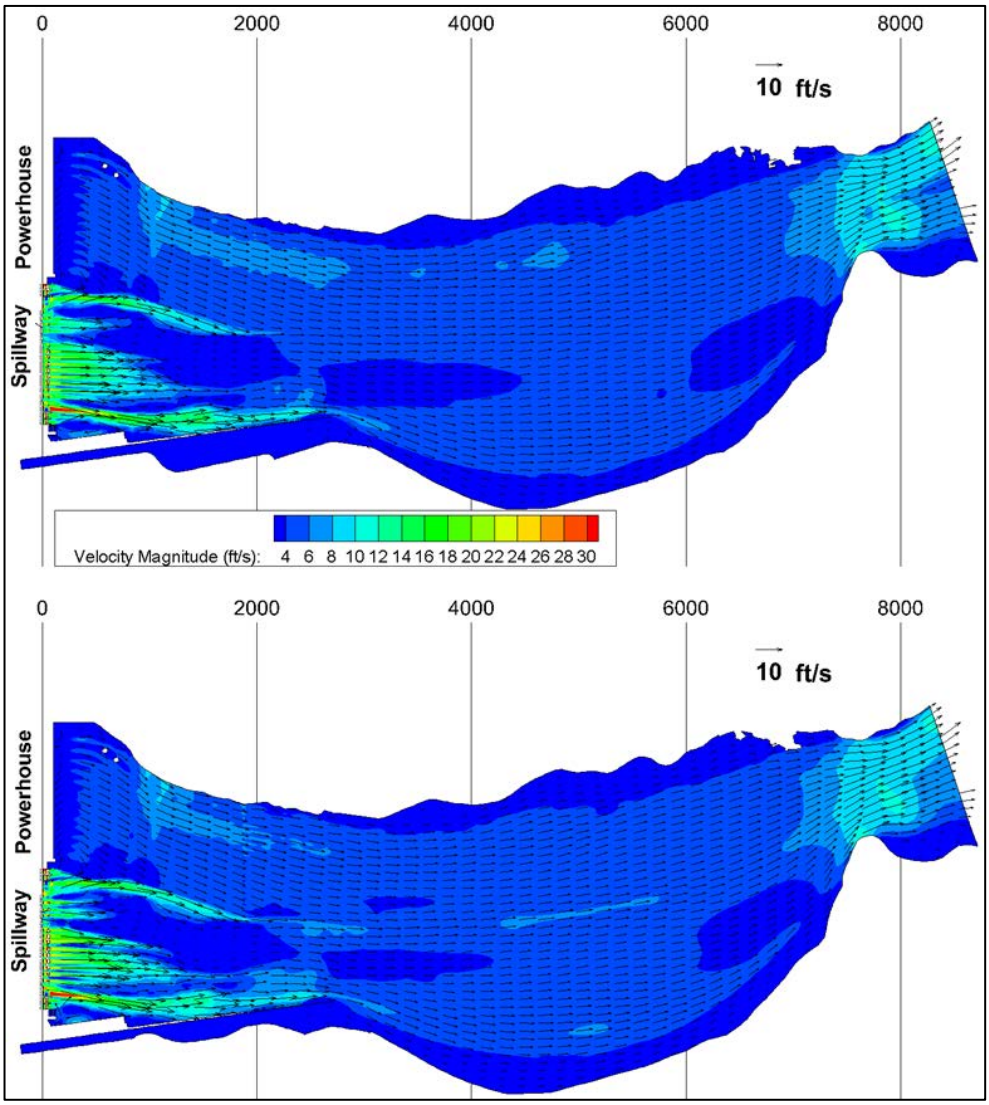

Figure C14 Contours of velocity magnitude and velocity vectors at 2m beneath the free surface. Top: Simulation 15. Bottom: Simulation 16.

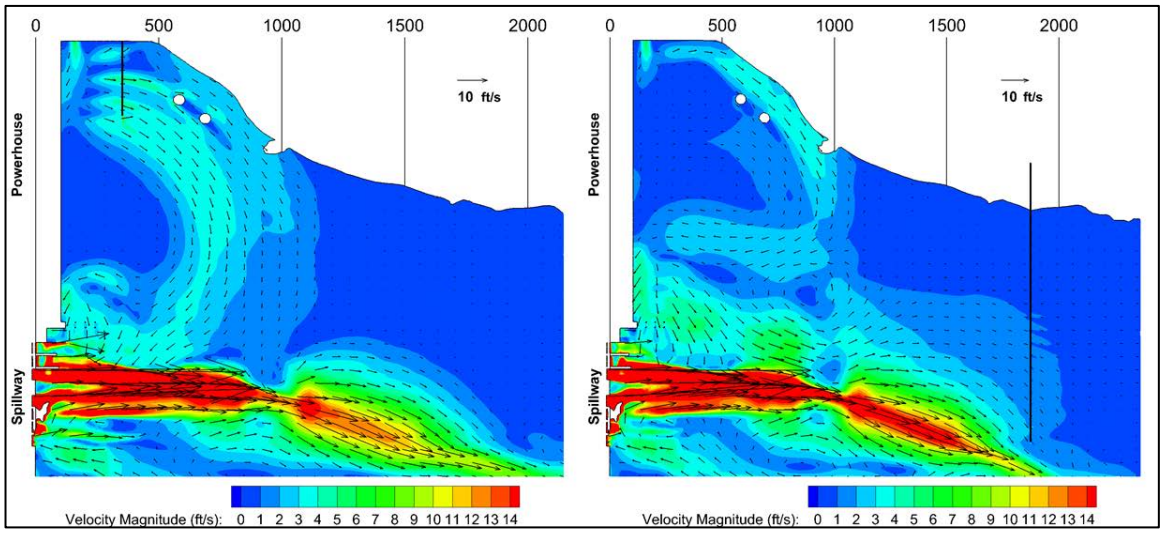

Figure C15 Contours of velocity magnitude and velocity vectors at 2m beneath the free surface near the dam. Left: Simulation 1. Right: Simulation2.

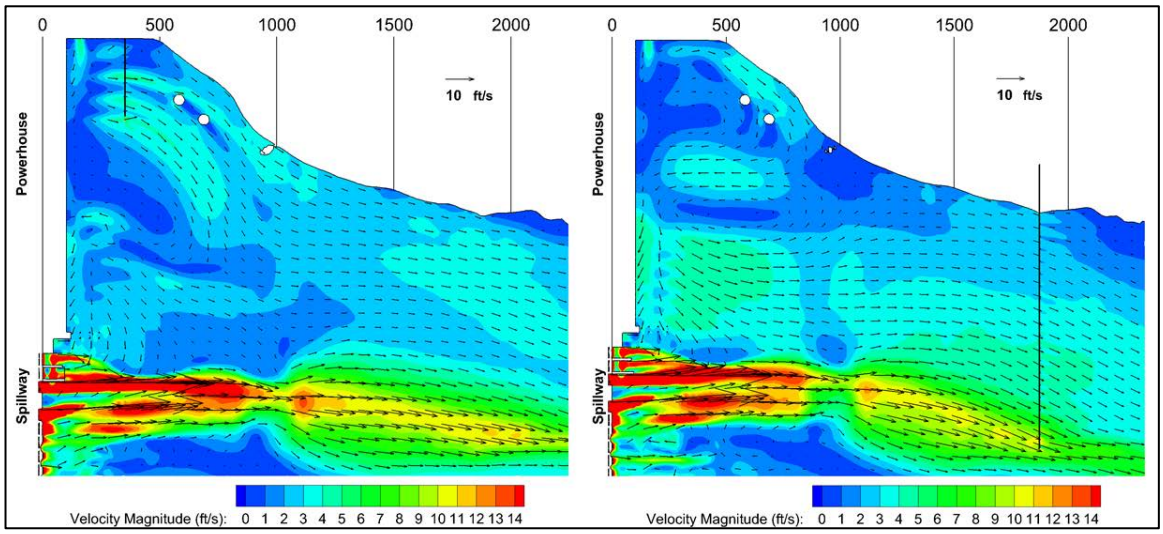

Figure C16 Contours of velocity magnitude and velocity vectors at 2m beneath the free surface near the dam. Left: Simulation 3. Right: Simulation4.

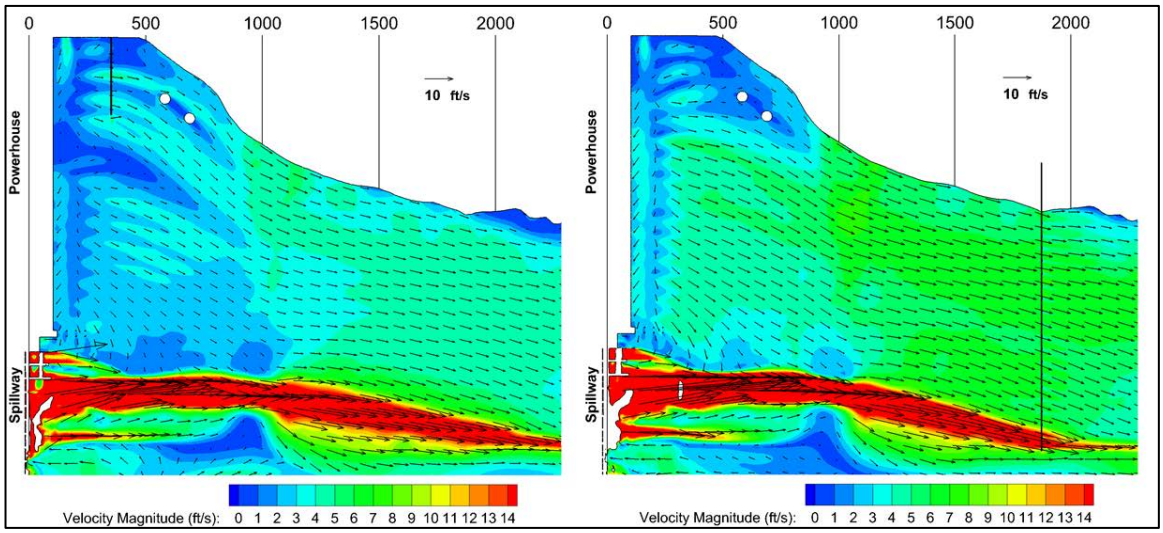

Figure C17 Contours of velocity magnitude and velocity vectors at 2m beneath the free surface near the dam. Left: Simulation 5. Right: Simulation 6.

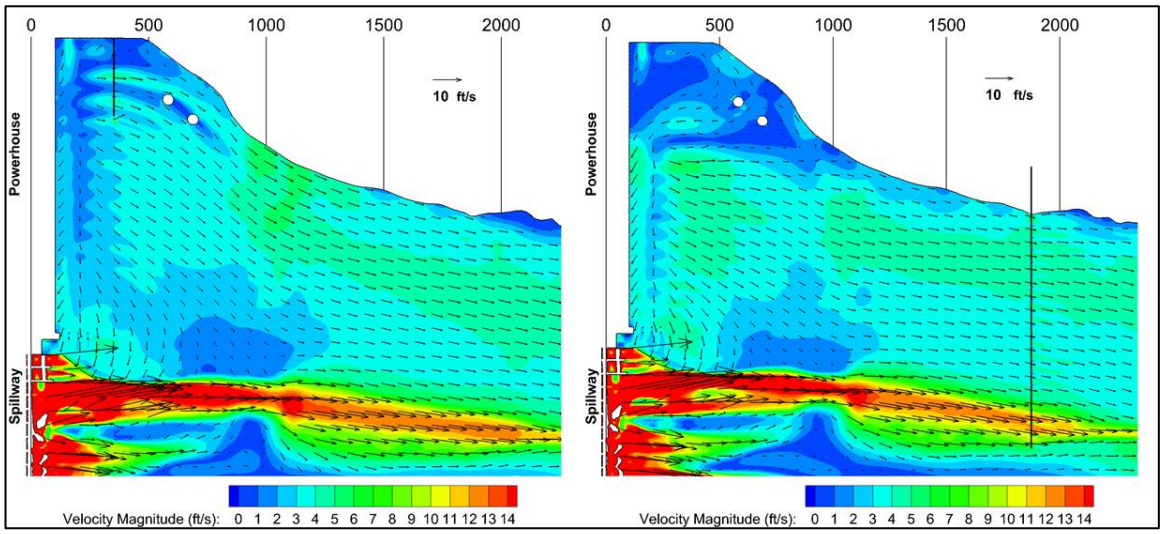

Figure C18 Contours of velocity magnitude and velocity vectors at 2m beneath the free surface near the dam. Left: Simulation 7. Right: Simulation 8.

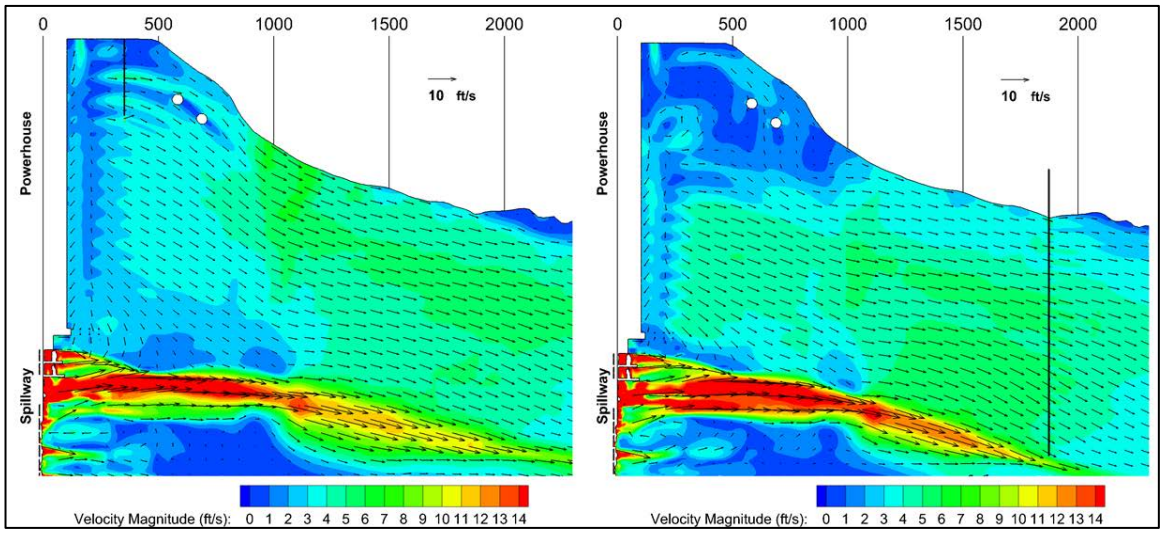

Figure C19 Contours of velocity magnitude and velocity vectors at 2m beneath the free surface near the dam. Left: Simulation 11. Right: Simulation 12.

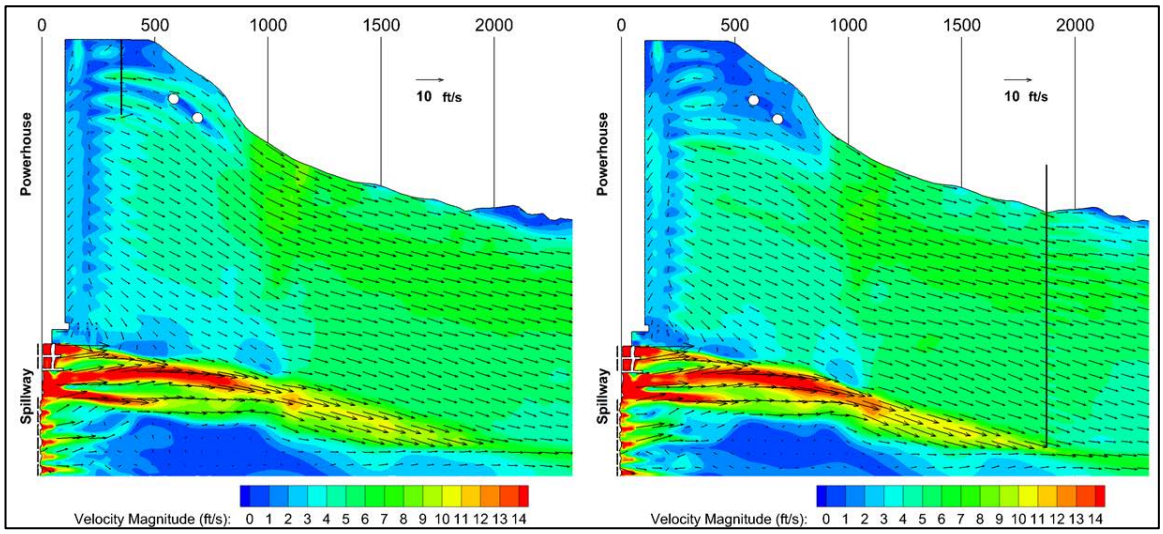

Figure C20 Contours of velocity magnitude and velocity vectors at 2m beneath the free surface near the dam. Left: Simulation 13. Right: Simulation 14.

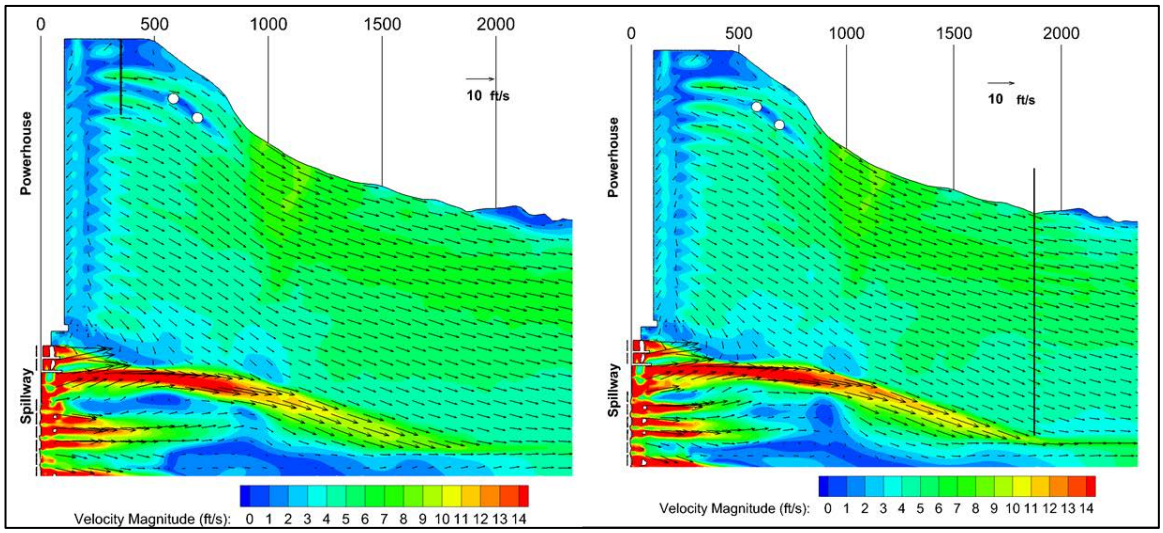

Figure C21 Contours of velocity magnitude and velocity vectors at 2m beneath the free surface near the dam. Left: Simulation 15. Right: Simulation 16.

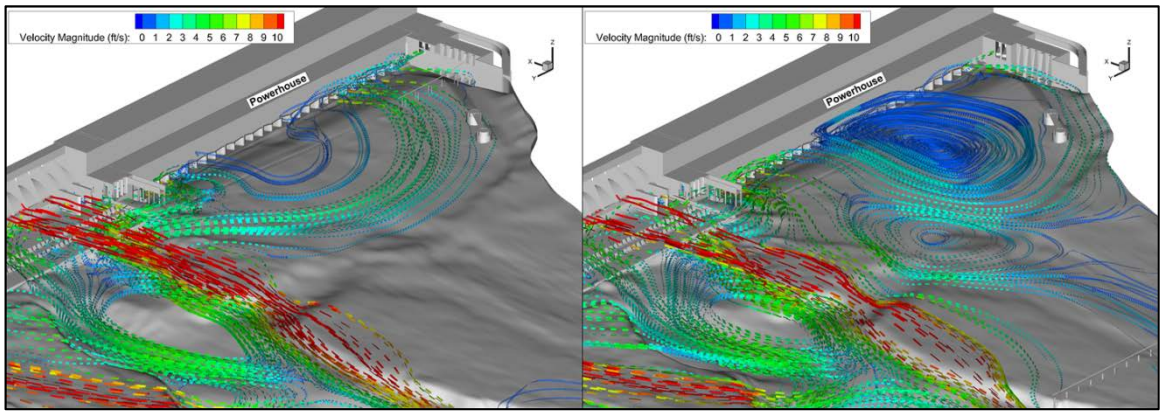

Figure C22 Streamlines in the southern region of the tailrace colored by velocity magnitude. Left: Simulation 1. Right: Simulation 2.

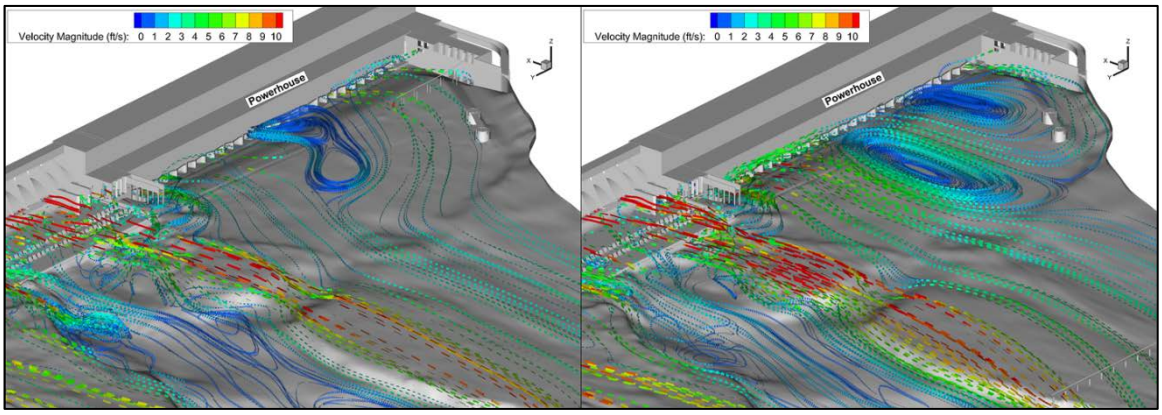

Figure C23 Streamlines in the southern region of the tailrace colored by velocity magnitude. Left: Simulation 3. Right: Simulation 4.

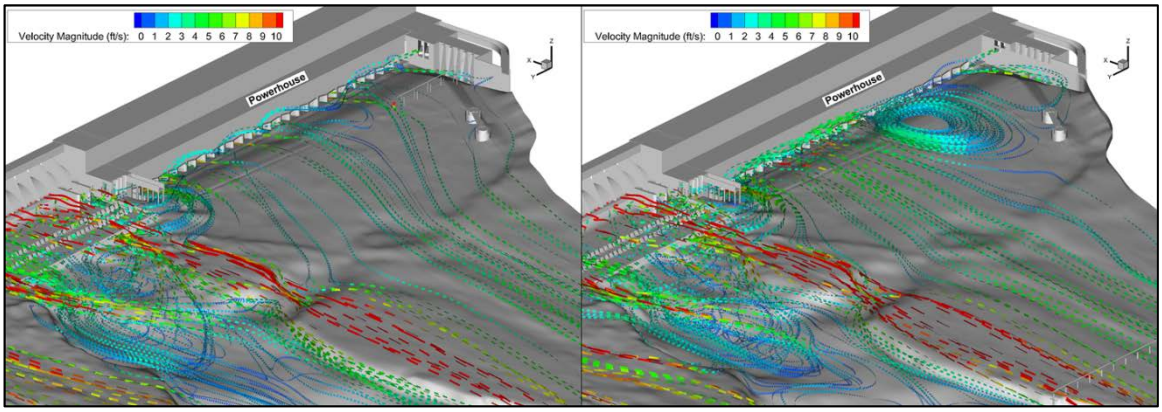

Figure C24 Streamlines in the southern region of the tailrace colored by velocity magnitude. Left: Simulation 5. Right: Simulation 6.

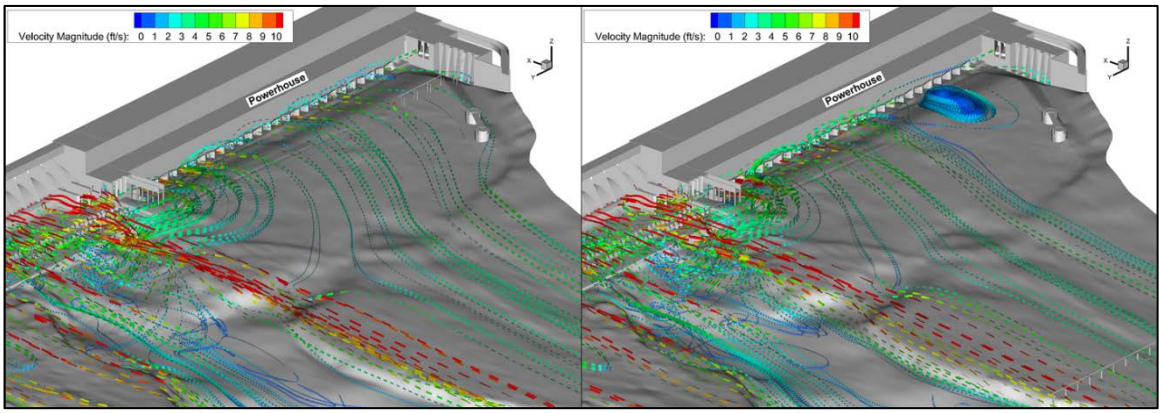

Figure C25 Streamlines in the southern region of the tailrace colored by velocity magnitude. Left: Simulation 7. Right: Simulation 8.

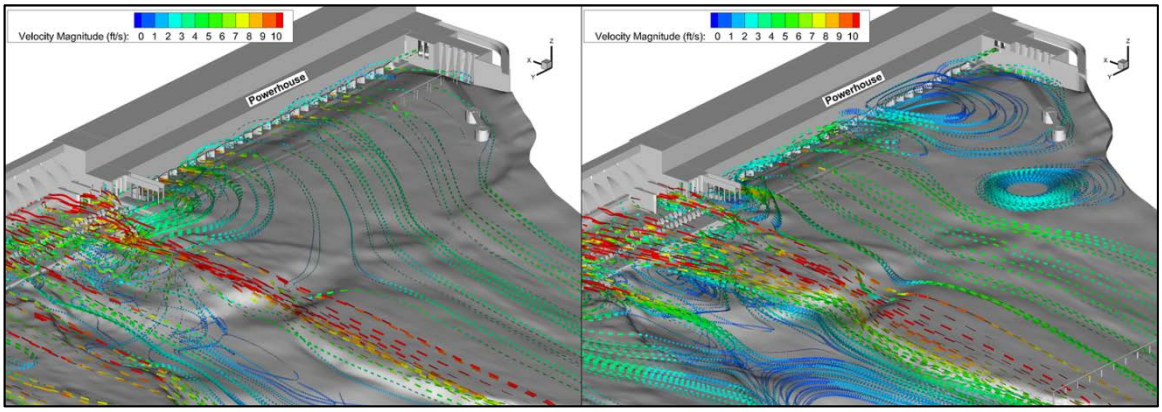

Figure C26 Streamlines in the southern region of the tailrace colored by velocity magnitude. Left: Simulation 11. Right: Simulation 12.

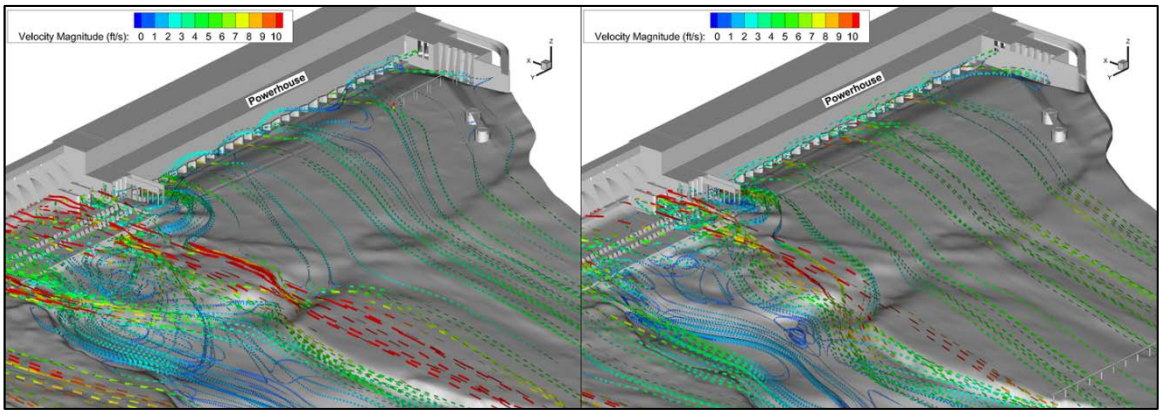

Figure C27 Streamlines in the southern region of the tailrace colored by velocity magnitude. Left: Simulation 13. Right: Simulation 14.

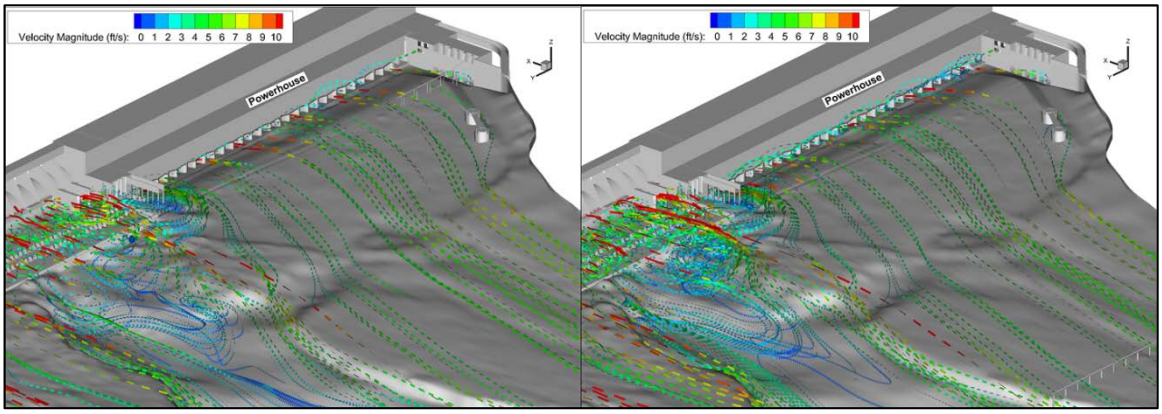

Figure C28 Streamlines in the southern region of the tailrace colored by velocity magnitude. Left: Simulation 15. Right: Simulation 16.

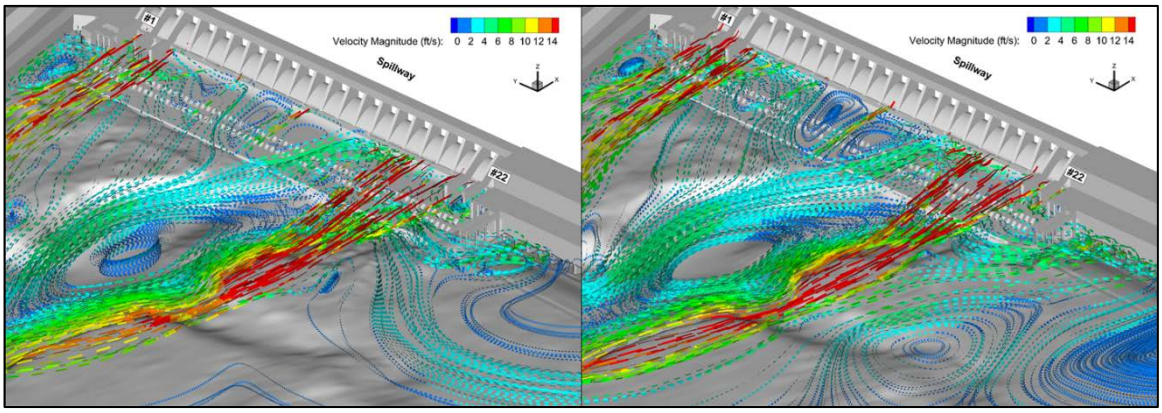

Figure C29 Streamlines in the northern region of the tailrace colored by velocity magnitude. Left: Simulation 1. Right: Simulation 2.

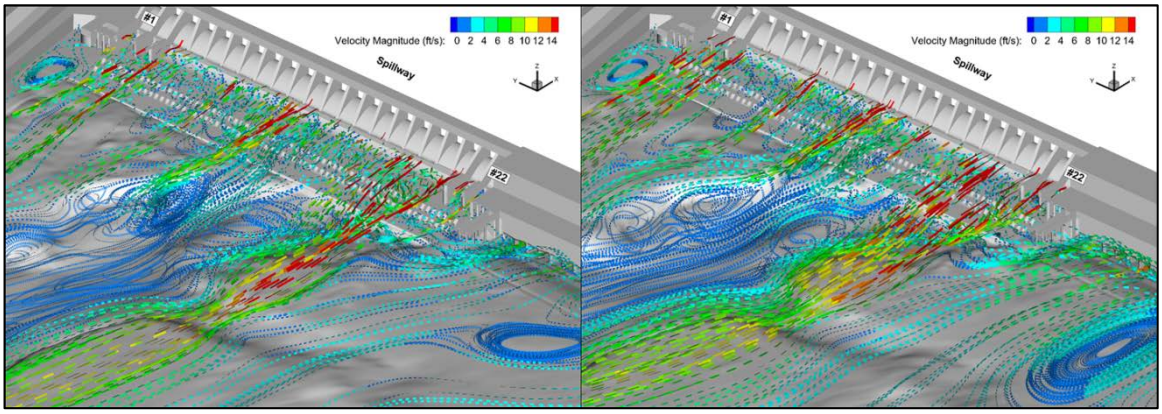

Figure C30 Streamlines in the northern region of the tailrace colored by velocity magnitude. Left: Simulation 3. Right: Simulation 4.

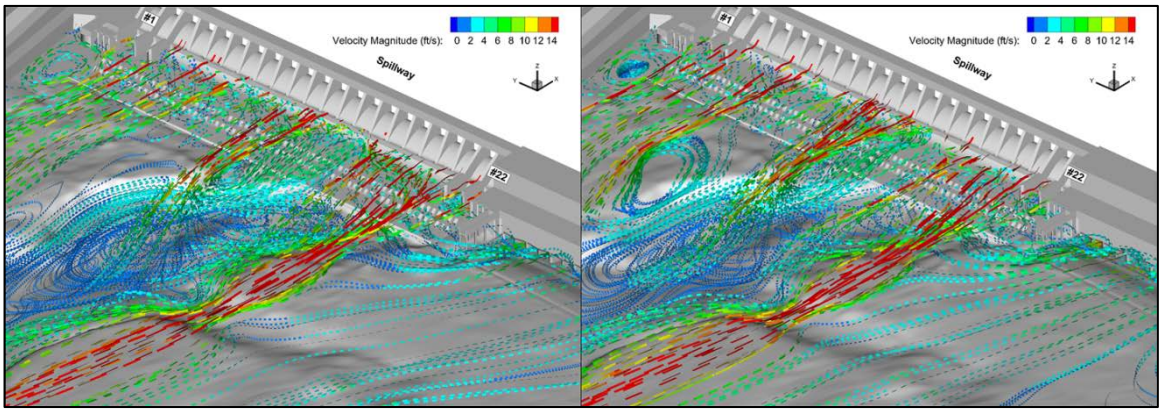

Figure C31 Streamlines in the northern region of the tailrace colored by velocity magnitude. Left: Simulation 5. Right: Simulation 6.

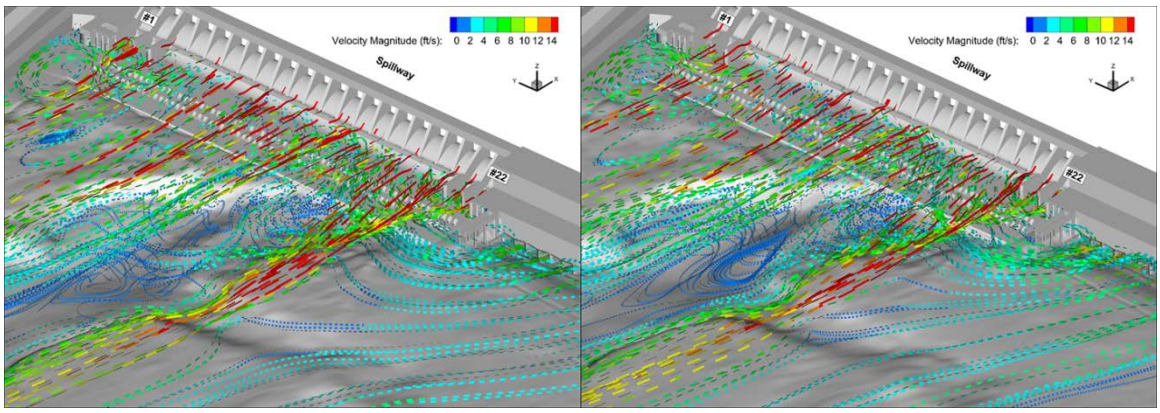

Figure C32 Streamlines in the northern region of the tailrace colored by velocity magnitude. Left: Simulation 7. Right: Simulation 8.

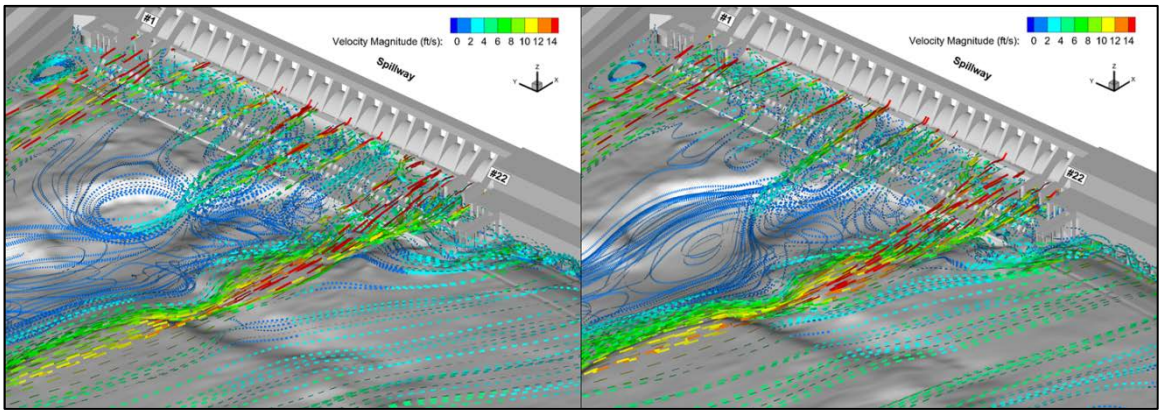

Figure C33 Streamlines in the northern region of the tailrace colored by velocity magnitude. Left: Simulation 11 Right: Simulation 12.

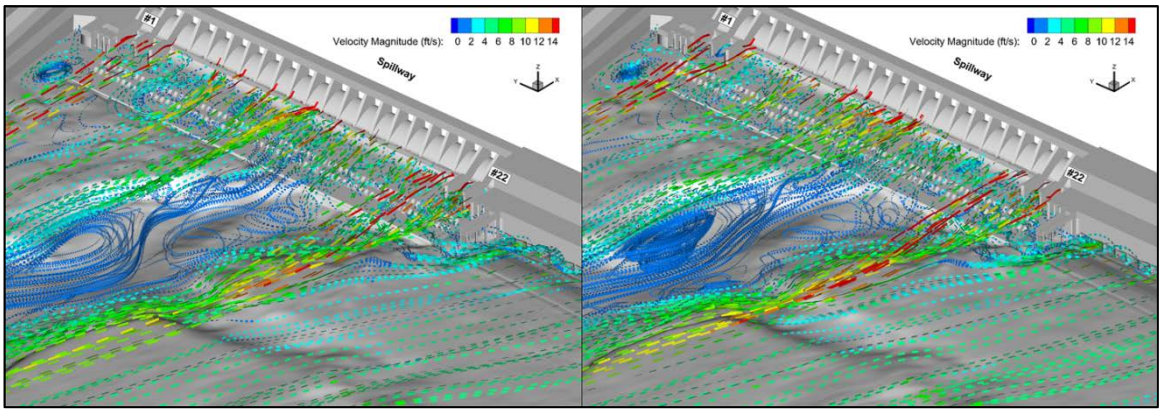

Figure C34 Streamlines in the northern region of the tailrace colored by velocity magnitude. Left: Simulation 13 Right: Simulation 14.

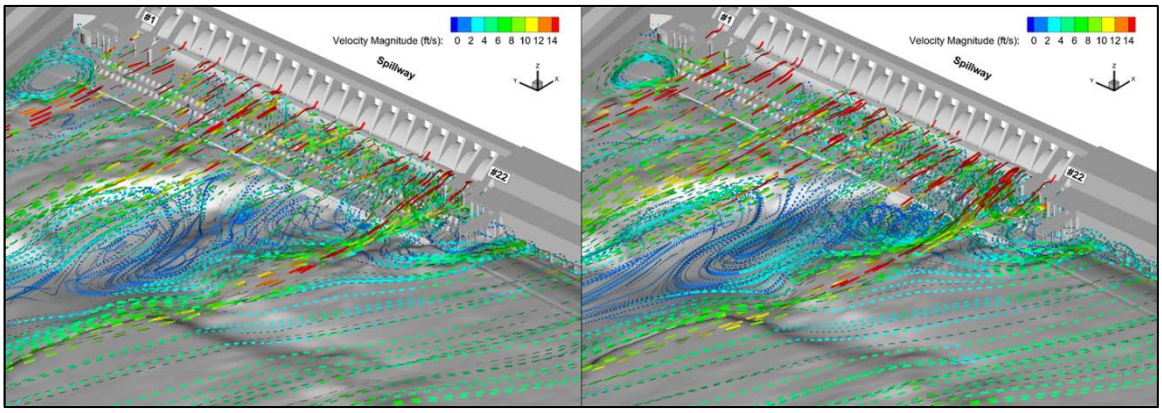

Figure C35 Streamlines in the northern region of the tailrace colored by velocity magnitude. Left: Simulation 15 Right: Simulation 16.

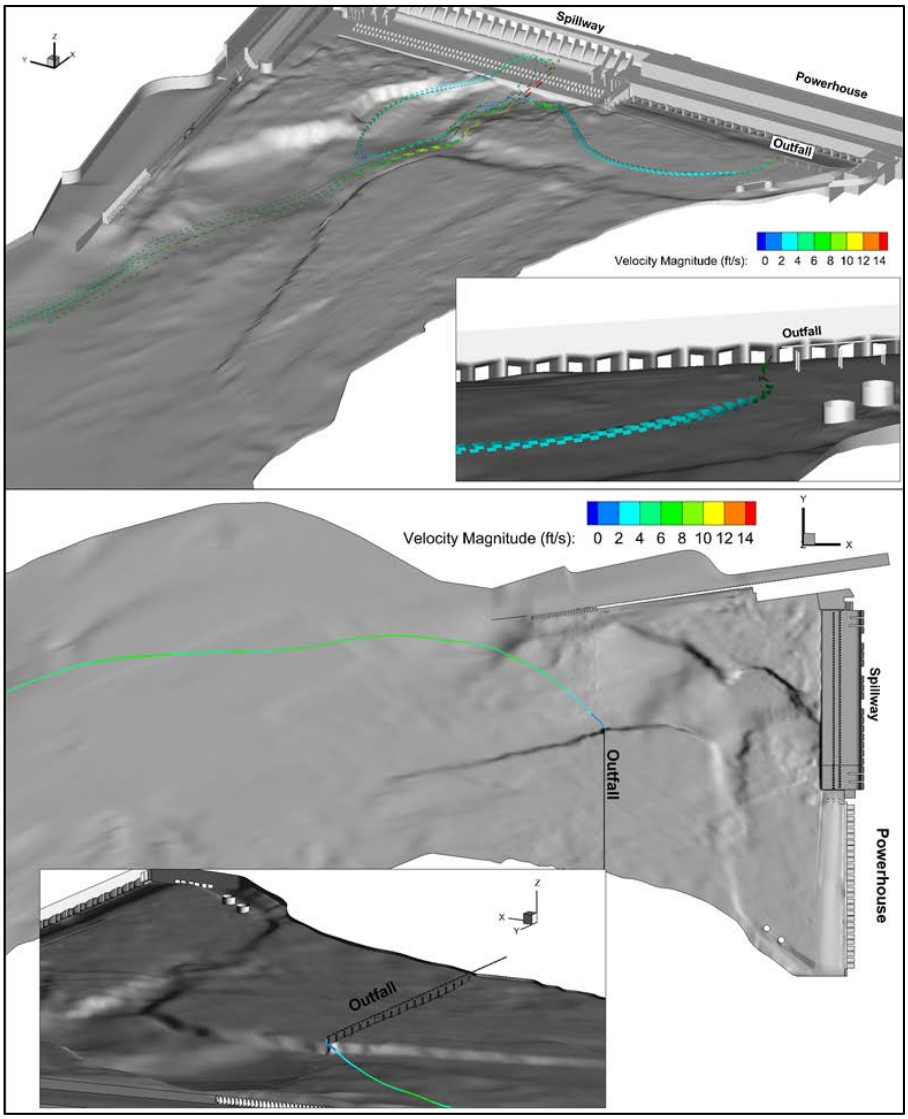

Figure C36. Streamlines released from the outfall colored by velocity magnitude. Top: Existing outfall (Simulation 1). Bottom: Proposed Outfall (Simulation 2).

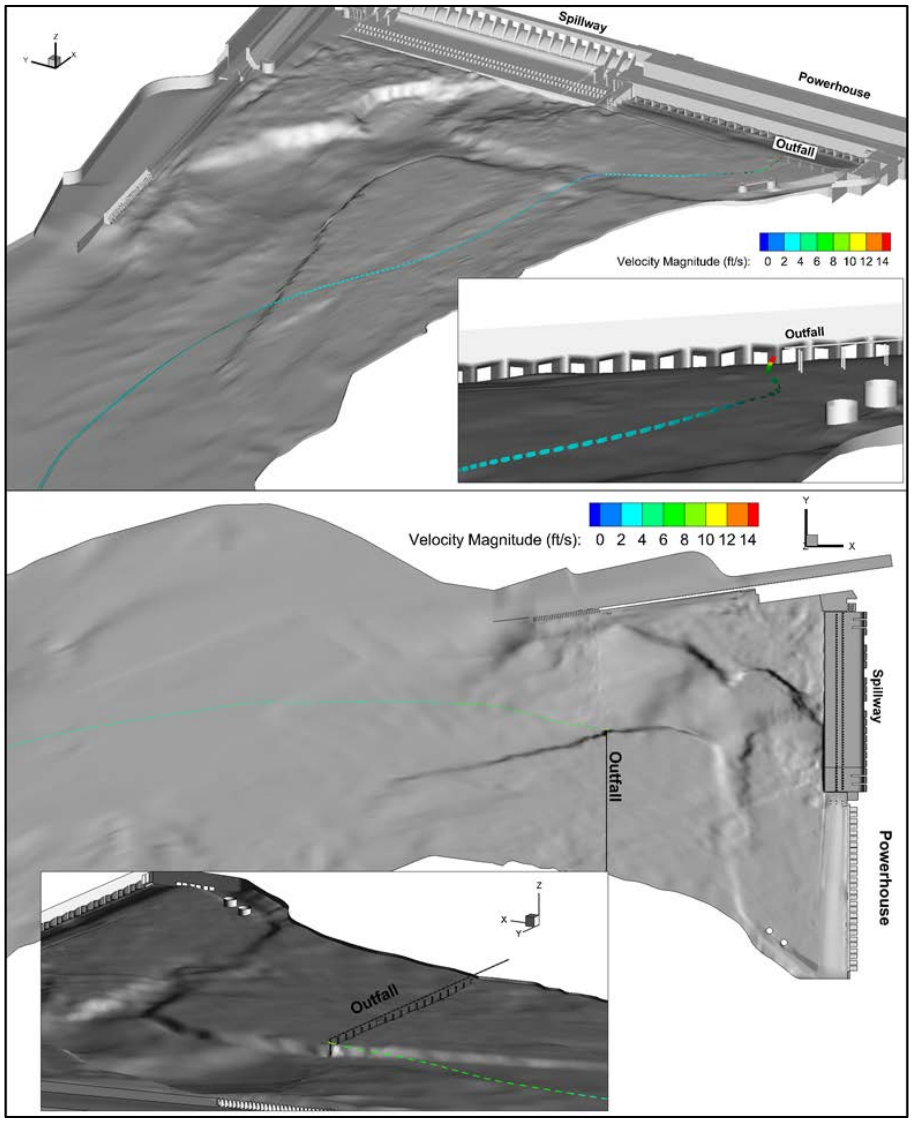

Figure C37. Streamlines released from the outfall colored by velocity magnitude. Top: Existing outfall (Simulation 3). Bottom: Proposed Outfall (Simulation 4).

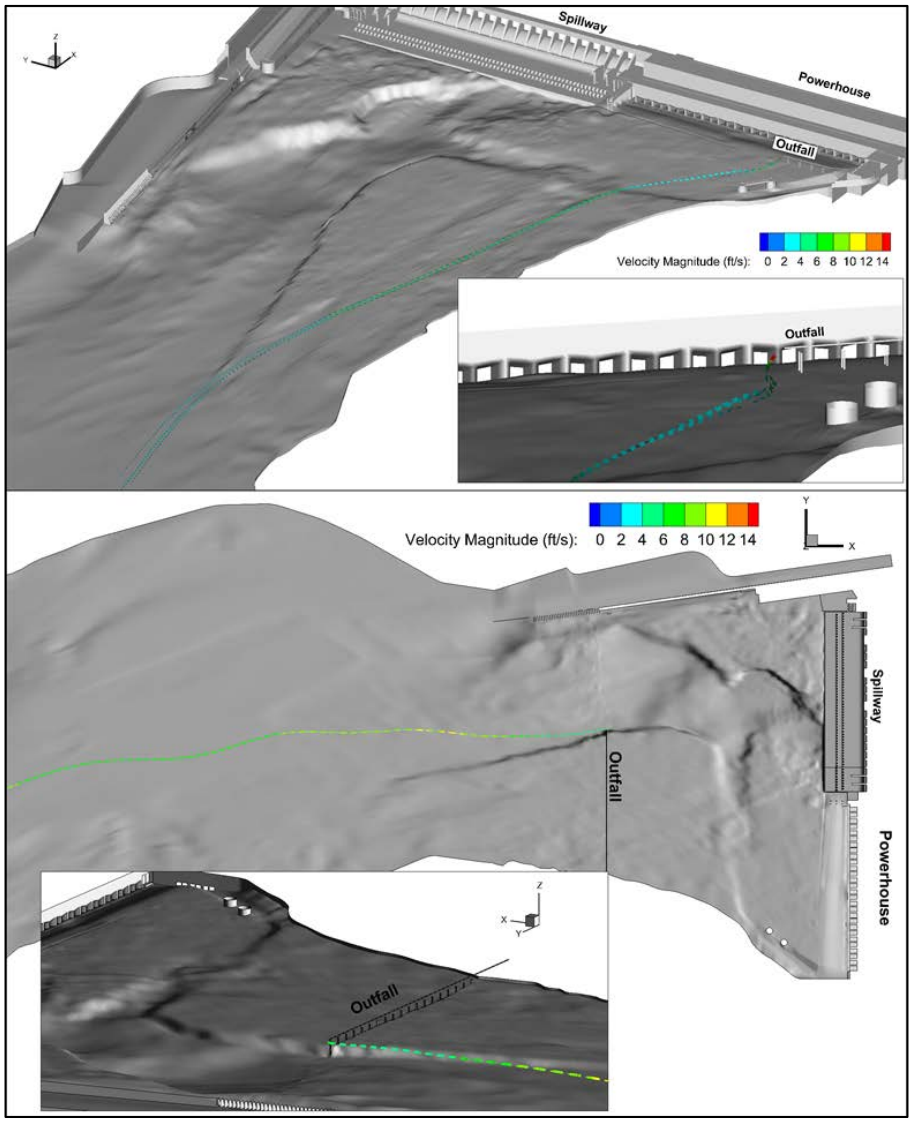

Figure C38. Streamlines released from the outfall colored by velocity magnitude. Top: Existing outfall (Simulation 5). Bottom: Proposed Outfall (Simulation 6).

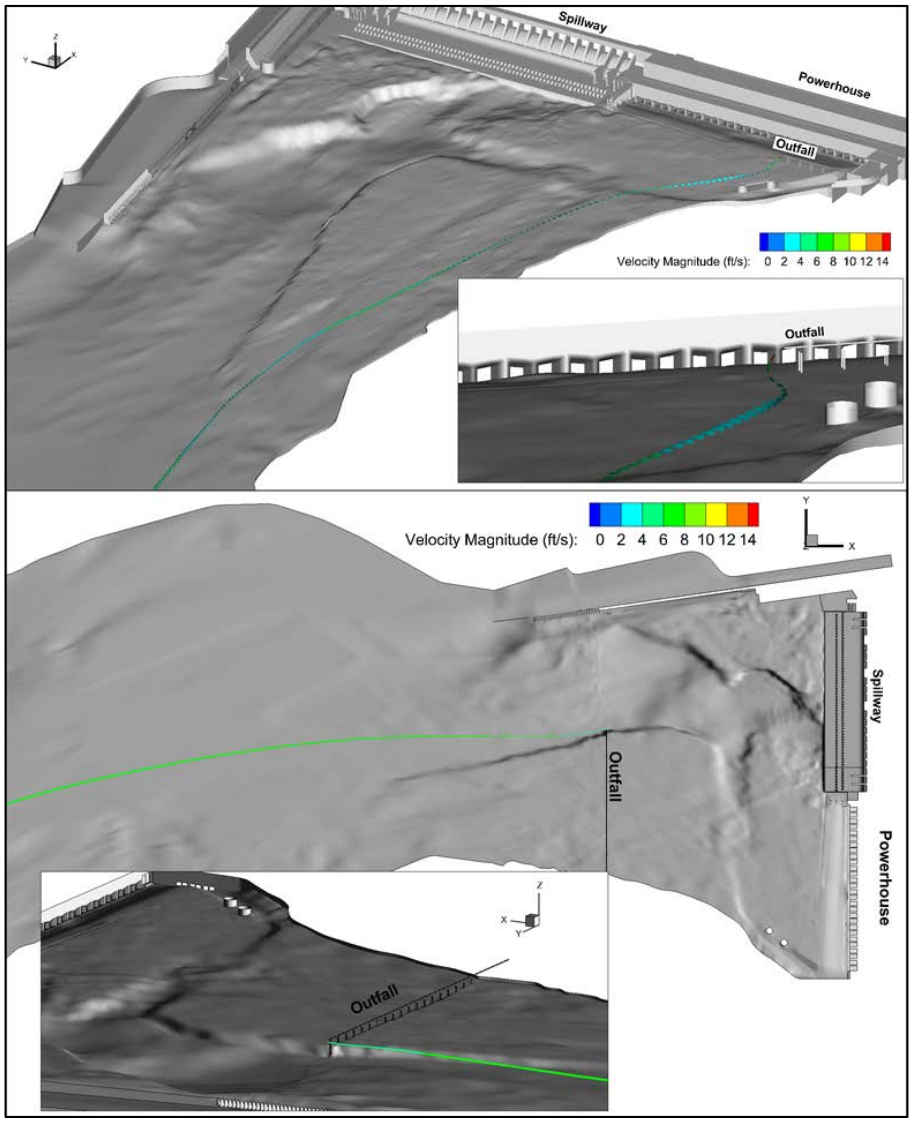

Figure C39. Streamlines released from the outfall colored by velocity magnitude. Top: Existing outfall (Simulation 7). Bottom: Proposed Outfall (Simulation 8).

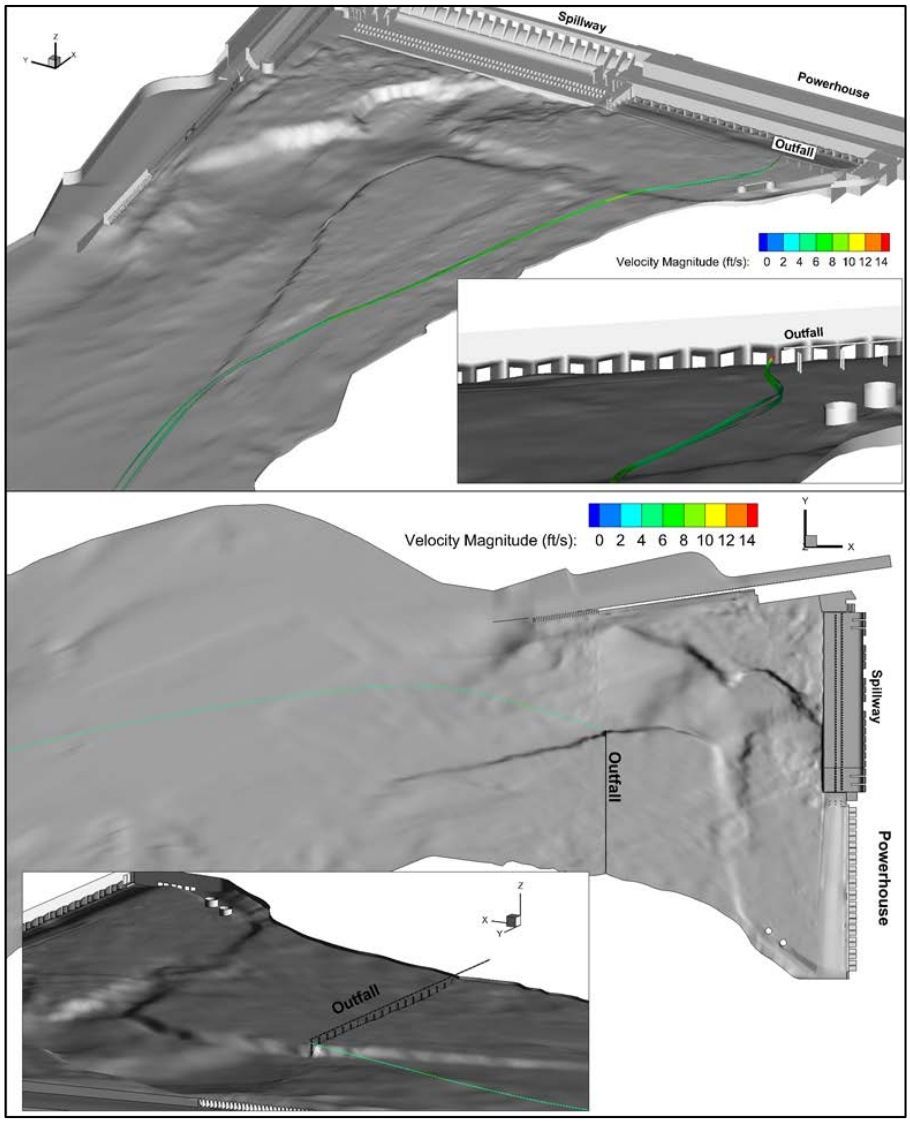

Figure C40. Streamlines released from the outfall colored by velocity magnitude. Top: Existing outfall (Simulation 11). Bottom: Proposed Outfall (Simulation 12).

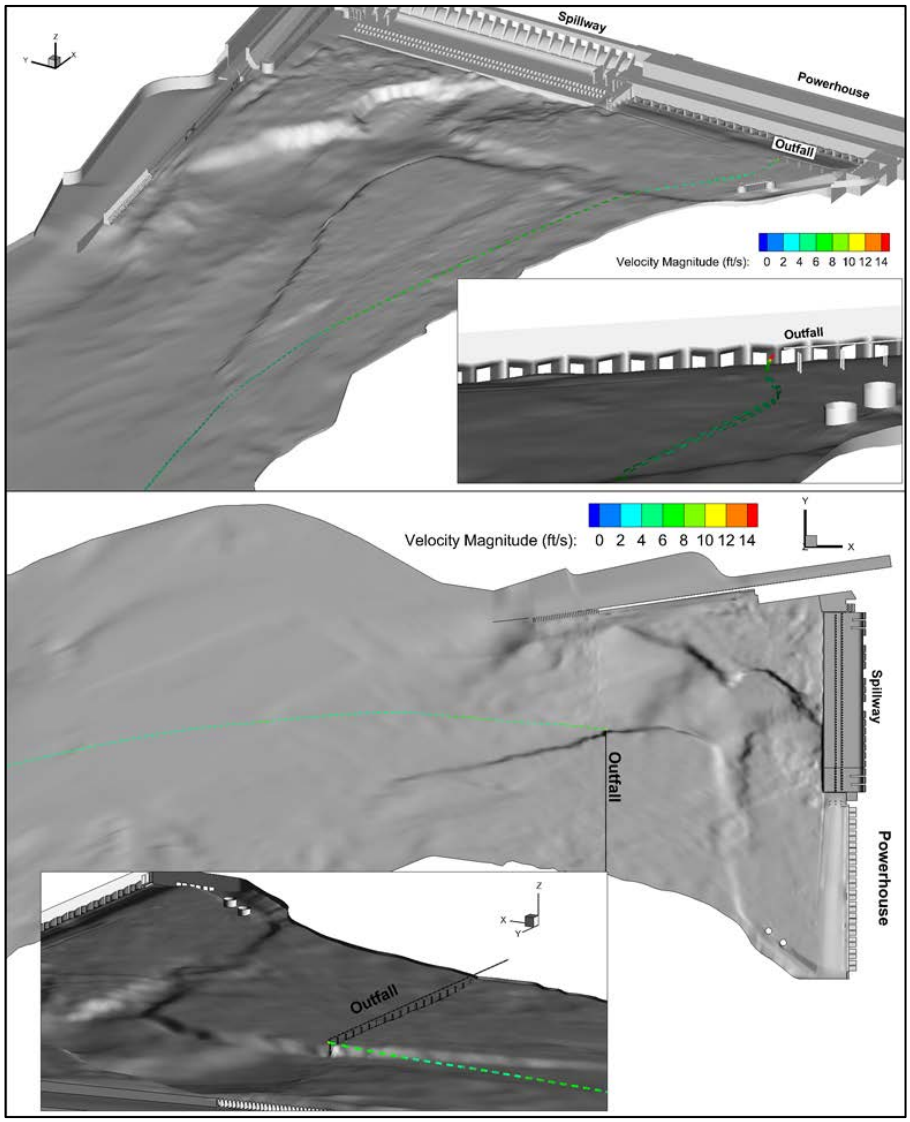

Figure C41. Streamlines released from the outfall colored by velocity magnitude. Top: Existing outfall (Simulation 13). Bottom: Proposed Outfall (Simulation 14).

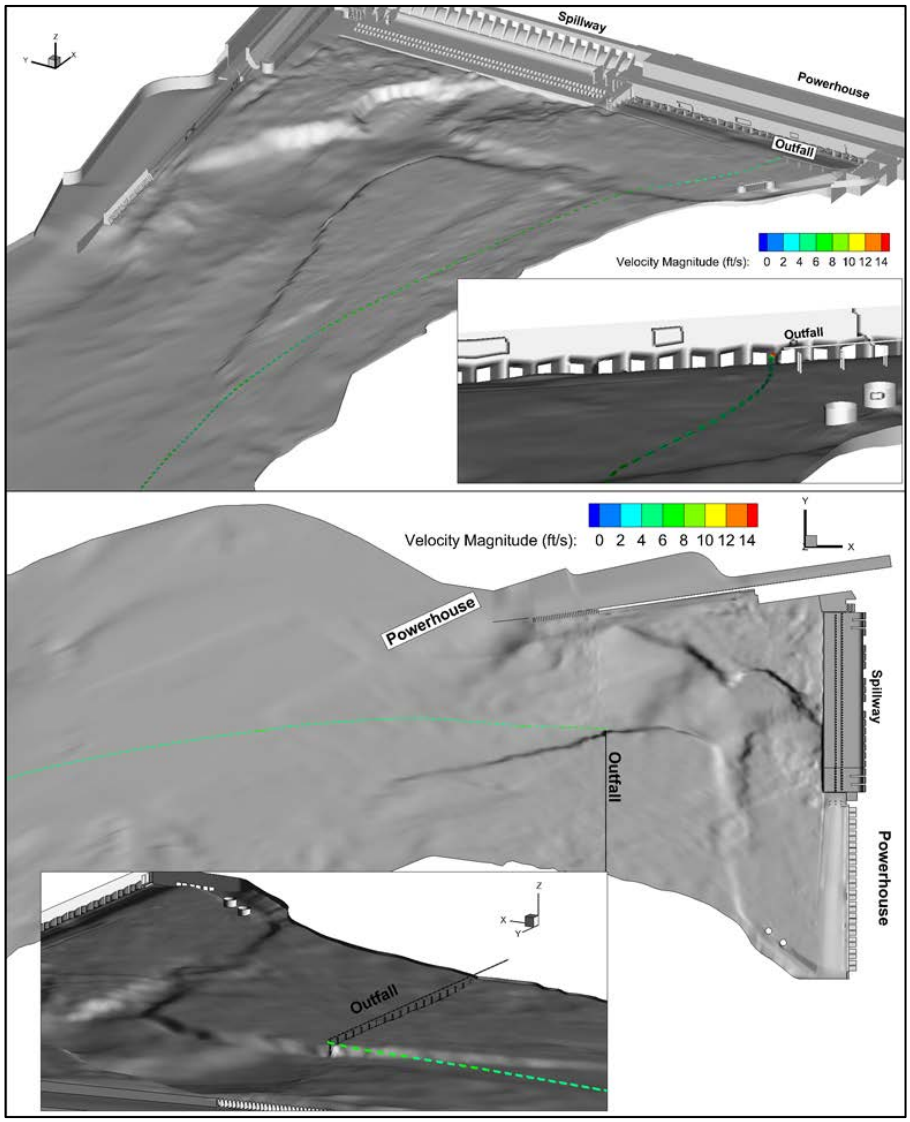

Figure C42. Streamlines released from the outfall colored by velocity magnitude. Top: Existing outfall (Simulation 15). Bottom: Proposed Outfall (Simulation 16).

APPENDIX D: PARTICLE TRACKS

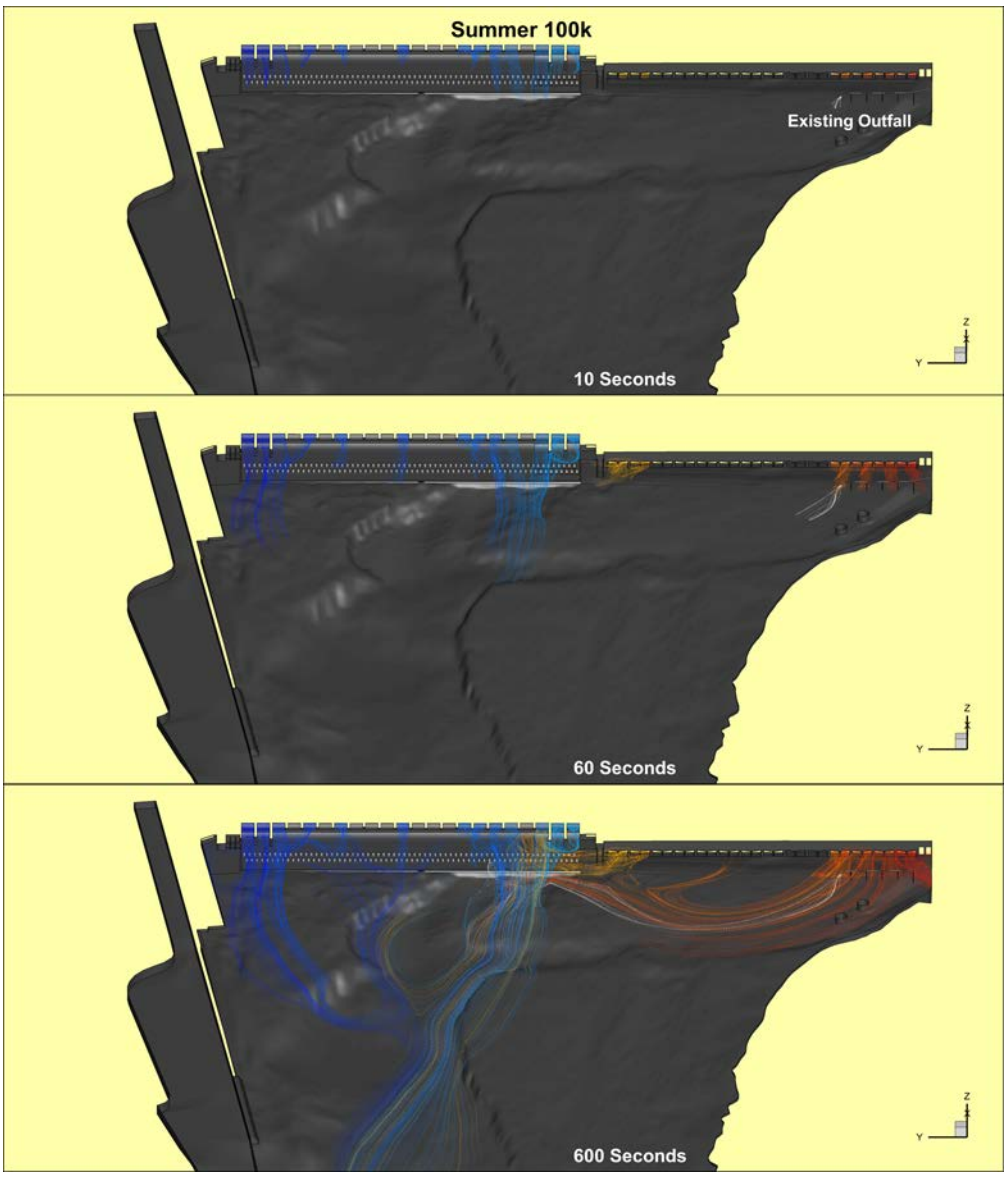

Figure D1. Particle tracks for 10 seconds, one minute and 10 minutes for Simulation 1.

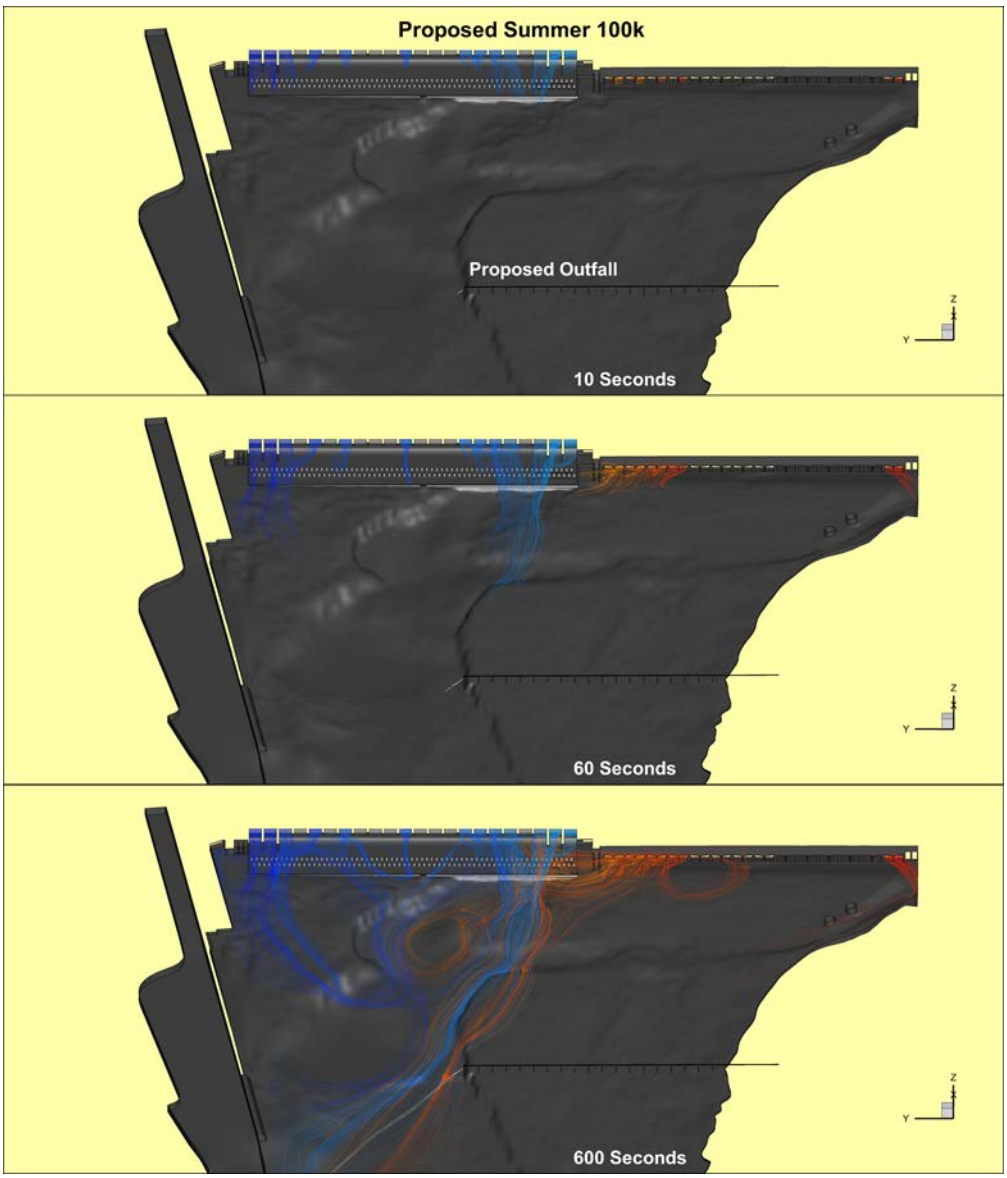

Figure D2. Particle tracks for 10 seconds, one minute and 10 minutes for Simulation 2.

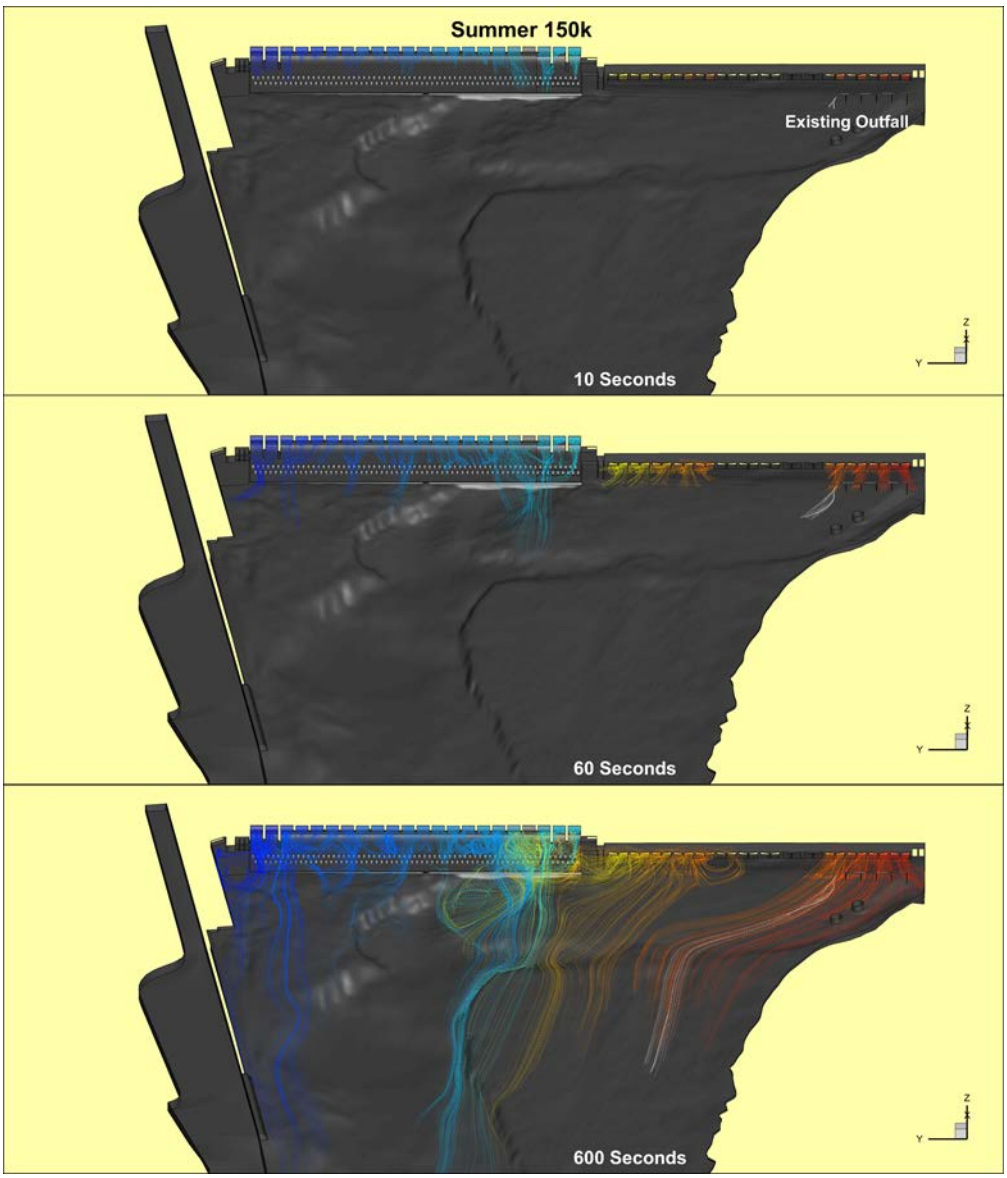

Figure D3. Particle tracks for 10 seconds, one minute and 10 minutes for Simulation 3.

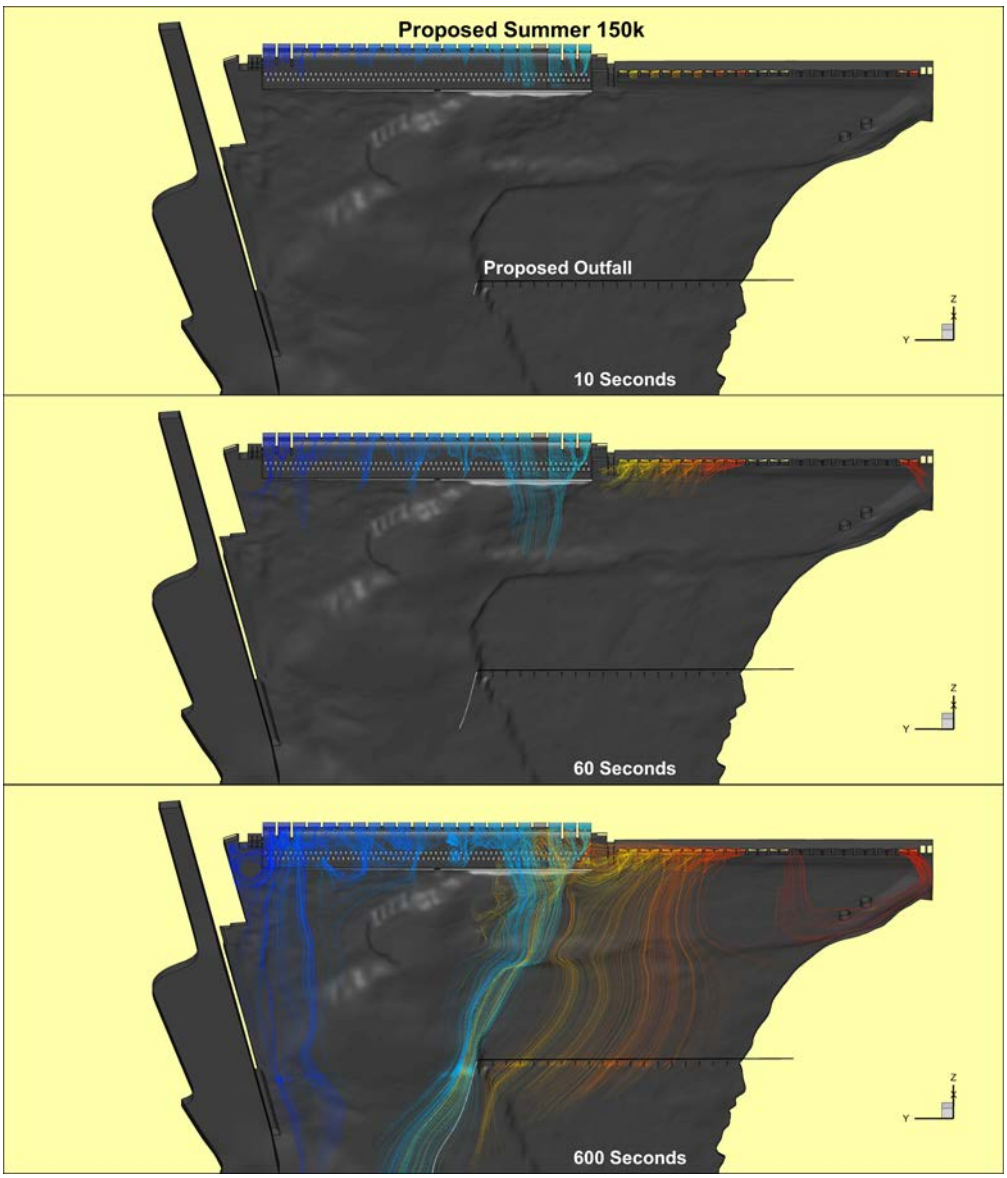

Figure D4. Particle tracks for 10 seconds, one minute and 10 minutes for Simulation 4.

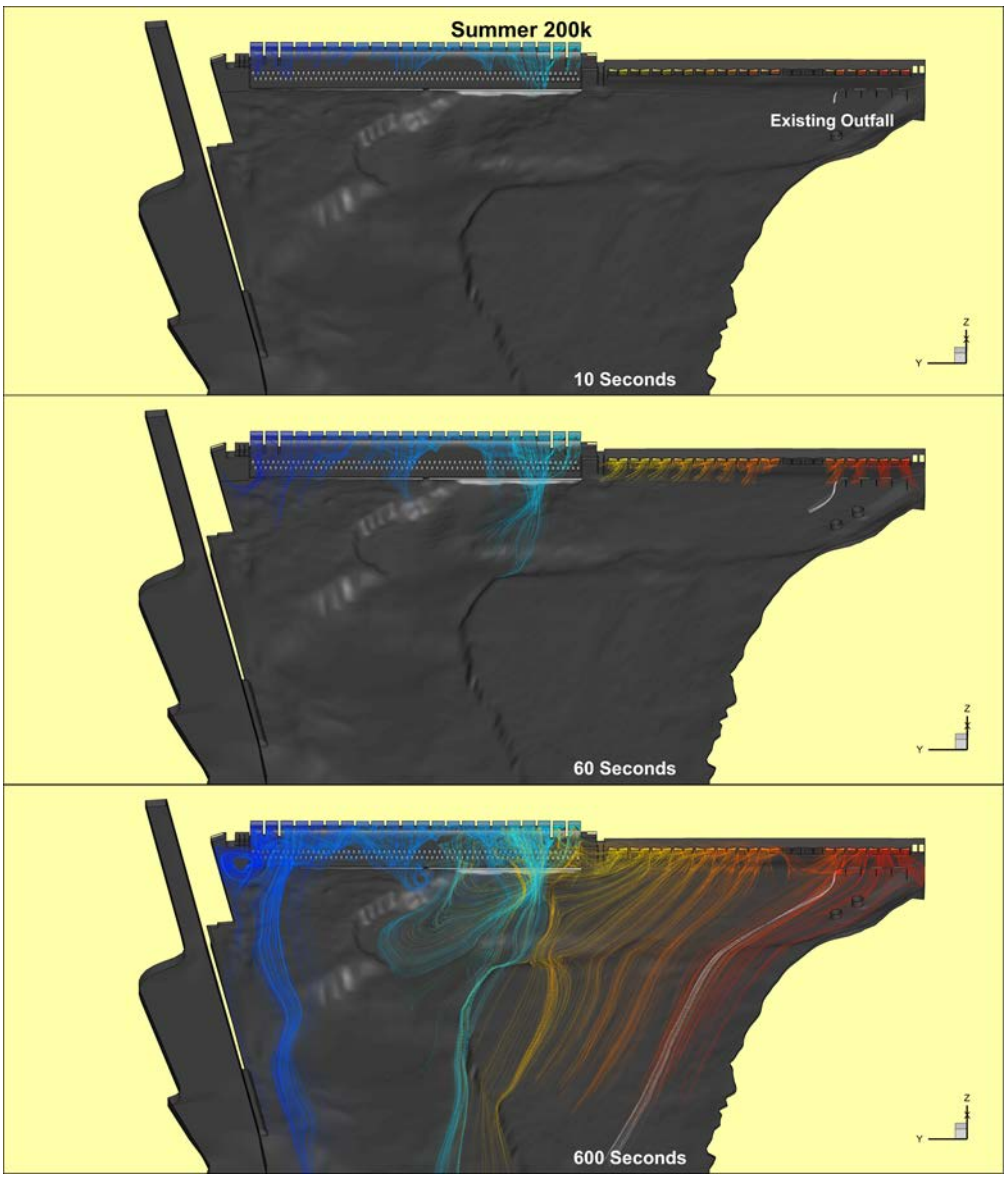

Figure D5. Particle tracks for 10 seconds, one minute and 10 minutes for Simulation 5.

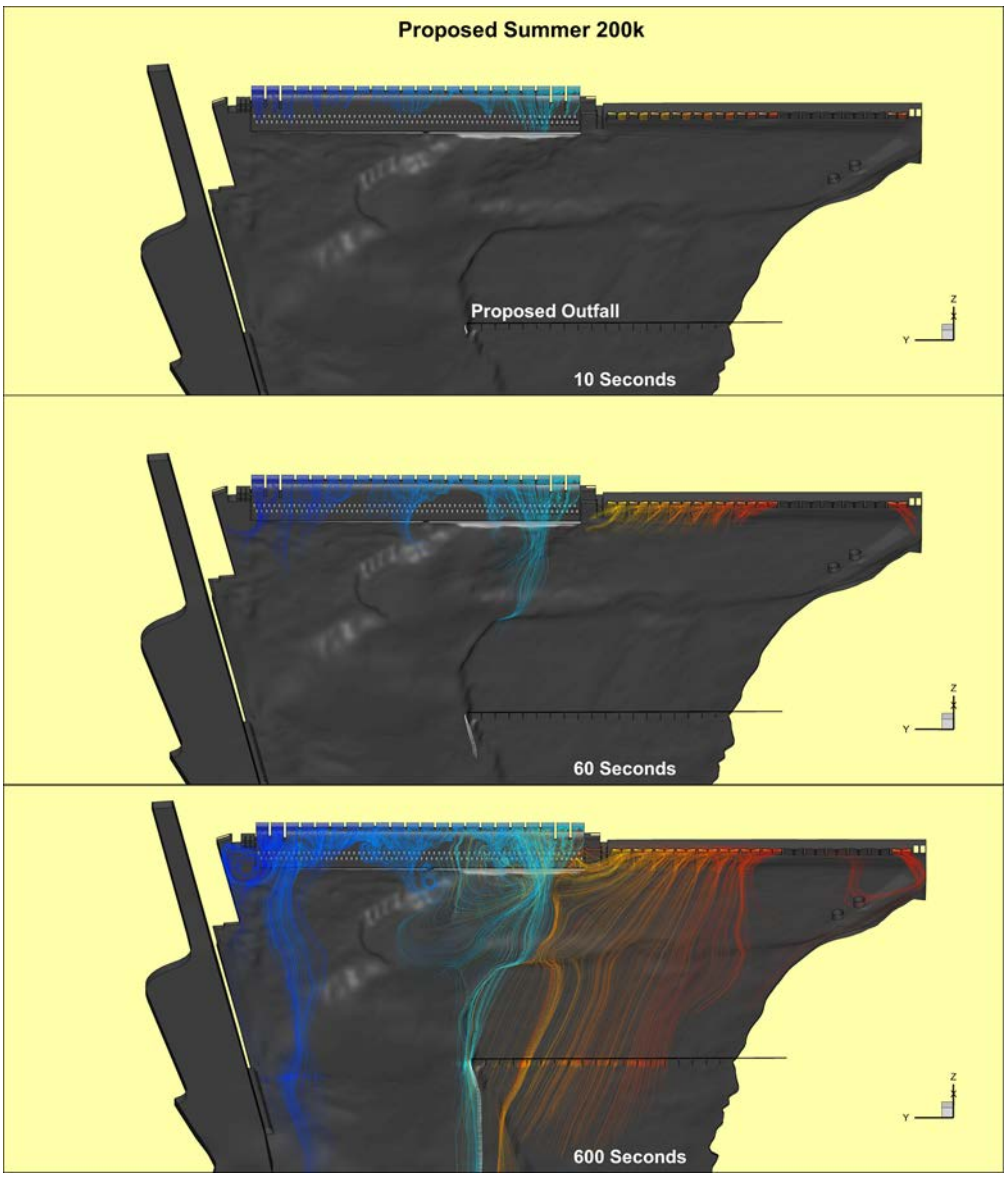

Figure D6. Particle tracks for 10 seconds, one minute and 10 minutes for Simulation 6.

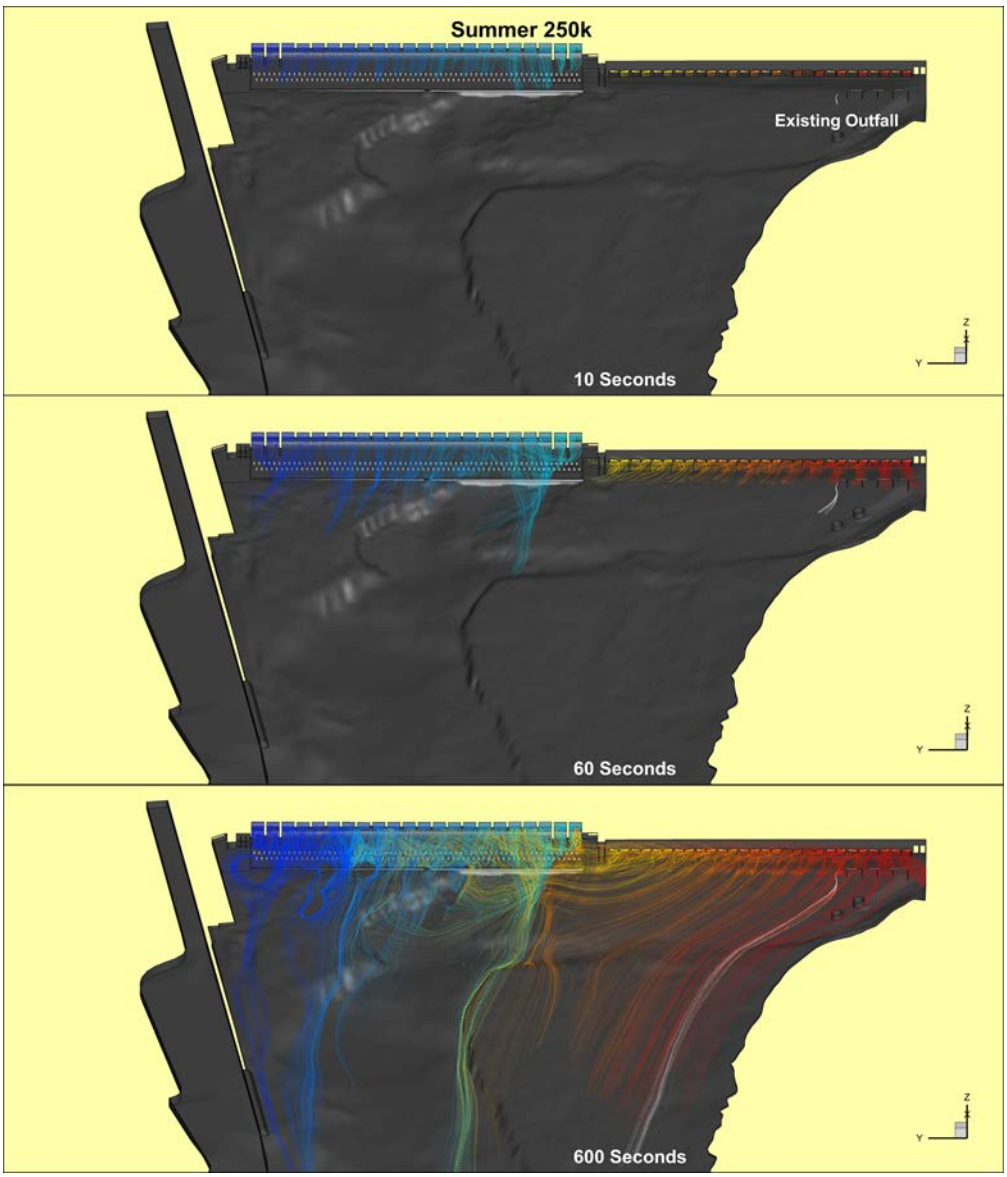

Figure D7. Particle tracks for 10 seconds, one minute and 10 minutes for Simulation 7.

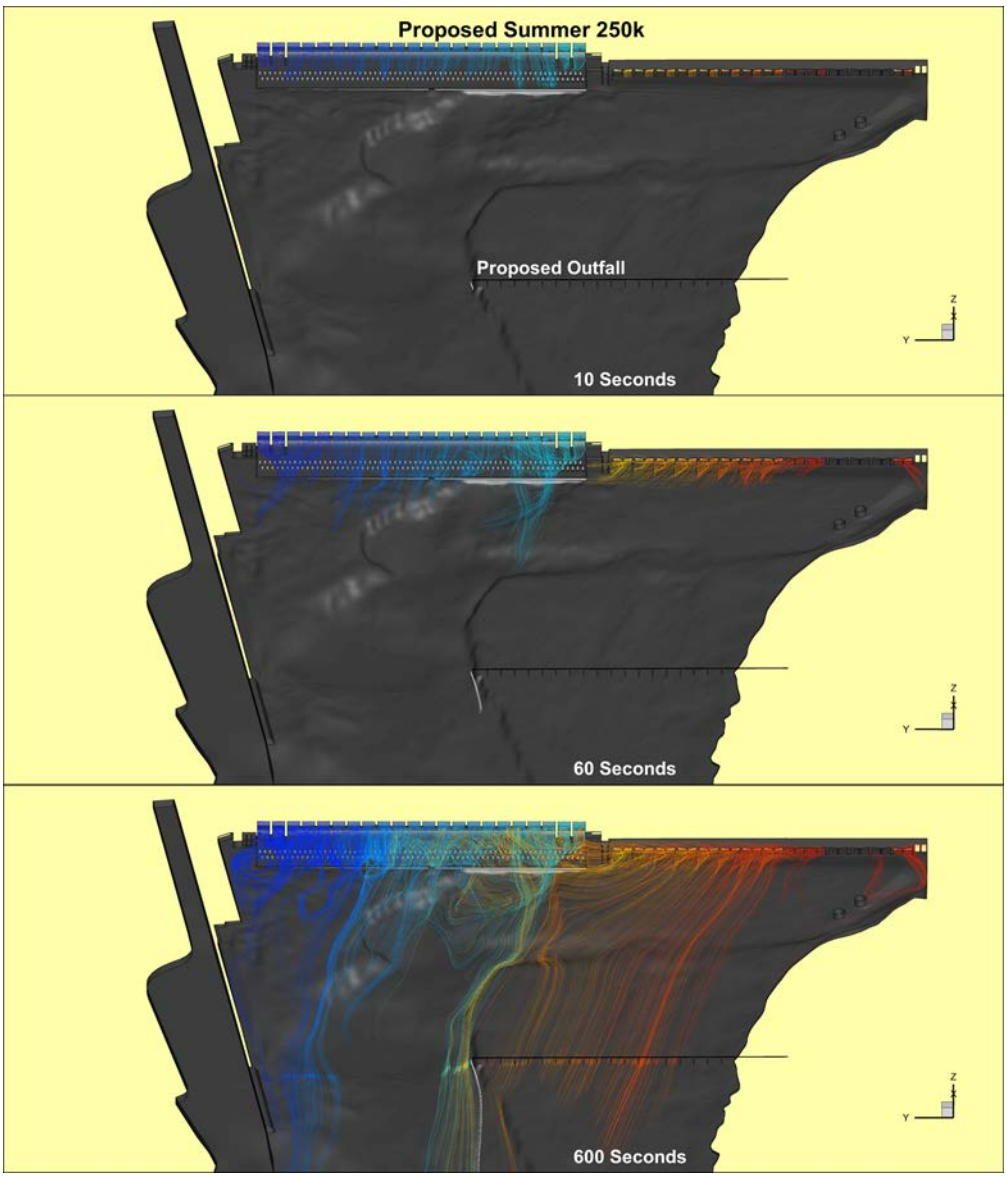

Figure D8. Particle tracks for 10 seconds, one minute and 10 minutes for Simulation 8.

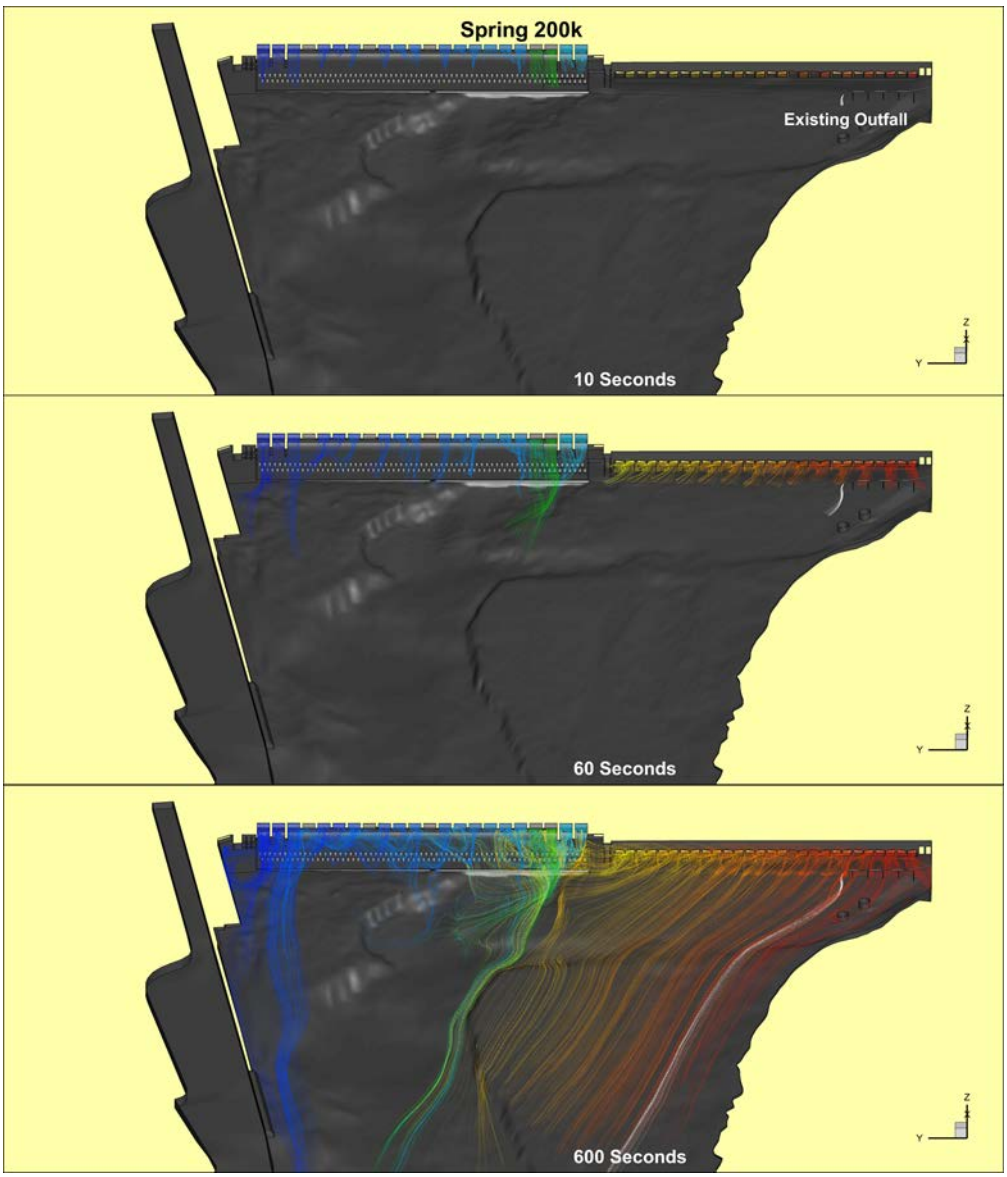

Figure D9. Particle tracks for 10 seconds, one minute and 10 minutes for Simulation 11.

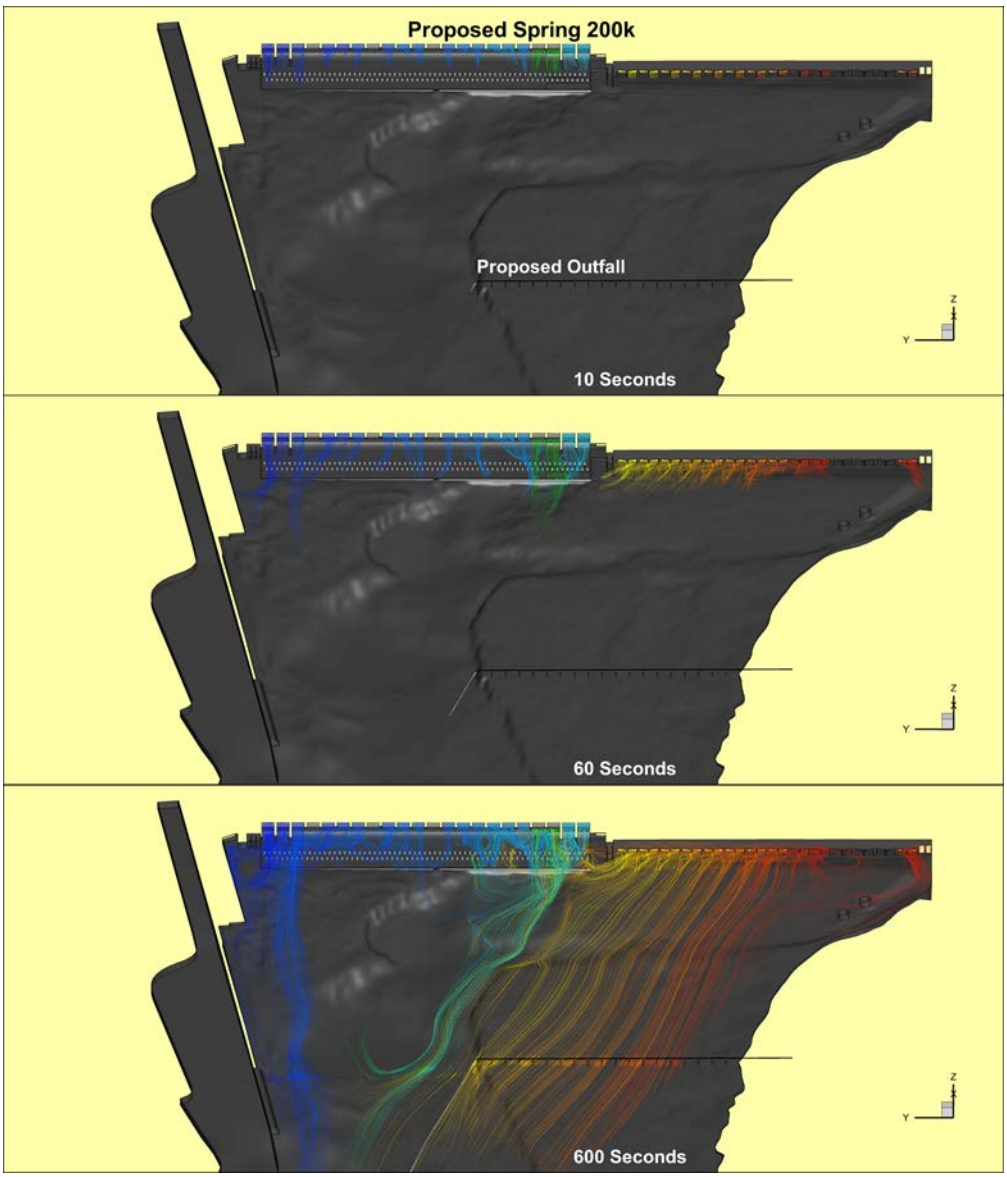

Figure D10. Particle tracks for 10 seconds, one minute and 10 minutes for Simulation 12.

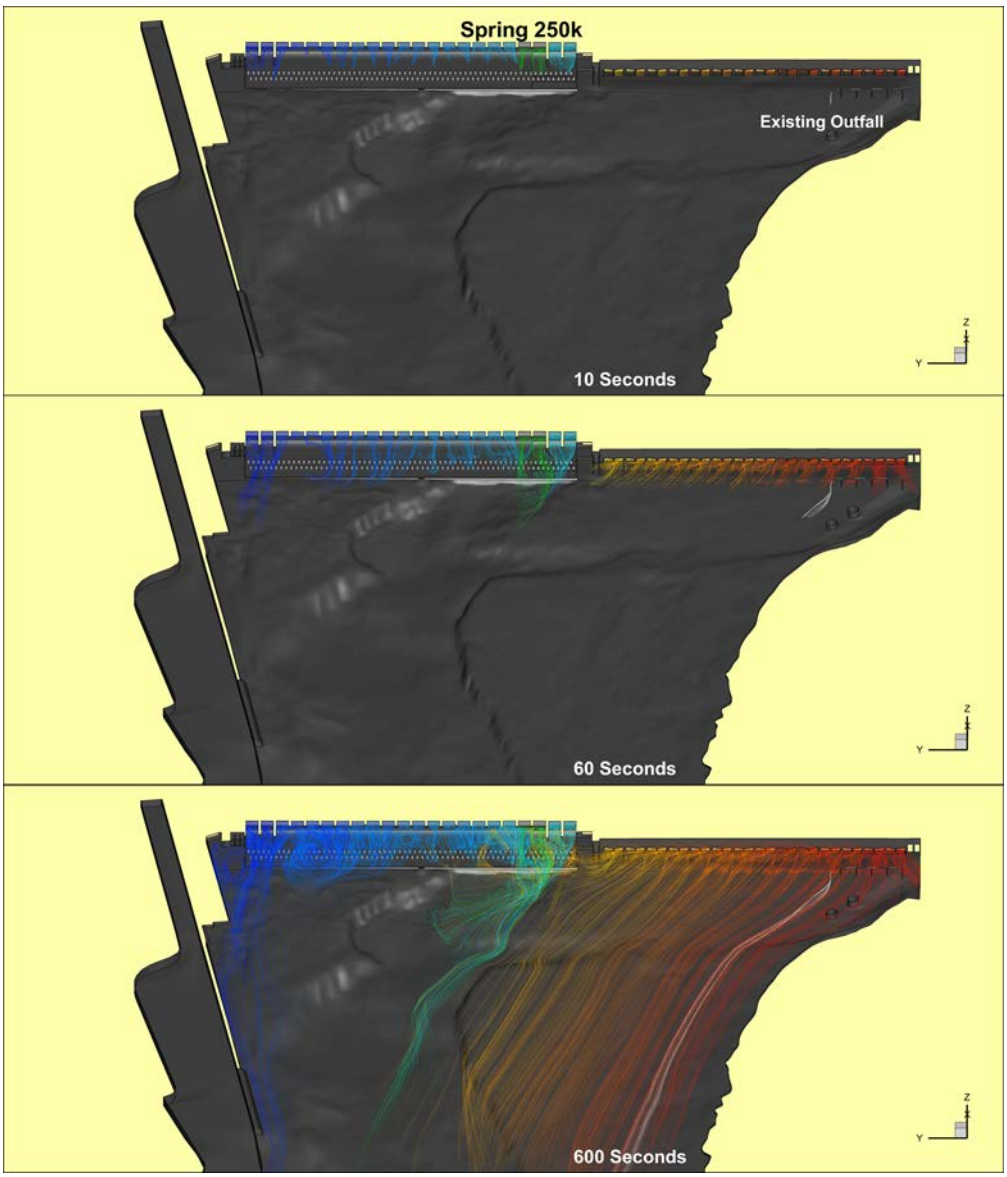

Figure D11. Particle tracks for 10 seconds, one minute and 10 minutes for Simulation 13.

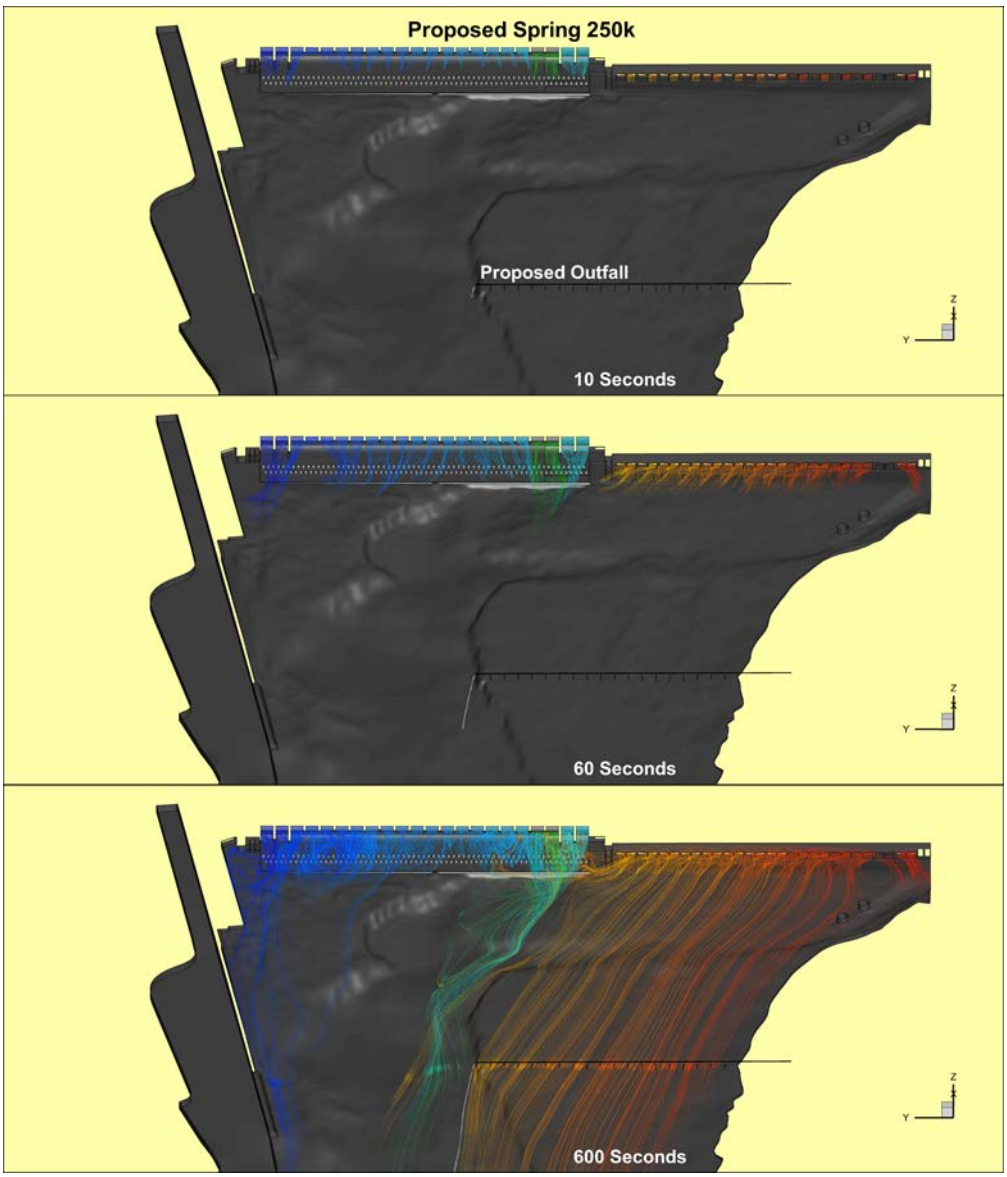

Figure D12. Particle tracks for 10 seconds, one minute and 10 minutes for Simulation 14.

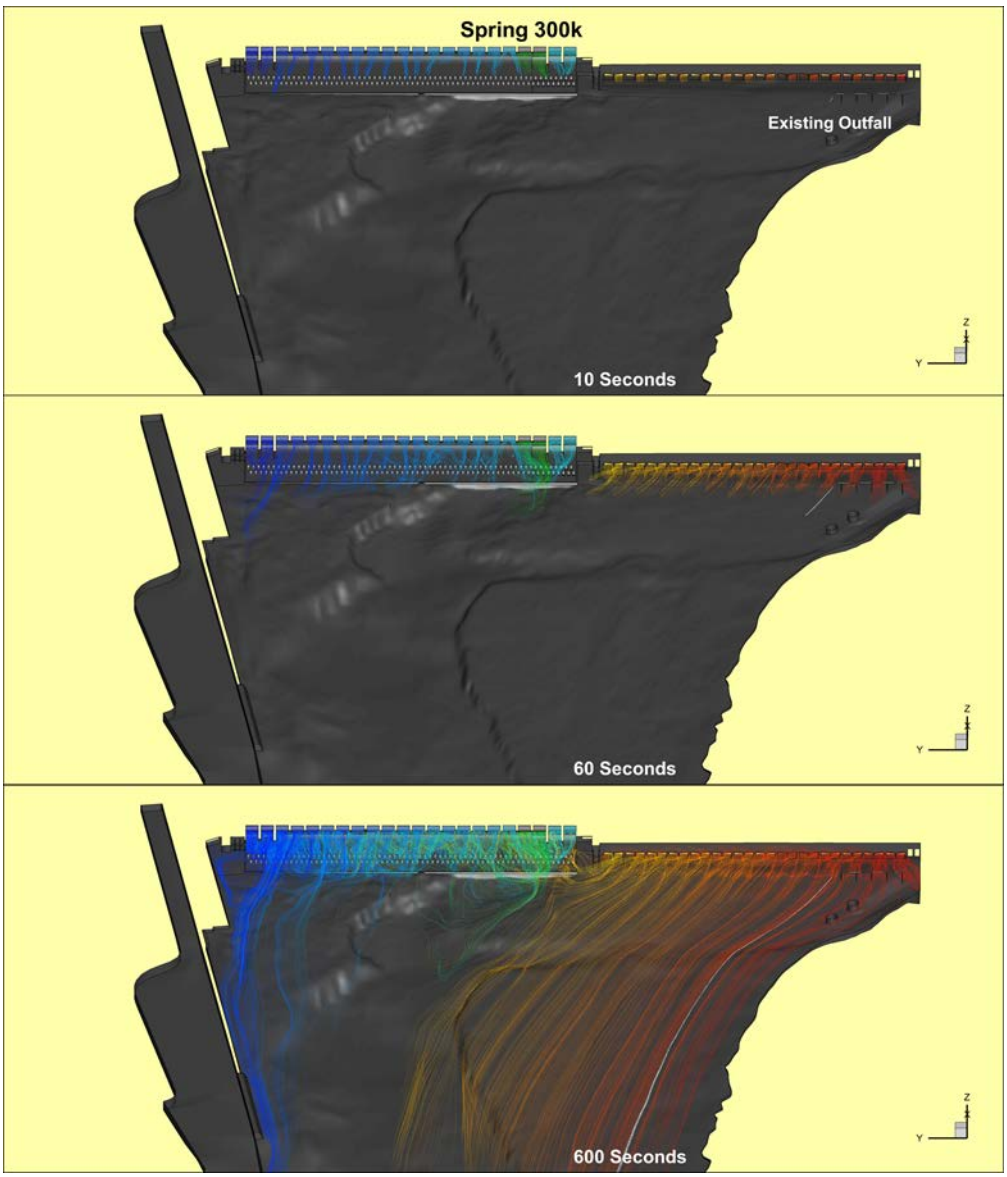

Figure D13. Particle tracks for 10 seconds, one minute and 10 minutes for Simulation 15.

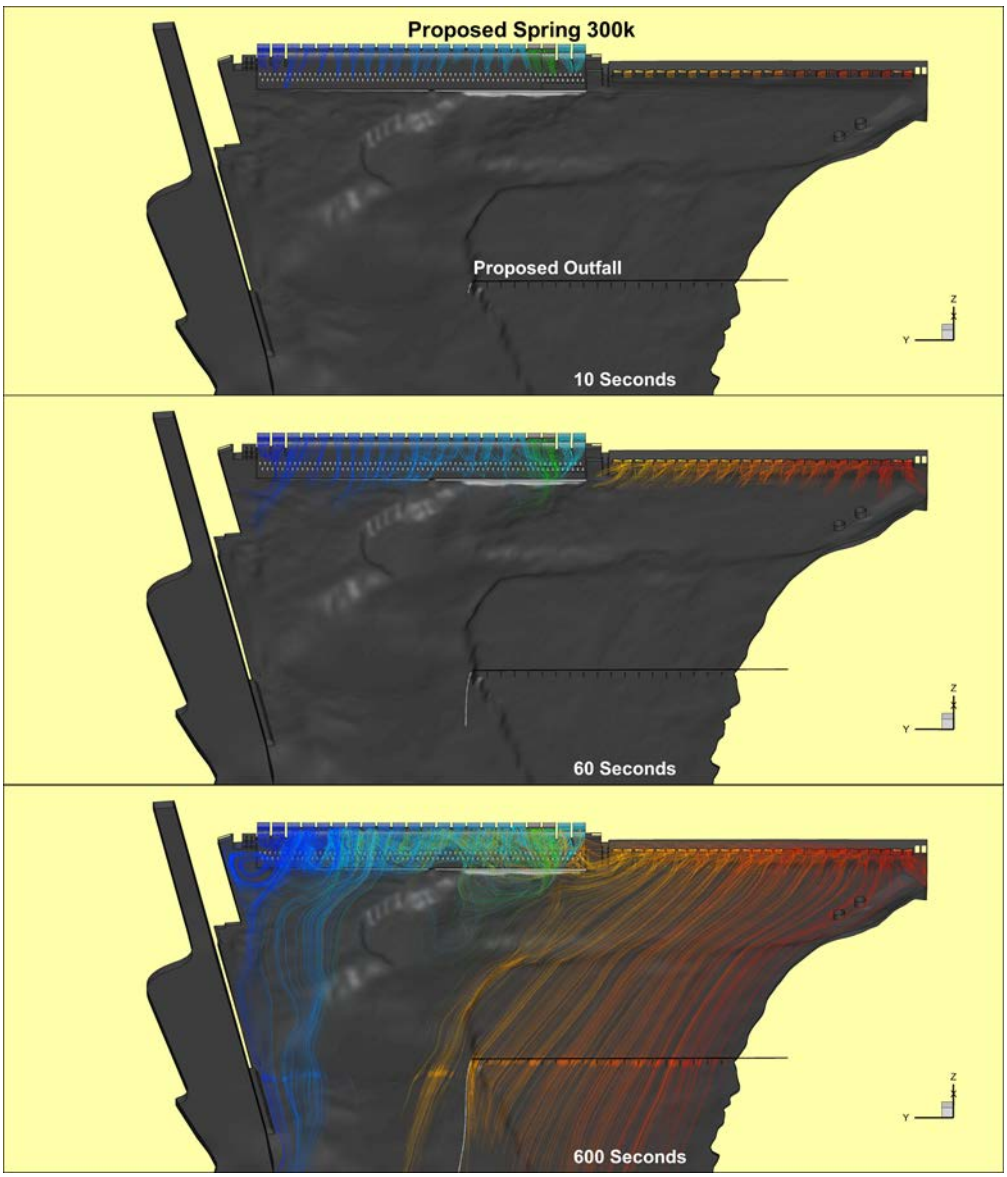

Figure D14. Particle tracks for 10 seconds, one minute and 10 minutes for Simulation 16.

APPENDIX E. EXPOSURE TABLES

Table E1 Exposure percentages after 10 seconds, 1 minute and 10 minutes for Simulation 1

Summer 100k- Exposure Percentage After 10 Seconds

Powerhouse Flow Exposure

	U1	U2	U3	U4	U5	U6	U7	U8	U9	U10	U11	U12	U13	U14	Outflow
Velocity	50	51	51	51	n/a	n/a	n/a	n/a	n/a	n/a	n/a	n/a	50	50	48
All	0	0	0	0	n/a	n/a	n/a	n/a	n/a	n/a	n/a	n/a	0	0	0

Spillway Flow Exposure

	S1	S2	S3	S4	S5	S6	S7	S8	S9	S10	S11	S12	S13	S14	S15	S16	S17	S18	S19	S20	S21	S22
Velocity	6	0	0	n/a	0	n/a	24.3	n/a	n/a	n/a	24	n/a	n/a	n/a	37.5	0	0	0	n/a	0	6	18
All	2	0	0	n/a	0	n/a	0	n/a	n/a	n/a	0	n/a	n/a	n/a	0	0	0	0	n/a	0	0	0

Summer 100k- Exposure Percentage After 1 Minute

Powerhouse Flow Exposure

	U1	U2	U3	U4	U5	U6	U7	U8	U9	U10	U11	U12	U13	U14	Outflow
Velocity	100	92	88	91	n/a	n/a	n/a	n/a	n/a	n/a	n/a	n/a	100	100	66
All	5	34	4	0	n/a	n/a	n/a	n/a	n/a	n/a	n/a	n/a	0	0	0

Spillway Flow Exposure

	S1	S2	S3	S4	S5	S6	S7	S8	S9	S10	S11	S12	S13	S14	S15	S16	S17	S18	S19	S20	S21	S22
Velocity	24	6	0	n/a	68	n/a	100	n/a	n/a	n/a	100	n/a	n/a	n/a	100	100	0	0	n/a	0	76	90
All	24	6	0	n/a	20	n/a	0	n/a	n/a	n/a	0	n/a	n/a	n/a	0	0	0	0	n/a	0	0	0

Summer 100k- Exposure Percentage After 10 Minutes

Powerhouse Flow Exposure

	U1	U2	U3	U4	U5	U6	U7	U8	U9	U10	U11	U12	U13	U14	Outflow
Velocity	100	100	100	100	n/a	n/a	n/a	n/a	n/a	n/a	n/a	n/a	100	100	100
All	54	82	12	0	n/a	n/a	n/a	n/a	n/a	n/a	n/a	n/a	0	0	0

Spillway Flow Exposure

	S1	S2	S3	S4	S5	S6	S7	S8	S9	S10	S11	S12	S13	S14	S15	S16	S17	S18	S19	S20	S21	S22
Velocity	100	100	100	n/a	100	n/a	100	n/a	n/a	n/a	100	n/a	n/a	n/a	100	100	40	50	n/a	86	94	92
All	52	8	0	n/a	28	n/a	10	n/a	n/a	n/a	14	n/a	n/a	n/a	0	0	0	0	n/a	0	0	0

Table E2 Exposure percentages after 10 seconds, 1 minute and 10 minutes for Simulation 2

Summer 100k Proposed- Exposure Percentage After 10 Seconds

Powerhouse Flow Exposure

	U1	U2	U3	U4	U5	U6	U7	U8	U9	U10	U11	U12	U13	U14	Outflow
Velocity	50	n/a	n/a	n/a	n/a	n/a	n/a	n/a	n/a	n/a	50	50	27	27	100
All	0	n/a	n/a	n/a	n/a	n/a	n/a	n/a	n/a	n/a	0	0	0	0	0

Spillway Flow Exposure

	S1	S2	S3	S4	S5	S6	S7	S8	S9	S10	S11	S12	S13	S14	S15	S16	S17	S18	S19	S20	S21	S22
Velocity	0	0	0	n/a	2.27	n/a	20.4	n/a	n/a	n/a	16	n/a	n/a	n/a	52.2	2	2	0	n/a	0	0	6
All	0	0	0	n/a	0	n/a	0	n/a	n/a	n/a	0	n/a	n/a	n/a	0	0	0	0	n/a	0	0	0

Summer 100k Proposed- Exposure Percentage After 1 Minute

Powerhouse Flow Exposure

	U1	U2	U3	U4	U5	U6	U7	U8	U9	U10	U11	U12	U13	U14	Outflow
Velocity	100	n/a	n/a	n/a	n/a	n/a	n/a	n/a	n/a	n/a	100	100	84	91	100
All	0	n/a	n/a	n/a	n/a	n/a	n/a	n/a	n/a	n/a	0	0	0	0	0

Spillway Flow Exposure

	S1	S2	S3	S4	S5	S6	S7	S8	S9	S10	S11	S12	S13	S14	S15	S16	S17	S18	S19	S20	S21	S22
Velocity	40	14	0	n/a	56.8	n/a	100	n/a	n/a	n/a	100	n/a	n/a	n/a	66	100	2	0	n/a	0	34	96
All	40	10	0	n/a	20.5	n/a	0	n/a	n/a	n/a	0	n/a	n/a	n/a	0	0	0	0	n/a	0	0	0

Summer 100k Proposed- Exposure Percentage After 10 Minutes

Powerhouse Flow Exposure

	U1	U2	U3	U4	U5	U6	U7	U8	U9	U10	U11	U12	U13	U14	Outflow
Velocity	100	n/a	n/a	n/a	n/a	n/a	n/a	n/a	n/a	n/a	100	100	100	100	100
All	18	n/a	n/a	n/a	n/a	n/a	n/a	n/a	n/a	n/a	0	0	0	1	0

Spillway Flow Exposure

	S1	S2	S3	S4	S5	S6	S7	S8	S9	S10	S11	S12	S13	S14	S15	S16	S17	S18	S19	S20	S21	S22
Velocity	100	100	100	n/a	100	n/a	100	n/a	n/a	n/a	100	n/a	n/a	n/a	89.4	100	68	12	n/a	68	100	100
All	48	60	4	n/a	40.9	n/a	6.77	n/a	n/a	n/a	0	n/a	n/a	n/a	19.1	18	14	6	n/a	16	20	12

Table E3 Exposure percentages after 10 seconds, 1 minute and 10 minutes for Simulation 3

Summer 150k- Exposure Percentage After 10 Seconds

Powerhouse Flow Exposure

	U1	U2	U3	U4	U5	U6	U7	U8	U9	U10	U11	U12	U13	U14	Outflow
Velocity	51	51	52	51	n/a	n/a	n/a	n/a	n/a	50	50	50	50	50	0
All	0	0	0	0	n/a	n/a	n/a	n/a	n/a	0	0	0	0	0	0

Spillway Flow Exposure

	S1	S2	S3	S4	S5	S6	S7	S8	S9	S10	S11	S12	S13	S14	S15	S16	S17	S18	S19	S20	S21	S22
Velocity	4	10	4	17.4	13.6	21.9	0	28.9	17.5	22	0	2	0	26	20	6.97	4	0	n/a	0	10	0
All	0	0	0	0	0	0	0	0	0	0	0	0	0	0	0	0	0	0	n/a	0	0	0

Summer 150k- Exposure Percentage After 1 Minute

Powerhouse Flow Exposure

	U1	U2	U3	U4	U5	U6	U7	U8	U9	U10	U11	U12	U13	U14	Outflow
Velocity	100	90	92	93	n/a	n/a	n/a	n/a	n/a	100	100	100	100	100	66
All	6	26	5	0	n/a	n/a	n/a	n/a	n/a	0	0	0	0	0	0

Spillway Flow Exposure

	S1	S2	S3	S4	S5	S6	S7	S8	S9	S10	S11	S12	S13	S14	S15	S16	S17	S18	S19	S20	S21	S22
Velocity	100	52	32	100	100	100	98	100	100	100	98	100	100	100	100	93	4	0	n/a	8	100	98
All	82	40	24	0	0	0	0	0	0	0	0	0	0	0	0	0	0	0	n/a	0	0	0

Summer 150k- Exposure Percentage After 10 Minutes

Powerhouse Flow Exposure

	U1	U2	U3	U4	U5	U6	U7	U8	U9	U10	U11	U12	U13	U14	Outflow
Velocity	100	100	100	100	n/a	n/a	n/a	n/a	n/a	100	100	100	100	100	100
All	60	87	6	0	n/a	n/a	n/a	n/a	n/a	0	0	0	0	0	0

Spillway Flow Exposure

	S1	S2	S3	S4	S5	S6	S7	S8	S9	S10	S11	S12	S13	S14	S15	S16	S17	S18	S19	S20	S21	S22
Velocity	100	100	100	100	100	100	100	100	100	100	100	100	100	100	100	100	96	16	n/a	80	100	100
All	100	100	100	100	100	92.7	76	80	15	40	16	16	2.1	0	0	0	0	0	n/a	0	0	0

Table E4 Exposure percentages after 10 seconds, 1 minute and 10 minutes for Simulation 4

Summer 150k Proposed- Exposure Percentage After 10 Seconds

Powerhouse Flow Exposure

	U1	U2	U3	U4	U5	U6	U7	U8	U9	U10	U11	U12	U13	U14	Outflow
Velocity	50	n/a	n/a	n/a	n/a	n/a	n/a	n/a	51	50	27	26	26	27	4
All	0	n/a	n/a	n/a	n/a	n/a	n/a	n/a	0	0	0	0	0	0	0

Spillway Flow Exposure

	S1	S2	S3	S4	S5	S6	S7	S8	S9	S10	S11	S12	S13	S14	S15	S16	S17	S18	S19	S20	S21	S22
Velocity	0	8	0	4	22.4	9.52	0	4	17.4	26	0	16	6	2	26.1	24.4	0	0	n/a	0	0	0
All	0	0	0	0	0	0	0	0	0	0	0	0	0	0	0	0	0	0	n/a	0	0	0

Summer 150k Proposed- Exposure Percentage After 1 Minute

Powerhouse Flow Exposure

	U1	U2	U3	U4	U5	U6	U7	U8	U9	U10	U11	U12	U13	U14	Outflow
Velocity	100	n/a	n/a	n/a	n/a	n/a	n/a	n/a	95	91	71	71	74	92	4
All	0	n/a	n/a	n/a	n/a	n/a	n/a	n/a	0	0	0	0	0	0	0

Spillway Flow Exposure

	S1	S2	S3	S4	S5	S6	S7	S8	S9	S10	S11	S12	S13	S14	S15	S16	S17	S18	S19	S20	S21	S22
Velocity	86	88	32	100	100	100	100	100	100	100	98	100	100	100	100	73.2	0	0	n/a	16	100	100
All	84	50	26	0	0	0	0	0	0	0	0	0	0	0	0	0	0	0	n/a	0	0	0

Summer 150k Proposed- Exposure Percentage After 10 Minutes

Powerhouse Flow Exposure

	U1	U2	U3	U4	U5	U6	U7	U8	U9	U10	U11	U12	U13	U14	Outflow
Velocity	100	n/a	n/a	n/a	n/a	n/a	n/a	n/a	100	100	100	100	100	100	4
All	70	n/a	n/a	n/a	n/a	n/a	n/a	n/a	9	20	7	0	0	0	0

Spillway Flow Exposure

	S1	S2	S3	S4	S5	S6	S7	S8	S9	S10	S11	S12	S13	S14	S15	S16	S17	S18	S19	S20	S21	S22
Velocity	100	96	100	100	100	100	100	100	100	100	100	100	100	100	100	100	100	48	n/a	64	100	100
All	100	88	94	100	100	92.9	74	62	28.3	40	52	40	0	14	0	0	0	0	n/a	0	0	0

Table E5 Exposure percentages after 10 seconds, 1 minute and 10 minutes for Simulation 5

Summer 200k- Exposure Percentage After 10 Seconds

Powerhouse Flow Exposure

	U1	U2	U3	U4	U5	U6	U7	U8	U9	U10	U11	U12	U13	U14	Outflow
Velocity	51	51	50	51	n/a	n/a	50	50	51	50	51	50	51	51	42
All	0	0	0	0	n/a	n/a	0	0	0	0	0	0	0	0	0

Spillway Flow Exposure

	S1	S2	S3	S4	S5	S6	S7	S8	S9	S10	S11	S12	S13	S14	S15	S16	S17	S18	S19	S20	S21	S22
Velocity	8	16	0	16.3	2	0	0	16.3	2.13	6	4.25	0	0	36.2	0	0	0	0	0	0	8	0
All	6	0	0	0	0	0	0	0	0	0	0	0	0	0	0	0	0	0	0	0	0	0

Summer 200k- Exposure Percentage After 1 Minute

Powerhouse Flow Exposure

	U1	U2	U3	U4	U5	U6	U7	U8	U9	U10	U11	U12	U13	U14	Outflow
Velocity	100	93	100	100	n/a	n/a	100	100	100	100	100	100	100	83.3	100
All	5	31	5	0	n/a	n/a	0	0	0	0	0	0	0	0	0

Spillway Flow Exposure

	S1	S2	S3	S4	S5	S6	S7	S8	S9	S10	S11	S12	S13	S14	S15	S16	S17	S18	S19	S20	S21	S22
Velocity	96	76	22	87.7	64	90	100	100	100	100	66	100	87.2	100	75.5	100	82	0	0	0	82	90
All	76	58	22	0	0	0	0	0	0	0	0	0	0	0	0	0	0	0	0	0	0	0

Summer 200k- Exposure Percentage After 10 Minutes

Powerhouse Flow Exposure

	U1	U2	U3	U4	U5	U6	U7	U8	U9	U10	U11	U12	U13	U14	Outflow
Velocity	100	100	100	100	n/a	n/a	100	100	100	100	100	100	100	100	100
All	58	83	60	7	n/a	n/a	0	0	0	0	0	0	0	0	4

Spillway Flow Exposure

	S1	S2	S3	S4	S5	S6	S7	S8	S9	S10	S11	S12	S13	S14	S15	S16	S17	S18	S19	S20	S21	S22
Velocity	100	100	100	100	100	98	100	100	100	100	100	100	100	100	100	100	96	82	50	32	88	100
All	100	100	74	79.6	56	58	71.4	68.9	83	78	25.5	52	59.6	46	2	0	0	0	0	0	0	0

Table E6 Exposure percentages after 10 seconds, 1 minute and 10 minutes for Simulation 6

Summer 200k Proposed- Exposure Percentage After 10 Seconds

Powerhouse Flow Exposure

	U1	U2	U3	U4	U5	U6	U7	U8	U9	U10	U11	U12	U13	U14	Outflow
Velocity	50	n/a	n/a	n/a	n/a	n/a	50	50	27	26	27	26	27	27	52
All	0	n/a	n/a	n/a	n/a	n/a	0	0	0	0	0	0	0	0	0

Spillway Flow Exposure

	S1	S2	S3	S4	S5	S6	S7	S8	S9	S10	S11	S12	S13	S14	S15	S16	S17	S18	S19	S20	S21	S22
Velocity	0	12	2	18	0	2	0	11.9	6	14	2	0	2.08	31.1	2.22	0	0	0	0	0	6	2
All	0	0	0	0	0	0	0	0	0	0	0	0	0	0	0	0	0	0	0	0	0	0

Summer 200k Proposed- Exposure Percentage After 1 Minute

Powerhouse Flow Exposure

	U1	U2	U3	U4	U5	U6	U7	U8	U9	U10	U11	U12	U13	U14	Outflow
Velocity	100	n/a	n/a	n/a	n/a	n/a	100	100	75	73	78	78	77	93	52
All	0	n/a	n/a	n/a	n/a	n/a	0	0	0	0	0	0	0	0	0

Spillway Flow Exposure

	S1	S2	S3	S4	S5	S6	S7	S8	S9	S10	S11	S12	S13	S14	S15	S16	S17	S18	S19	S20	S21	S22
Velocity	91.8	77.6	10	96	90	84	100	100	100	90	68	98	100	100	88.9	100	92	2	0	0	86	100
All	81.6	58	8	0	0	0	0	0	0	0	0	0	0	0	0	0	0	0	0	0	0	0

Summer 200k Proposed- Exposure Percentage After 10 Minutes

Powerhouse Flow Exposure

	U1	U2	U3	U4	U5	U6	U7	U8	U9	U10	U11	U12	U13	U14	Outflow
Velocity	100	n/a	n/a	n/a	n/a	n/a	100	100	100	100	100	100	100	100	52
All	55	n/a	n/a	n/a	n/a	n/a	14	47	0	0	0	0	0	0	0

Spillway Flow Exposure

	S1	S2	S3	S4	S5	S6	S7	S8	S9	S10	S11	S12	S13	S14	S15	S16	S17	S18	S19	S20	S21	S22
Velocity	100	98	100	100	100	100	100	100	100	100	100	100	100	100	100	100	100	96	80	32	98	100
All	100	98	80	94	74	76	88	86	86	44	22	38	43.8	37.8	0	0	0	0	0	0	0	0

Table E7 Exposure percentages after 10 seconds, 1 minute and 10 minutes for Simulation 7

Summer 250k- Exposure Percentage After 10 Seconds

Powerhouse Flow Exposure

	U1	U2	U3	U4	U5	U6	U7	U8	U9	U10	U11	U12	U13	U14	Outflow
Velocity	51	51	50	50	50	50	51	50	50	50	50	50	50	50	6
All	0	0	0	0	0	0	0	0	0	0	0	0	0	0	0

Spillway Flow Exposure

	S1	S2	S3	S4	S5	S6	S7	S8	S9	S10	S11	S12	S13	S14	S15	S16	S17	S18	S19	S20	S21	S22
Velocity	12	2	0	2	0	0	0	2	0	0	0	0	0	0	0	0	8	0	0	0	0	0
All	10	0	0	0	0	0	0	0	0	0	0	0	0	0	0	0	0	0	0	0	0	0

Summer 250k- Exposure Percentage After 1 Minute

Powerhouse Flow Exposure

	U1	U2	U3	U4	U5	U6	U7	U8	U9	U10	U11	U12	U13	U14	Outflow
Velocity	100	90	100	100	100	100	100	99	100	100	100	100	100	100	100
All	5	29	4	0	0	0	0	0	0	0	0	0	0	0	0

Spillway Flow Exposure

	S1	S2	S3	S4	S5	S6	S7	S8	S9	S10	S11	S12	S13	S14	S15	S16	S17	S18	S19	S20	S21	S22
Velocity	76	64	74	81.6	100	66	20	64	52	94	82	86	90	98	98	98	88	0	18	22	46	32
All	22	28	74	36.7	21.3	0	0	0	0	0	0	0	0	0	0	0	0	0	0	0	0	0

Summer 250k- Exposure Percentage After 10 Minutes

Powerhouse Flow Exposure

	U1	U2	U3	U4	U5	U6	U7	U8	U9	U10	U11	U12	U13	U14	Outflow
Velocity	100	100	100	100	100	100	100	100	100	100	100	100	100	100	100
All	55	80	70	5	0	0	0	0	0	0	0	0	2	0	100

Spillway Flow Exposure

	S1	S2	S3	S4	S5	S6	S7	S8	S9	S10	S11	S12	S13	S14	S15	S16	S17	S18	S19	S20	S21	S22
Velocity	100	100	100	100	100	100	86	94	96	100	100	100	100	100	100	100	100	24	96	94	100	90
All	76	90	96	81.6	68.1	50	8	16	0	0	0	0	0	2	2	0	0	0	2	0	0	0

Table E8 Exposure percentages after 10 seconds, 1 minute and 10 minutes for Simulation 8

Summer 250k Proposed- Exposure Percentage After 10 Seconds

Powerhouse Flow Exposure

	U1	U2	U3	U4	U5	U6	U7	U8	U9	U10	U11	U12	U13	U14	Outflow
Velocity	51	n/a	n/a	n/a	50	27.1	28	26	27	25	26	27	26	28	100
All	0	n/a	n/a	n/a	0	0	0	0	0	0	0	0	0	0	0

Spillway Flow Exposure

	S1	S2	S3	S4	S5	S6	S7	S8	S9	S10	S11	S12	S13	S14	S15	S16	S17	S18	S19	S20	S21	S22
Velocity	10	10	0	4.1	0	0	0	0	0	0	0	0	0	0	0	2	6	0	0	0	0	0
All	0	0	0	0	0	0	0	0	0	0	0	0	0	0	0	0	0	0	0	0	0	0

Summer 250k Proposed- Exposure Percentage After 1 Minute

Powerhouse Flow Exposure

	U1	U2	U3	U4	U5	U6	U7	U8	U9	U10	U11	U12	U13	U14	Outflow
Velocity	98	n/a	n/a	n/a	100	68.7	82	87	95	95	98	99	97	98	100
All	0	n/a	n/a	n/a	0	0	0	0	0	0	0	0	0	0	0

Spillway Flow Exposure

	S1	S2	S3	S4	S5	S6	S7	S8	S9	S10	S11	S12	S13	S14	S15	S16	S17	S18	S19	S20	S21	S22
Velocity	98	74	80	90	92	48	16	80	66	94	72	74	80	100	100	98	78	8	20	14	42	46
All	30	16	76	16	12	0	0	0	0	0	0	0	0	0	0	0	0	0	0	0	0	0

Summer 250k Proposed- Exposure Percentage After 10 Minutes

Powerhouse Flow Exposure

	U1	U2	U3	U4	U5	U6	U7	U8	U9	U10	U11	U12	U13	U14	Outflow
Velocity	100	n/a	n/a	n/a	100	100	100	100	100	100	100	100	100	99	100
All	52	n/a	n/a	n/a	38.5	65.6	25	1	1	2	4	5	2	4	0

Spillway Flow Exposure

	S1	S2	S3	S4	S5	S6	S7	S8	S9	S10	S11	S12	S13	S14	S15	S16	S17	S18	S19	S20	S21	S22
Velocity	100	100	100	100	100	100	82	82	78	100	98	100	100	100	100	100	92	26	98	94	100	100
All	88	78	98	98	72	56	8	10	0	0	0	0	0	0	0	0	0	0	0	0	0	0

Table E9 Exposure percentages after 10 seconds, 1 minute and 10 minutes for Simulation 11

Spring 200k- Exposure Percentage After 10 Seconds

Powerhouse Flow Exposure

	U1	U2	U3	U4	U5	U6	U7	U8	U9	U10	U11	U12	U13	U14	Outflow
Velocity	51	51	50	50	50	51	51	50	50	50	50	50	50	50	34
All	0	0	0	0	0	0	0	0	0	0	0	0	0	0	0

Spillway Flow Exposure

	S1	S2	S3	S4	S5	S6	S7	S8	S9	S10	S11	S12	S13	S14	S15	S16	S17	S18	S19	S20	S21	S22
Velocity	0	8	0	n/a	0	12.2	6.21	n/a	0	29.2	6	n/a	0	23.9	0	46.9	30.6	0	0	0	6	4
All	0	0	0	n/a	0	0	0	n/a	0	0	0	n/a	0	0	0	0	0	0	0	0	0	0

Spring 200k- Exposure Percentage After 1 Minute

Powerhouse Flow Exposure

	U1	U2	U3	U4	U5	U6	U7	U8	U9	U10	U11	U12	U13	U14	Outflow
Velocity	100	89	100	100	100	100	100	99	100	100	100	100	100	100	100
All	5	28	4	0	0	0	0	0	0	0	0	0	0	0	0

Spillway Flow Exposure

	S1	S2	S3	S4	S5	S6	S7	S8	S9	S10	S11	S12	S13	S14	S15	S16	S17	S18	S19	S20	S21	S22
Velocity	62	62	0	n/a	100	100	100	n/a	100	100	98	n/a	100	97.9	100	100	100	100	0	0	76	100
All	62	50	0	n/a	0	0	0	n/a	0	0	0	n/a	0	0	0	0	0	0	0	0	0	0

Spring 200k- Exposure Percentage After 10 Minutes

Powerhouse Flow Exposure

	U1	U2	U3	U4	U5	U6	U7	U8	U9	U10	U11	U12	U13	U14	Outflow
Velocity	100	100	100	100	100	100	100	100	100	100	100	100	100	100	100
All	56	81	82	4	0	0	0	0	0	0	0	0	0	0	4

Spillway Flow Exposure

	S1	S2	S3	S4	S5	S6	S7	S8	S9	S10	S11	S12	S13	S14	S15	S16	S17	S18	S19	S20	S21	S22
Velocity	100	98	84	n/a	100	100	100	n/a	100	100	100	n/a	100	100	100	100	100	100	100	100	100	100
All	96	94	0	n/a	88	69.4	60	n/a	75.6	48	18	n/a	4	8.16	0	0	0	0	0	0	0	0

Table E10 Exposure percentages after 10 seconds, 1 minute and 10 minutes for Simulation 12

Spring 200k Proposed- Exposure Percentage After 10 Seconds

Powerhouse Flow Exposure

	U1	U2	U3	U4	U5	U6	U7	U8	U9	U10	U11	U12	U13	U14	Outflow
Velocity	51	n/a	n/a	n/a	50	51	50	27	26	27	27	27	27	28	100
All	0	n/a	n/a	n/a	0	0	0	0	0	0	0	0	0	0	0

Spillway Flow Exposure

	S1	S2	S3	S4	S5	S6	S7	S8	S9	S10	S11	S12	S13	S14	S15	S16	S17	S18	S19	S20	S21	S22
Velocity	0	0	0	n/a	0	22.2	0	n/a	4.08	46	8.16	n/a	0	28.6	4	31.8	4.08	0	0	0	4	4
All	0	0	0	n/a	0	0	0	n/a	0	0	0	n/a	0	0	0	0	0	0	0	0	0	0

Spring 200k Proposed- Exposure Percentage After 1 Minute

Powerhouse Flow Exposure

	U1	U2	U3	U4	U5	U6	U7	U8	U9	U10	U11	U12	U13	U14	Outflow
Velocity	100	n/a	n/a	n/a	100	100	100	82	95	85	81	79	76	95	100
All	0	n/a	n/a	n/a	0	0	0	0	0	0	0	0	0	0	0

Spillway Flow Exposure

	S1	S2	S3	S4	S5	S6	S7	S8	S9	S10	S11	S12	S13	S14	S15	S16	S17	S18	S19	S20	S21	S22
Velocity	63.2	70	0	n/a	100	100	100	n/a	100	100	100	n/a	100	100	100	100	100	97.9	62	34	92	98
All	61.2	68	0	n/a	0	0	0	n/a	0	0	0	n/a	0	0	0	0	0	0	0	0	0	0

Spring 200k Proposed- Exposure Percentage After 10 Minutes

Powerhouse Flow Exposure

	U1	U2	U3	U4	U5	U6	U7	U8	U9	U10	U11	U12	U13	U14	Outflow
Velocity	100	n/a	n/a	n/a	100	100	100	100	100	100	100	100	100	100	100
All	64	n/a	n/a	n/a	33.3	22.9	0	0	0	0	0	0	0	0	0

Spillway Flow Exposure

	S1	S2	S3	S4	S5	S6	S7	S8	S9	S10	S11	S12	S13	S14	S15	S16	S17	S18	S19	S20	S21	S22
Velocity	100	100	100	n/a	100	100	100	n/a	100	100	100	n/a	100	100	100	100	100	100	100	100	100	100
All	100	96	2	n/a	60	64.4	22	n/a	69.4	48	16.3	n/a	30.6	2	0	0	0	0	0	0	0	0

Table E11 Exposure percentages after 10 seconds, 1 minute and 10 minutes for Simulation 13

Spring 250k- Exposure Percentage After 10 Seconds

Powerhouse Flow Exposure

	U1	U2	U3	U4	U5	U6	U7	U8	U9	U10	U11	U12	U13	U14	Outflow
Velocity	51	51	50	50	50	50	50	50	50	50	50	50	51	50	0
All	0	0	0	0	0	0	0	0	0	0	0	0	0	0	0

Spillway Flow Exposure

	S1	S2	S3	S4	S5	S6	S7	S8	S9	S10	S11	S12	S13	S14	S15	S16	S17	S18	S19	S20	S21	S22
Velocity	2	0	0	38.1	30	0	0	0	0	0	2.22	6	0	6	0	12	6	2	10.4	0	0	0
All	0	0	0	0	0	0	0	0	0	0	0	0	0	0	0	0	0	0	0	0	0	0

Spring 250k- Exposure Percentage After 1 Minute

Powerhouse Flow Exposure

	U1	U2	U3	U4	U5	U6	U7	U8	U9	U10	U11	U12	U13	U14	Outflow
Velocity	100	84	88	93	100	88.5	93	85	92	93	92	97	100	100	6
All	5	33	1	0	0	0	0	0	0	0	0	0	0	0	0

Spillway Flow Exposure

	S1	S2	S3	S4	S5	S6	S7	S8	S9	S10	S11	S12	S13	S14	S15	S16	S17	S18	S19	S20	S21	S22
Velocity	58	36	64	93	100	100	98	100	100	100	100	100	100	100	100	100	100	100	77.1	20	76	78
All	52	34	54	46.5	0	0	0	0	0	0	0	0	0	0	0	0	0	0	0	0	0	0

Spring 250k- Exposure Percentage After 10 Minutes

Powerhouse Flow Exposure

	U1	U2	U3	U4	U5	U6	U7	U8	U9	U10	U11	U12	U13	U14	Outflow
Velocity	100	99	92	96	100	88.5	93	85	100	100	100	100	100	100	6
All	55	79	12	0	0	0	0	0	0	0	0	1	3	2	0

Spillway Flow Exposure

	S1	S2	S3	S4	S5	S6	S7	S8	S9	S10	S11	S12	S13	S14	S15	S16	S17	S18	S19	S20	S21	S22
Velocity	100	98	100	100	100	100	100	100	100	100	100	100	100	100	100	100	100	100	100	100	100	100
All	100	84	68	76.6	16	42	56	24	34	32	31.1	26	6.5	0	0	0	0	0	0	0	0	0

Table E12 Exposure percentages after 10 seconds, 1 minute and 10 minutes for Simulation 14

Spring 250k Proposed- Exposure Percentage After 10 Seconds

Powerhouse Flow Exposure

	U1	U2	U3	U4	U5	U6	U7	U8	U9	U10	U11	U12	U13	U14	Outflow
Velocity	51	n/a	50	50	25	26	29	27	26	27	27	27	27	28	42
All	0	n/a	0	0	0	0	0	0	0	0	0	0	0	0	0

Spillway Flow Exposure

	S1	S2	S3	S4	S5	S6	S7	S8	S9	S10	S11	S12	S13	S14	S15	S16	S17	S18	S19	S20	S21	S22
Velocity	0	6	0	47.9	16	4	0	8	0	0	4.64	4	0	28.6	8.33	12	34	4	12	0	0	2
All	0	0	0	0	0	0	0	0	0	0	0	0	0	0	0	0	0	0	0	0	0	0

Spring 250k Proposed- Exposure Percentage After 1 Minute

Powerhouse Flow Exposure

	U1	U2	U3	U4	U5	U6	U7	U8	U9	U10	U11	U12	U13	U14	Outflow
Velocity	100	n/a	100	100	76	76	82	82	98	85	84	81	76	95	42
All	2	n/a	0	0	0	0	0	0	0	0	0	0	0	0	0

Spillway Flow Exposure

	S1	S2	S3	S4	S5	S6	S7	S8	S9	S10	S11	S12	S13	S14	S15	S16	S17	S18	S19	S20	S21	S22
Velocity	80	94	58	93.9	100	100	100	100	100	100	100	100	100	100	100	100	100	100	76	54	76	82
All	80	58	46	40.8	0	0	0	0	0	0	0	0	0	0	0	0	0	0	0	0	0	0

Spring 250k Proposed- Exposure Percentage After 10 Minutes

Powerhouse Flow Exposure

	U1	U2	U3	U4	U5	U6	U7	U8	U9	U10	U11	U12	U13	U14	Outflow
Velocity	100	n/a	100	100	79.2	76	82	82	98	87	98	100	100	100	42
All	41	n/a	69	56	3.1	0	0	0	0	0	0	0	0	0	0

Spillway Flow Exposure

	S1	S2	S3	S4	S5	S6	S7	S8	S9	S10	S11	S12	S13	S14	S15	S16	S17	S18	S19	S20	S21	S22
Velocity	100	100	98	100	100	100	100	100	100	100	100	100	100	100	100	100	100	100	100	100	100	100
All	100	82	74	81.6	30	44	69.4	28	15.5	20	27.9	6	0	0	0	0	0	0	0	0	0	0

Table E13. Exposure percentages after 10 seconds, 1 minute and 10 minutes for Simulation 15

Spring 300k- Exposure Percentage After 10 Seconds

Powerhouse Flow Exposure

	U1	U2	U3	U4	U5	U6	U7	U8	U9	U10	U11	U12	U13	U14	Outflow
Velocity	27	26	26	26	25	26	29	27	27	27	27	27	27	28	100
All	0	0	0	0	0	0	0	0	0	0	0	0	0	0	0

Spillway Flow Exposure

	S1	S2	S3	S4	S5	S6	S7	S8	S9	S10	S11	S12	S13	S14	S15	S16	S17	S18	S19	S20	S21	S22
Velocity	2	0	0	2	4	0	2	0	0	0	8	0	0	6	6.12	6	0	0	6	0	0	0
All	0	0	0	0	0	0	0	0	0	0	0	0	0	0	0	0	0	0	0	0	0	0

Spring 300k- Exposure Percentage After 1 Minute

Powerhouse Flow Exposure

	U1	U2	U3	U4	U5	U6	U7	U8	U9	U10	U11	U12	U13	U14	Outflow
Velocity	100	81	87	82	95.8	81.2	84	80	91	92	89	92	92	94	100
All	13	0	0	0	0	0	0	0	0	0	0	0	0	0	0

Spillway Flow Exposure

	S1	S2	S3	S4	S5	S6	S7	S8	S9	S10	S11	S12	S13	S14	S15	S16	S17	S18	S19	S20	S21	S22
Velocity	92	80	2	60	100	98	100	94	100	100	100	96	100	100	100	100	100	87.8	94	62	66	86
All	20	38	0	12	0	0	0	0	0	0	0	0	0	0	0	0	0	0	0	0	0	0

Spring 300k- Exposure Percentage After 10 Minutes

Powerhouse Flow Exposure

	U1	U2	U3	U4	U5	U6	U7	U8	U9	U10	U11	U12	U13	U14	Outflow
Velocity	100	94	88	82	95.8	81.2	84	80	91	92	99	100	100	100	100
All	41	5	0	0	0	0	0	0	0	0	0	0	0	0	0

Spillway Flow Exposure

	S1	S2	S3	S4	S5	S6	S7	S8	S9	S10	S11	S12	S13	S14	S15	S16	S17	S18	S19	S20	S21	S22
Velocity	100	100	68	84	100	100	100	100	100	100	100	100	100	100	100	100	100	100	100	100	100	100
All	74	84	2	2	24	14	44	46	26	34	10	26	16	12	16.3	18	16	2.04	2	4	4	2

Table E14 Exposure percentages after 10 seconds, 1 minute and 10 minutes for Simulation 16

Spring 300k Proposed- Exposure Percentage After 10 Seconds

Powerhouse Flow Exposure

	U1	U2	U3	U4	U5	U6	U7	U8	U9	U10	U11	U12	U13	U14	Outflow
Velocity	27	26	26	26	25	26	29	27	26	27	26	27	26	27	42
All	0	0	0	0	0	0	0	0	0	0	0	0	0	0	0

Spillway Flow Exposure

	S1	S2	S3	S4	S5	S6	S7	S8	S9	S10	S11	S12	S13	S14	S15	S16	S17	S18	S19	S20	S21	S22
Velocity	2	2	0	2	4.34	2	0	0	4	2	0	0	0	0	8.2	4	0	10	0	0	2	0
All	0	0	0	0	0	0	0	0	0	0	0	0	0	0	0	0	0	0	0	0	0	0

Spring 300k Proposed- Exposure Percentage After 1 Minute

Powerhouse Flow Exposure

	U1	U2	U3	U4	U5	U6	U7	U8	U9	U10	U11	U12	U13	U14	Outflow
Velocity	100	86	83	80	79.2	89.6	95	92	100	92	93	92	78	94	42
All	3	32	0	0	0	0	0	0	0	0	0	0	0	0	0

Spillway Flow Exposure

	S1	S2	S3	S4	S5	S6	S7	S8	S9	S10	S11	S12	S13	S14	S15	S16	S17	S18	S19	S20	S21	S22
Velocity	96	66	58	58	100	100	90	64.6	90	88	98	100	100	100	93.8	100	100	92	54	62	62	76
All	26	20	58	10	0	0	0	0	0	0	0	0	0	0	0	0	0	0	0	0	0	0

Spring 300k Proposed- Exposure Percentage After 10 Minutes

Powerhouse Flow Exposure

	U1	U2	U3	U4	U5	U6	U7	U8	U9	U10	U11	U12	U13	U14	Outflow
Velocity	100	97	88	80	80.2	90.6	97	92	100	100	100	100	100	100	42
All	26	79	4	0	0	0	0	0	0	0	0	0	0	0	0

Spillway Flow Exposure

	S1	S2	S3	S4	S5	S6	S7	S8	S9	S10	S11	S12	S13	S14	S15	S16	S17	S18	S19	S20	S21	S22
Velocity	100	100	80	94	100	100	96	97.9	94	96	100	100	100	100	100	100	100	100	100	100	100	100
All	94	98	76	90	93.5	82	34	39.6	54	46	46	48	32	44	46.9	40	30	8	6	10	12	6

Table E15 Exposure time percentages after 10 seconds, 1 minute and 10 minutes for Simulation 1

Summer 100k- Exposure Time Percentage After 10 Seconds

Powerhouse Flow Exposure

	U1	U2	U3	U4	U5	U6	U7	U8	U9	U10	U11	U12	U13	U14	Outflow
Velocity	38.6	38.6	38.4	38.4	n/a	n/a	n/a	n/a	n/a	n/a	n/a	n/a	37.9	37.8	3.76
All	0	0	0	0	n/a	n/a	n/a	n/a	n/a	n/a	n/a	n/a	0	0	0

Spillway Flow Exposure

	S1	S2	S3	S4	S5	S6	S7	S8	S9	S10	S11	S12	S13	S14	S15	S16	S17	S18	S19	S20	S21	S22
Velocity	0	0	0	n/a	1.76	n/a	9.8	n/a	n/a	n/a	9.65	n/a	n/a	n/a	12.2	0	0	0	n/a	0	3.47	1.48
All	0	0	0	n/a	0	n/a	0	n/a	n/a	n/a	0	n/a	n/a	n/a	0	0	0	0	n/a	0	0	0

Summer 100k- Exposure Time Percentage After 1 Minute

Powerhouse Flow Exposure

	U1	U2	U3	U4	U5	U6	U7	U8	U9	U10	U11	U12	U13	U14	Outflow
Velocity	73.4	69.4	67.8	63.1	n/a	n/a	n/a	n/a	n/a	n/a	n/a	n/a	79.6	73.4	25
All	0.75	7.47	1.13	0	n/a	n/a	n/a	n/a	n/a	n/a	n/a	n/a	0	0	0

Spillway Flow Exposure

	S1	S2	S3	S4	S5	S6	S7	S8	S9	S10	S11	S12	S13	S14	S15	S16	S17	S18	S19	S20	S21	S22
Velocity	4.77	1.13	0	n/a	18.3	n/a	76.2	n/a	n/a	n/a	41.1	n/a	n/a	n/a	44.1	49.4	0	0	n/a	0	15.5	21.4
All	5.61	0.76	0	n/a	1.04	n/a	0	n/a	n/a	n/a	0	n/a	n/a	n/a	0	0	0	0	n/a	0	0	0

Summer 100k- Exposure Time Percentage After 10 Minutes

Powerhouse Flow Exposure

	U1	U2	U3	U4	U5	U6	U7	U8	U9	U10	U11	U12	U13	U14	Outflow
Velocity	97.1	96.8	84.1	90.7	n/a	n/a	n/a	n/a	n/a	n/a	n/a	n/a	41.5	36.1	75.1
All	6.65	42.7	3.06	0	n/a	n/a	n/a	n/a	n/a	n/a	n/a	n/a	0	0	0

Spillway Flow Exposure

	S1	S2	S3	S4	S5	S6	S7	S8	S9	S10	S11	S12	S13	S14	S15	S16	S17	S18	S19	S20	S21	S22
Velocity	56.3	57.8	58.8	n/a	51.4	n/a	58.9	n/a	n/a	n/a	58.7	n/a	n/a	n/a	11.4	13.7	19.5	5.6	n/a	16.5	49.6	31.2
All	6.27	0.64	0	n/a	2.71	n/a	2.04	n/a	n/a	n/a	0.55	n/a	n/a	n/a	0	0	0	0	n/a	0	0	0

Table E16 Exposure time percentages after 10 seconds, 1 minute and 10 minutes for Simulation 2

Summer 100k Proposed- Exposure Time Percentage After 10 Seconds															
Powerhouse Flow Exposure															
	U1	U2	U3	U4	U5	U6	U7	U8	U9	U10	U11	U12	U13	U14	Outflow
Velocity	38.7	n/a	n/a	n/a	n/a	n/a	n/a	n/a	n/a	n/a	38.2	38.1	16.9	19.9	90.1
All	0	n/a	n/a	n/a	n/a	n/a	n/a	n/a	n/a	n/a	0	0	0	0	0

Spillway Flow Exposure																					
	S1	S2	S3	S4	S5	S6	S7	S8	S9	S10	S11	S12	S13	S14	S15	S16	S17	S18	S19	S20	S21	S22
Velocity	0	0	0	n/a	0	n/a	2.97	n/a	n/a	n/a	6.25	n/a	n/a	n/a	11.6	1.77	0.38	0	n/a	0	0	0.85
All	0	0	0	n/a	0	n/a	0	n/a	n/a	n/a	0	n/a	n/a	n/a	0	0	0	0	n/a	0	0	0

Summer 100k Proposed- Exposure Time Percentage After 1 Minute															
Powerhouse Flow Exposure															
	U1	U2	U3	U4	U5	U6	U7	U8	U9	U10	U11	U12	U13	U14	Outflow
Velocity	74.3	n/a	n/a	n/a	n/a	n/a	n/a	n/a	n/a	n/a	70.3	73.7	49.6	39.1	98.4
All	0	n/a	n/a	n/a	n/a	n/a	n/a	n/a	n/a	n/a	0	0	0	0	0

Spillway Flow Exposure																					
	S1	S2	S3	S4	S5	S6	S7	S8	S9	S10	S11	S12	S13	S14	S15	S16	S17	S18	S19	S20	S21	S22
Velocity	14.5	3.13	0	n/a	18.7	n/a	73.2	n/a	n/a	n/a	58.6	n/a	n/a	n/a	4.89	44.2	0.21	0	n/a	0	12.9	33.7
All	12.9	0.56	0	n/a	1.71	n/a	0	n/a	n/a	n/a	0	n/a	n/a	n/a	0	0	0	0	n/a	0	0	0

Summer 100k Proposed- Exposure Time Percentage After 10 Minutes															
Powerhouse Flow Exposure															
	U1	U2	U3	U4	U5	U6	U7	U8	U9	U10	U11	U12	U13	U14	Outflow
Velocity	97	n/a	n/a	n/a	n/a	n/a	n/a	n/a	n/a	n/a	59.6	61	51.4	45.4	19.1
All	12.2	n/a	n/a	n/a	n/a	n/a	n/a	n/a	n/a	n/a	0	0	0	0.02	0

Spillway Flow Exposure																					
	S1	S2	S3	S4	S5	S6	S7	S8	S9	S10	S11	S12	S13	S14	S15	S16	S17	S18	S19	S20	S21	S22
Velocity	52.6	51.4	58.2	n/a	50.4	n/a	58.8	n/a	n/a	n/a	72.1	n/a	n/a	n/a	22.7	33.8	38.2	2.62	n/a	24.7	58	32.2
All	14.4	5.19	0.04	n/a	8.39	n/a	0.8	n/a	n/a	n/a	4.3	n/a	n/a	n/a	1.18	1.23	1.92	0.76	n/a	0.25	2.06	0.46

Table E17 Exposure time percentages after 10 seconds, 1 minute and 10 minutes for Simulation 3

Summer 150k- Exposure Percentage After 10 Seconds

Powerhouse Flow Exposure

	U1	U2	U3	U4	U5	U6	U7	U8	U9	U10	U11	U12	U13	U14	Outflow
Velocity	51	51	52	51	n/a	n/a	n/a	n/a	n/a	50	50	50	50	50	0
All	0	0	0	0	n/a	n/a	n/a	n/a	n/a	0	0	0	0	0	0

Spillway Flow Exposure

	S1	S2	S3	S4	S5	S6	S7	S8	S9	S10	S11	S12	S13	S14	S15	S16	S17	S18	S19	S20	S21	S22
Velocity	4	10	4	17.4	13.6	21.9	0	28.9	17.5	22	0	2	0	26	20	6.97	4	0	n/a	0	10	0
All	0	0	0	0	0	0	0	0	0	0	0	0	0	0	0	0	0	0	n/a	0	0	0

Summer 150k- Exposure Percentage After 1 Minute

Powerhouse Flow Exposure

	U1	U2	U3	U4	U5	U6	U7	U8	U9	U10	U11	U12	U13	U14	Outflow
Velocity	100	90	92	93	n/a	n/a	n/a	n/a	n/a	100	100	100	100	100	66
All	6	26	5	0	n/a	n/a	n/a	n/a	n/a	0	0	0	0	0	0

Spillway Flow Exposure

	S1	S2	S3	S4	S5	S6	S7	S8	S9	S10	S11	S12	S13	S14	S15	S16	S17	S18	S19	S20	S21	S22
Velocity	100	52	32	100	100	100	98	100	100	100	98	100	100	100	100	93	4	0	n/a	8	100	98
All	82	40	24	0	0	0	0	0	0	0	0	0	0	0	0	0	0	0	n/a	0	0	0

Summer 150k- Exposure Percentage After 10 Minutes

Powerhouse Flow Exposure

	U1	U2	U3	U4	U5	U6	U7	U8	U9	U10	U11	U12	U13	U14	Outflow
Velocity	100	100	100	100	n/a	n/a	n/a	n/a	n/a	100	100	100	100	100	100
All	60	87	6	0	n/a	n/a	n/a	n/a	n/a	0	0	0	0	0	0

Spillway Flow Exposure

	S1	S2	S3	S4	S5	S6	S7	S8	S9	S10	S11	S12	S13	S14	S15	S16	S17	S18	S19	S20	S21	S22
Velocity	100	100	100	100	100	100	100	100	100	100	100	100	100	100	100	100	96	16	n/a	80	100	100
All	100	100	100	100	100	92.7	76	80	15	40	16	16	2.1	0	0	0	0	0	n/a	0	0	0

Table E18 Exposure time percentages after 10 seconds, 1 minute and 10 minutes for Simulation 4

Summer 150k Proposed- Exposure Time Percentage After 10 Seconds

Powerhouse Flow Exposure

	U1	U2	U3	U4	U5	U6	U7	U8	U9	U10	U11	U12	U13	U14	Outflow
Velocity	38.8	n/a	n/a	n/a	n/a	n/a	n/a	n/a	38.3	38.5	16.9	17	16.9	17	0.01
All	0	n/a	n/a	n/a	n/a	n/a	n/a	n/a	0	0	0	0	0	0	0

Spillway Flow Exposure

	S1	S2	S3	S4	S5	S6	S7	S8	S9	S10	S11	S12	S13	S14	S15	S16	S17	S18	S19	S20	S21	S22
Velocity	0	1.56	0	1.48	8.3	2.49	0	2.6	3.51	6.65	0	3.55	1.23	1.34	8.19	5.22	0	0	n/a	0	0	0
All	0	0	0	0	0	0	0	0	0	0	0	0	0	0	0	0	0	0	n/a	0	0	0

Summer 150k Proposed- Exposure Time Percentage After 1 Minute

Powerhouse Flow Exposure

	U1	U2	U3	U4	U5	U6	U7	U8	U9	U10	U11	U12	U13	U14	Outflow
Velocity	68.6	n/a	n/a	n/a	n/a	n/a	n/a	n/a	62.1	63.2	38.1	42.6	48.2	46.6	0
All	0	n/a	n/a	n/a	n/a	n/a	n/a	n/a	0	0	0	0	0	0	0

Spillway Flow Exposure

	S1	S2	S3	S4	S5	S6	S7	S8	S9	S10	S11	S12	S13	S14	S15	S16	S17	S18	S19	S20	S21	S22
Velocity	24.5	54.7	18.5	59.5	76.6	63.5	42.8	66.9	68.2	70.7	24.9	58.9	66.9	59.7	51.8	18.9	0	0	n/a	3	34.3	41.5
All	17.5	6.25	4.53	0	0	0	0	0	0	0	0	0	0	0	0	0	0	0	n/a	0	0	0

Summer 150k Proposed- Exposure Time Percentage After 10 Minutes

Powerhouse Flow Exposure

	U1	U2	U3	U4	U5	U6	U7	U8	U9	U10	U11	U12	U13	U14	Outflow
Velocity	96.8	n/a	n/a	n/a	n/a	n/a	n/a	n/a	64.2	68.9	70	57.3	50.8	44.7	0
All	30.7	n/a	n/a	n/a	n/a	n/a	n/a	n/a	2.21	6.9	3.01	0	0	0	0

Spillway Flow Exposure

	S1	S2	S3	S4	S5	S6	S7	S8	S9	S10	S11	S12	S13	S14	S15	S16	S17	S18	S19	S20	S21	S22
Velocity	61.6	50.1	56.9	59.1	47.9	47.5	63.5	62.4	75.7	86.5	77.3	73.9	66.7	68.2	25.6	36.1	49	11.6	n/a	24.8	40.6	35.5
All	49.2	32.1	14.2	19.9	16	13.8	7.85	5.4	1.51	1.81	2.73	3.24	0	0.62	0	0	0	0	n/a	0	0	0

Table E19 Exposure time percentages after 10 seconds, 1 minute and 10 minutes for Simulation 5

Summer 200k- Exposure Time Percentage After 10 Seconds															
Powerhouse Flow Exposure															
	U1	U2	U3	U4	U5	U6	U7	U8	U9	U10	U11	U12	U13	U14	Outflow
Velocity	38.7	38.6	38.4	38.4	n/a	n/a	38.2	38	38.1	38.2	38	37.9	37.8	37.9	1.01
All	0	0	0	0	n/a	n/a	0	0	0	0	0	0	0	0	0

Spillway Flow Exposure																					
	S1	S2	S3	S4	S5	S6	S7	S8	S9	S10	S11	S12	S13	S14	S15	S16	S17	S18	S19	S20	S21	S22
Velocity	2.72	6.49	0	4.28	0.34	0	0	8.33	1.73	1.28	0.76	0	0	16.9	0	0.17	0	0	0	0	2.24	0
All	1.58	0	0	0	0	0	0	0	0	0	0	0	0	0	0	0	0	0	0	0	0	0

Summer 200k- Exposure Time Percentage After 1 Minute															
Powerhouse Flow Exposure															
	U1	U2	U3	U4	U5	U6	U7	U8	U9	U10	U11	U12	U13	U14	Outflow
Velocity	72.4	68.4	72.7	67.2	n/a	n/a	80.7	68.6	73.8	73.9	74.4	75.7	75.9	73.1	47.8
All	0.74	5.73	0.94	0	n/a	n/a	0	0	0	0	0	0	0	0	0

Spillway Flow Exposure																					
	S1	S2	S3	S4	S5	S6	S7	S8	S9	S10	S11	S12	S13	S14	S15	S16	S17	S18	S19	S20	S21	S22
Velocity	37.8	29	2.94	36.5	27	35.9	58.6	54.9	62.4	63.2	30.3	54.6	20.7	27.5	7.71	46.6	28	0	0	0	16.5	32.4
All	23.6	5.41	2.93	0	0	0	0	0	0	0	0	0	0	0	0	0	0	0	0	0	0	0

Summer 200k- Exposure Time Percentage After 10 Minutes															
Powerhouse Flow Exposure															
	U1	U2	U3	U4	U5	U6	U7	U8	U9	U10	U11	U12	U13	U14	Outflow
Velocity	95.7	79.1	616	89.5	n/a	n/a	82.9	76.4	81	76.3	74	61.9	63.9	60.5	29.4
All	13.9	49.8	8.36	0.26	n/a	n/a	0	0	0	0	0	0	0	0	0.04

Spillway Flow Exposure																					
	S1	S2	S3	S4	S5	S6	S7	S8	S9	S10	S11	S12	S13	S14	S15	S16	S17	S18	S19	S20	S21	S22
Velocity	55	51.6	39.3	34.1	36.8	48.2	40.1	33.2	50.9	59.7	64.7	56.4	48.7	60.9	58.4	51	58.4	55.8	26	24.3	39.2	57
All	34.6	33.0	11.6	9.4	6.9	11.4	11.0	6.8	11.3	9.7	2.4	6.1	8.2	5.2	0.0	0.0	0.0	0.0	0.0	0.0	0.0	0.0

Table E20 Exposure time percentages after 10 seconds, 1 minute and 10 minutes for Simulation 6

Summer 200k Proposed- Exposure Time Percentage After 10 Seconds															
Powerhouse Flow Exposure															
	U1	U2	U3	U4	U5	U6	U7	U8	U9	U10	U11	U12	U13	U14	Outflow
Velocity	39	n/a	n/a	n/a	n/a	n/a	38.6	38.4	17	16.8	16.7	16.9	17	16.7	0.58
All	0	n/a	n/a	n/a	n/a	n/a	0	0	0	0	0	0	0	0	0

Spillway Flow Exposure																					
	S1	S2	S3	S4	S5	S6	S7	S8	S9	S10	S11	S12	S13	S14	S15	S16	S17	S18	S19	S20	S21	S22
Velocity	0.0	3.8	0.9	5.0	0.0	0.3	0.0	6.4	0.5	2.5	0.2	0.0	0.3	14.4	0.3	0.0	0.0	0.0	0.0	0.0	2.2	1.0
All	0	0	0	0	0	0	0	0	0	0	0	0	0	0	0	0	0	0	0	0	0	0

Summer 200k Proposed- Exposure Time Percentage After 1 Minute															
Powerhouse Flow Exposure															
	U1	U2	U3	U4	U5	U6	U7	U8	U9	U10	U11	U12	U13	U14	Outflow
Velocity	68.2	n/a	n/a	n/a	n/a	n/a	70.9	63.9	35.7	37.3	45.1	484	49.7	50.3	0.09
All	0	n/a	n/a	n/a	n/a	n/a	0	0	0	0	0	0	0	0	0

Spillway Flow Exposure																					
	S1	S2	S3	S4	S5	S6	S7	S8	S9	S10	S11	S12	S13	S14	S15	S16	S17	S18	S19	S20	S21	S22
Velocity	30.4	22.8	2.21	45.3	33.4	35.4	32.4	22.7	65.2	58.9	27.8	44.7	38.1	36.5	12.3	57.9	36.3	0.45	0	0	42.8	35.7
All	20.6	7.11	1.82	0	0	0	0	0	0	0	0	0	0	0	0	0	0	0	0	0	0	0

Summer 200k Proposed- Exposure Time Percentage After 10 Minutes															
Powerhouse Flow Exposure															
	U1	U2	U3	U4	U5	U6	U7	U8	U9	U10	U11	U12	U13	U14	Outflow
Velocity	96.4	n/a	n/a	n/a	n/a	n/a	67.4	81.2	46.3	38.8	46.1	46.7	41.3	59.7	0.01
All	21.9	n/a	n/a	n/a	n/a	n/a	4.23	12	0	0	0	0	0	0	0

Spillway Flow Exposure																					
	S1	S2	S3	S4	S5	S6	S7	S8	S9	S10	S11	S12	S13	S14	S15	S16	S17	S18	S19	S20	S21	S22
Velocity	60.5	58	39.4	46.1	48.9	46.5	38.3	42	49	67.9	74.5	65.8	61.2	57.2	41.1	66.9	79.7	58.8	17.2	1.9	47.9	48.3
All	44.5	41.2	5.67	19	14.6	12.3	10.2	17.7	8.7	5.19	1.61	2.16	3.45	2.9	0	0	0	0	0	0	0	0

Table E21 Exposure time percentages after 10 seconds, 1 minute and 10 minutes for Simulation 7

Summer 250k- Exposure Time Percentage After 10 Seconds

Powerhouse Flow Exposure

	U1	U2	U3	U4	U5	U6	U7	U8	U9	U10	U11	U12	U13	U14	Outflow
Velocity	39	38.9	38.7	38.6	38.9	38.7	38.7	38.4	38.4	38.5	38.3	38.3	38.6	38.2	0.01
All	0	0	0	0	0	0	0	0	0	0	0	0	0	0	0

Spillway Flow Exposure

	S1	S2	S3	S4	S5	S6	S7	S8	S9	S10	S11	S12	S13	S14	S15	S16	S17	S18	S19	S20	S21	S22
Velocity	3.26	0.25	0	0.92	0	0	0	0.08	0	0	0	0	0	0	0	0	2.68	0	0	0	0	0
All	3.18	0	0	0	0	0	0	0	0	0	0	0	0	0	0	0	0	0	0	0	0	0

Summer 250k- Exposure Time Percentage After 1 Minute

Powerhouse Flow Exposure

	U1	U2	U3	U4	U5	U6	U7	U8	U9	U10	U11	U12	U13	U14	Outflow
Velocity	71.3	66.8	71.8	73.2	75.4	71.1	74.5	71.9	75.4	75.9	75.5	76.7	71.9	70.5	66.7
All	0.64	6.01	0.61	0	0	0	0	0	0	0	0	0	0	0	0

Spillway Flow Exposure

	S1	S2	S3	S4	S5	S6	S7	S8	S9	S10	S11	S12	S13	S14	S15	S16	S17	S18	S19	S20	S21	S22
Velocity	21	17.3	13.3	345	44.9	27.2	11.5	22.5	15.5	40.5	34.4	47	48.1	42.3	49.2	55.4	34.4	0	3.16	3.06	7.76	9.74
All	9.61	3.97	13.3	2.75	3.24	0	0	0	0	0	0	0	0	0	0	0	0	0	0	0	0	0

Summer 250k- Exposure Time Percentage After 10 Minutes

Powerhouse Flow Exposure

	U1	U2	U3	U4	U5	U6	U7	U8	U9	U10	U11	U12	U13	U14	Outflow
Velocity	95.5	86.8	63.9	64.7	82.4	91.6	91.2	88.6	77.7	62.5	71.4	65.8	51.3	49.2	34.8
All	11.4	54.4	15.3	0.8	0	0	0	0	0	0	0	0	0	1.08	14

Spillway Flow Exposure

	S1	S2	S3	S4	S5	S6	S7	S8	S9	S10	S11	S12	S13	S14	S15	S16	S17	S18	S19	S20	S21	S22
Velocity	52	53.4	51.9	42.5	59.3	64.4	35.3	39.6	16.6	40	49.5	87.3	89.9	80.3	67.6	78.6	62.8	11.1	52.7	70	57.4	58.3
All	18.9	17.8	19.5	13.1	8.6	9.69	0.44	1.97	0	0	0	0	0	0.14	0.08	0	0	0	0.01	0	0	0

Table E22 Exposure time percentages after 10 seconds, 1 minute and 10 minutes for Simulation 8

Summer 250k Proposed- Exposure Time Percentage After 10 Seconds															
Powerhouse Flow Exposure															
	U1	U2	U3	U4	U5	U6	U7	U8	U9	U10	U11	U12	U13	U14	Outflow
Velocity	37.9	n/a	n/a	n/a	38.3	17.5	18.1	17.6	17.4	17.2	17.5	17.4	17.4	17.9	6.82
All	0	n/a	n/a	n/a	0	0	0	0	0	0	0	0	0	0	0

Spillway Flow Exposure																					
	S1	S2	S3	S4	S5	S6	S7	S8	S9	S10	S11	S12	S13	S14	S15	S16	S17	S18	S19	S20	S21	S22
Velocity	1.78	1.79	0	1.62	0	0	0	0	0	0	0	0	0	0	0	0.59	2.82	0	0	0	0	0
All	0	0	0	0	0	0	0	0	0	0	0	0	0	0	0	0	0	0	0	0	0	0

Summer 250k Proposed- Exposure Time Percentage After 1 Minute															
Powerhouse Flow Exposure															
	U1	U2	U3	U4	U5	U6	U7	U8	U9	U10	U11	U12	U13	U14	Outflow
Velocity	66.7	n/a	n/a	n/a	60.4	28.9	29.9	33.4	41.6	41.7	47.4	48.3	50.1	43.5	4.38
All	0	n/a	n/a	n/a	0	0	0	0	0	0	0	0	0	0	0

Spillway Flow Exposure																					
	S1	S2	S3	S4	S5	S6	S7	S8	S9	S10	S11	S12	S13	S14	S15	S16	S17	S18	S19	S20	S21	S22
Velocity	22.3	15.9	9.37	37.9	35.6	24.7	9.47	29.8	23.3	42.6	33.3	39.6	40.7	50.7	48.6	48.4	44.7	2.83	6.07	1.49	5.47	4.43
All	3.21	2.19	8.17	1.01	0.95	0	0	0	0	0	0	0	0	0	0	0	0	0	0	0	0	0

Summer 250k Proposed- Exposure Time Percentage After 10 Minutes															
Powerhouse Flow Exposure															
	U1	U2	U3	U4	U5	U6	U7	U8	U9	U10	U11	U12	U13	U14	Outflow
Velocity	93.8	n/a	n/a	n/a	68.8	55.4	52.3	66.6	77	74.6	66.3	54.5	47.1	45.1	0.43
All	14.9	n/a	n/a	n/a	21.6	28.3	5.42	0	0	0	0.38	1.13	1.99	1.18	0

Spillway Flow Exposure																					
	S1	S2	S3	S4	S5	S6	S7	S8	S9	S10	S11	S12	S13	S14	S15	S16	S17	S18	S19	S20	S21	S22
Velocity	46.2	48.2	46	46.3	48.9	44.2	15.8	44.5	16.2	35.8	60.3	88	90.7	80.7	73.3	67.4	68.9	17.7	70.3	71.1	63.8	52.3
All	13.2	9.94	27.6	12.5	7.91	2.8	0.66	0.4	0	0	0	0	0	0	0	0	0	0	0	0	0	0

Table E23 Exposure time percentages after 10 seconds, 1 minute and 10 minutes for Simulation 11

Spring 200k- Exposure Time Percentage After 10 Seconds

Powerhouse Flow Exposure

	U1	U2	U3	U4	U5	U6	U7	U8	U9	U10	U11	U12	U13	U14	Outflow
Velocity	38.8	38.7	38.5	38.5	38.6	38.5	38.4	38.3	38.2	38.4	38.1	38.1	38.1	38	0.54
All	0	0	0	0	0	0	0	0	0	0	0	0	0	0	0

Spillway Flow Exposure

	S1	S2	S3	S4	S5	S6	S7	S8	S9	S10	S11	S12	S13	S14	S15	S16	S17	S18	S19	S20	S21	S22
Velocity	0	2.23	0	n/a	0	5.61	2.35	n/a	0	14.3	1.13	n/a	0	8.43	0	1	17.8	8.42	0	0	0.8	0.57
All	0	0	0	n/a	0	0	0	n/a	0	0	0	n/a	0	0	0	0	0	0	0	0	0	0

Spring 200k- Exposure Time Percentage After 1 Minute

Powerhouse Flow Exposure

	U1	U2	U3	U4	U5	U6	U7	U8	U9	U10	U11	U12	U13	U14	Outflow
Velocity	72.1	67.9	73.3	74.6	76.5	72.3	74.8	71.8	75.4	75.3	75.4	76.4	76.1	73.2	63.6
All	0.77	5.97	0.71	0	0	0	0	0	0	0	0	0	0	0	0

Spillway Flow Exposure

	S1	S2	S3	S4	S5	S6	S7	S8	S9	S10	S11	S12	S13	S14	S15	S16	S17	S18	S19	S20	S21	S22
Velocity	15.9	13.5	0	n/a	58.2	64	66	n/a	58.5	70.2	61.5	n/a	54.1	63.3	62.7	42.5	42.2	52.2	0	0	25	35.2
All	11.1	6.94	0	n/a	0	0	0	n/a	0	0	0	n/a	0	0	0	0	0	0	0	0	0	0

Spring 200k- Exposure Time Percentage After 10 Minutes

Powerhouse Flow Exposure

	U1	U2	U3	U4	U5	U6	U7	U8	U9	U10	U11	U12	U13	U14	Outflow
Velocity	93.5	70.7	53.4	49.2	53.1	55.4	65.4	67.4	72.8	71	77	62.4	62.2	65	20.7
All	12.9	40.9	10.7	0.42	0	0	0	0	0	0	0	0	0	0	9.71

Spillway Flow Exposure

	S1	S2	S3	S4	S5	S6	S7	S8	S9	S10	S11	S12	S13	S14	S15	S16	S17	S18	S19	S20	S21	S22
Velocity	54	46.4	25.8	n/a	36.6	30.1	34.3	n/a	57.5	54.7	77.2	n/a	90.8	77	98.7	68.9	69.5	49.7	58.1	78.8	76.1	75.6
All	37.2	31.8	0	n/a	21.7	10.4	9.28	n/a	8.65	5.56	1.17	n/a	0.07	0.41	0	0	0	0	0	0	0	0

Table E24 Exposure time percentages after 10 seconds, 1 minute and 10 minutes for Simulation 12

Spring 200k Proposed- Exposure Time Percentage After 10 Seconds

Powerhouse Flow Exposure

	U1	U2	U3	U4	U5	U6	U7	U8	U9	U10	U11	U12	U13	U14	Outflow
Velocity	38.8	n/a	n/a	n/a	38.5	38.6	38.3	17.2	16.7	17.2	17.1	17	17	17	1.96
All	0	n/a	n/a	n/a	0	0	0	0	0	0	0	0	0	0	0

Spillway Flow Exposure

	S1	S2	S3	S4	S5	S6	S7	S8	S9	S10	S11	S12	S13	S14	S15	S16	S17	S18	S19	S20	S21	S22
Velocity	0	0	0	n/a	0.27	9.42	0.11	n/a	0.75	16.7	1.95	n/a	0	11.6	0.38	12.8	0.53	0	0	0	0.14	0.31
All	0	0	0	n/a	0	0	0	n/a	0	0	0	n/a	0	0	0	0	0	0	0	0	0	0

Spring 200k Proposed- Exposure Time Percentage After 1 Minute

Powerhouse Flow Exposure

	U1	U2	U3	U4	U5	U6	U7	U8	U9	U10	U11	U12	U13	U14	Outflow
Velocity	70.7	n/a	n/a	n/a	77.1	73.8	69.7	35.6	45.1	45.2	47.4	47.6	48.1	50	0.32
All	0	n/a	n/a	n/a	0	0	0	0	0	0	0	0	0	0	0

Spillway Flow Exposure

	S1	S2	S3	S4	S5	S6	S7	S8	S9	S10	S11	S12	S13	S14	S15	S16	S17	S18	S19	S20	S21	S22
Velocity	16.9	11	0	n/a	57.7	61.9	69.1	n/a	64.1	75.3	60.3	n/a	58	65.8	61	44.2	48.9	38.8	23.8	4.7	40	47.5
All	11.3	6.39	0	n/a	0	0	0	n/a	0	0	0	n/a	0	0	0	0	0	0	0	0	0	0

Spring 200k Proposed- Exposure Time Percentage After 10 Minutes

Powerhouse Flow Exposure

	U1	U2	U3	U4	U5	U6	U7	U8	U9	U10	U11	U12	U13	U14	Outflow
Velocity	96.8	n/a	n/a	n/a	73.2	62.3	38.2	13.8	34.4	36.1	46.9	49.4	49.7	63	1.96
All	31.2	n/a	n/a	n/a	4.81	4.2	0	0	0	0	0	0	0	0	0

Spillway Flow Exposure

	S1	S2	S3	S4	S5	S6	S7	S8	S9	S10	S11	S12	S13	S14	S15	S16	S17	S18	S19	S20	S21	S22
Velocity	55.6	59.4	43.8	n/a	35.7	35.1	40.4	n/a	53.2	60.4	80.7	n/a	78.5	73.7	59.4	57.7	57.1	63.5	61.6	68.6	76.5	72.3
All	35.7	43.6	0.01	n/a	9.46	13.4	4.85	n/a	12	5.65	0.67	n/a	0.82	0.06	0	0	0	0	0	0	0	0

Table E25 Exposure time percentages after 10 seconds, 1 minute and 10 minutes for Simulation 13

Spring 250k- Exposure Time Percentage After 10 Seconds

Powerhouse Flow Exposure

	U1	U2	U3	U4	U5	U6	U7	U8	U9	U10	U11	U12	U13	U14	Outflow
Velocity	40	39.8	39.2	48.6	39.2	39	39	38.9	38.4	37.8	38.3	38.9	38.6	38.8	0
All	0	0	0	0	0	0	0	0	0	0	0	0	0	0	0

Spillway Flow Exposure

	S1	S2	S3	S4	S5	S6	S7	S8	S9	S10	S11	S12	S13	S14	S15	S16	S17	S18	S19	S20	S21	S22
Velocity	0.69	0	0	12.3	10.7	0	0	0	0	0	0.36	2.78	0	3.66	0	3.21	1.19	0.34	2.5	0	0	0
All	0	0	0	0	0	0	0	0	0	0	0	0	0	0	0	0	0	0	0	0	0	0

Spring 250k- Exposure Time Percentage After 1 Minute

Powerhouse Flow Exposure

	U1	U2	U3	U4	U5	U6	U7	U8	U9	U10	U11	U12	U13	U14	Outflow
Velocity	68.8	60.7	61.9	62.7	70.5	59.4	65.3	62.1	66.7	66.7	65.7	69.1	65.8	62.4	0.49
All	0.49	5.2	0.34	0	0	0	0	0	0	0	0	0	0	0	0

Spillway Flow Exposure

	S1	S2	S3	S4	S5	S6	S7	S8	S9	S10	S11	S12	S13	S14	S15	S16	S17	S18	S19	S20	S21	S22
Velocity	21.2	9.65	26	43.9	62.2	51.8	46.2	46.8	58.1	55.5	54	67.2	65	57.1	63.5	63.4	69.6	57.5	37.9	4.36	54.9	26.4
All	6.01	2.1	5.67	3.81	0	0	0	0	0	0	0	0	0	0	0	0	0	0	0	0	0	0

Spring 250k- Exposure Time Percentage After 10 Minutes

Powerhouse Flow Exposure

	U1	U2	U3	U4	U5	U6	U7	U8	U9	U10	U11	U12	U13	U14	Outflow
Velocity	88	56.1	29.9	26.5	27.9	19.9	21.9	21.1	36.8	42.4	53.8	60.9	61.2	65.1	0.05
All	11.5	28.3	0	0	0	0	0	0	0	0	0	0.1	0.54	0.33	0

Spillway Flow Exposure

	S1	S2	S3	S4	S5	S6	S7	S8	S9	S10	S11	S12	S13	S14	S15	S16	S17	S18	S19	S20	S21	S22
Velocity	54.9	55.1	56.2	61.2	83.7	73.2	59.7	82.5	80.5	81.5	81.6	85	84.3	82.2	69.7	63.7	69.6	73.9	69.5	81.9	81.8	80.3
All	41.7	37.4	30.2	20.8	1.16	8.44	8.36	3.55	4.89	3.82	1.34	1.83	0.08	0	0	0	0	0	0	0	0	0

Table E26 Exposure time percentages after 10 seconds, 1 minute and 10 minutes for Simulation 14

Spring 250k Proposed- Exposure Time Percentage After 10 Seconds															
Powerhouse Flow Exposure															
	U1	U2	U3	U4	U5	U6	U7	U8	U9	U10	U11	U12	U13	U14	Outflow
Velocity	39.2	n/a	39.6	39.7	16.8	17	17.6	17.3	16.7	17.2	17.1	17.1	17	17.1	0.1
All	0	n/a	0	0	0	0	0	0	0	0	0	0	0	0	0

Spillway Flow Exposure																					
	S1	S2	S3	S4	S5	S6	S7	S8	S9	S10	S11	S12	S13	S14	S15	S16	S17	S18	S19	S20	S21	S22
Velocity	0	3.52	0	32.4	4.82	2.01	0	1.3	0	0	1.32	0.56	0	12.5	0.55	2.46	7.62	1.7	6.05	0	0	0.19
All	0	0	0	0	0	0	0	0	0	0	0	0	0	0	0	0	0	0	0	0	0	0

Spring 250k Proposed- Exposure Time Percentage After 1 Minute															
Powerhouse Flow Exposure															
	U1	U2	U3	U4	U5	U6	U7	U8	U9	U10	U11	U12	U13	U14	Outflow
Velocity	69.7	n/a	77.3	67.7	46.4	34.5	36.2	39.9	49.5	45.7	57.8	47.7	48.1	51.3	0.02
All	0.03	n/a	0	0	0	0	0	0	0	0	0	0	0	0	0

Spillway Flow Exposure																					
	S1	S2	S3	S4	S5	S6	S7	S8	S9	S10	S11	S12	S13	S14	S15	S16	S17	S18	S19	S20	S21	S22
Velocity	19.6	37.5	22.7	35.1	51.1	54.3	51.7	65.6	34	55.3	52.4	63.5	66.6	68.4	56.3	60.4	54.4	55.5	35.3	13.5	42.8	33.2
All	12.3	6.47	6.21	4.6	0	0	0	0	0	0	0	0	0	0	0	0	0	0	0	0	0	0

Spring 250k Proposed- Exposure Time Percentage After 10 Minutes															
Powerhouse Flow Exposure															
	U1	U2	U3	U4	U5	U6	U7	U8	U9	U10	U11	U12	U13	U14	Outflow
Velocity	95.9	n/a	62	43.5	13	13	12.1	9.2	22.2	16.3	31.2	41.4	58.9	68.4	0
All	7.71	n/a	23.7	7.88	0.02	0	0	0	0	0	0	0	0	0	0

Spillway Flow Exposure																					
	S1	S2	S3	S4	S5	S6	S7	S8	S9	S10	S11	S12	S13	S14	S15	S16	S17	S18	S19	S20	S21	S22
Velocity	62.5	68.3	49.1	49.8	63.1	71.1	69.7	81.6	79.1	83.6	72.6	87.6	87	78.8	57.9	61.5	51.2	71.8	59.1	78.4	74.1	76
All	49.1	35.7	22.1	15.1	4.53	7.96	14.6	1.82	1.74	1.82	2.76	0.3	0	0	0	0	0	0	0	0	0	0

Table E27 Exposure time percentages after 10 seconds, 1 minute and 10 minutes for Simulation 15

Spring 300k- Exposure Time Percentage After 10 Seconds

Powerhouse Flow Exposure

	U1	U2	U3	U4	U5	U6	U7	U8	U9	U10	U11	U12	U13	U14	Outflow
Velocity	17.6	17	16.9	16.6	16.8	17	17.5	17	17	17	17	17	17	17	52.9
All	0	0	0	0	0	0	0	0	0	0	0	0	0	0	0

Spillway Flow Exposure

	S1	S2	S3	S4	S5	S6	S7	S8	S9	S10	S11	S12	S13	S14	S15	S16	S17	S18	S19	S20	S21	S22
Velocity	0.04	0	0	0.5	2.86	0	0.23	0	0	0	0.62	0	0	0.5	2.73	0.88	0	0	0.6	0	0	0
All	0	0	0	0	0	0	0	0	0	0	0	0	0	0	0	0	0	0	0	0	0	0

Spring 300k- Exposure Time Percentage After 1 Minute

Powerhouse Flow Exposure

	U1	U2	U3	U4	U5	U6	U7	U8	U9	U10	U11	U12	U13	U14	Outflow
Velocity	63.9	52.2	53.7	52.2	56.9	46.4	52.7	51.3	57.2	57.8	57.3	57.8	57.2	54.3	40.3
All	0.91	0	0	0	0	0	0	0	0	0	0	0	0	0	0

Spillway Flow Exposure

	S1	S2	S3	S4	S5	S6	S7	S8	S9	S10	S11	S12	S13	S14	S15	S16	S17	S18	S19	S20	S21	S22
Velocity	21.4	19.3	0.18	28	62.3	55.2	59.5	48.3	48.9	45.3	49.9	42.1	37.3	23.9	44.1	444	57.8	47.6	40.6	19.2	9.85	9
All	1.41	1.83	0	1.17	0	0	0	0	0	0	0	0	0	0	0	0	0	0	0	0	0	0

Spring 300k- Exposure Time Percentage After 10 Minutes

Powerhouse Flow Exposure

	U1	U2	U3	U4	U5	U6	U7	U8	U9	U10	U11	U12	U13	U14	Outflow
Velocity	87.8	48.6	28.1	19	23.3	14.4	14.6	13.4	20	22.3	33.2	44	39.2	54.5	4.01
All	2.81	0.6	0	0	0	0	0	0	0	0	0	0	0	0	0

Spillway Flow Exposure

	S1	S2	S3	S4	S5	S6	S7	S8	S9	S10	S11	S12	S13	S14	S15	S16	S17	S18	S19	S20	S21	S22
Velocity	38.2	34.3	21.1	28.3	33.5	36.2	47.5	48.9	53.1	56.4	75.2	59.1	56.4	63.5	63.6	61.7	69.6	68.8	65	64.7	56.7	59.1
All	4.34	4.89	0.02	2.7	0.9	0.33	1.27	2.09	1.06	1.16	0.75	0.56	0.27	0.14	0.39	0.32	0.3	0.02	0.01	0.02	0.02	0.01

Table E28 Exposure time percentages after 10 seconds, 1 minute and 10 minutes for Simulation 16

Spring 300k Proposed- Exposure Time Percentage After 10 Seconds															
Powerhouse Flow Exposure															
	U1	U2	U3	U4	U5	U6	U7	U8	U9	U10	U11	U12	U13	U14	Outflow
Velocity	17.4	17	16.9	16.8	17.2	17	17.5	16.9	16.7	17	17	17.1	16.3	16.8	0.11
All	0	0	0	0	0	0	0	0	0	0	0	0	0	0	0

Spillway Flow Exposure																					
	S1	S2	S3	S4	S5	S6	S7	S8	S9	S10	S11	S12	S13	S14	S15	S16	S17	S18	S19	S20	S21	S22
Velocity	0.2	0.1	0	0.16	0.99	1.02	0	0	1.63	0.21	0	0	0	0	3.02	0.7	0	1.35	0	0	0.64	0
All	0	0	0	0	0	0	0	0	0	0	0	0	0	0	0	0	0	0	0	0	0	0

Spring 300k Proposed- Exposure Time Percentage After 1 Minute															
Powerhouse Flow Exposure															
	U1	U2	U3	U4	U5	U6	U7	U8	U9	U10	U11	U12	U13	U14	Outflow
Velocity	66.1	48.7	54.9	52.8	49.2	42.8	45.3	45.1	57	48.4	52.9	51.5	49.6	53.1	0.02
All	0.13	3.71	0	0	0	0	0	0	0	0	0	0	0	0	0

Spillway Flow Exposure																					
	S1	S2	S3	S4	S5	S6	S7	S8	S9	S10	S11	S12	S13	S14	S15	S16	S17	S18	S19	S20	S21	S22
Velocity	14.7	11.1	13.8	20.5	56.4	57.8	36.7	35.8	52.1	40.8	57	42.7	42.8	34.3	46.5	54.3	58.3	57.2	21.1	8.02	5.81	10.8
All	1.96	2.85	13.8	0.9	0	0	0	0	0	0	0	0	0	0	0	0	0	0	0	0	0	0

Spring 300k Proposed- Exposure Time Percentage After 10 Minutes															
Powerhouse Flow Exposure															
	U1	U2	U3	U4	U5	U6	U7	U8	U9	U10	U11	U12	U13	U14	Outflow
Velocity	87.3	42.9	26.5	25.6	17	15.1	17.3	16.4	28.2	37.6	45.6	44.8	49.1	56.6	0
All	3.84	22	0.1	0	0	0	0	0	0	0	0	0	0	0	0

Spillway Flow Exposure																					
	S1	S2	S3	S4	S5	S6	S7	S8	S9	S10	S11	S12	S13	S14	S15	S16	S17	S18	S19	S20	S21	S22
Velocity	51.6	54.5	31.8	50.7	49.3	58.4	45.9	42.7	50.8	41.1	60	60.3	48.2	54.4	70.5	62.5	75.2	71.6	69.2	64.8	57.7	62.9
All	11.1	15.8	18.6	19.6	11.8	5.53	2.77	2.46	5.34	1.94	3.11	3.73	1.63	3.17	3.24	3.19	1.58	0.55	0.28	0.81	0.84	0.45

APPENDIX F. PREDATION CRITERIA

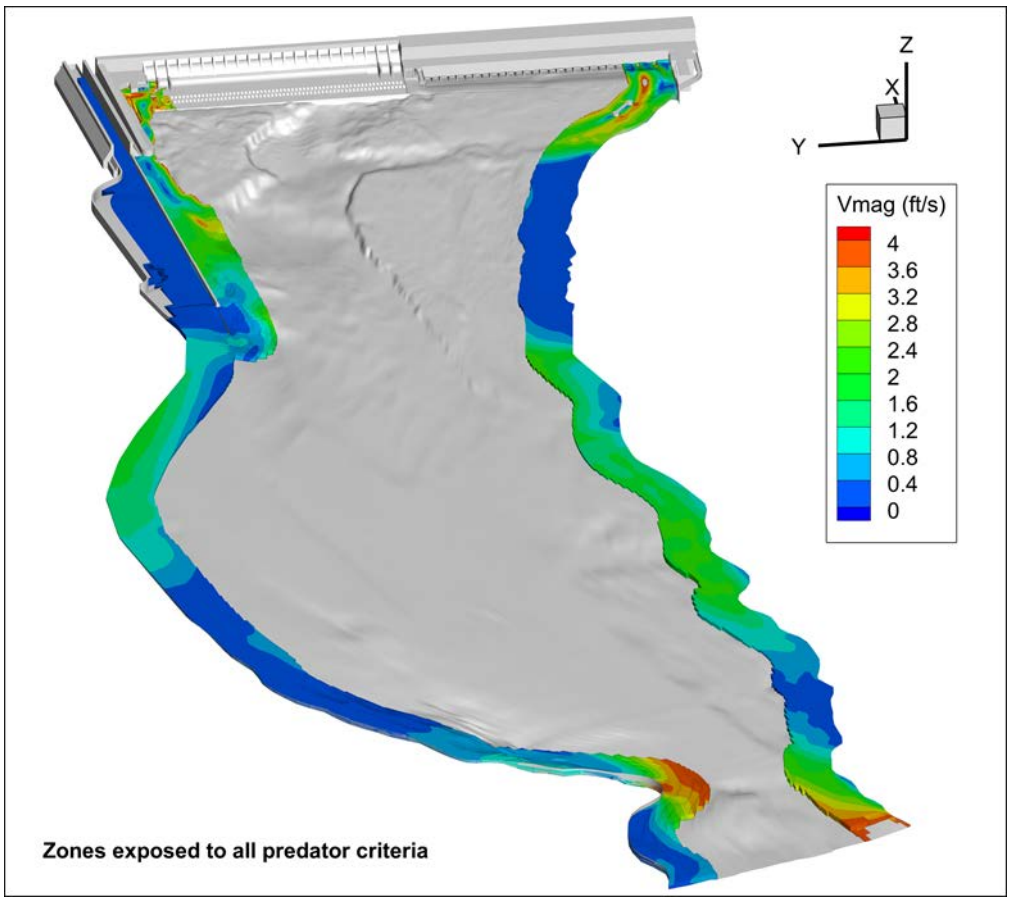

Figure F1. Zone exposed to all predation criteria colored by velocity magnitude for Simulation 1.

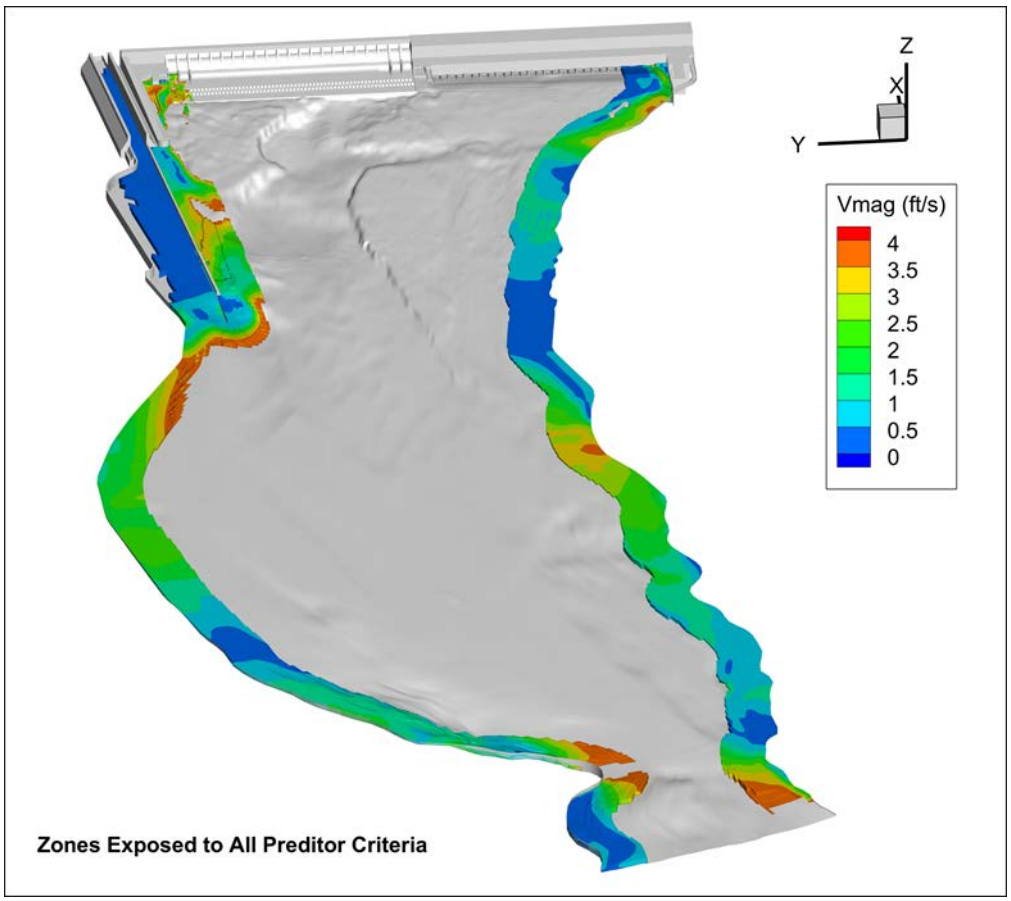

Figure F2. Zone exposed to all predation criteria colored by velocity magnitude for Simulation 2

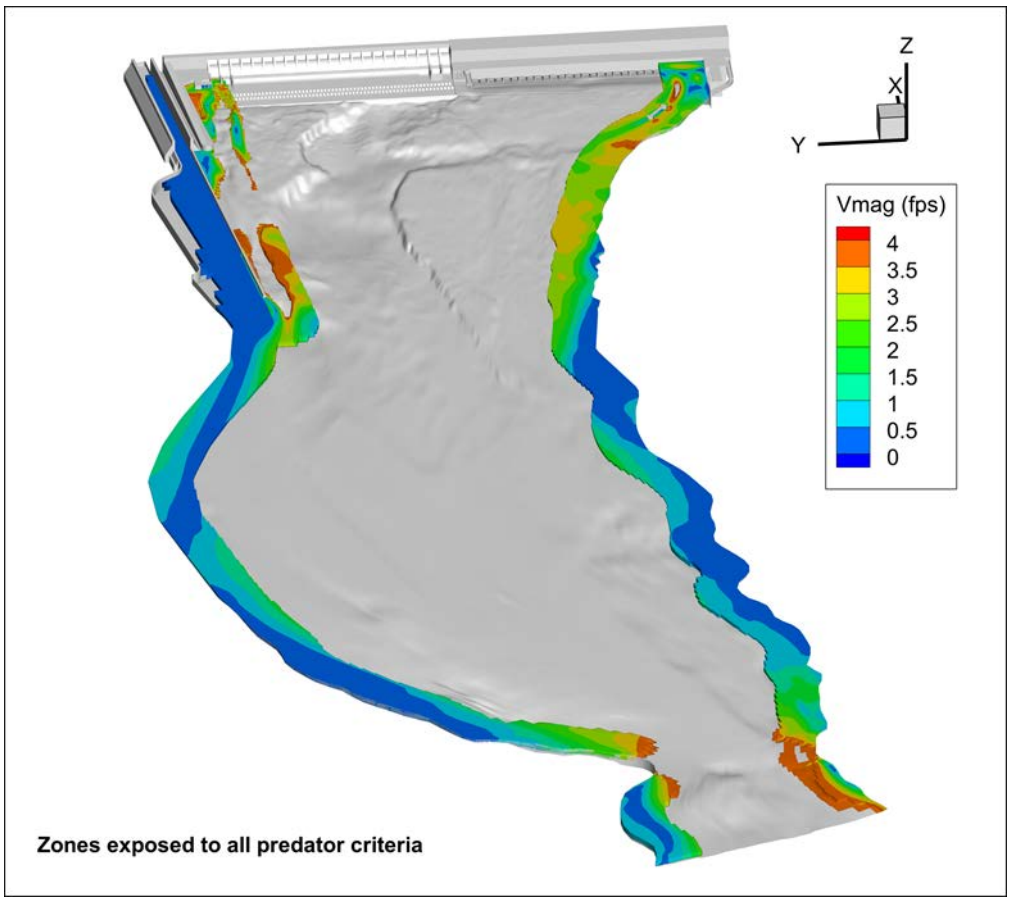

Figure F3. Zone exposed to all predation criteria colored by velocity magnitude for Simulation 3

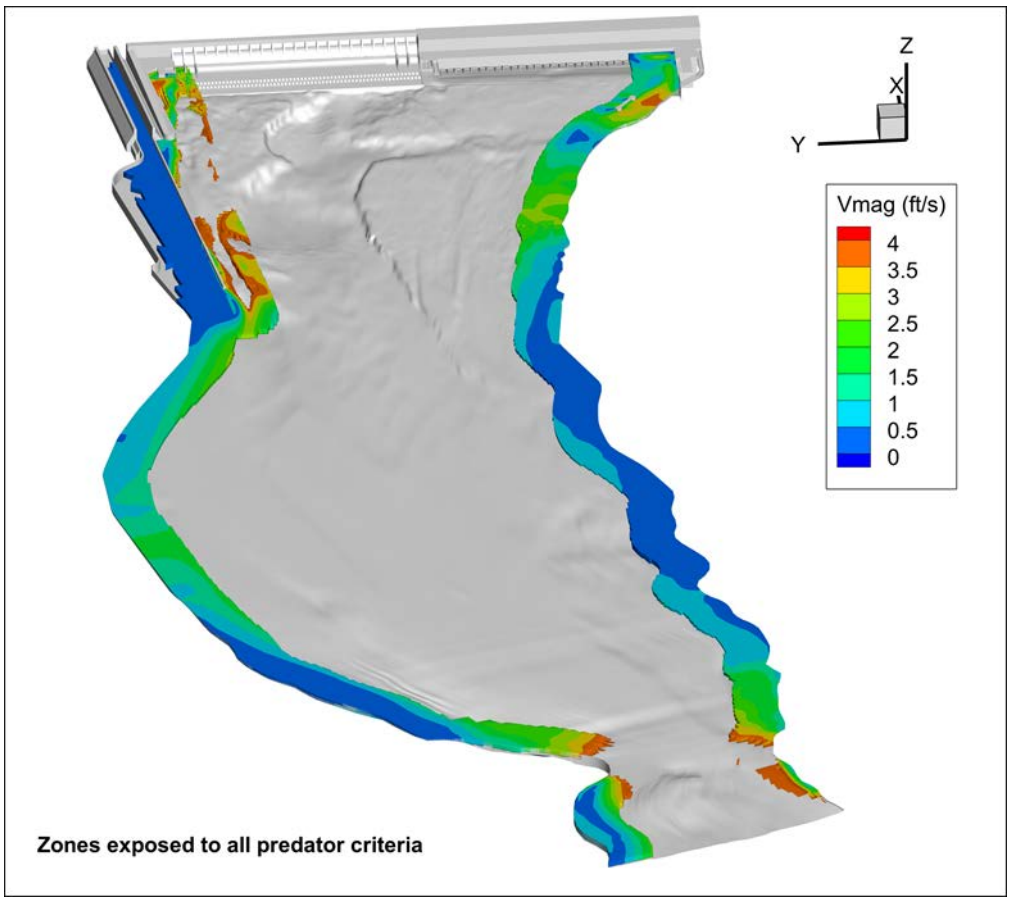

Figure F4. Zone exposed to all predation criteria colored by velocity magnitude for Simulation 4

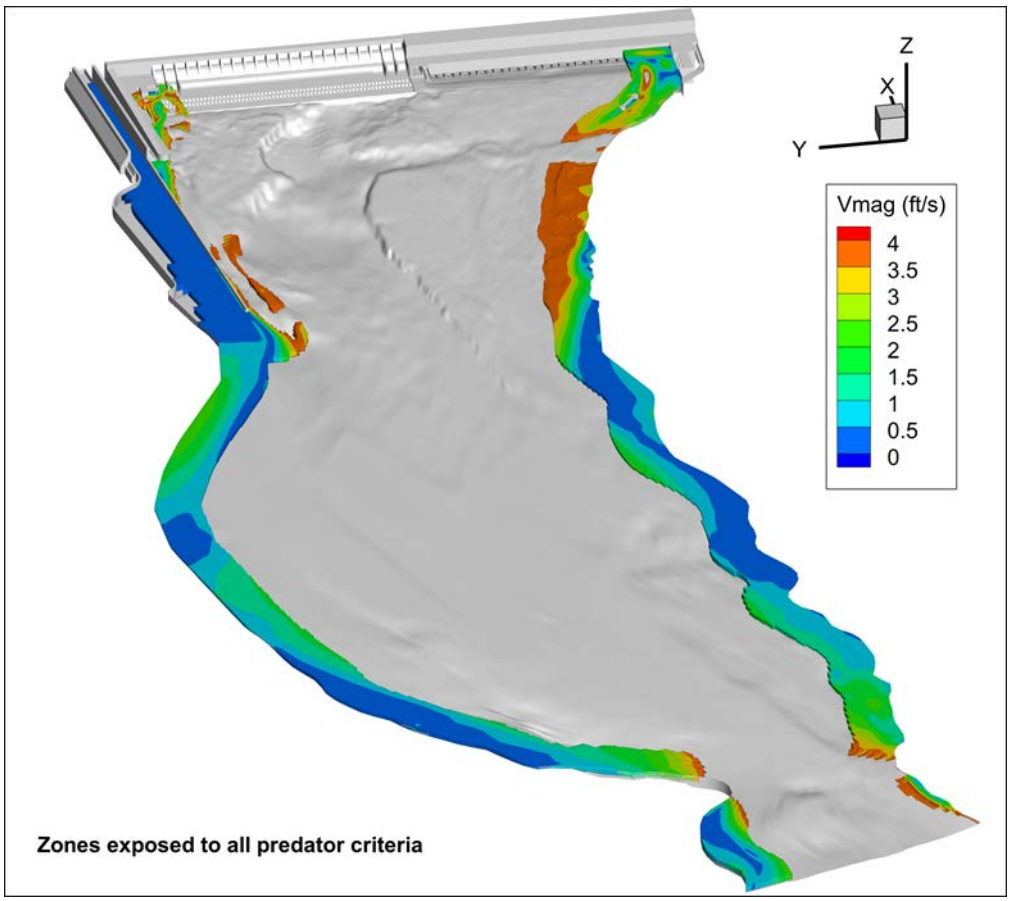

Figure F5. Zone exposed to all predation criteria colored by velocity magnitude for Simulation 5

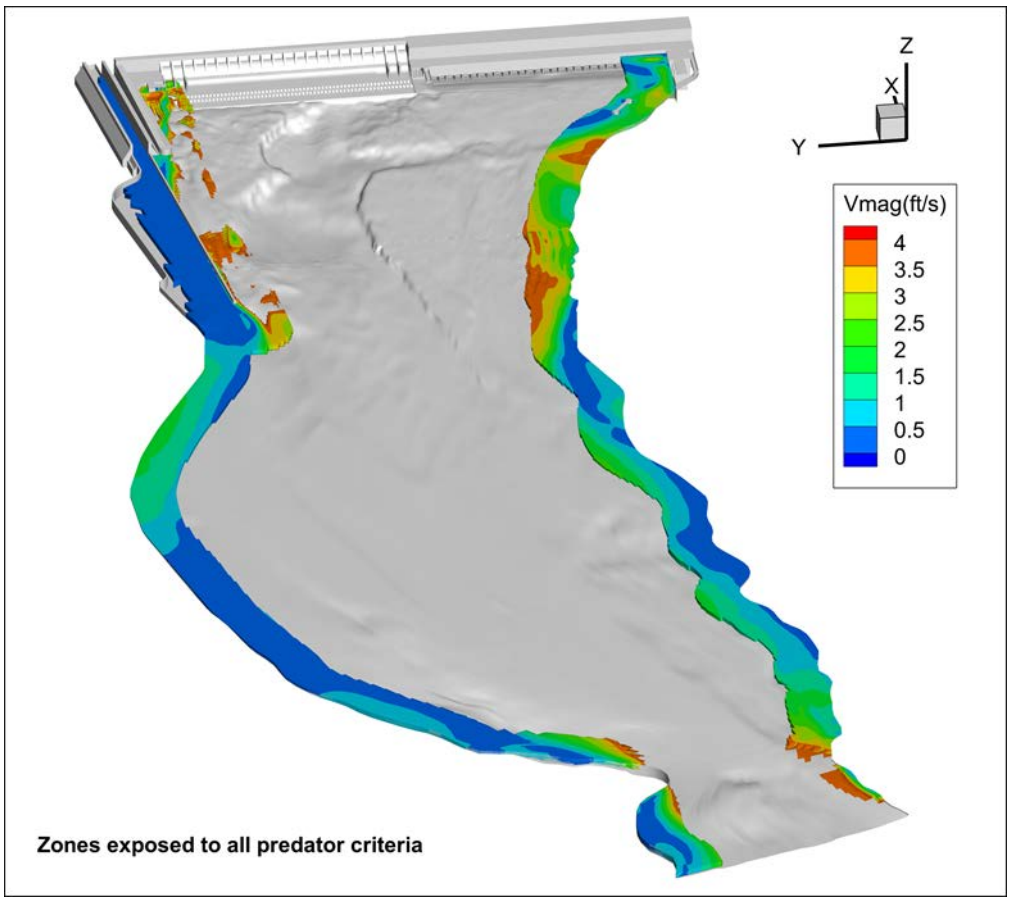

Figure F6. Zone exposed to all predation criteria colored by velocity magnitude for Simulation 6

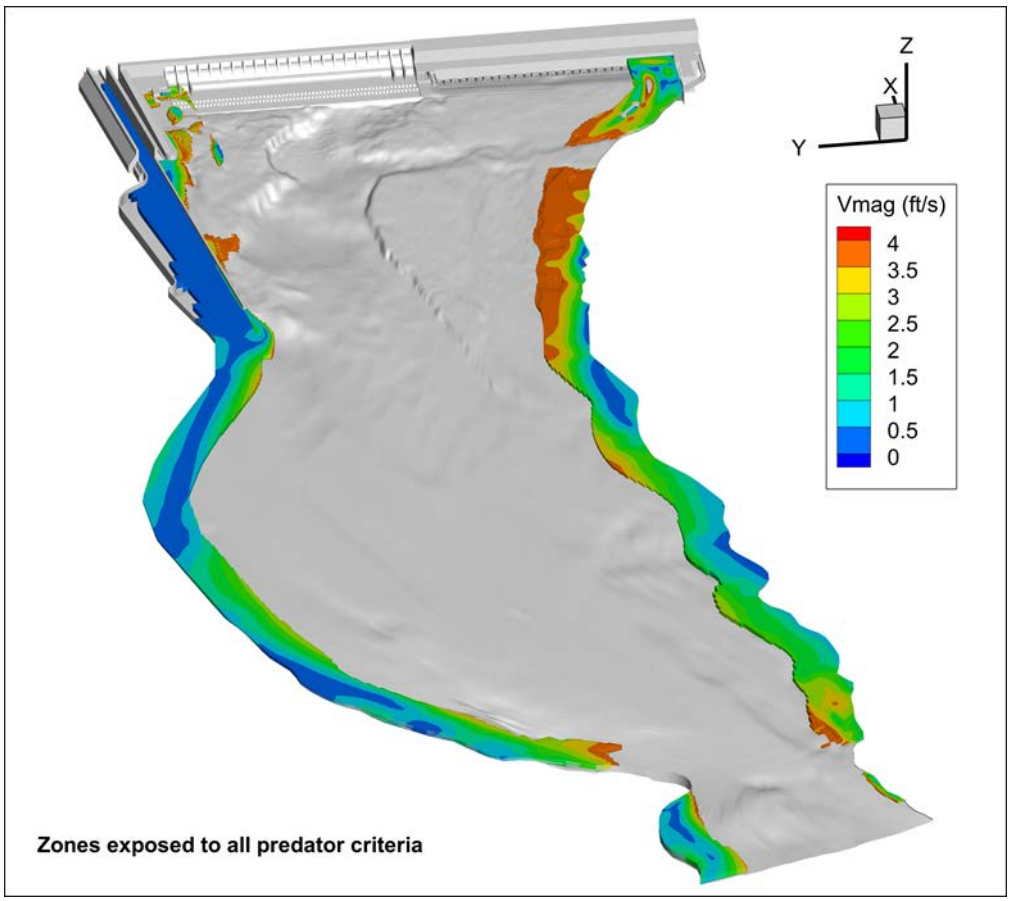

Figure F7. Zone exposed to all predation criteria colored by velocity magnitude for Simulation 7

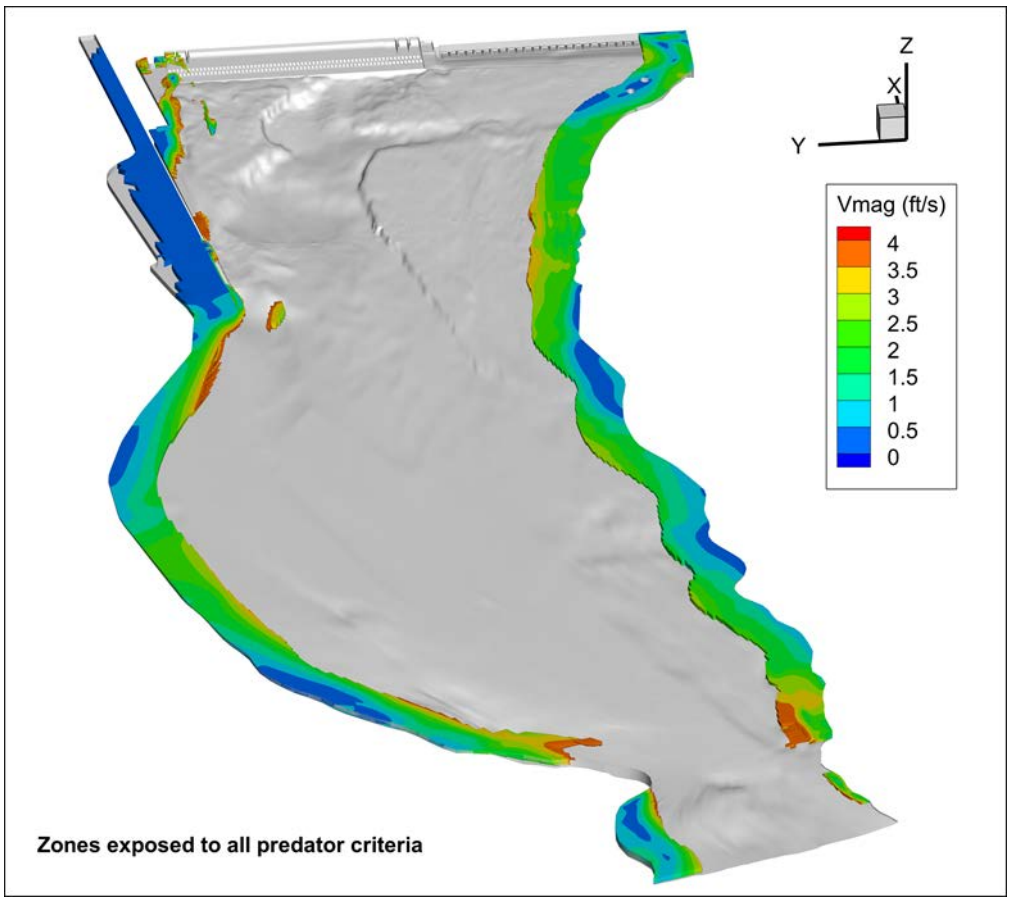

Figure F8. Zone exposed to all predation criteria colored by velocity magnitude for Simulation 8

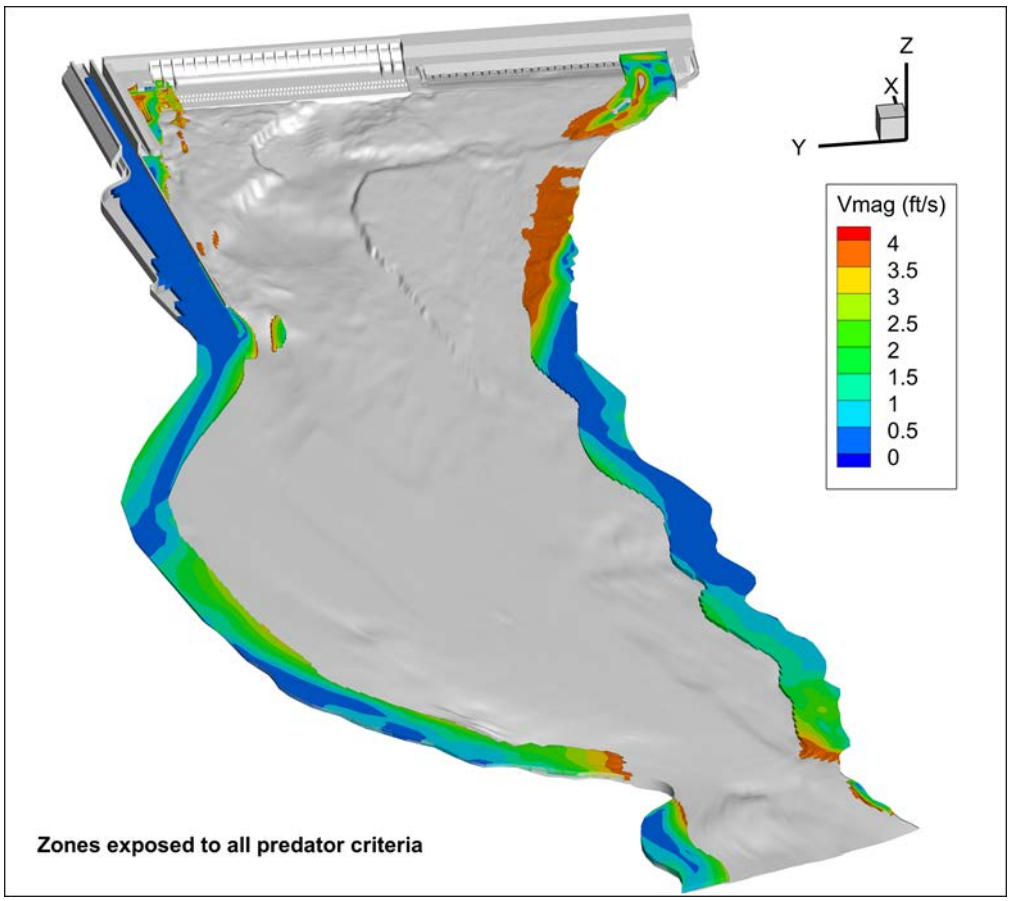

Figure F9. Zone exposed to all predation criteria colored by velocity magnitude for Simulation 11

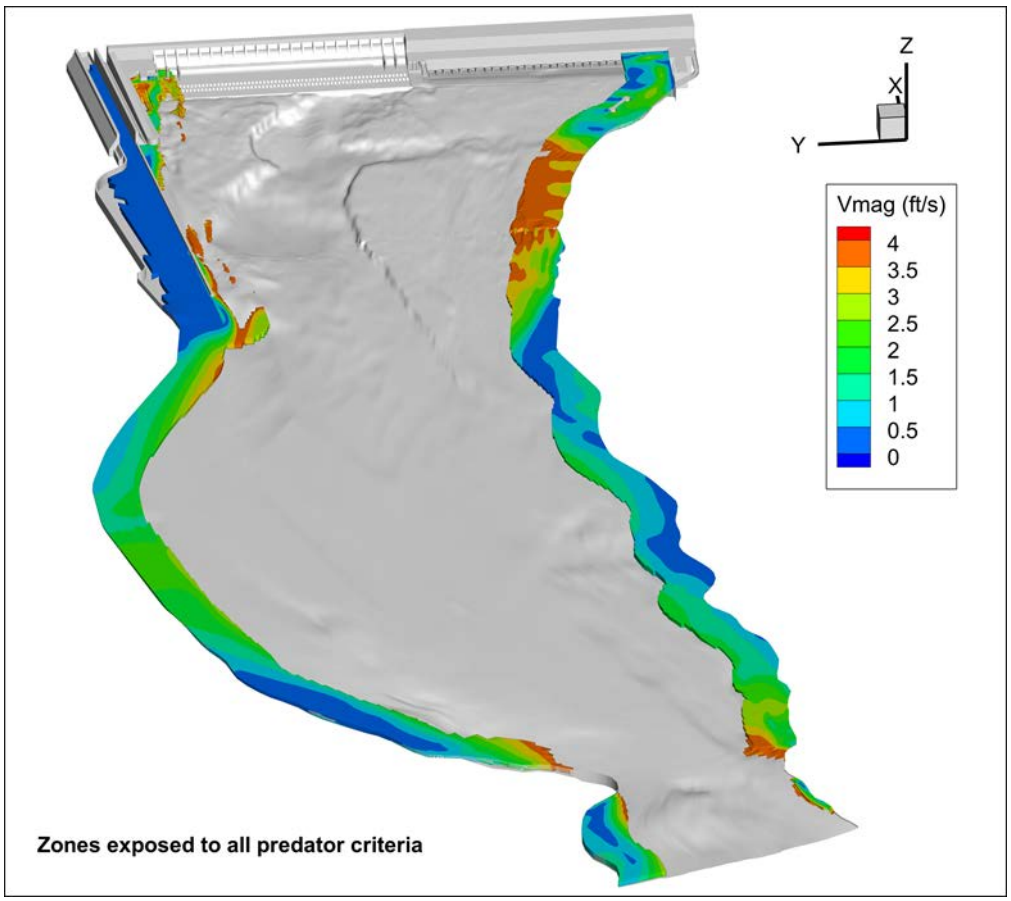

Figure F10. Zone exposed to all predation criteria colored by velocity magnitude for Simulation 12

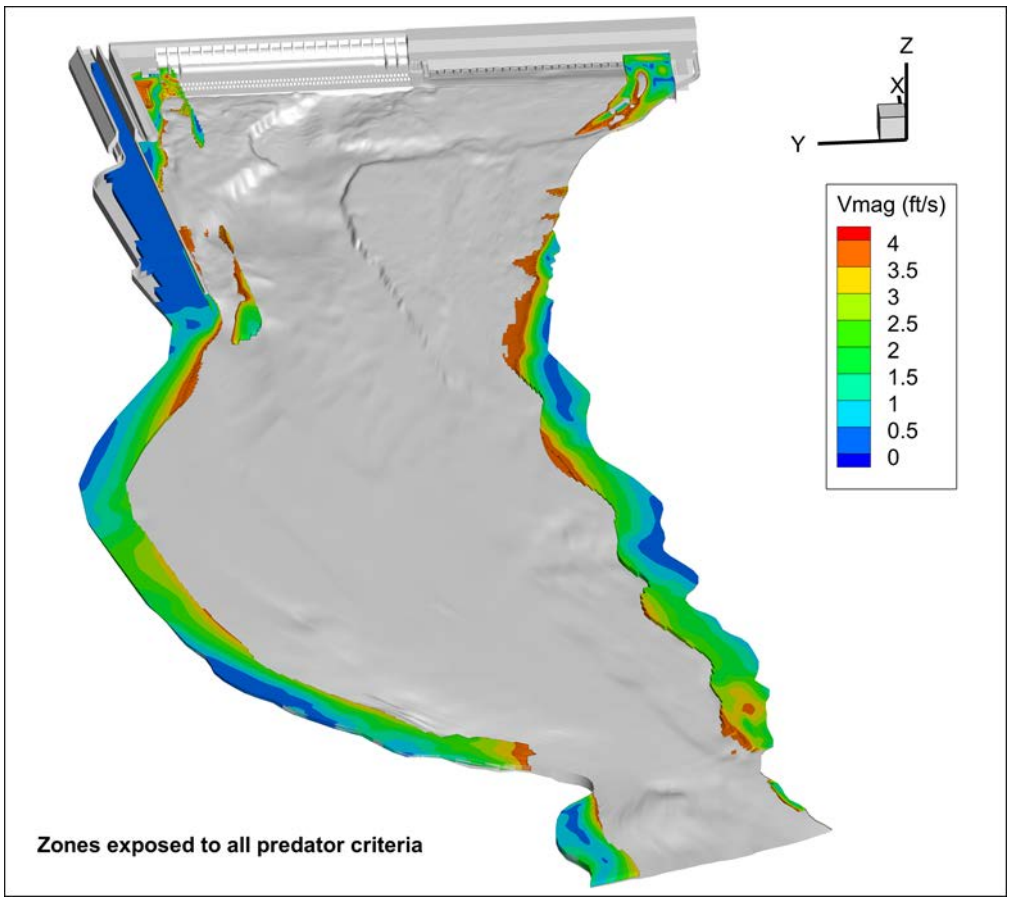

Figure F11. Zone exposed to all predation criteria colored by velocity magnitude for Simulation 13

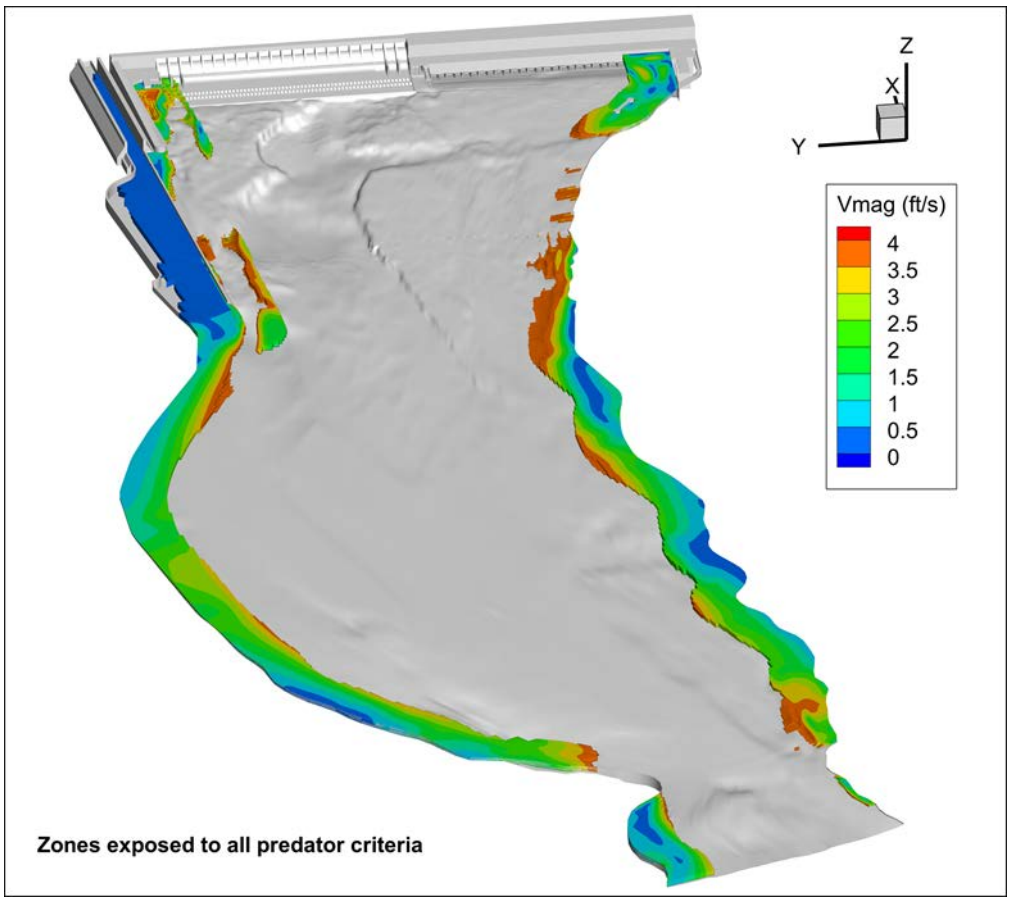

Figure F12. Zone exposed to all predation criteria colored by velocity magnitude for Simulation 14

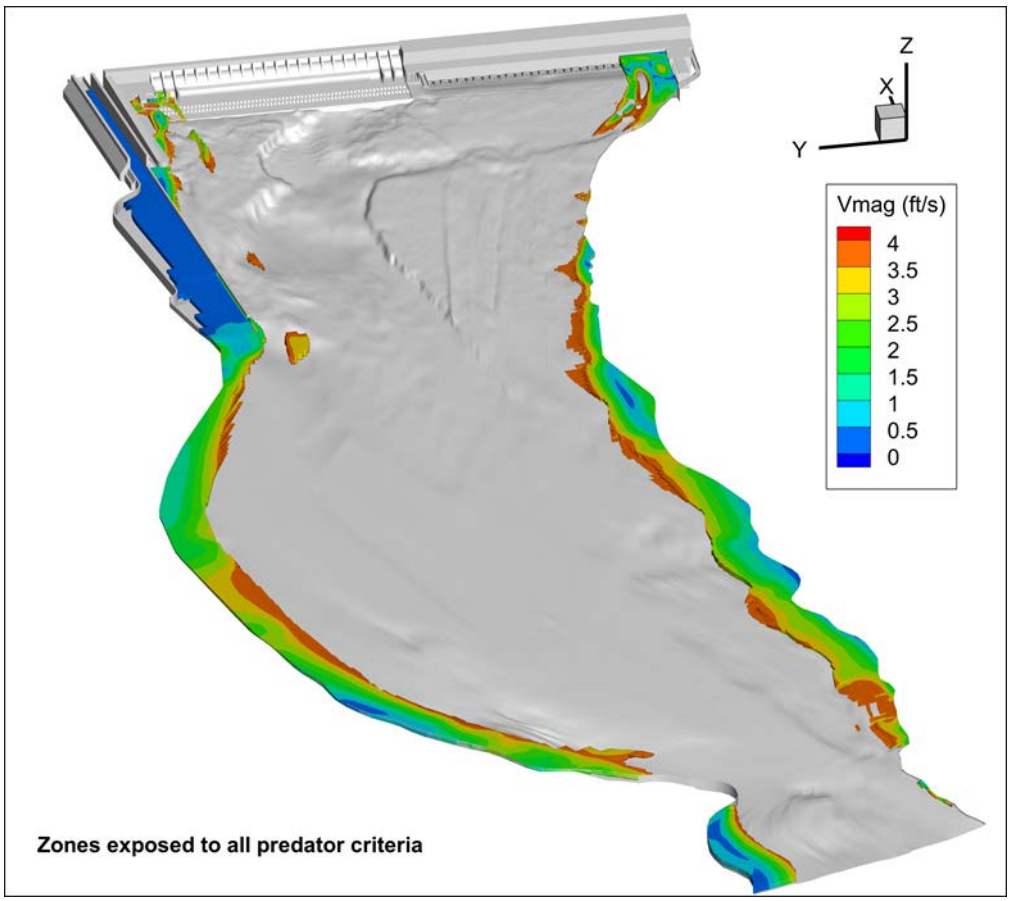

Figure F13. Zone exposed to all predation criteria colored by velocity magnitude for Simulation 15

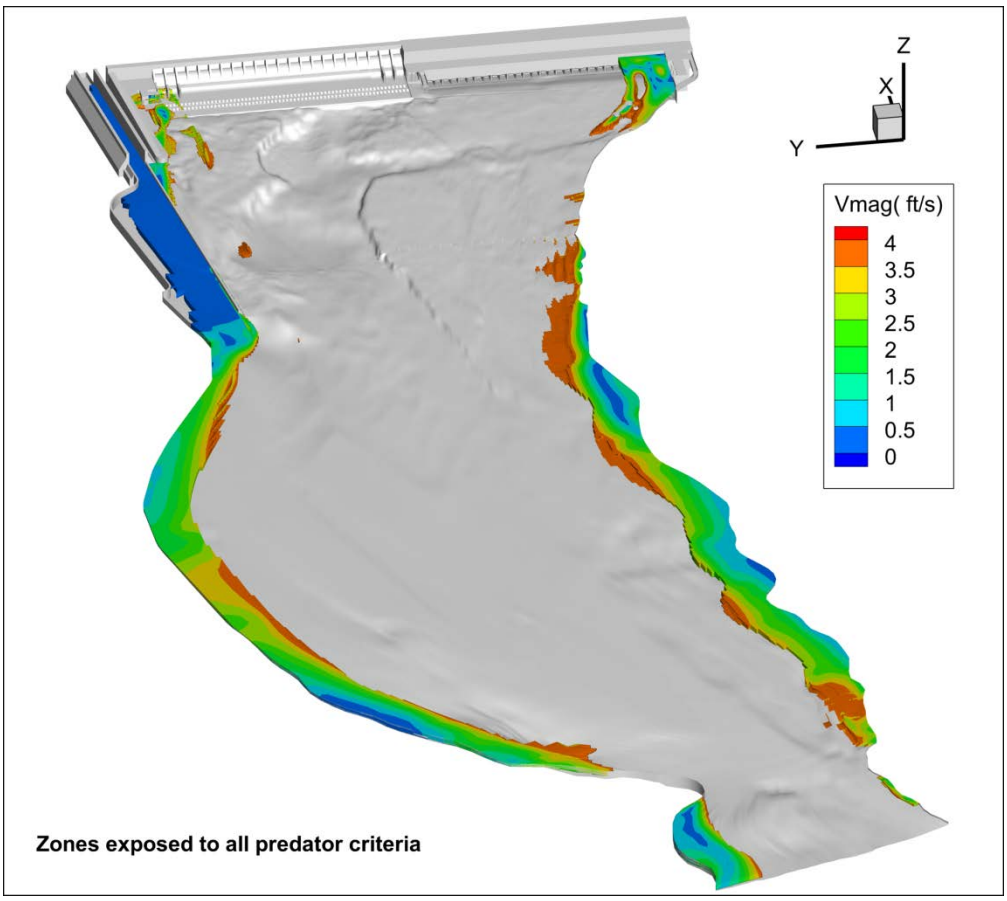

Figure F14. Zone exposed to all predation criteria colored by velocity magnitude for Simulation 16

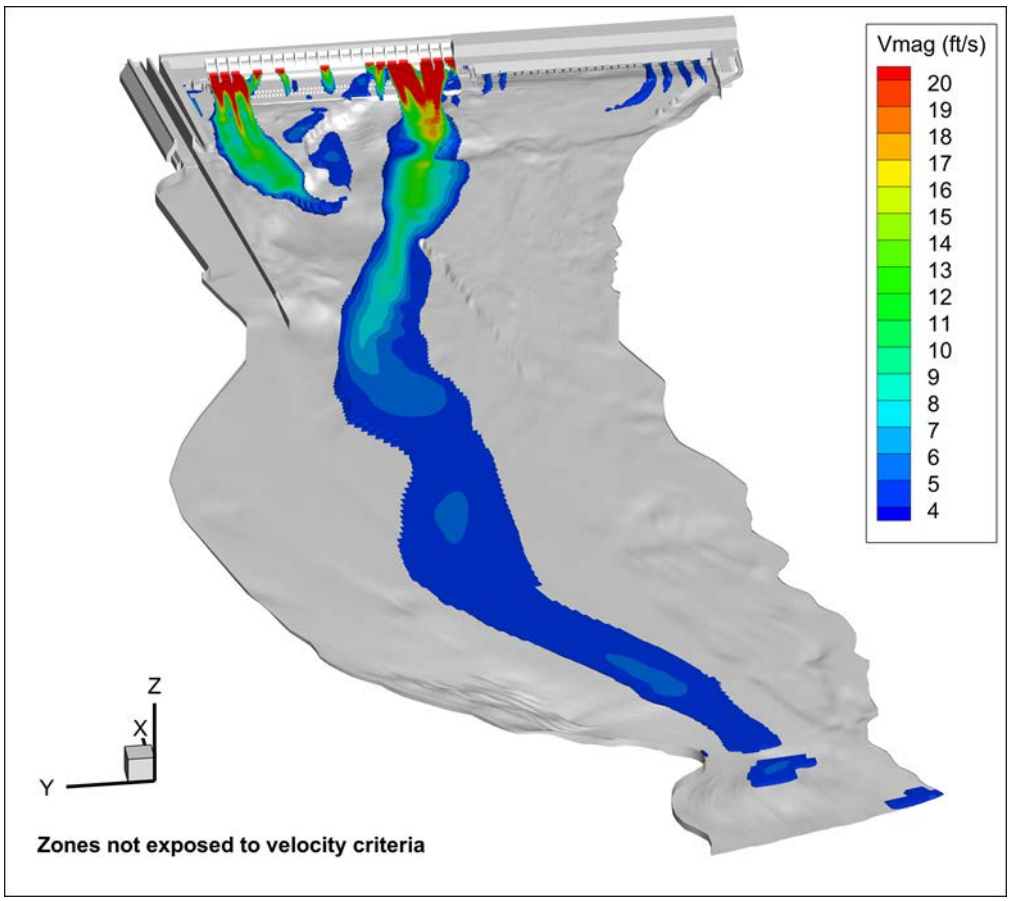

Figure F15. Zones with velocity magnitude greater than 4 ft/s colored by velocity magnitude for Simulation 1

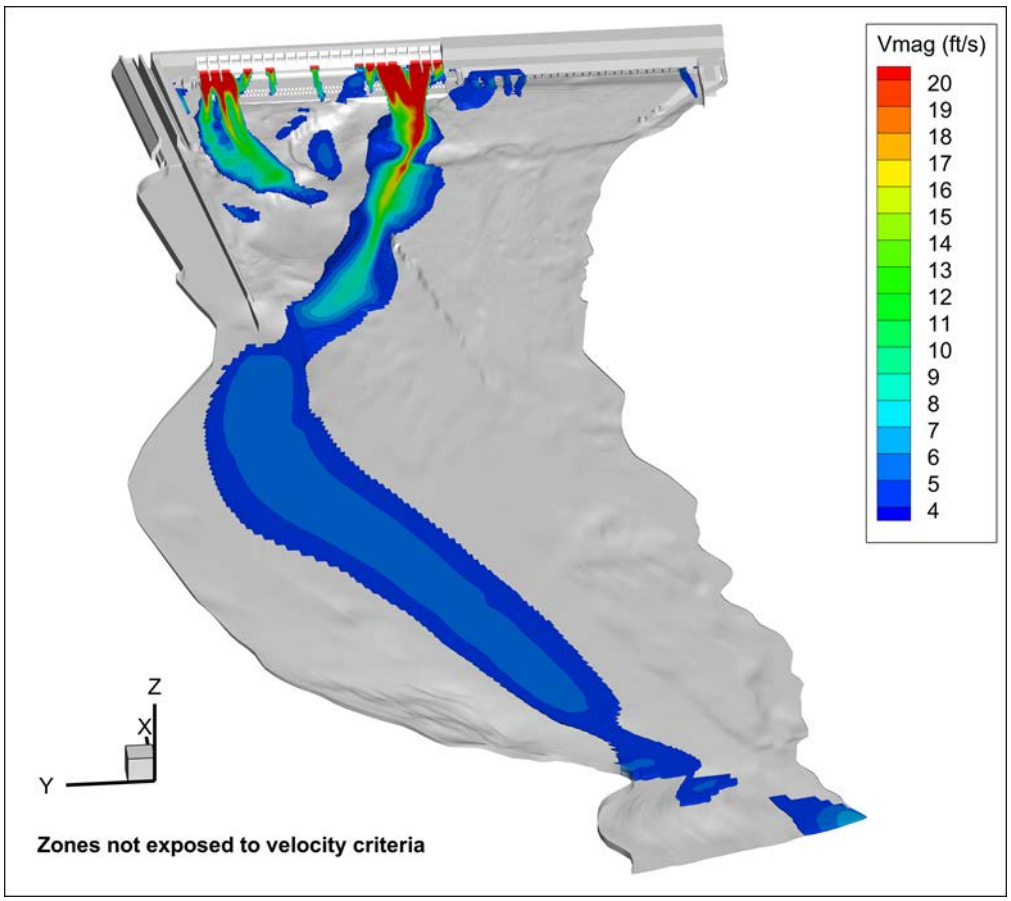

Figure F16. Zones with velocity magnitude greater than 4 ft/s colored by velocity magnitude for Simulation 2

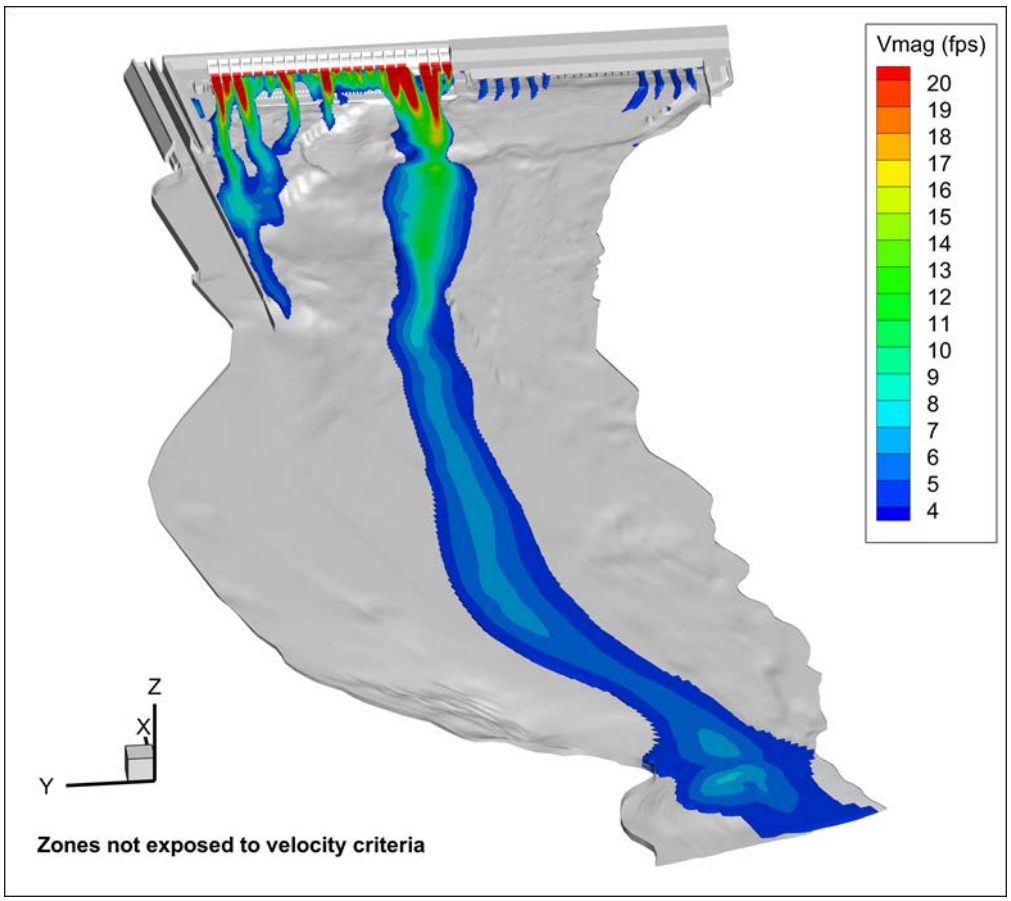

Figure F17. Zones with velocity magnitude greater than 4 ft/s colored by velocity magnitude for Simulation 3

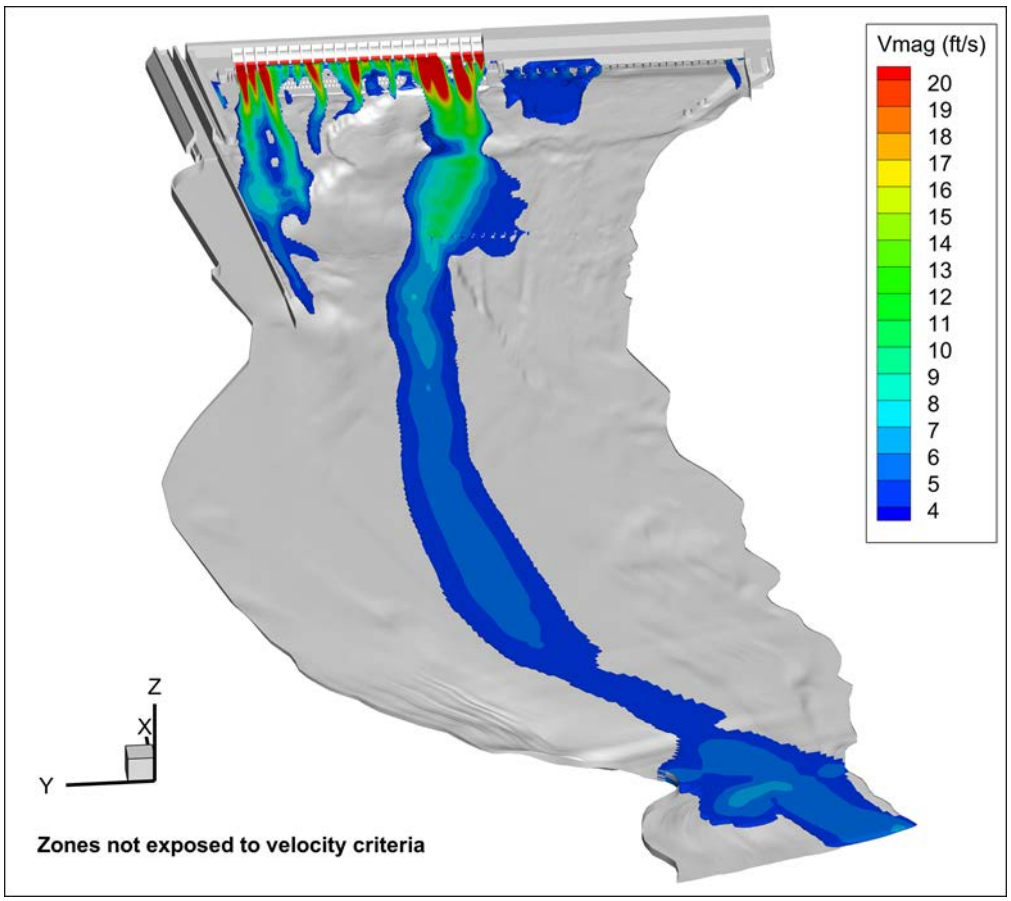

Figure F18. Zones with velocity magnitude greater than 4 ft/s colored by velocity magnitude for Simulation 4

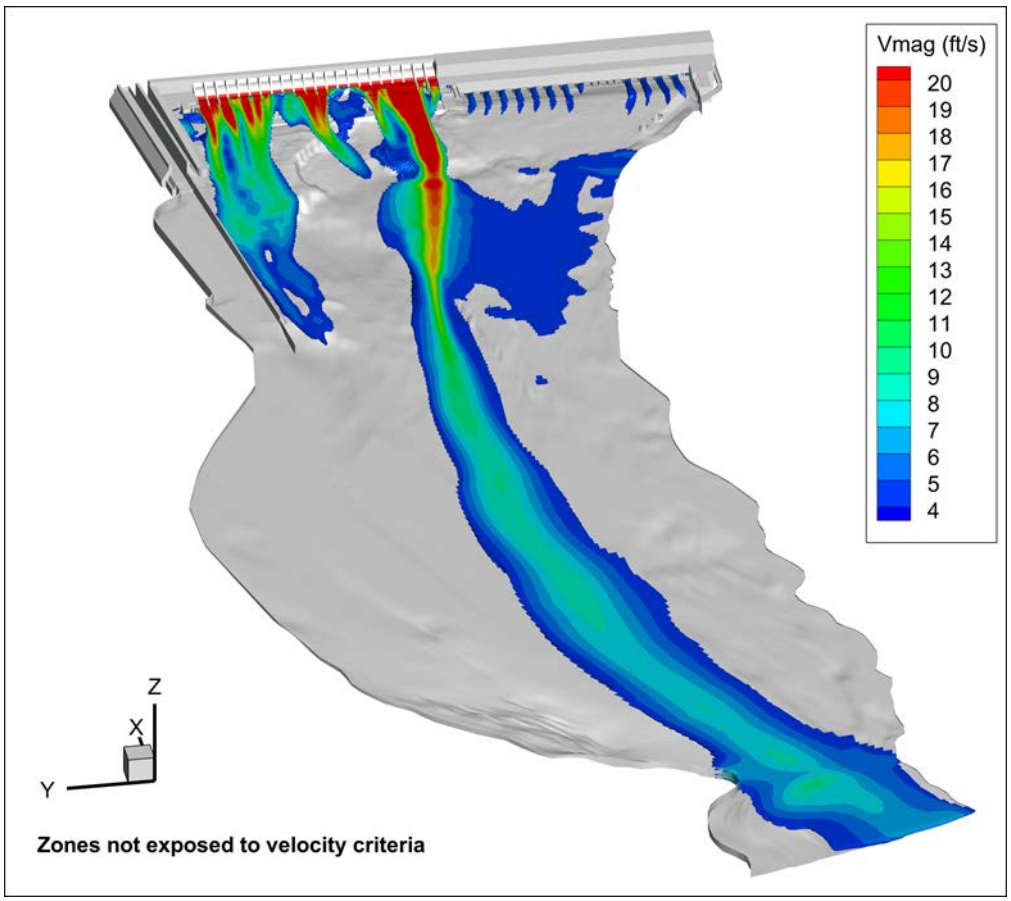

Figure F19. Zones with velocity magnitude greater than 4 ft/s colored by velocity magnitude for Simulation 5

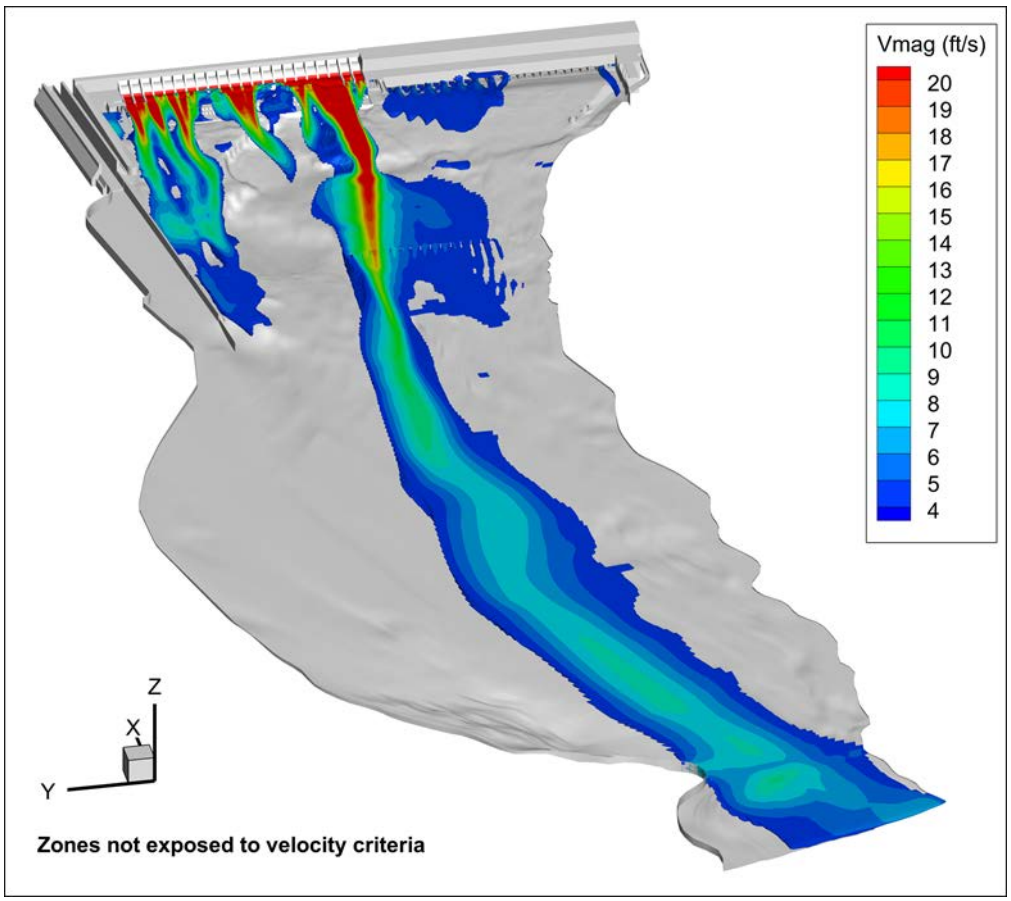

Figure F20. Zones with velocity magnitude greater than 4 ft/s colored by velocity magnitude for Simulation 6

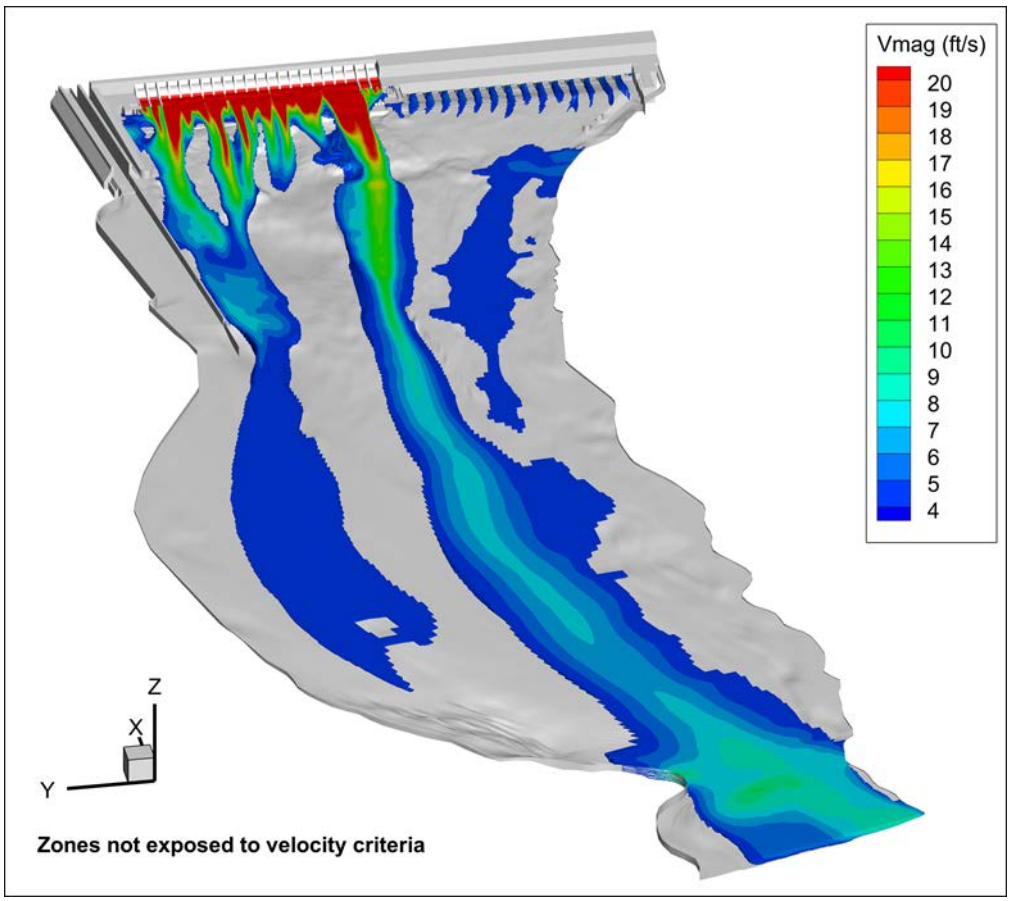

Figure F21. Zones with velocity magnitude greater than 4 ft/s colored by velocity magnitude for Simulation 7

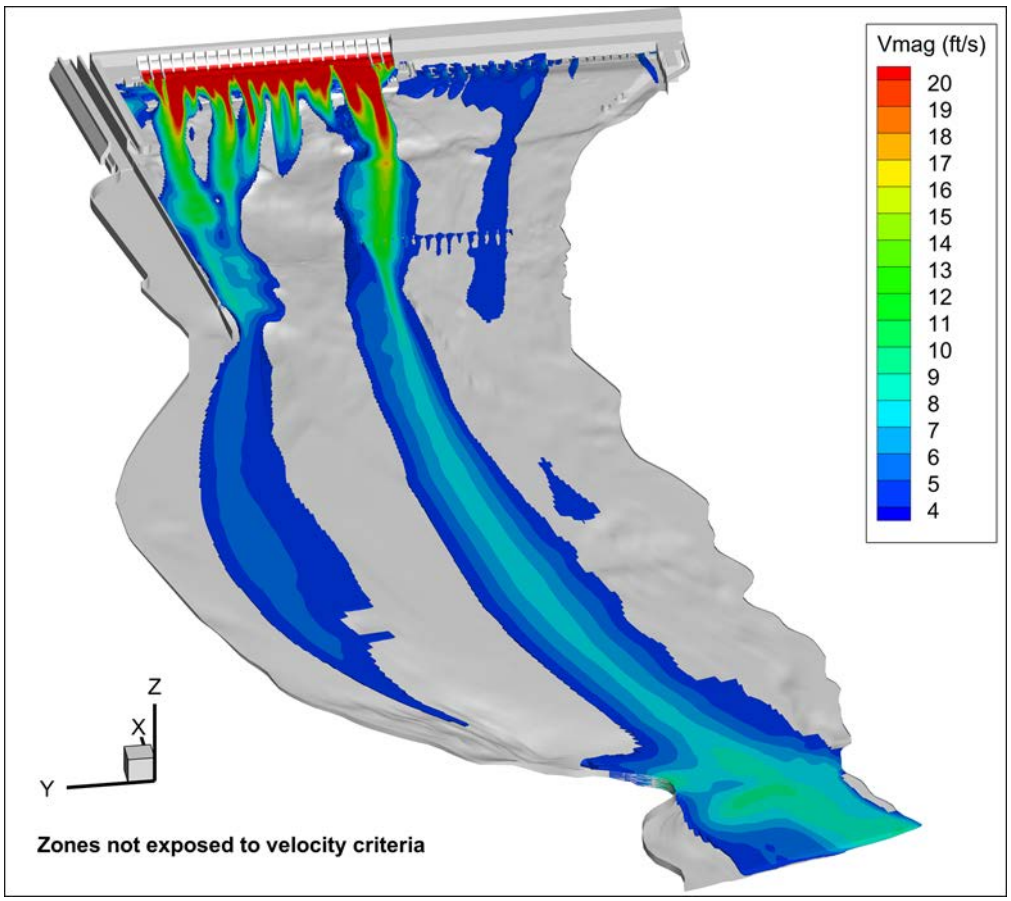

Figure F22. Zones with velocity magnitude greater than 4 ft/s colored by velocity magnitude for Simulation 8

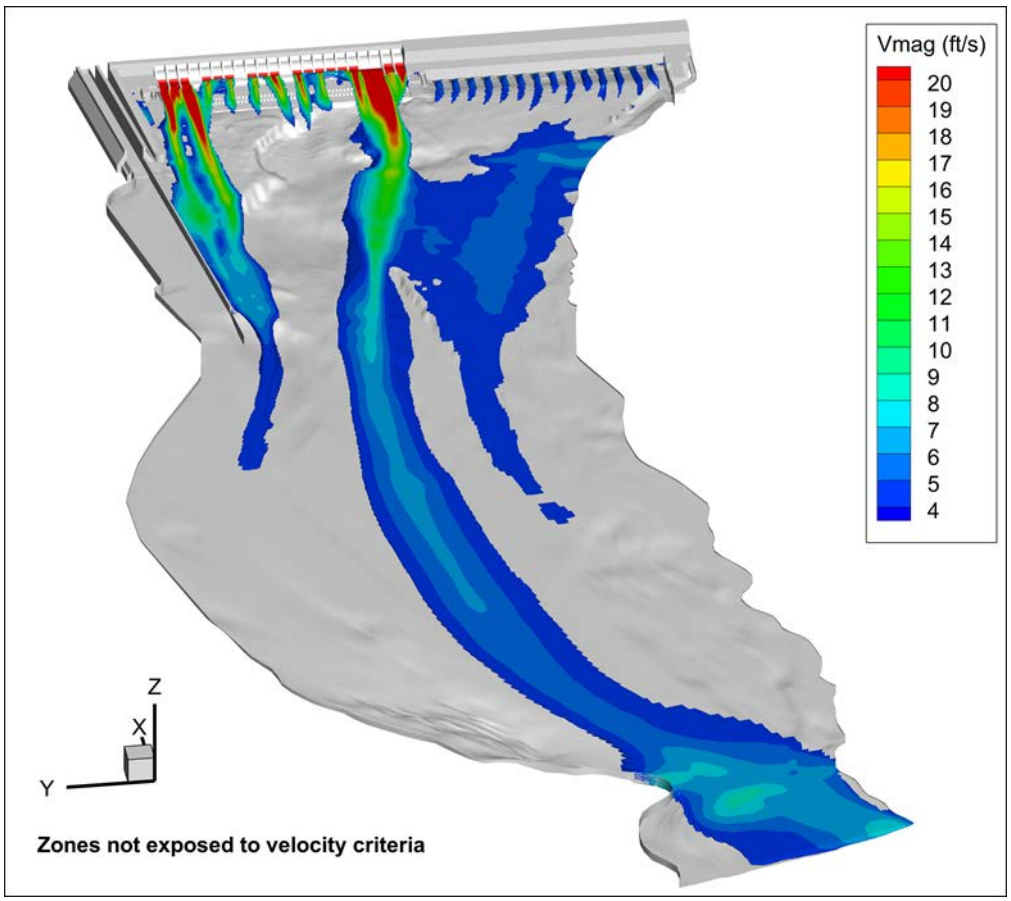

Figure F23. Zones with velocity magnitude greater than 4 ft/s colored by velocity magnitude for Simulation 11

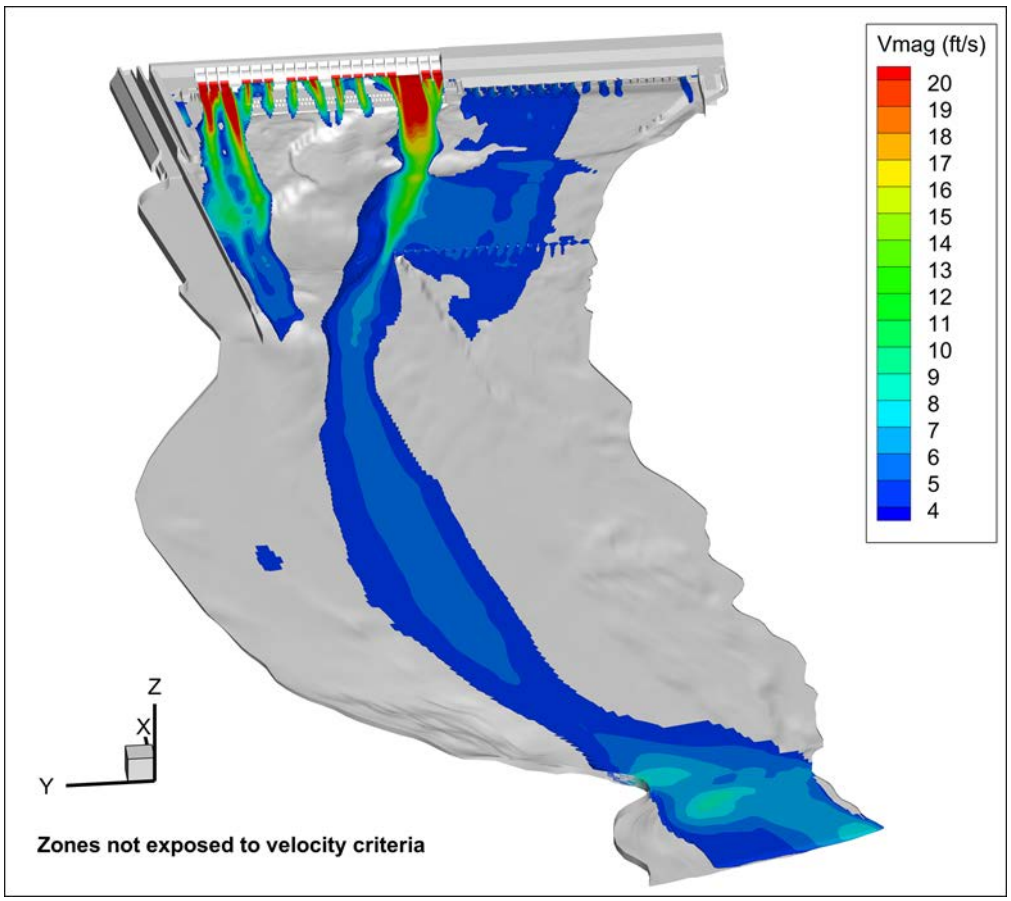

Figure F24. Zones with velocity magnitude greater than 4 ft/s colored by velocity magnitude for Simulation 12

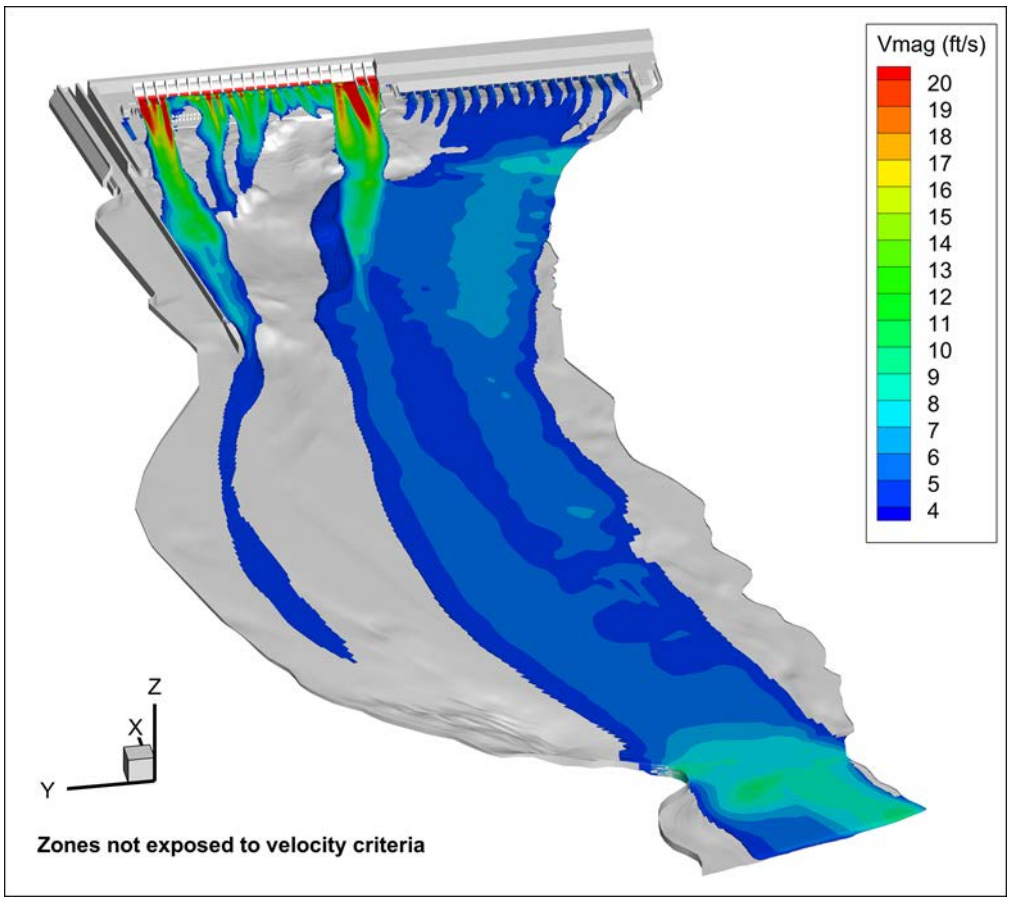

Figure F25. Zones with velocity magnitude greater than 4 ft/s colored by velocity magnitude for Simulation 13

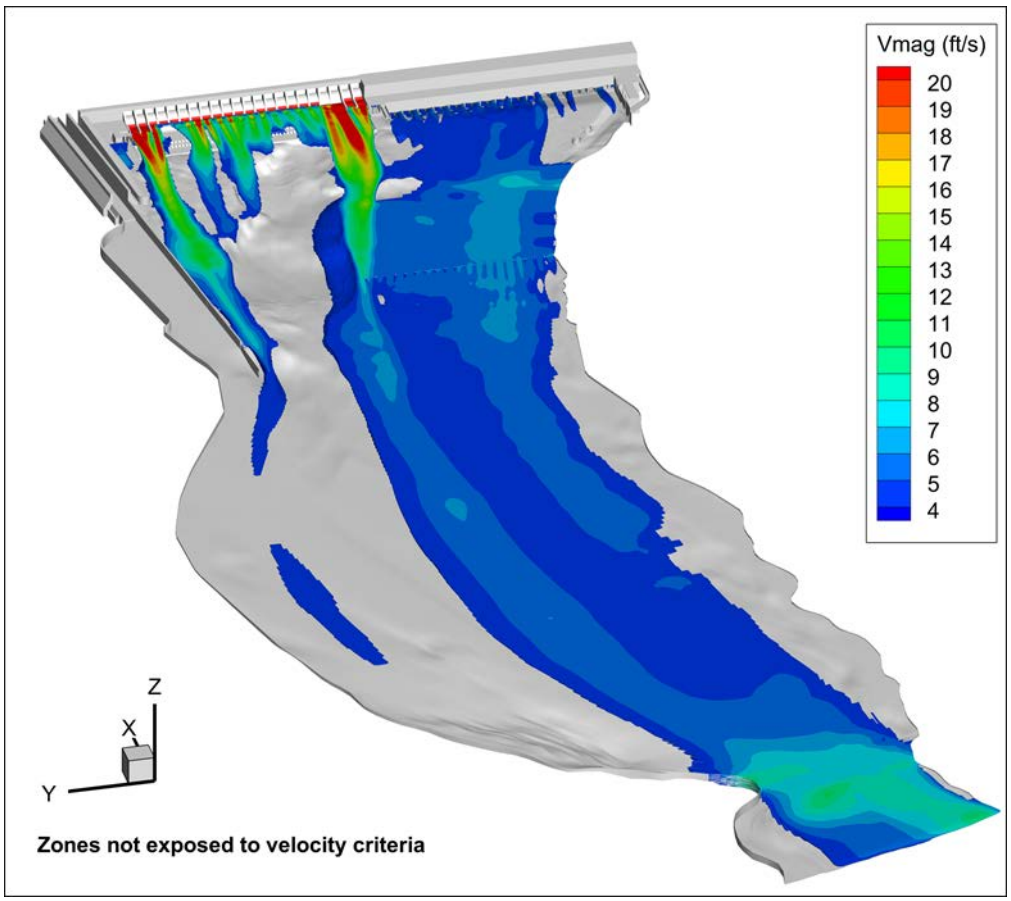

Figure F26. Zones with velocity magnitude greater than 4 ft/s colored by velocity magnitude for Simulation 14.

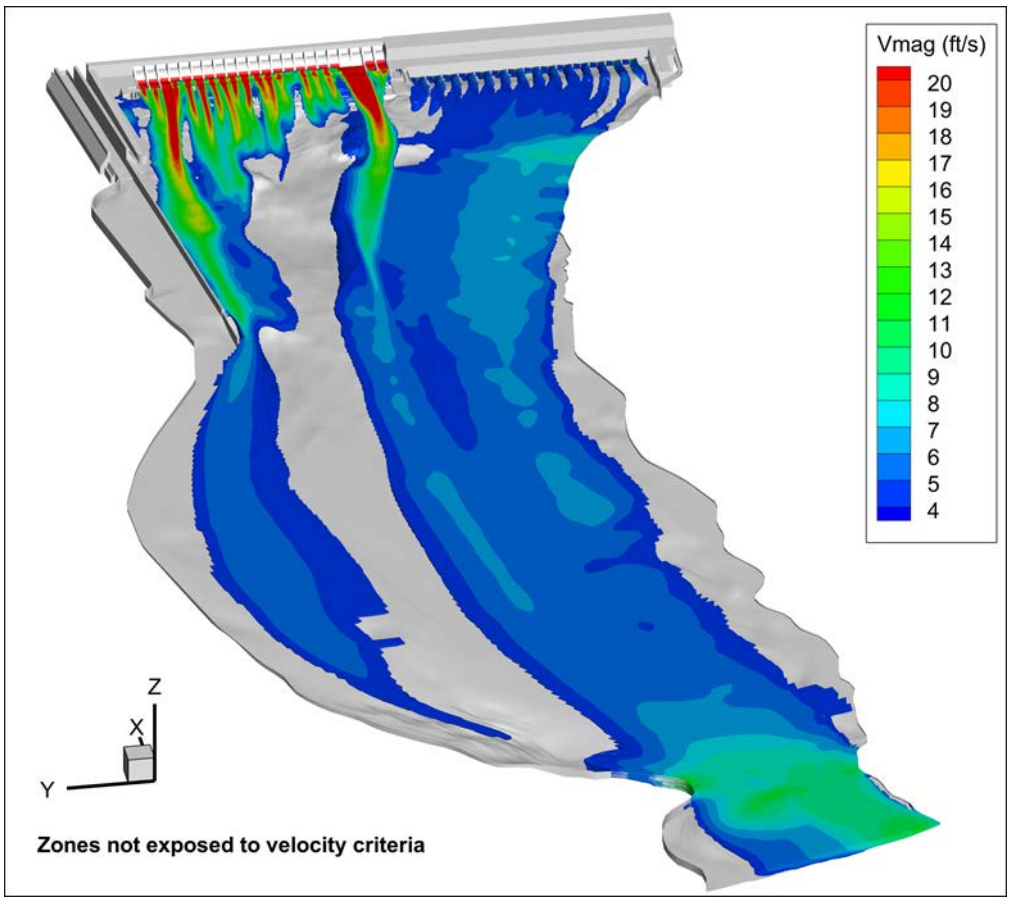

Figure F27. Zones with velocity magnitude greater than 4 ft/s colored by velocity magnitude for Simulation 15

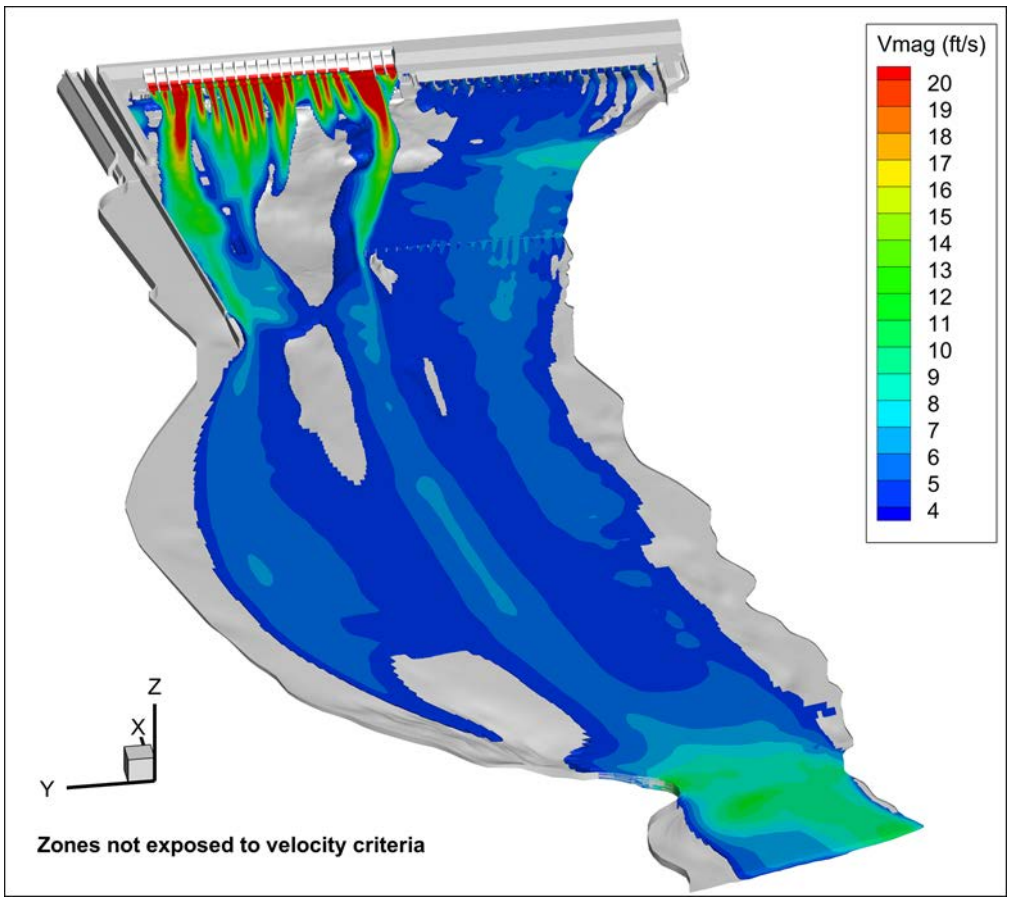

Figure F28. Zones with velocity magnitude greater than 4 ft/s colored by velocity magnitude for Simulation 16

APPENDIX G. RIGID-LID MODEL TWO PHASE FLOW PLOTS

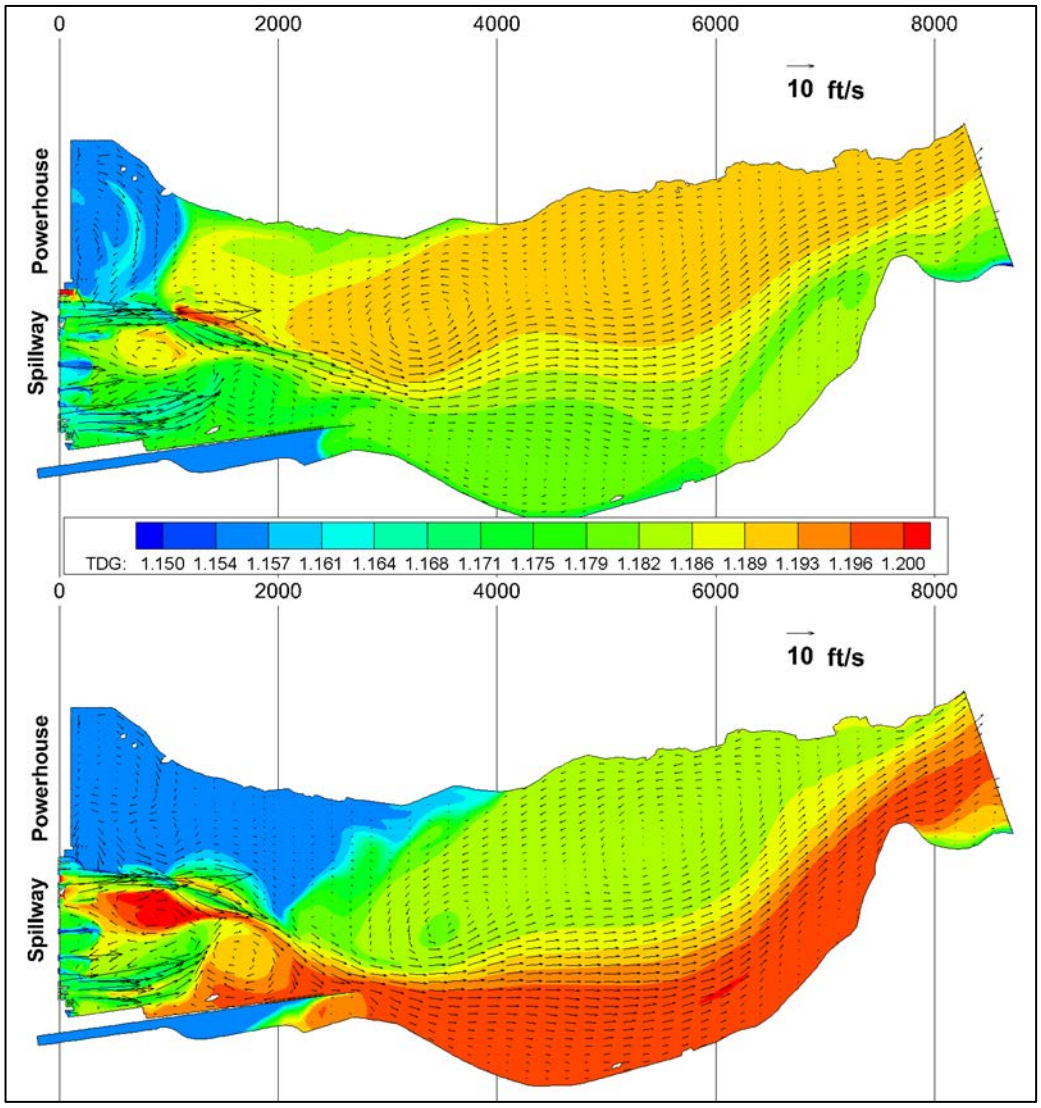

Figure G1. Contours of TDG and velocity vectors at 2m beneath the free surface. Top: Simulation 1. Bottom: Simulation 2

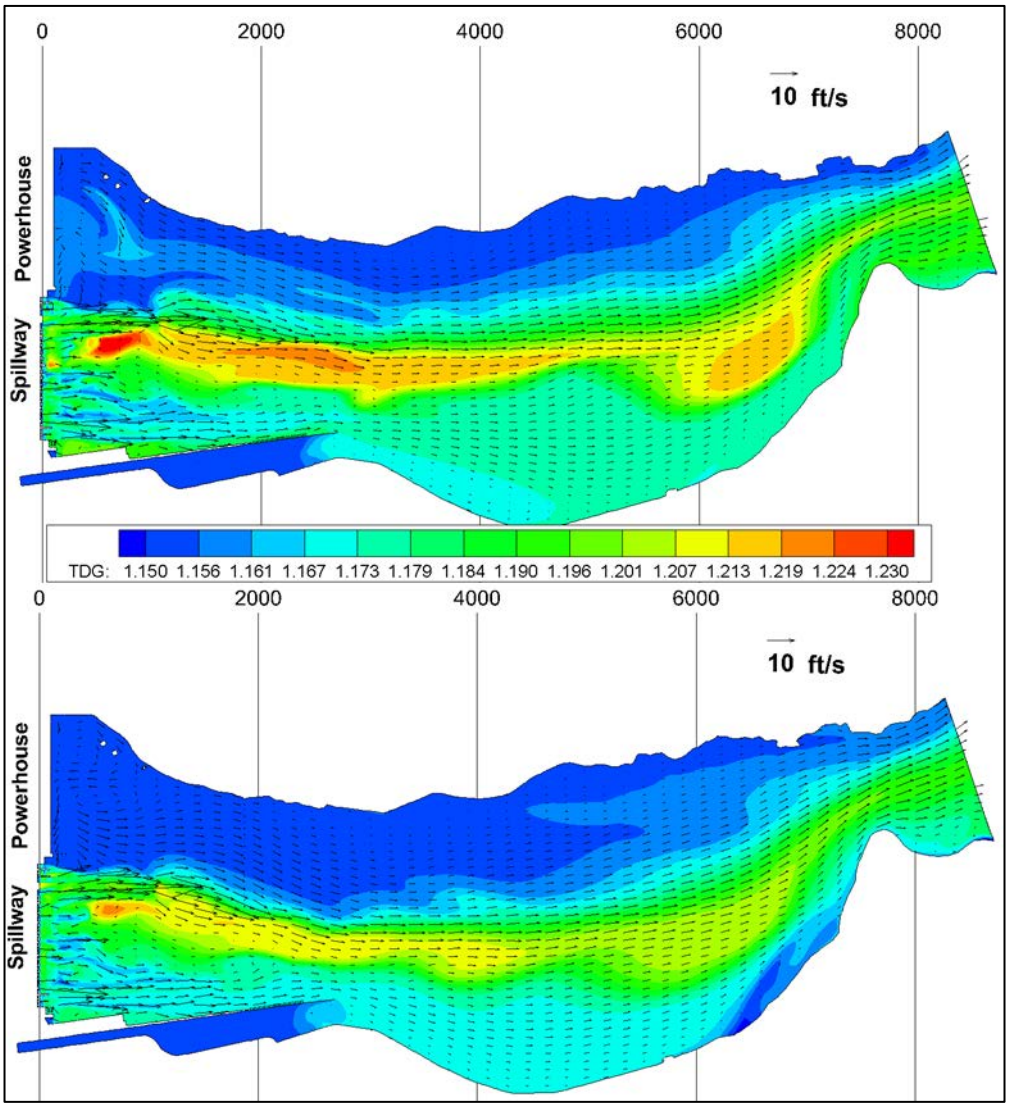

Figure G2. Contours of TDG and velocity vectors at 2m beneath the free surface. Top: Simulation 3. Bottom: Simulation 4

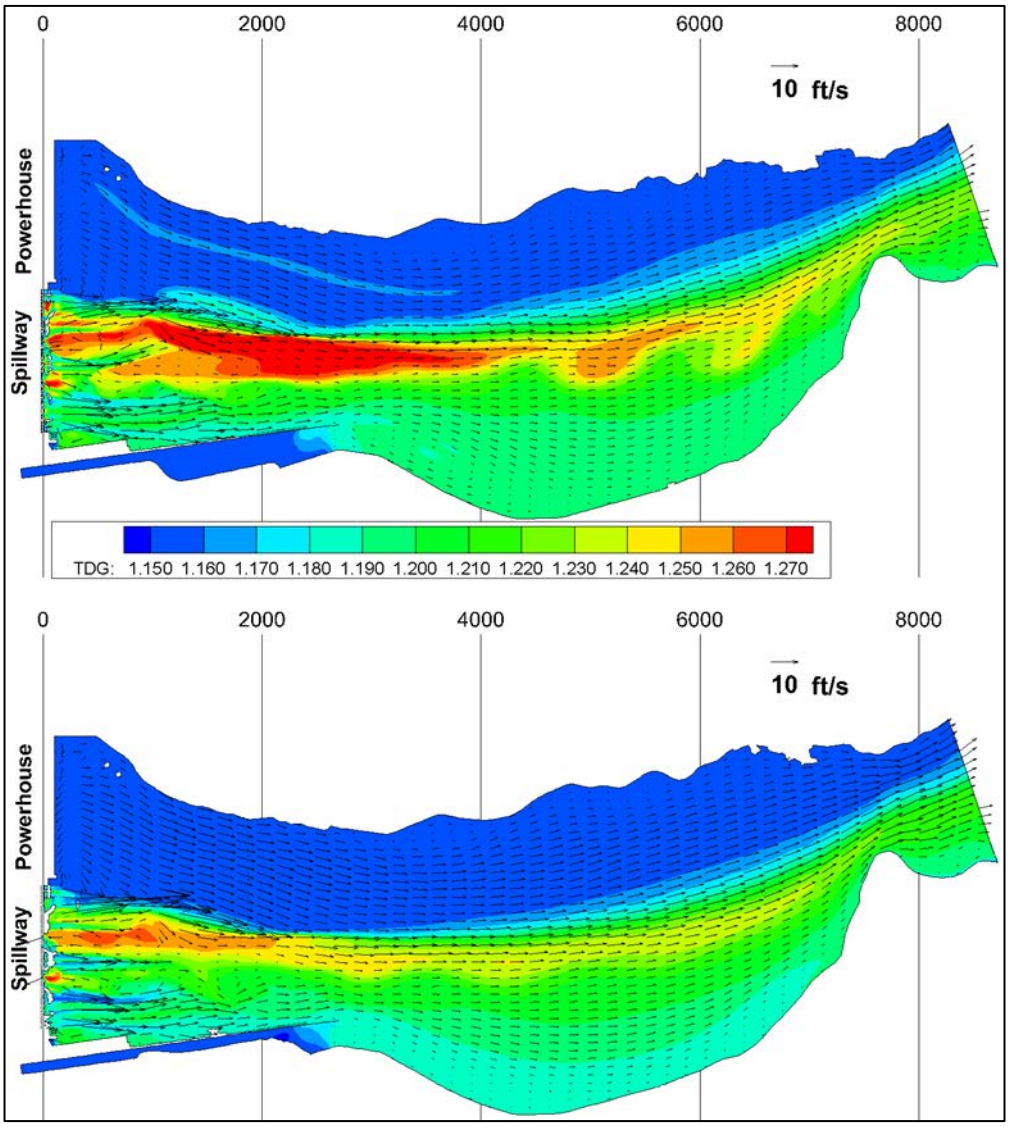

Figure G3. Contours of TDG and velocity vectors at 2m beneath the free surface. Top: Simulation 5. Bottom: Simulation 6

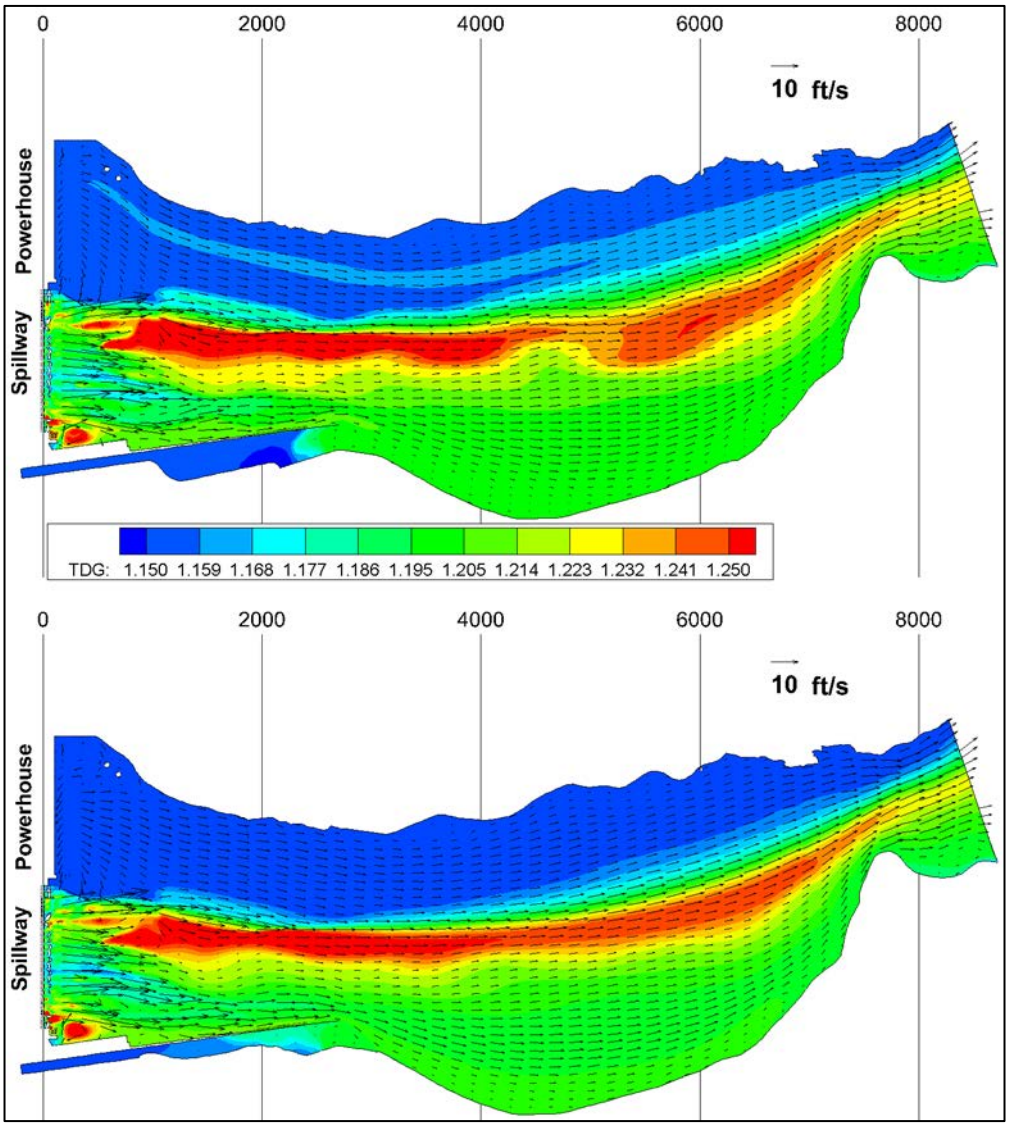

Figure G4. Contours of TDG and velocity vectors at 2m beneath the free surface. Top: Simulation 7. Bottom: Simulation 8

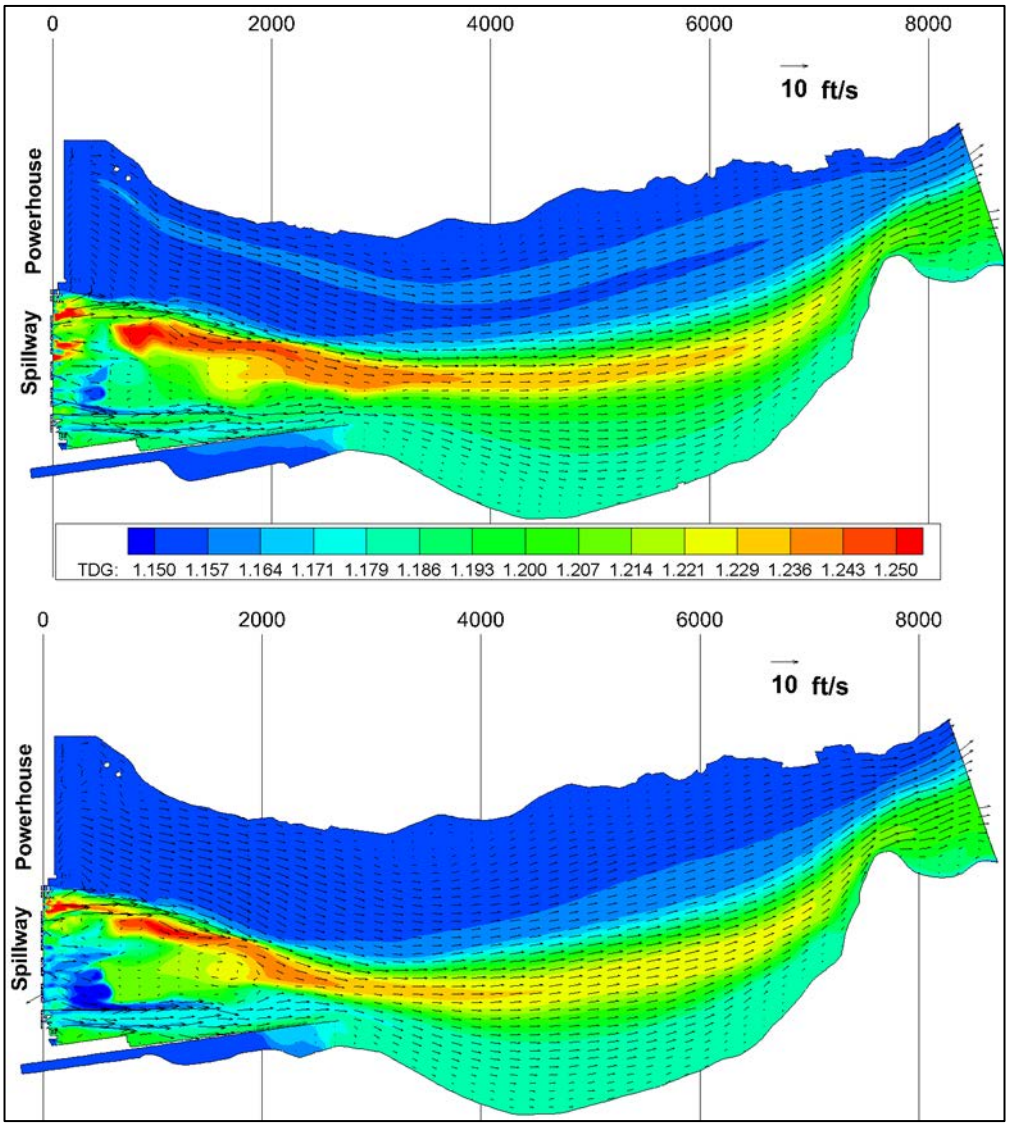

Figure G5. Contours of TDG and velocity vectors at 2m beneath the free surface. Top: Simulation 11. Bottom: Simulation 12

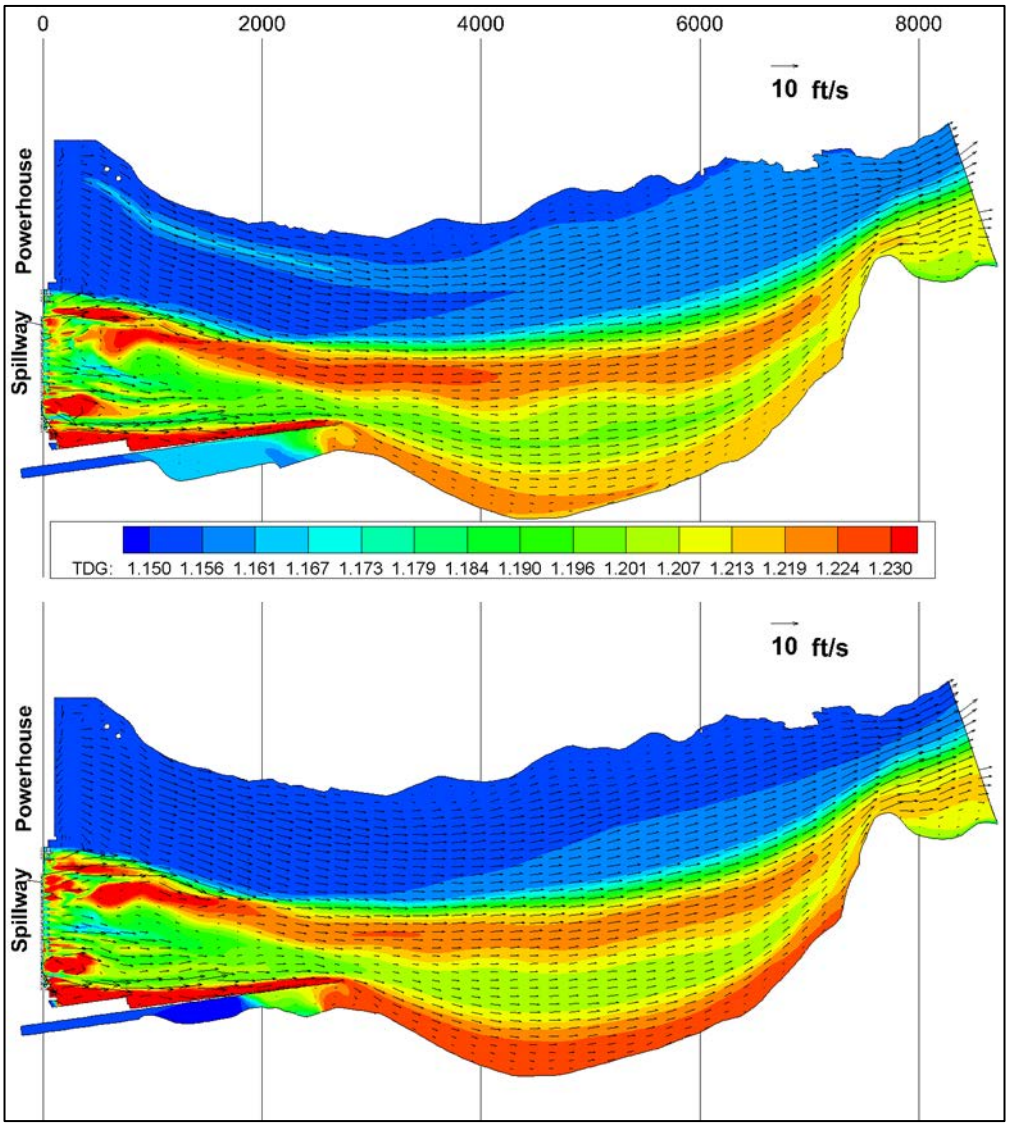

Figure G6. Contours of TDG and velocity vectors at 2m beneath the free surface. Top: Simulation 13. Bottom: Simulation 14

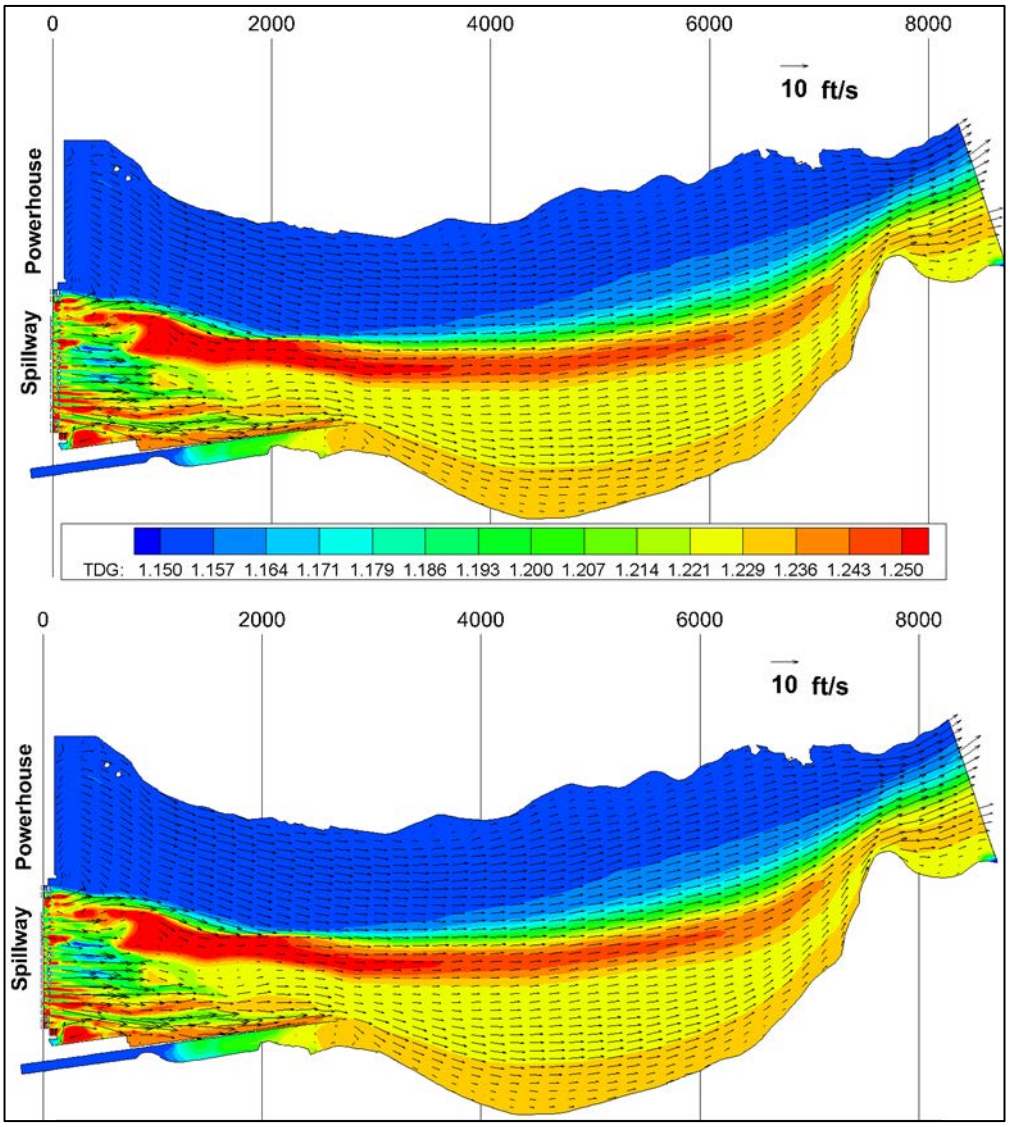

Figure G7. Contours of TDG and velocity vectors at 2m beneath the free surface. Top: Simulation 15. Bottom: Simulation 16

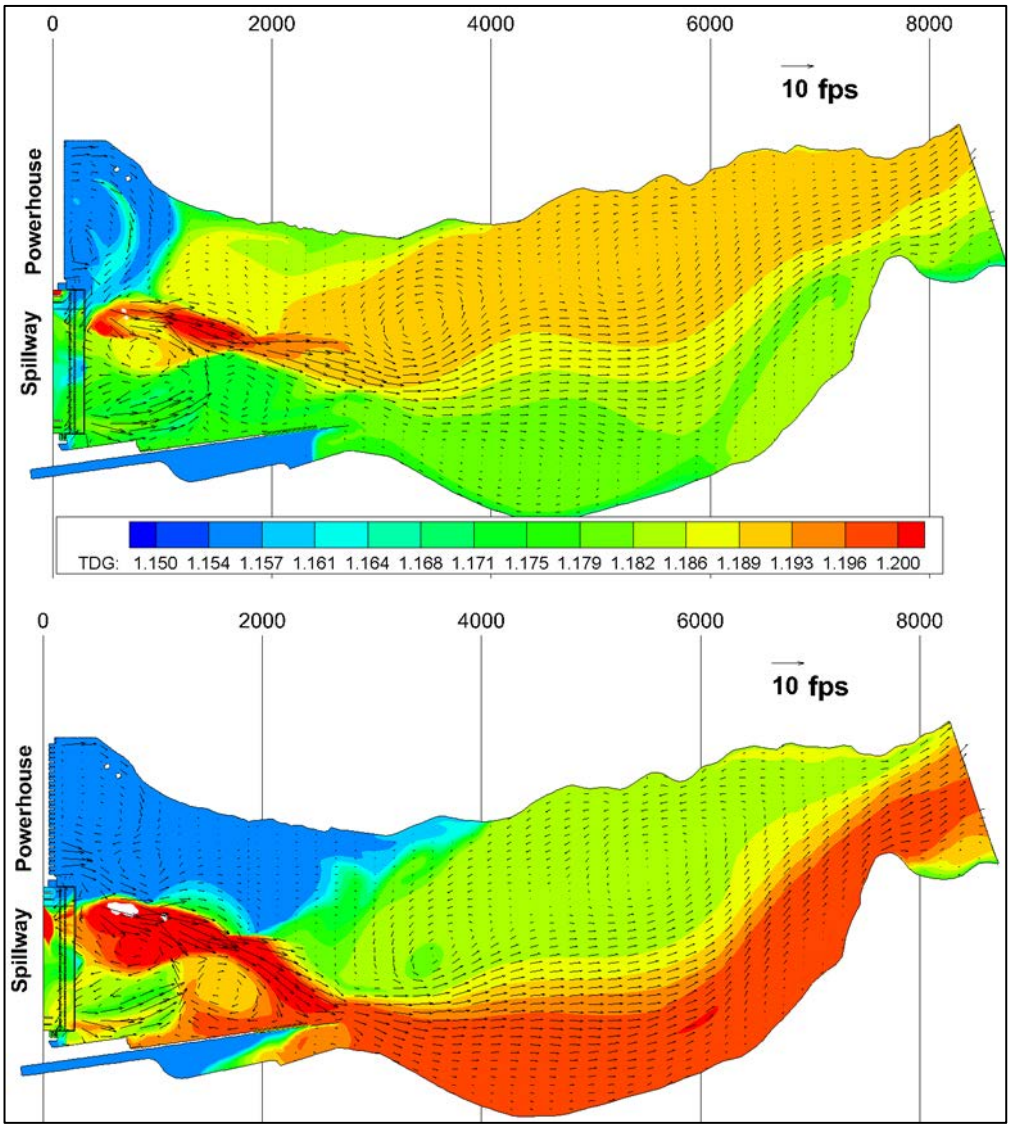

Figure G8. Contours of TDG and velocity vectors at the river bed. Top: Simulation 1. Bottom: Simulation 2

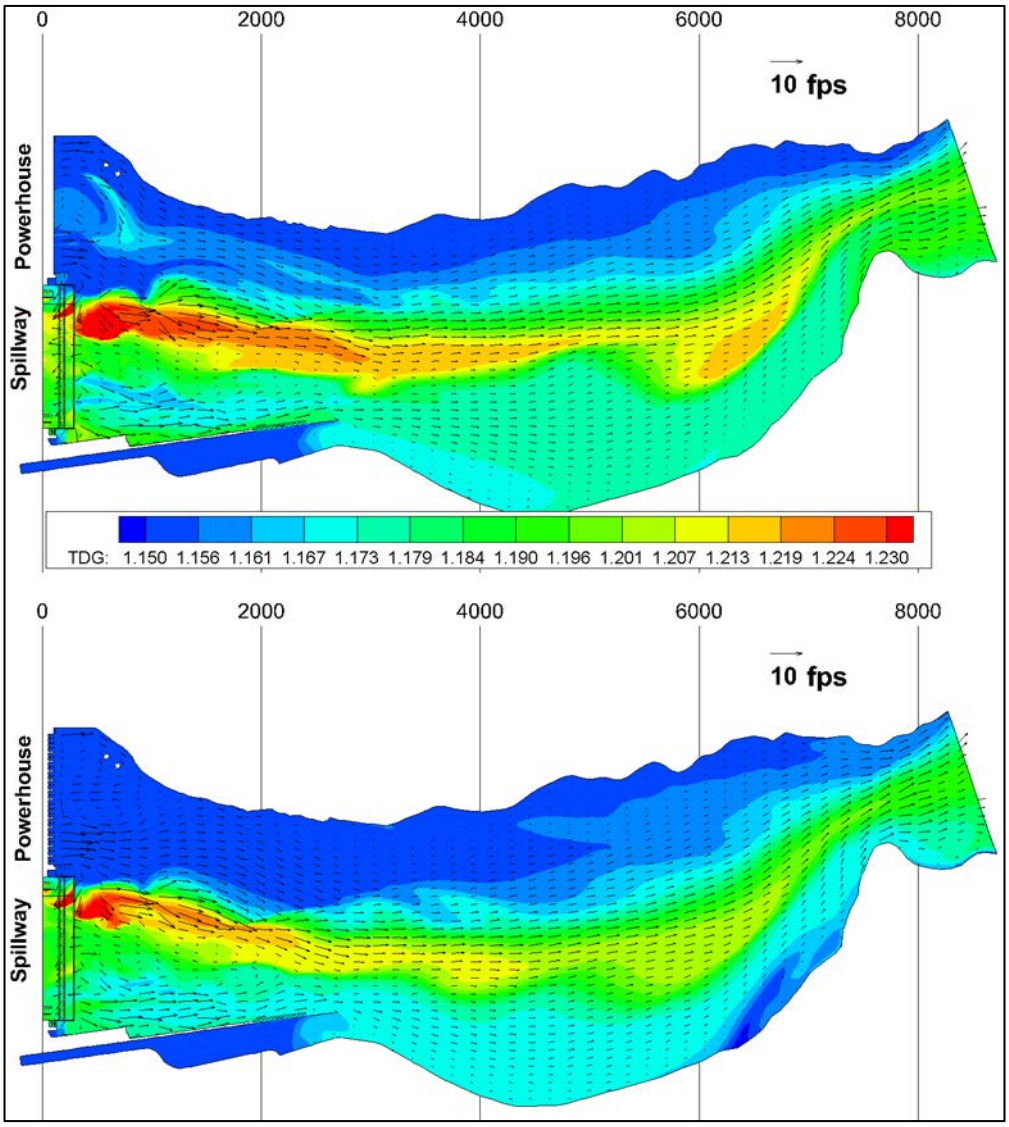

Figure G9. Contours of TDG and velocity vectors at the river bed. Top: Simulation 3. Bottom: Simulation 4

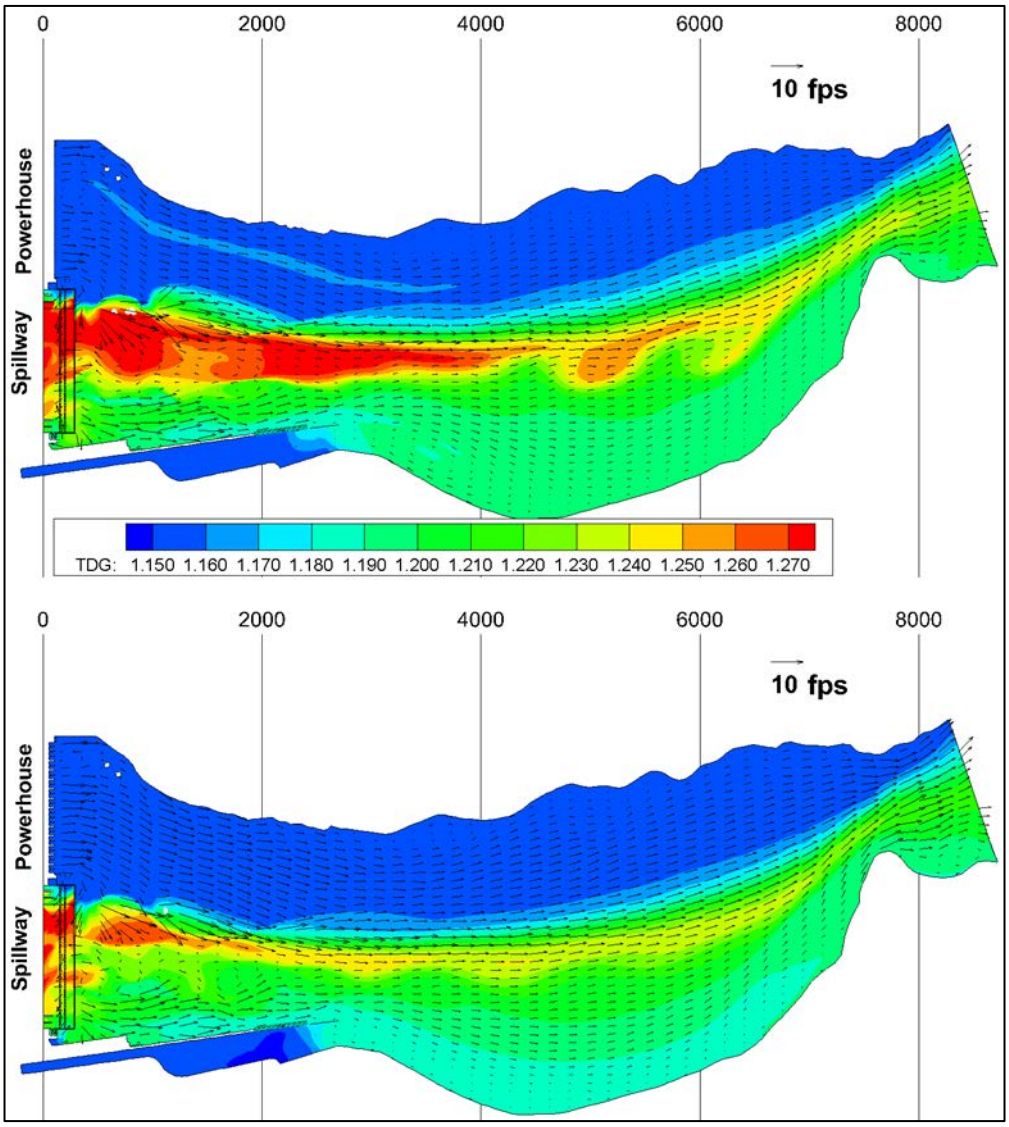

Figure G10. Contours of TDG and velocity vectors at the river bed. Top: Simulation 5. Bottom: Simulation 6

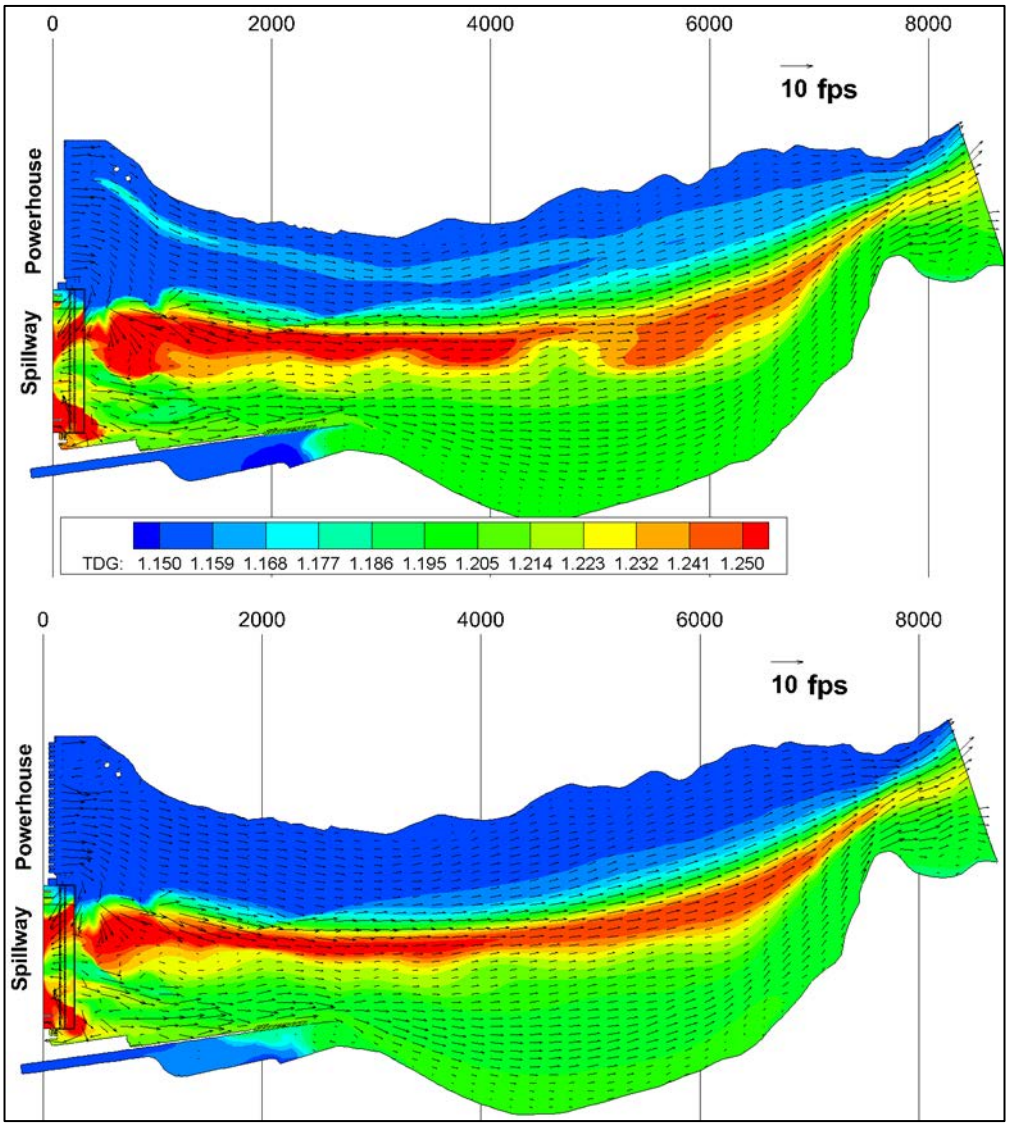

Figure G11. Contours of TDG and velocity vectors at the river bed. Top: Simulation 7. Bottom: Simulation 8

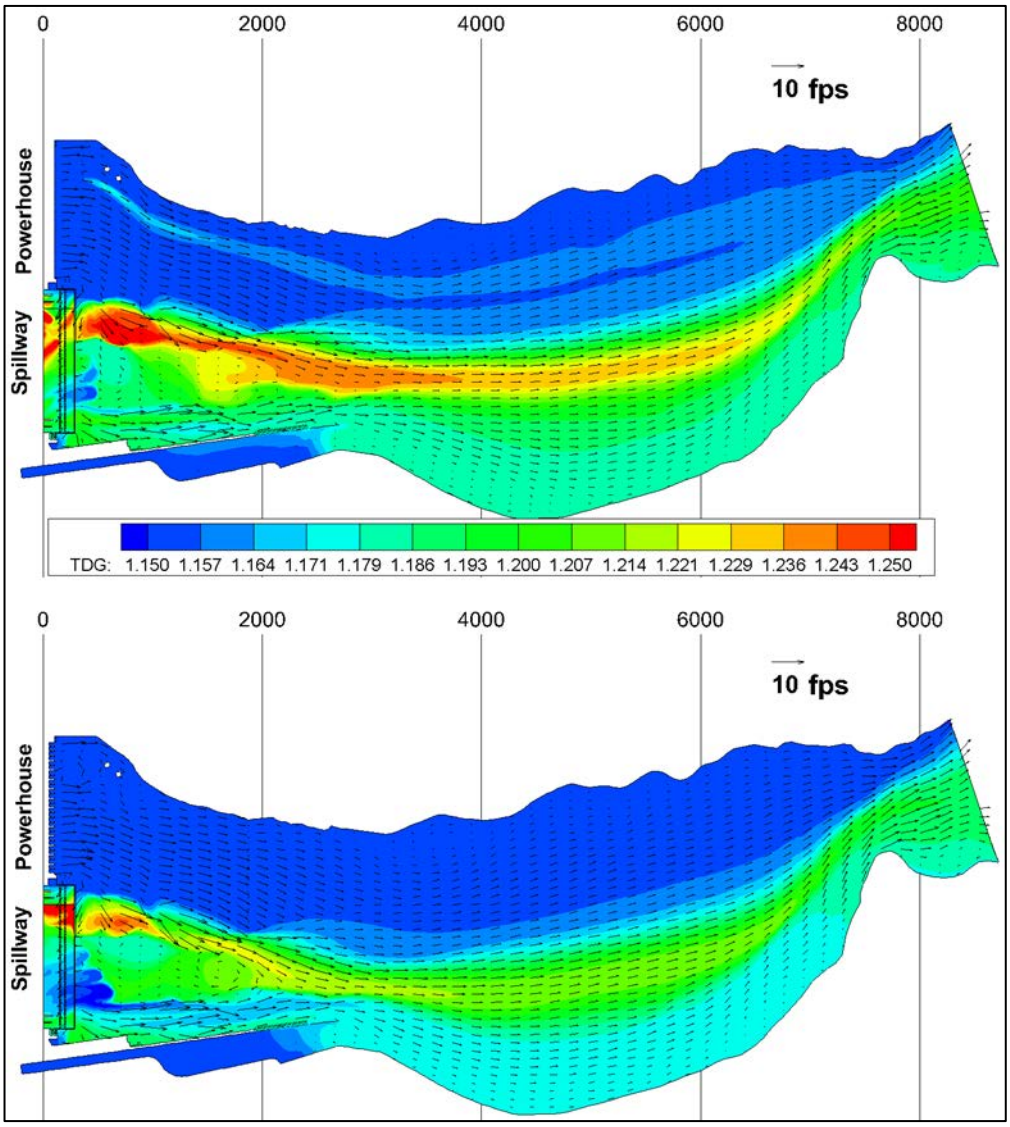

Figure G12. Contours of TDG and velocity vectors at the river bed. Top: Simulation 11. Bottom: Simulation 12

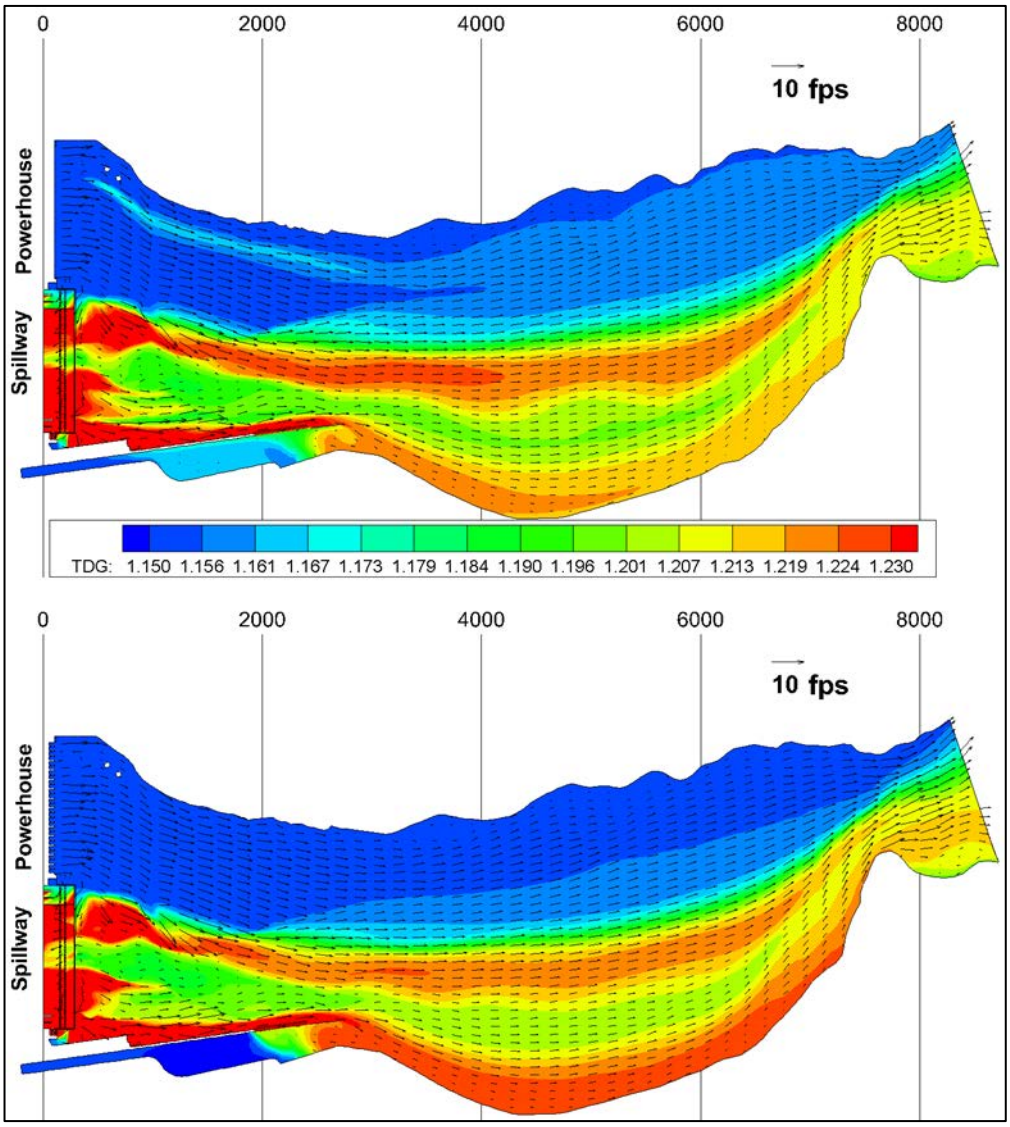

Figure G13. Contours of TDG and velocity vectors at the river bed. Top: Simulation 13. Bottom: Simulation 14

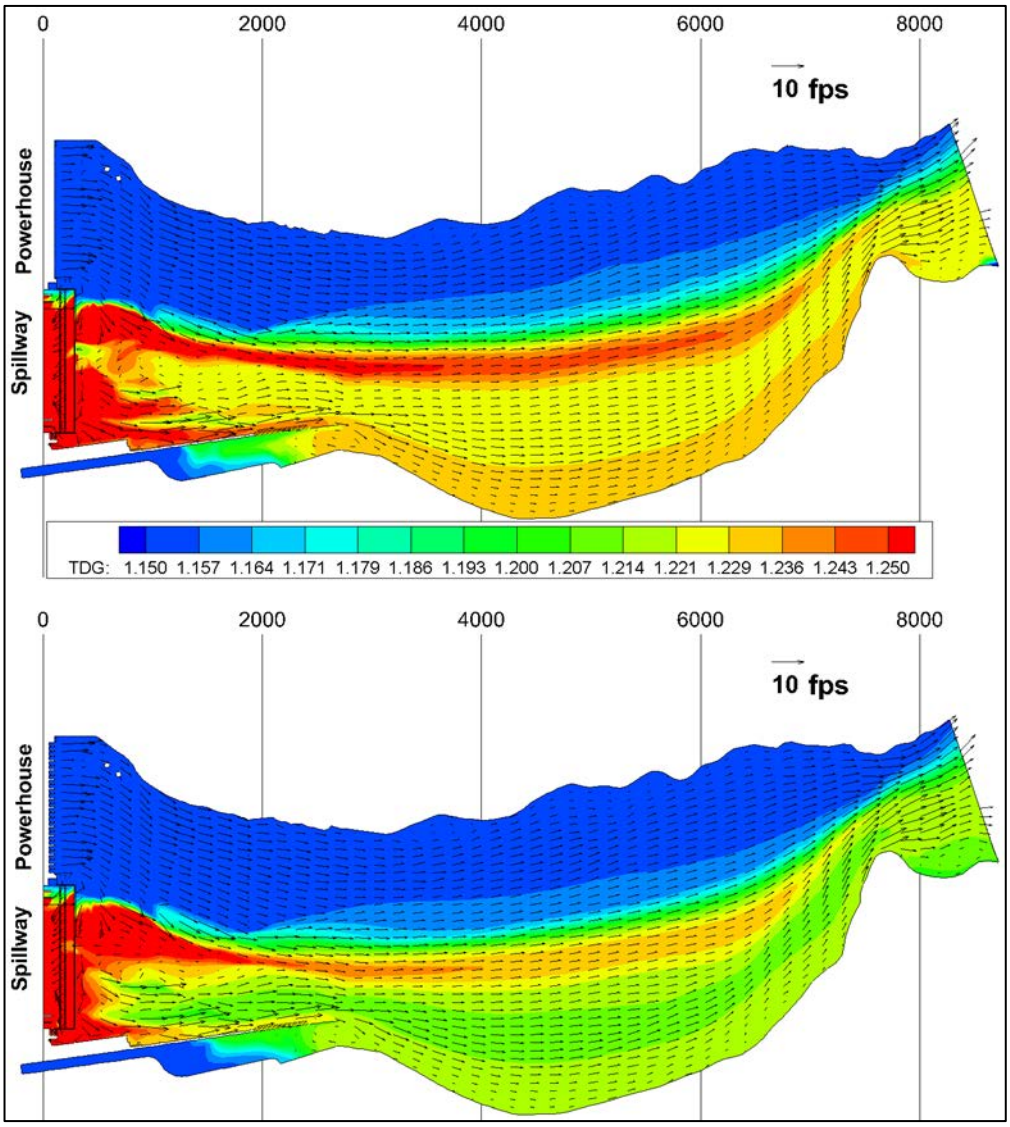

Figure G14. Contours of TDG and velocity vectors at the river bed. Top: Simulation 15. Bottom: Simulation 16

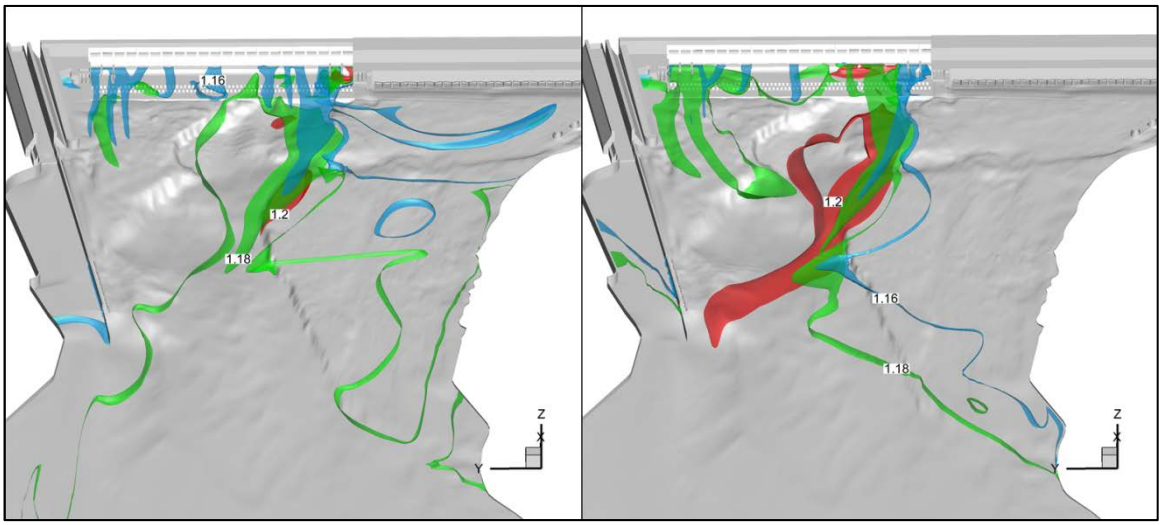

Figure G15. Isosurfaces of TDG. Left: Simulation 1. Right: Simulation 2

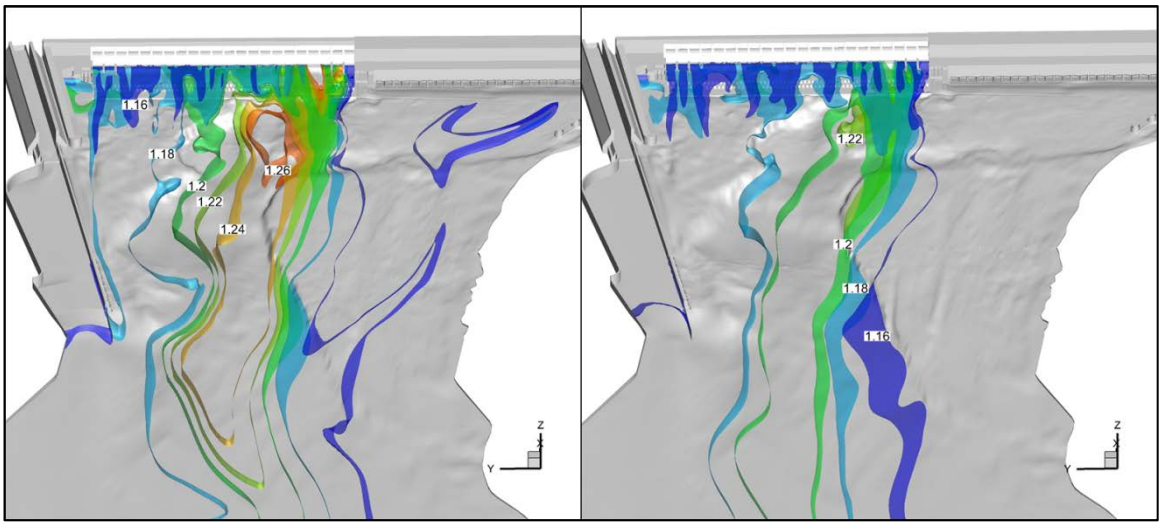

Figure G16. Isosurfaces of TDG. Left: Simulation 3. Right: Simulation 4

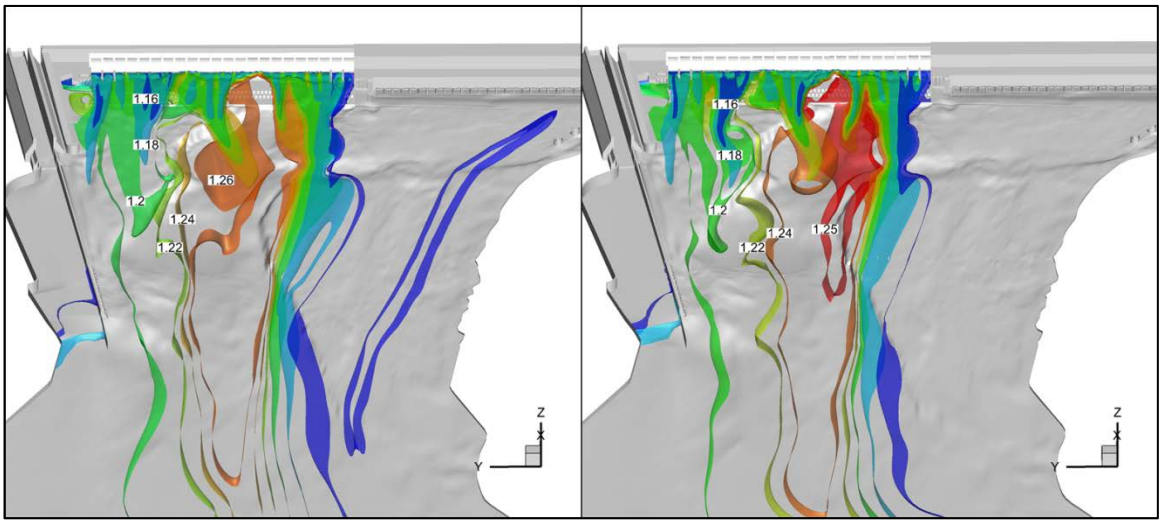

Figure G17. Isosurfaces of TDG. Left: Simulation 5. Right: Simulation 6

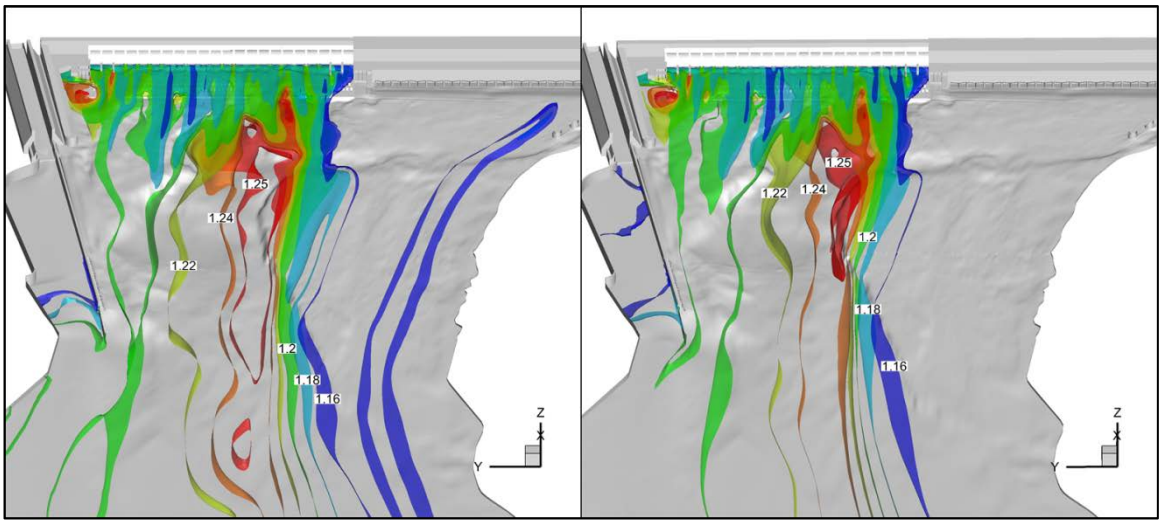

Figure G18. Isosurfaces of TDG. Left: Simulation 7. Right: Simulation 8

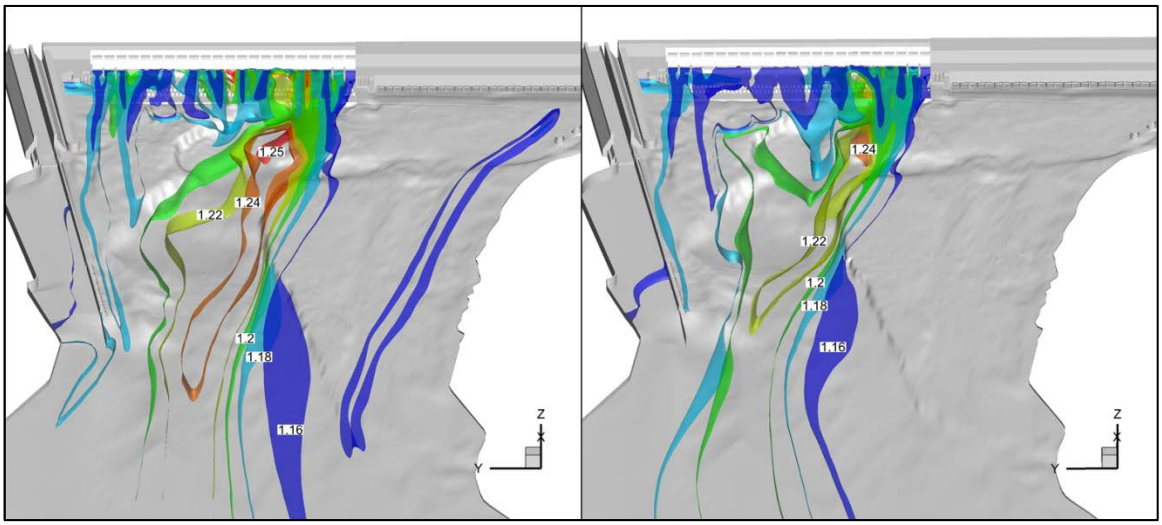

Figure G19. Isosurfaces of TDG. Left: Simulation 11. Right: Simulation 12

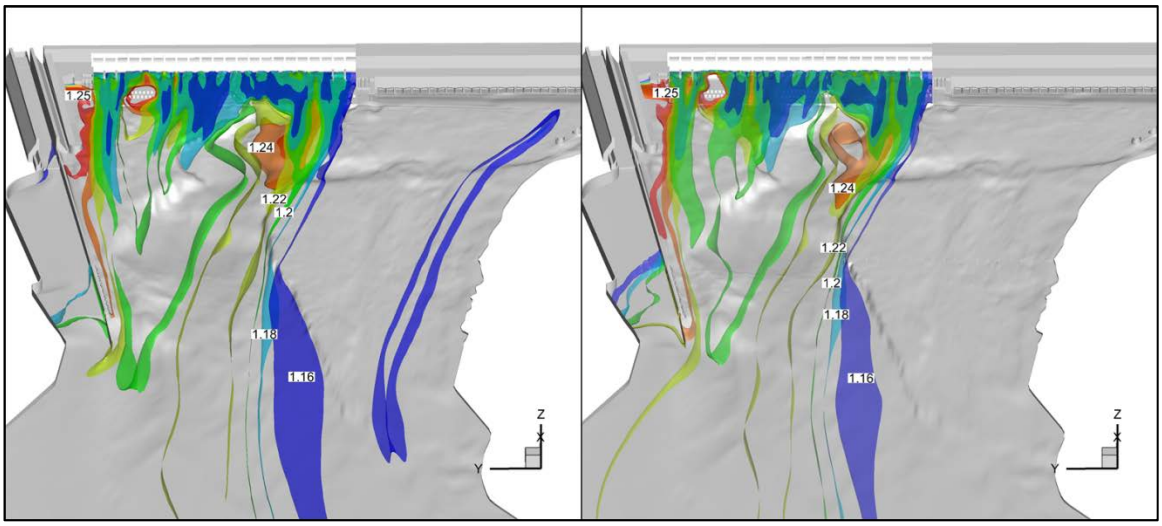

Figure G20. Isosurfaces of TDG. Left: Simulation 13. Right: Simulation 14

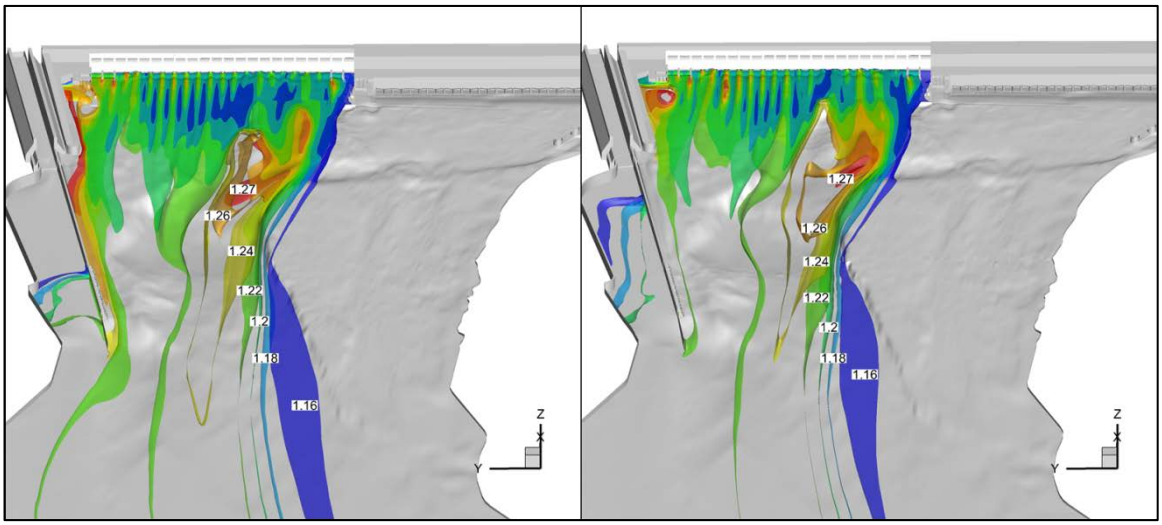

Figure G21. Isosurfaces of TDG. Left: Simulation 15. Right: Simulation 16

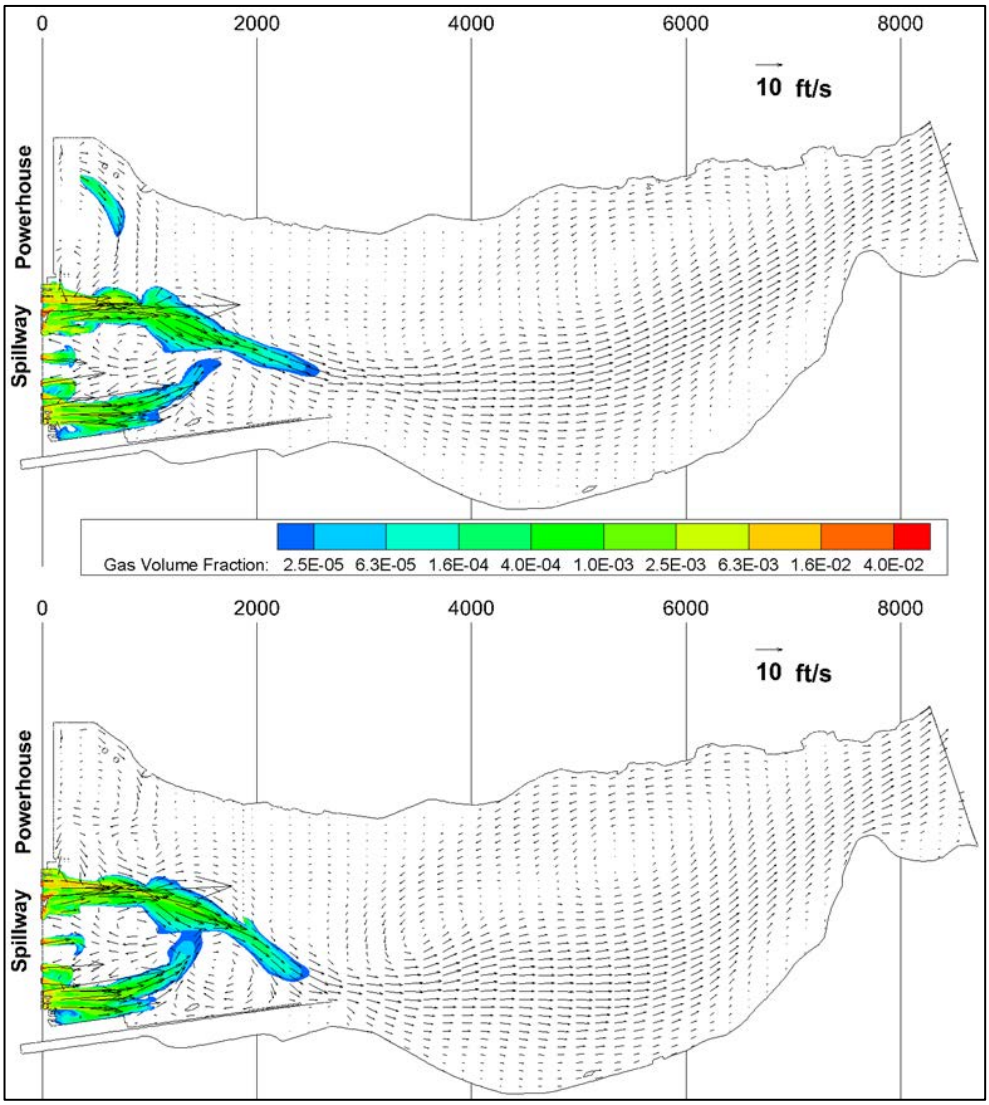

Figure G22. Contours of gas volume fraction and velocity vectors at 2m beneath the free surface. Top: Simulation 1. Bottom: Simulation 2

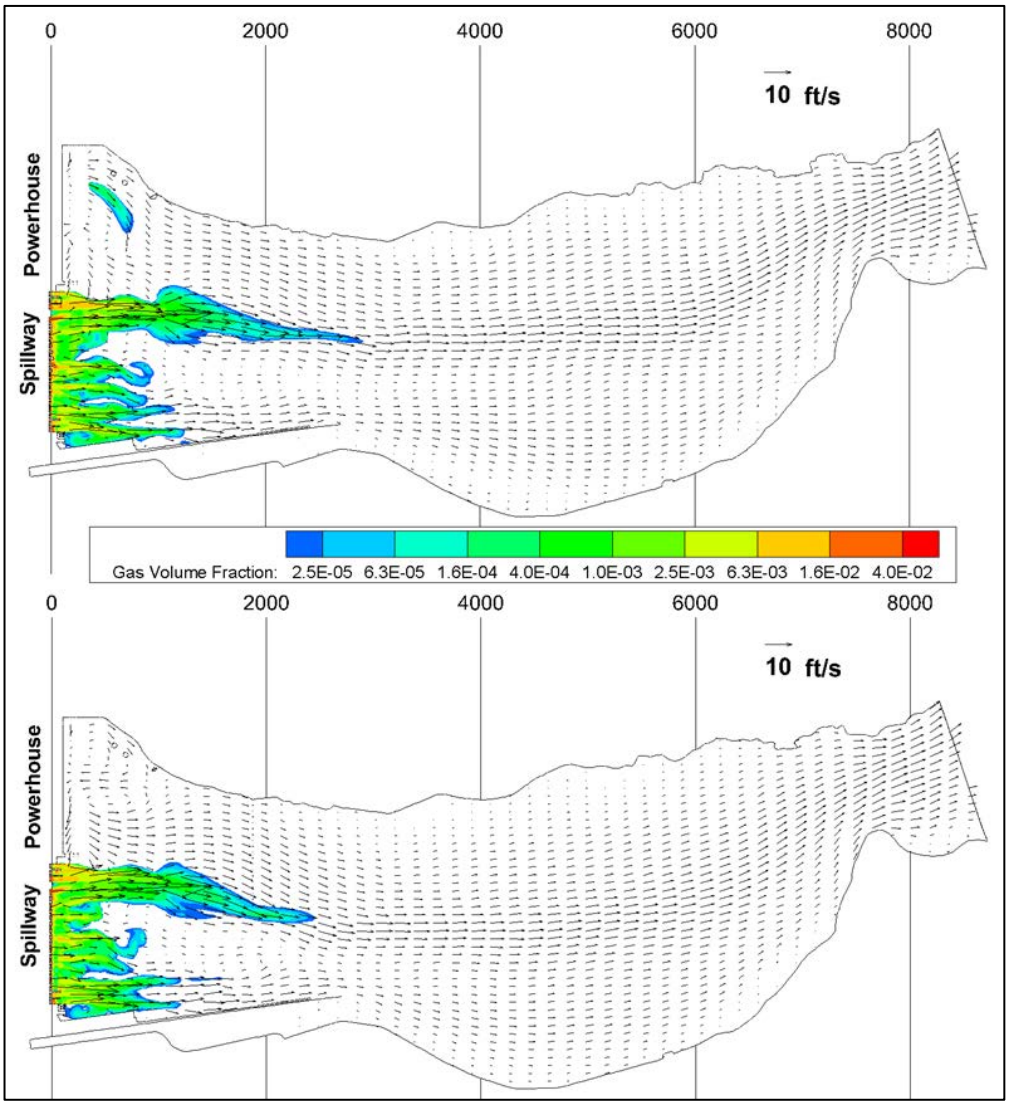

Figure G23. Contours of gas volume fraction and velocity vectors at 2m beneath the free surface. Top: Simulation 3. Bottom: Simulation 4

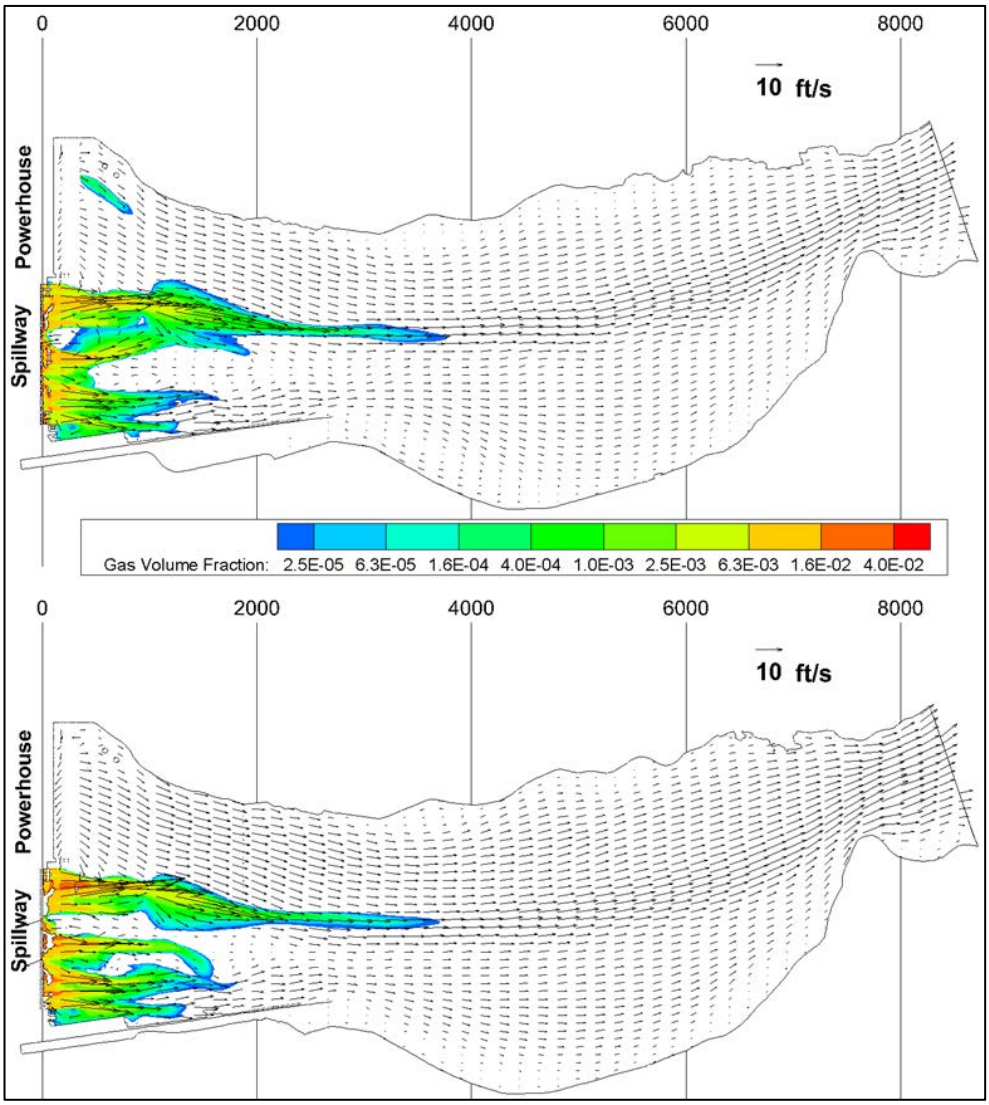

Figure G24. Contours of gas volume fraction and velocity vectors at 2m beneath the free surface. Top: Simulation 5. Bottom: Simulation 6

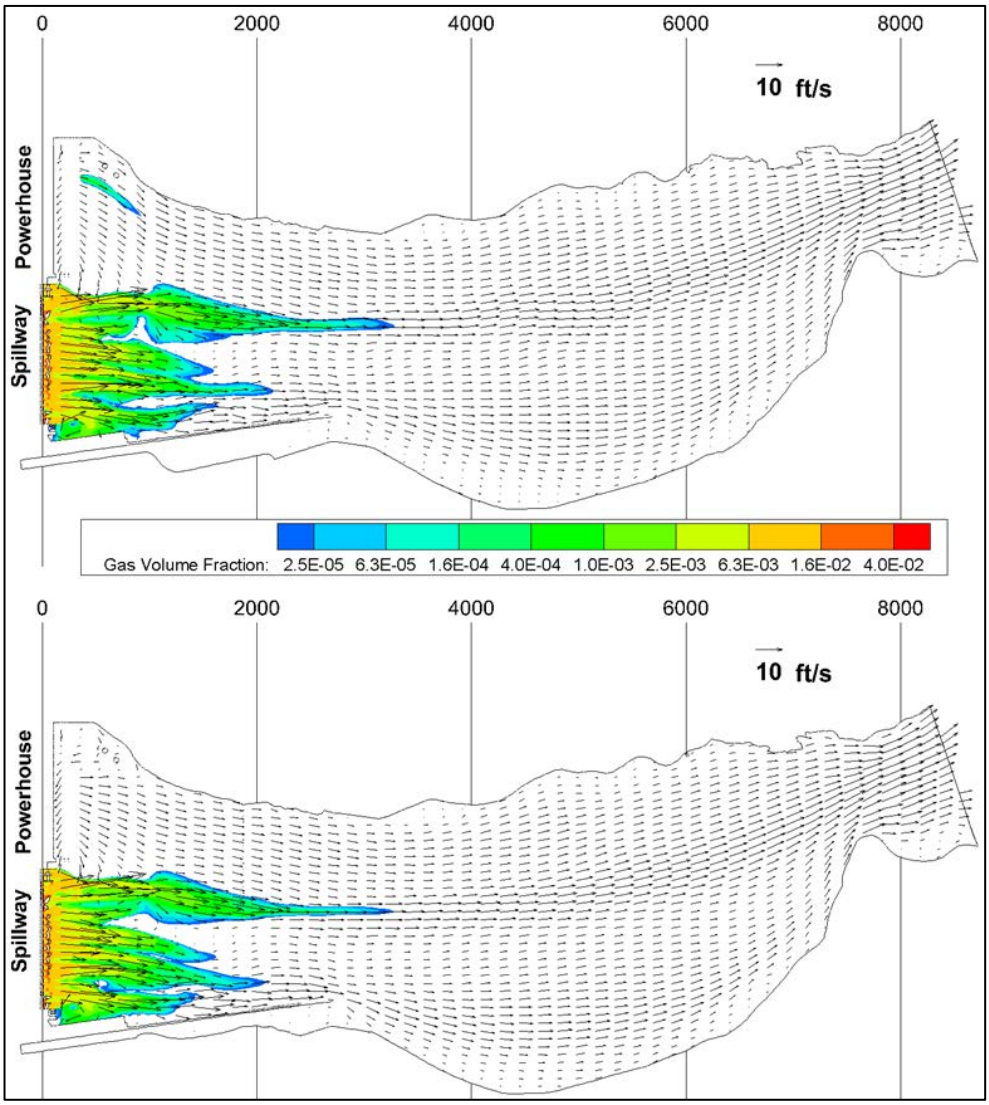

Figure G25. Contours of gas volume fraction and velocity vectors at 2m beneath the free surface. Top: Simulation 7. Bottom: Simulation 8

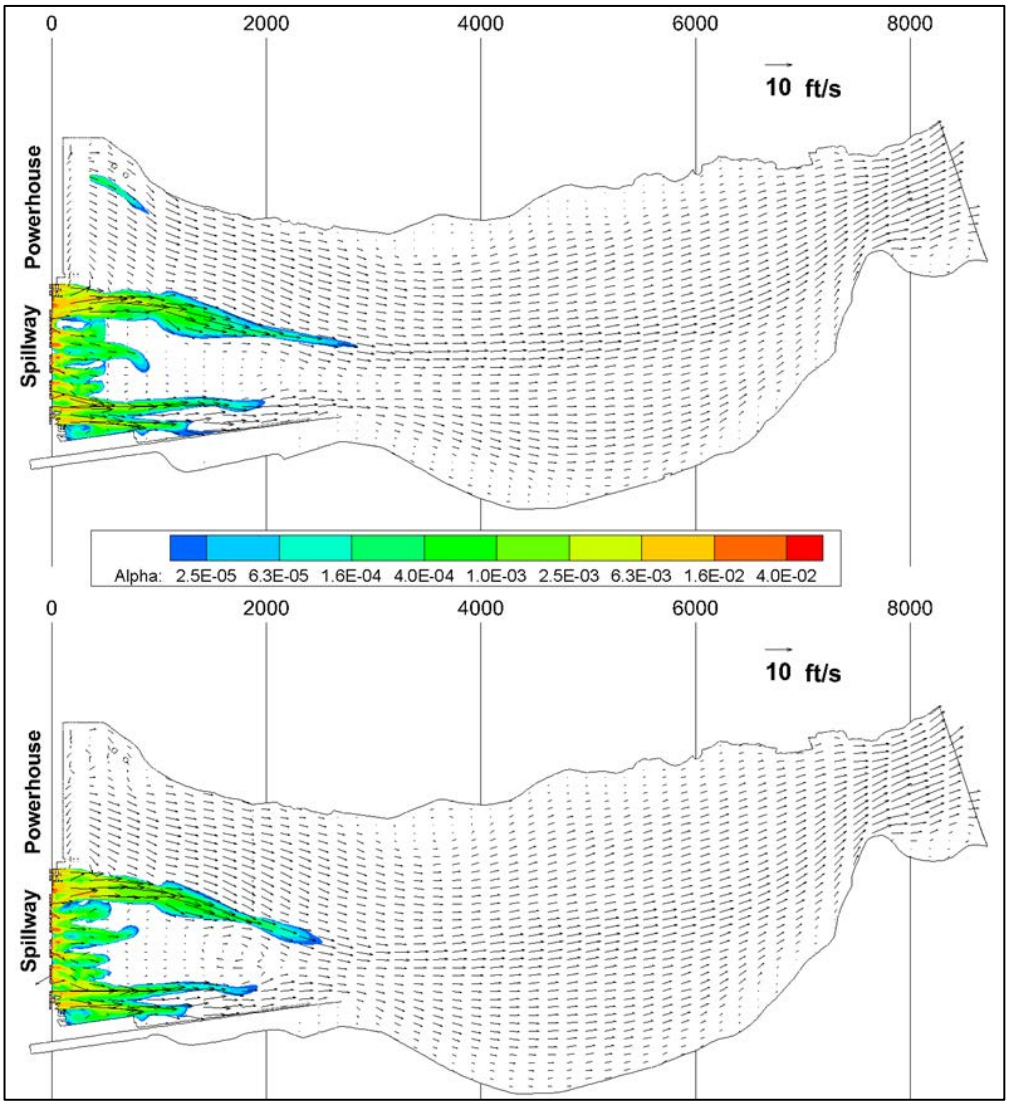

Figure G26. Contours of gas volume fraction and velocity vectors at 2m beneath the free surface. Top: Simulation 11. Bottom: Simulation 12

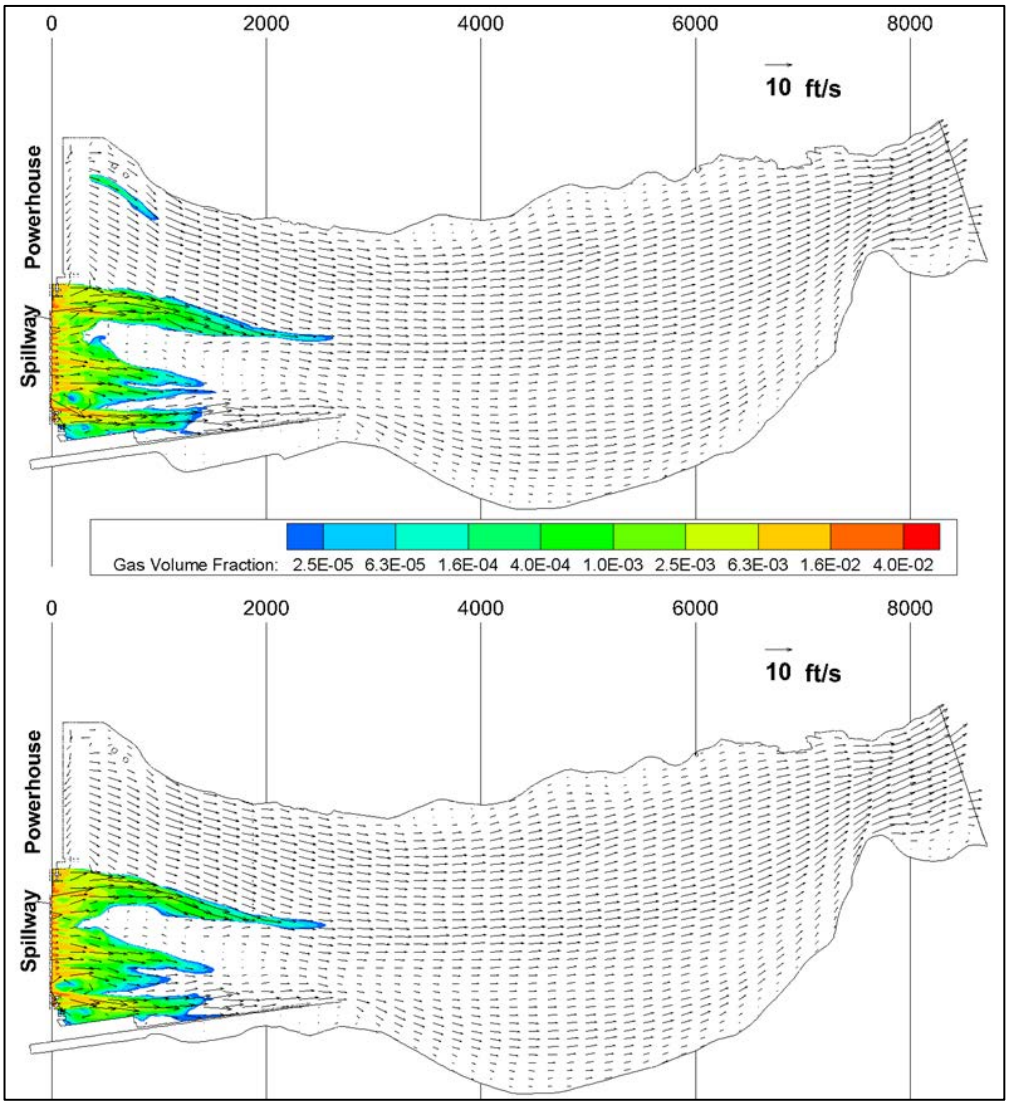

Figure G27. Contours of gas volume fraction and velocity vectors at 2m beneath the free surface. Top: Simulation 13. Bottom: Simulation 14

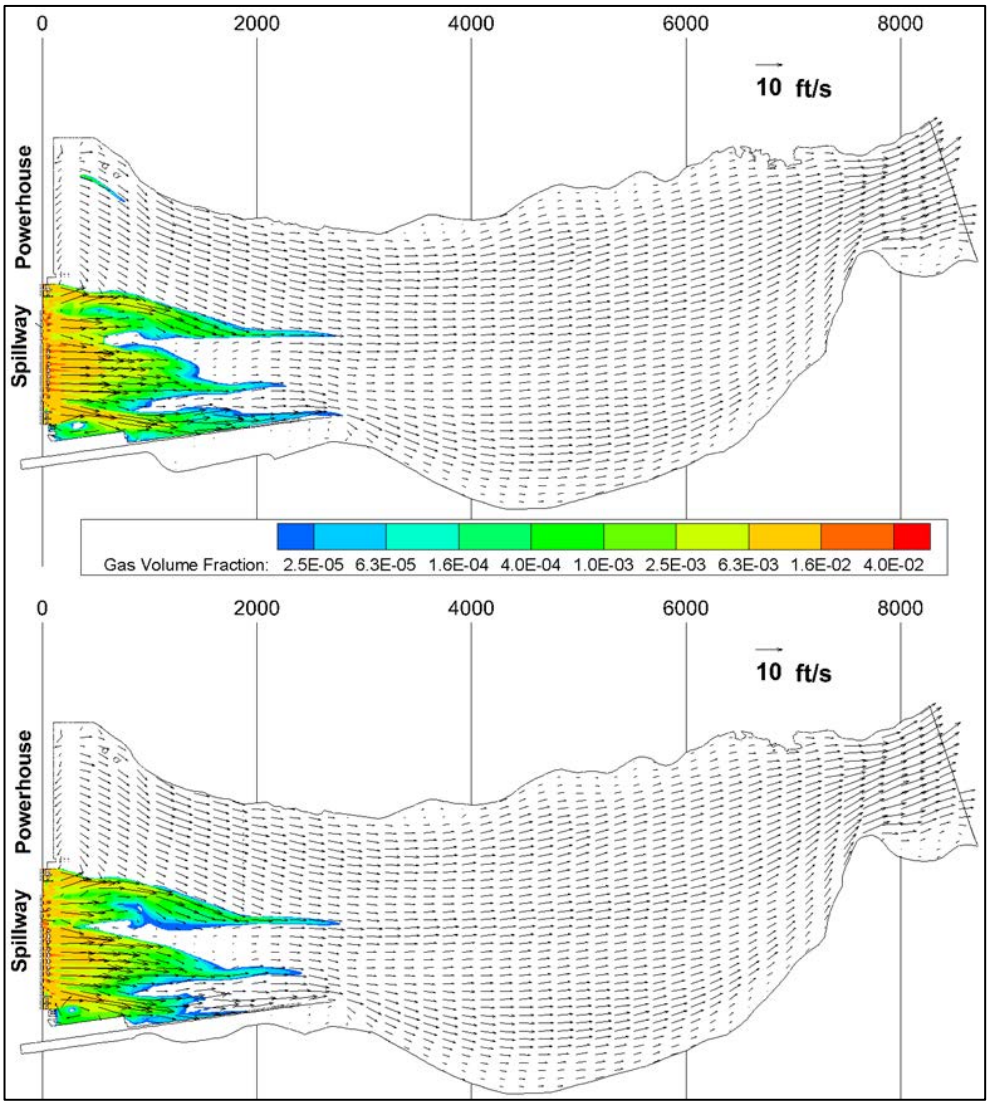

Figure G28. Contours of gas volume fraction and velocity vectors at 2m beneath the free surface. Top: Simulation 15. Bottom: Simulation 16

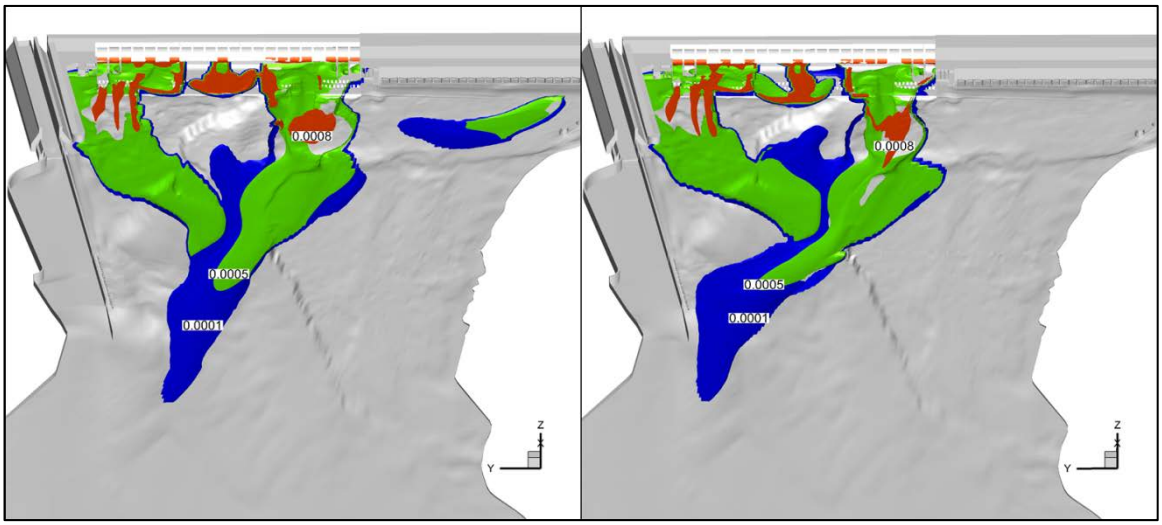

Figure G29. Isosurfaces of bubble diameter. Left: Simulation 1. Right: Simulation 2.

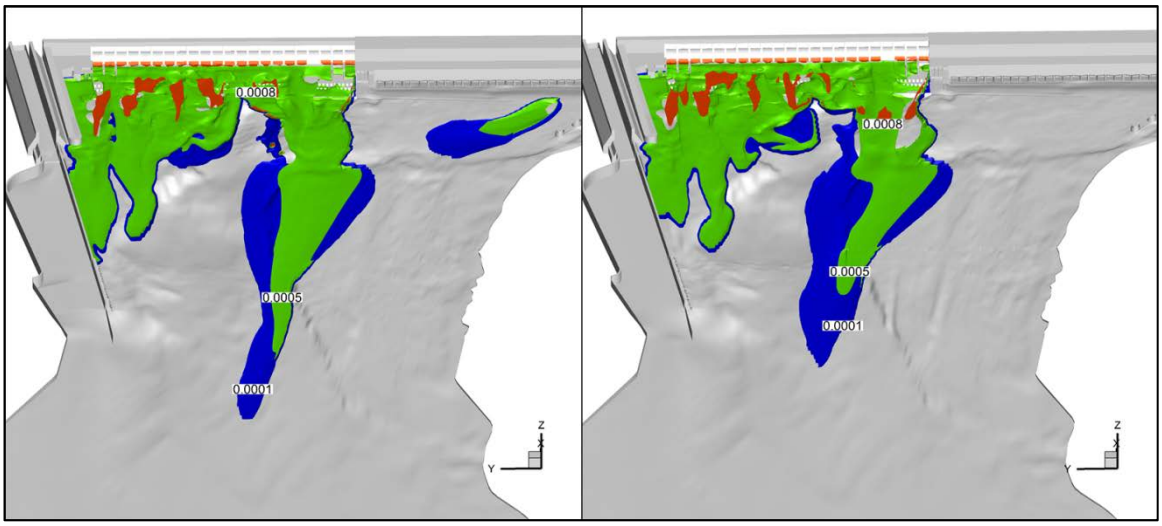

Figure G30. Isosurfaces of bubble diameter. Left: Simulation 3. Right: Simulation 4

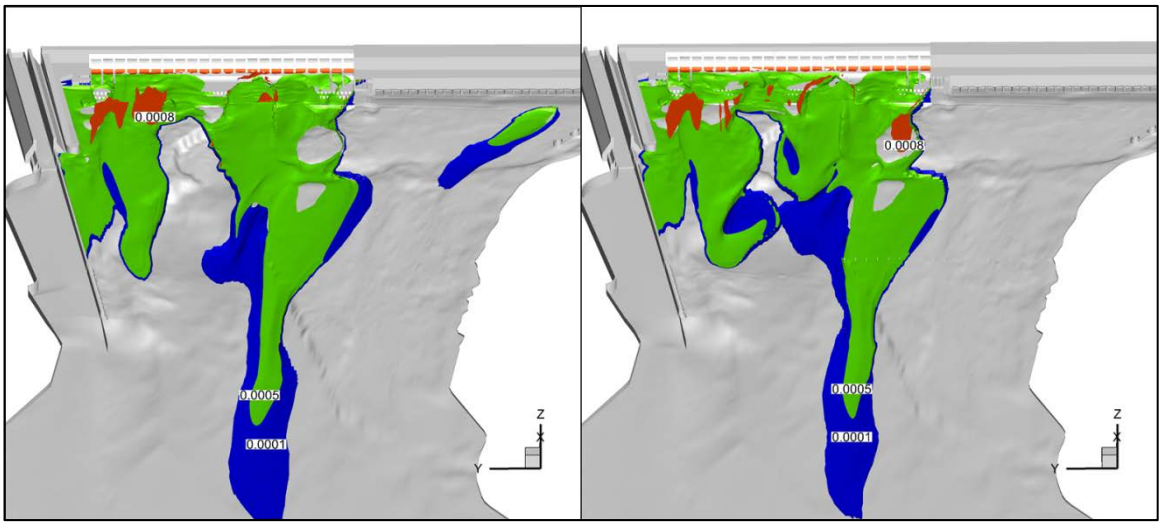

Figure G31. Isosurfaces of bubble diameter. Left: Simulation 5. Right: Simulation 6

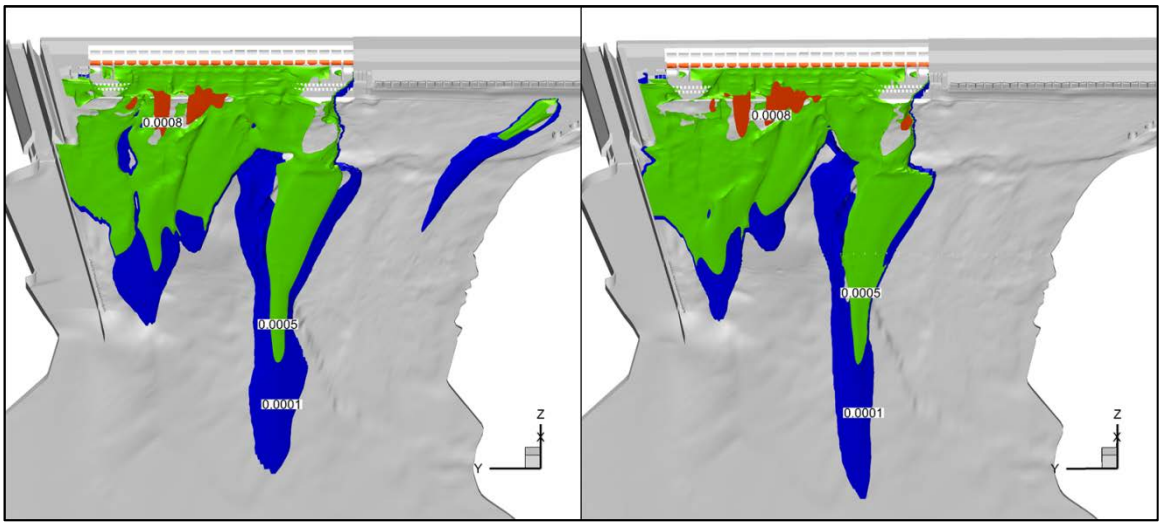

Figure G32. Isosurfaces of bubble diameter. Left: Simulation 7. Right: Simulation 8

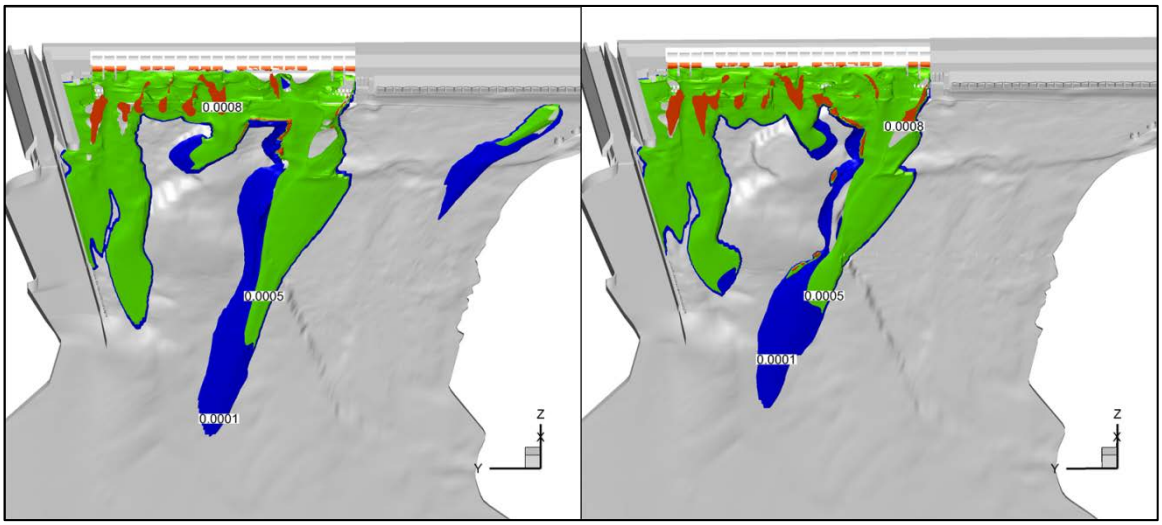

Figure G33. Isosurfaces of bubble diameter. Left: Simulation 11. Right: Simulation 12

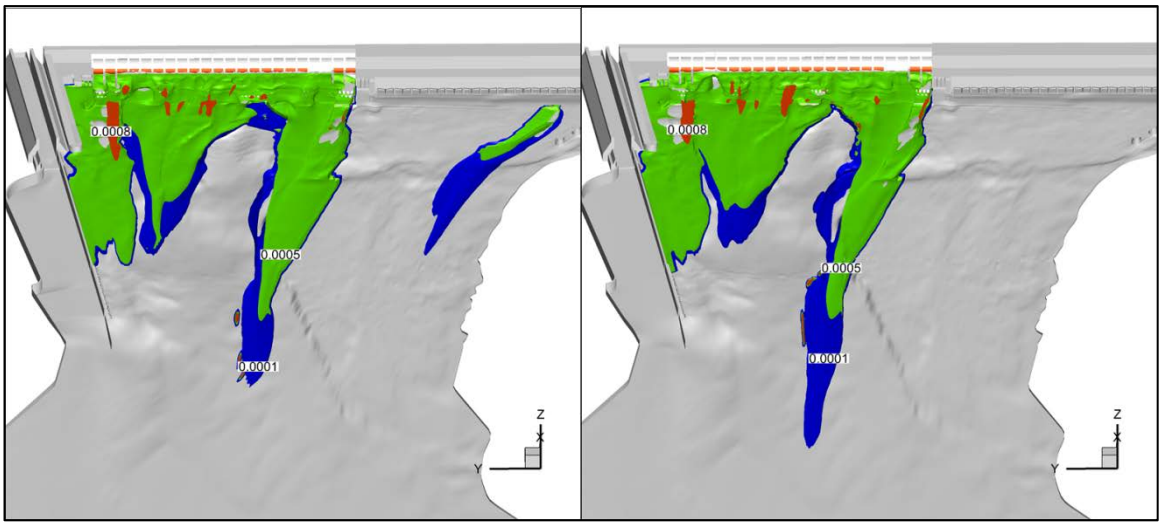

Figure G34. Isosurfaces of bubble diameter. Left: Simulation 13. Right: Simulation 14

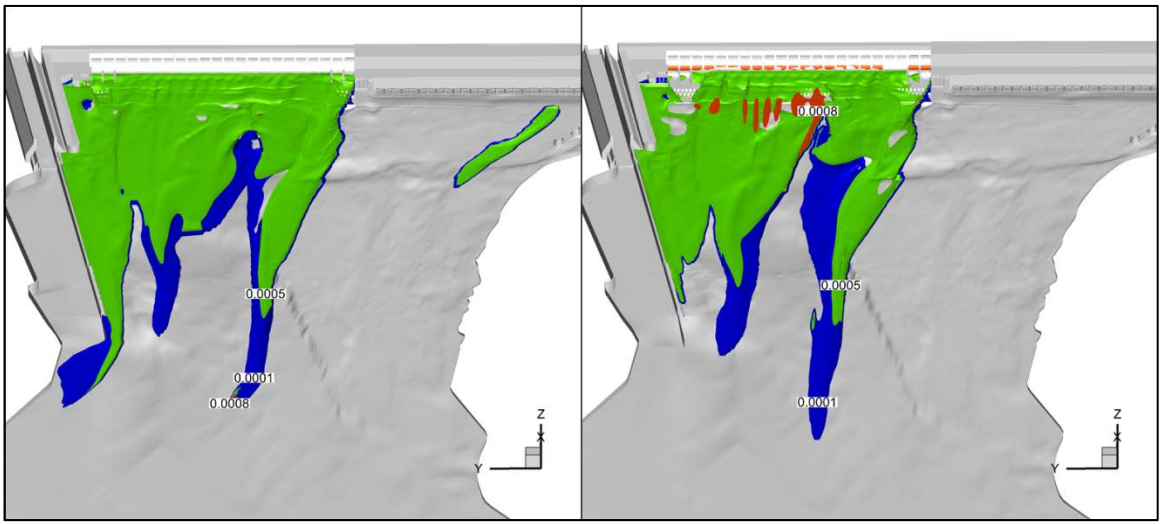

Figure G35. Isosurfaces of bubble diameter. Left: Simulation 15. Right: Simulation 16